(Abbreviated Title)

EFFECTS OF ULTRASONIC VIBRATIONS ON HEAT TRANSFER TO LIQUIDS

(Abbreviated Title)

EFFECTS OF ULTRASONIC VIBRATIONS ON HEAT TRANSFER TO LIQUIDS

EFFECTS OF ULTRASONIC VIBRATIONS ON HEAT TRANSFER

TO LIQUIDS BY NATURAL CONVECTION AND BY BOILING

EFFECTS OF ULTRASONIC VIBRATIONS ON HEAT TRANSFER

TO LIQUIDS BY NATURAL CONVECTION AND BY BOILING

by

SAU WAI WONG, B.Eng., M.Eng.(Chem.)

A thesis submitted to the Faculty of Graduate Studies

and Research in partial fulfilment of the

requirements for the degree of

Doctor of Philosophy

Chemical Engineering Department,
McGill University,
Montreal.   1st October, 1966

Ph.D. Thesis   Chemical Engineering

EFFECTS OF ULTRASONIC VIBRATIONS ON HEAT TRANSFER

TO LIQUIDS BY NATURAL CONVECTION AND BY BOILING

SAU WAI WONG

ABSTRACT

        The effects of ultrasonic vibrations on heat transfer to
water and methanol by natural convection and by boiling were measured
at three acoustic energy levels with frequency ranging from 20.6 to 306
kcps, using electrically heated platinum wires of diameters 0.007 and
0.010 in. Up to an eight-fold increase in heat transfer coefficient was
obtained in natural convection, but the effects diminished with increased
temperature difference and became negligible in the well-developed nucle-
ate boiling region. High-speed photographs showed that the increase was
due to the motion of cavitation bubbles on the wire surface. The heat
transfer results were correlated as a function of local cavitation acti-
vity values measured by a technique developed for this work.

        Ultrasonic vibrations at a frequency of 20.6 kcps had a
negligible effect on the burnout heat flux and the critical temperature
difference in methanol at $113^{\circ}F$ using platinum wire of 0.007 in. dia-
meter.

ACKNOWLEDGEMENTS

TABLE OF CONTENTS

LIST OF ILLUSTRATIONS

Page

Part II

LIST OF TABLES

GENERAL INTRODUCTION

In recent years, there has been increased interest in the effects of vibrations on heat transfer. These studies are conducted because most industrial applications involve systems with some degree of relative vibration or pulsation of the fluid and the surface. Other investigators, however, have studied the problem with the object of increasing the heat transfer rate.

The limited number of papers published on the influence of vibrations on boiling heat transfer is mainly concerned with the increase of the value of burnout heat flux or that of the critical temperature difference. Such information is useful for design calculations in such high power density systems as rocket engines and nuclear reactors. The results of these studies have varied from no effect to almost a 100% increase in the value of the burnout heat flux. The effects of vibrations on nucleate boiling, however, have hardly been touched upon.

In convective heat transfer, most of the work done is for gases. In the case of a liquid where the existence of two phases is possible, less information is available and the results from these studies show a wide discrepancy.

It was the purpose of this study to establish the important variables in heat transfer to liquids by natural convection as well as by boiling in sound fields of 20 to 300 kcps and for sound pressures well above the cavitation threshold of the liquid. Attempts were made to determine the controlling mechanism in these processes. One of

the limitations in this type of study is that specific results will be strongly dependent on the geometry of the system. In the present work, local values of the amplitude of vibration in the heat transfer surface were measured directly.

LITERATURE SURVEY

I.   INTRODUCTION

Boiling heat transfer data are generally presented graphi-
cally with log (q/A) as the ordinate and log (Δt) as the abscissa,where
(q/A) is the heat flux density and (Δt) is the temperature difference
between the heating surface and the fluid saturation temperature. The
data plotted this way yield the characteristic boiling curve which has
a similar shape for all fluid-surface combinations. The data shown in
Figure 1 were obtained by Nukiyama[1] in 1934 for water boiling at atmos-
pheric pressure on a submerged, electrically heated, platinum wire. In
the region AB, the liquid water is being superheated by natural convec-
tion. As the temperature difference increases, nucleate boiling (BC)
takes place where vapor bubbles form at specific points on the heating
surface. In this range the heat flux increases rapidly with a moderate
increase in wire temperature as new active points appear. At point C,
the heat flux goes through a maximum, the peak heat flux, at a tempera-
ture difference called the "critical Δ t". Beyond the critical Δt
value, a large fraction of the heating surface is covered by vapor,
which, because of its poor thermal conductivity, tends to insulate the
surface. The insulating effect of the vapor becomes so large at the
"critical Δt" that the heat flux diminishes as the temperature differ-
ence is further increased. This corresponds to the transition-film
boiling   region CD. In the film boiling region DEF,a stable film
of vapor covers the heating surface and heat is transferred through the

FIGURE 1

BOILING OF WATER AT 212°F ON AN ELECTRICALLY HEATED

PLATINUM WIRE, SHOWING DIFFERENT REGIONS
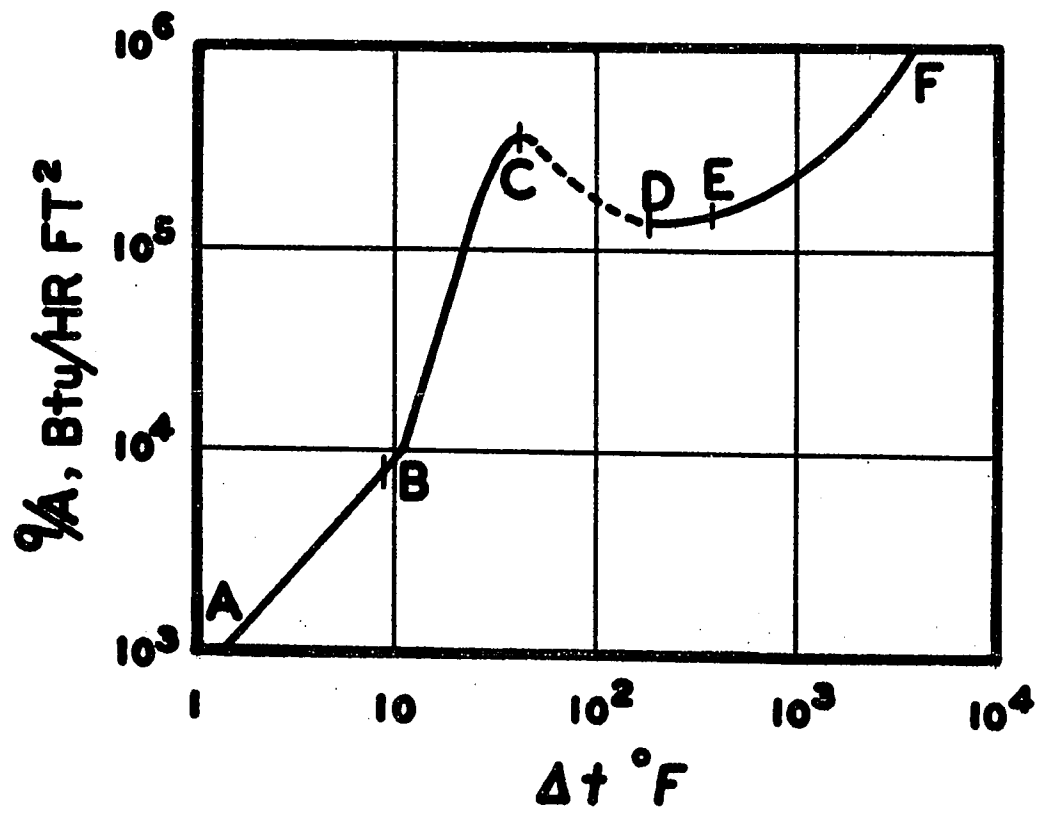
vapor film by conduction, convection and radiation.

The heat flux corresponding to the value at point C on the boiling curve sometimes is referred to as the burnout heat flux. In systems where heat is supplied by an electric heater or where the energy-generation rates are relatively independent of material temperatures as in the case of a pressurized-water nuclear reactor, an increase in heat flux beyond the peak value causes the temperature of the heater to jump suddenly to a very high value which usually exceeds the melting point of the heating element.

In spite of the extensive studies that have been made on boiling heat transfer, there exists today no consistent analytical method for predicting nucleate boiling heat fluxes and the peak value. Recent studies[2,3,4,5], however, have indicated that at lower heat fluxes, the important heat transfer mechanism is the agitation and stirring action of single bubbles in the superheated liquid layer adjacent to the heating surface. At higher heat fluxes, the mechanism of latent heat transport predominates and it is believed that in the vicinity of the peak heat flux, latent heat transport alone accounts for the total flux. It becomes obvious that the heat flux at a certain Δt is directly proportional to the frequency of bubble emission and the number of nucleation sites on the heating surface. One is thus led to the conjecture on the effect of a sound field on these two variables, and hence the effect of this field on boiling heat transfer rates.

In the case of natural convective heat transfer, it is expected that the heat transfer rates will be increased under the

influence of a sound field. The imposition of acoustic pulsation should create disturbances in the relatively stagnant film of liquid near the heating surface.

It has been mentioned that wide discrepancy exists in the published data on the effects of acoustic vibrations on heat transfer by convection as well as by boiling. The confusion is partly due to the various methods used to measure and report the values of the amplitude of vibration. In the case of a liquid, this in turn is due to the difficulty in measuring the amplitude of vibration directly. The interaction of the sound waves with the heat transfer surface and the container walls may set up a certain standing wave pattern. The effects of vibrations on heat transfer in many cases, may depend on the location of the heat transfer surface in the sound field. As a result, it is very difficult to compare these data on a common basis. In order to determine the mechanism which may be important in affecting the rate of heat transfer in a sound field, it is advantageous to review some concepts and definitions.

II. BACKGROUND INFORMATION

"Ultrasonic vibrations" refers to vibrations of sound waves at frequencies above the frequencies of audible sound which generally ranges from 30 to 20,000 cps. When a liquid is subjected to ultrasonic vibrations, small bubbles may be generated. The collapse of these bubbles may bring about drastic effects such as chemical reaction, erosion, emission of light (sonoluminescence) and radiation of sound. In fact, the formation and collapse of these small bubbles, which is called acoustic cavitation, can be expected to have a pronounced effect upon any boundary layer in which they are found. The amount of acoustic energy necessary to cause cavitation is termed the "cavitation threshold".

The tensile strength of a homogeneous liquid may be defined as the limiting negative pressure that such a liquid will withstand before it ruptures to form a new stable phase. Theoretical studies[6] based on the kinetic theory of liquids show that the tensile strength within a liquid is very large, for example in water of the order of 10^3 atm. These values are exceedingly high compared with the acoustic cavitation threshold values which range from 1 to 40 atm. under varying experimental conditions. Most liquids, unless they are specially treated, contain dissolved gases or other inhomogeneities which are generally called "nuclei" or "microbubbles". They are believed to be small air- or vapor-filled cavities stabilized in cracks on the surface of small particles suspended in the liquid, and are weak spots within the liquid. In order to have cavitation, it would be necessary only to overcome the surface tension forces of these nuclei rather than the intermolecular

bonding forces of the liquid. The strength of a nucleus depends very much on its size. As a result, the gas content of the liquid is an important variable in the study of acoustic cavitation. Other parameters include hydrostatic pressure, frequency, temperature, viscosity and other liquid properties.

Gaseous Cavitation

With water and using a focussing system at 60 kcps, Blake[7] has shown that there are three distinct types of cavitation. At very low pressures, large visible bubbles, which do not produce sound are formed in gassy water (water more or less saturated with gas). This is termed quiet degassing. At higher pressures, a more or less continuous stream of smaller gas bubbles is observed. These stable bubbles are originated at the focus of the sound field and they are accompanied by a soft hissing sound. Blake has observed that there is a critical pressure, or threshold, for the formation of these streamers and that the rate of formation is very sensitive to changes in the sound pressure amplitude. This second type of cavitation is called gaseous cavitation. Like the quiet degassing, gaseous cavitation only occurs in water that is almost saturated with gas. For a sound field of 60 kcps, Blake reported a sound pressure amplitude of about 0.25 atm. to be the threshold value for quiet degassing and about 1.25 atm. for gaseous cavitation. The boundary where the two types of cavitation are divided is not too well defined. Many investigators[8,9,10] have combined the two and termed them as gaseous cavitation.

As mentioned above, cavitation nuclei are small air- or vapor-filled cavities stabilized in cracks on the surface of small particles suspended in liquid. On the basis of a microscopic examination of water, Rosenberg[11] reported that these particles are mainly dust particles ranging from 0.5μ to 10μ in diameter. It appears that some mechanism must exist by which a nucleus can increase its air content and grow to a large visible bubble when it is situated in an acoustic pressure field. In a recent study by Barger[8] on the effect of suspended particle size on cavitation threshold, the water used was filtered through a 0.45μ filter. It was assumed that the diameter of the particles remaining in the water must have been less than about 0.5μ and that the radius of the small bubbles that were drawn from the cracks was less than about 0.2μ. With a sound pressure of 0.45 atm. and a frequency of 27 kcps, the resulting cavitating bubbles had a mean radius of about 40μ.

A theory called rectified diffusion was first proposed by Blake[7] and later elaborated by Hsieh and Plesset[12] to explain the growth of a cavity by a net influx of gas as it oscillates in the acoustic pressure field. According to this theory, a small bubble filled with gas is assumed to pulsate in phase with the pressure amplitude of the acoustic field. For this phase relationship to occur, the bubble resonance frequency must be larger than the driving frequency. If the bubble was initially in equilibrium with its surroundings, gas will tend to diffuse out when the bubble is compressed and in when the bubble is expanded. This is because the pressure of the air in the bubble is less

than the equilibrium air saturation pressure in the surrounding liquid when the bubble is expanded beyond its equilibrium radius and greater than the equilibrium air saturation pressure when the bubble is compressed. Since the surface area of the bubble is larger when the bubble is expanded, the bubble experiences a net gain of air during each cycle of motion.

Several equations[7,12,13] have been proposed to determine the mass transfer rate of gas into the bubble by rectified diffusion. The most complete derivation has been presented by Hsieh and Plesset[12] and the final equation is as follows:

$$\frac{dm}{dt} = \frac{8\,\bar{\pi}}{3}\ \mathscr{D}\ c_s\ R_o\ (\frac{P_p}{P_o})^2 \tag{1}$$

where $\mathscr{D}$ = diffusivity of the gas through the liquid, cm^2/sec

c_s = saturation gas content of the liquid at P_o, cc/lit

P_o = ambient pressure in the liquid, atm

P_p = peak acoustic pressure, atm

R_o = mean bubble radius, cm.

Eq. (1) was derived under the assumption that the applied acoustic pressure is small, that is, for small-amplitude linear oscillations. The effect of frequency is also assumed to be negligible.

Eq. (1) was used by Strasberg[14] to obtain the threshold pressure for rectified diffusion. The threshold pressure is taken to be the critical pressure for which the rate of air diffusing into the bubble is equal to the rate of air diffusing out of the bubble. The result can be expressed as

$$\frac{P_{cv}}{P_o} = [\ (\frac{3}{2})(\ 1 + \frac{2\sigma}{R_o P_o} - \frac{C_A}{C_s}) \ ]^{1/2} \qquad (2)$$

where P_{cv} = threshold pressure for rectified diffusion, atm

σ = surface tension, dyne/cm

C_A = actual gas content of the liquid, cc/lit

P_o, R_o and C_s are defined as before.

Strasberg compared the threshold pressure values predicted by Eq. (2) with a limited amount of experimental data and showed that they have the same order of magnitude. However, in deriving Eq. (1), Hsieh and Plesset have emphasized the assumption of $(P_p/P_o) \ll 1$ so that the linearization procedure may be carried out. Eq. (2) is thus subjected to the same limitation. In fact, for water that is saturated with air at t = 20°C and P_o = 1 atm., one can easily show that the inequality $R_o \geq 220 \mu$ must hold for $(P_p/P_o) \leq 0.10$. For partially degassed water, Eq. (2) is limited to even larger values of R_o. On the other hand, cavitation bubbles have been observed to grow from sub-visible size[8,10]. It is evident that Eq. (2) cannot give reliable quantitative results.

Vaporous Cavitation

In degassed water, vaporous cavitation will occur. This is characterized by sporadic ruptures of cavities and sharp snapping sounds. According to Blake[7], the small explosive ruptures can be observed when the sound pressure amplitude is about 4 atm. (at 60 kcps). The ruptures are caused by the violent collapse of very short-lived bubbles, each bubble producing an audible snap at the climax of its

cycle of growth and collapse. The gas content of the liquid is again
an important variable. While Blake used completely degassed water,
Barger[8] was able to achieve vaporous cavitation with water of gas con-
centration half of the saturation value. The threshold pressure found
by Barger for frequencies smaller than 200 kcps, was larger than 3 atm.

The growth of vaporous cavitation bubbles cannot be
explained by rectified diffusion. The complete collapse of bubbles in
this region indicates that the gas content of the bubbles must be negli-
gible with respect to the amount of gas that would be necessary to sta-
bilize the final pre-collapse bubble radius.

The first theoretical treatment of the dynamics of a
sub-visible nucleus in a sound field was given by Noltingk and Neppiras[15,16].
They assumed that the liquid is incompressible, the gas content in the
bubble is constant and that there is no vapor in it. The applied acous-
tic pressure wave is taken to be sinusoidal, and the diameter of a
bubble is always much less than the wavelength. Numerical solutions of
the equation of motion relating the kinetic energy of the associated
mass of liquid and the total work done in overcoming surface tension,
the pressure of the gas and that of the liquid have been calculated for
a number of values of the parameters: acoustic pressure, frequency,
initial bubble radius. All calculations were for an ambient pressure
of 1 atm. The results are presented in curves of radius versus time
for the growth and collapse of the bubble. These solutions show that
the bubble (nucleus) initially increases in size to a maximum radius
during the tension phase of the acoustic cycle, and then collapses

during the compression phase. At the end of the first acoustic cycle, the bubble radius is calculated to be equal or less than the initial radius. Noltingk and Neppiras did not continue their calculations beyond this point because the calculated bubble interface velocity became larger than the speed of sound in water, a condition that invalidates the incompressibility assumption.

Their results also showed that the maximum radius of the bubble is inversely proportional to the driving frequency, and directly proportional to the applied acoustic pressure. For a specified driving frequency and acoustic pressure, it is shown that there exists a minimum and maximum bubble radius for which cavitation can set in. Bubbles with radii smaller than the minimum value are bubbles for which the surface tension forces are not exceeded by the applied acoustic pressure. The maximum value of the bubble radius should not exceed the resonant size of the bubble. Noltingk and Neppiras have shown that bubbles with radii larger than the maximum value exhibit a complex oscillation, but do not collapse.

It should be noted that because of the complexity of the problem, many simplifying assumptions have been made. Dissipative effects such as sound radiation, heat conduction and viscosity have been ignored by Noltingk and Neppiras. Recently, Flynn[17] has shown these dissipative effects have a pronounced effect on the motion of a bubble. Calculations of Noltingk and Neppiras show that the lifetime of a bubble is less than an acoustic cycle. This contradicts most experimental observations. Using high-speed photography, Willard[10], as well as

Barger[8], observed the lifetime of a vaporous cavitation bubble to be hundreds of acoustic cycles. Consequently, results of Noltingk and Neppiras may be taken as qualitative.

Experimental Determinations of Cavitation Threshold

A great number of papers has been published on the dependence of acoustic cavitation threshold on the state of the liquid, the acoustic frequency, liquid properties, etc. Frequently, the measured threshold values have been inconsistent. This is mainly due to the various definitions of cavitation used by different experimenters, different experimental procedures, and poor control of the exact state of the liquid. It should be noted, however, that such control is generally very difficult to accomplish in practice.

As was discussed in the theory of acoustic cavitation, the gas content of the liquid is the most important variable affecting the cavitation threshold. The most complete study of this variable was given by Galloway[9] who used a focussed system with frequencies ranging from 20 to 40 kcps. The sound pressure at the focus was determined from the reading taken by a pressure probe which was positioned at the secondary maxima of the standing pressure wave. The cavitation threshold depended heavily upon the gas content of the liquid for gas contents greater than 5% of the saturation value. The results were presented in graphical form for distilled water and petroleum ether. Whether the gaseous cavitation or vaporous cavitation occurred depended on the gas content of the liquid. When the gas content was of the order of 10% of

the saturation value, vaporous cavitation occurred. Strasberg[14] has also studied the effect of gas content on acoustic cavitation threshold. Various empirical equations are shown in Table I.

Galloway[9] also studied the effect of temperature on the cavitation threshold of distilled water, synthetic seawater, petroleum ether, and a 0.1 mole fraction dioxane-water mixture for different degrees of gas content over a range of 0° to 50°C. The cavitation threshold of all samples decreased linearly with increasing temperature. Similar results for water at 60 kcps were obtained by Blake[7], whose empirical equation is given in Table I.

A change in the temperature of the liquid changes the surface tension, the vapor pressure, the viscosity, as well as the degree of saturation of the liquid. The temperature dependence of cavitation threshold, however, cannot be attributed to viscosity, since viscosity has a hyperbolic rather than linear dependence on temperature. Galloway[9] also attempted to correlate cavitation threshold with the surface tension of the liquid without success. He concluded that the temperature dependence of cavitation threshold was due to the dependence of gas solubility on temperature.

The effect of temperature was also studied by Connolly and Fox[18] using both focussed waves and plane progressive waves at 1 mcps for gassy water at temperatures between 0° and 30°C. The gas content of water was kept constant at the saturation value at 30°C. It was found that the measured value of cavitation threshold was not a linear function of temperature, but increased by a factor of 2.5 between

TABLE I

CORRELATIONS FOR ACOUSTIC CAVITATION THRESHOLD

BLAKE

$$P_{cv} = 0.07 \ (\ T_s - T) + 1 \quad \text{atm} \qquad (T = 10^o \text{ to } 50^o C)$$

GALLOWAY

$$P_{cv} = P_z \ (\ 1 - T/273) \qquad (T = 0^o \text{ to } 50^o C)$$

CONNOLLY AND FOX

$$P_{cv} = 1.75 + 0.176 \ (C_s - C_A) \qquad (T = 0^o \text{ to } 30^o C)$$

STRASBERG

$$P_{cv} = 2 + 4.8 \ (1 - C_A/20)$$

where T = temperature, in $^o C$

T_s = saturation temperature of the liquid, in $^o C$

P_z = P_{cv} evaluated at $0^o C$

C_A = actual gas content in cc/liter

C_s = gas content when the liquid is saturated, in cc/liter.

30° and 0°C. A method of correlation based on the degree of undersaturation of the liquid was proposed by Connolly and Fox. As the temperature is decreased, water becomes less and less saturated. The undersaturation is then defined as the difference between the saturated gas content and the actual gas content present in the liquid. The measured values of cavitation threshold varied linearly with the degree of undersaturation. The final equation is shown in Table I.

Briggs et al.[19] studied the effect of variation of viscosity on cavitation threshold in liquids at a frequency of 25 kcps. The cavitation threshold changed by less than a factor of 3 over a range of viscosities from 0.007 poise to 8.0 poise, the threshold increasing with increasing viscosity. On the basis of these data, it appears that the viscosity of the liquid is not a very important parameter in determining the cavitation threshold.

The first complete study on the frequency dependence of the acoustic cavitation threshold was made by Esche[20]. Nine different experimental arrangements were set up to determine the threshold at nine frequencies from dc to 3.3 mcps. The water was described as distilled, filtered, and degassed, but the actual gas content was not measured. The results were presented graphically[21]. For degassed water the cavitation threshold remains nearly constant at 1 atm. for frequencies below 10 kcps, and increases rapidly above 100 kcps. At 5 mcps Esche reported a value of 100 atm. for cavitation threshold. These results, however, have been shown to be in wide discrepancy with those reported by other experimenters[8].Consequently, Esche's results are only qualitative.

Recently, a more elaborate study has been made by Barger[8] using water at seven different frequencies varying from 27 to 1,160 kcps. The gas content of water covered a very wide range and the suspended particle size was carefully controlled. As expected, the cavitation threshold depended heavily on the gas content of the liquid. The cavitation threshold increases rapidly for frequencies above 350 kcps. The effect of gas content became negligible when the frequency was 350 kcps or above. With the same gas content, there was no measurable difference in the cavitation thresholds of the samples of water that had been filtered through a filter with pore size of 0.45μ and those that had not been filtered.

Finally, on the effect of the hydrostatic pressure, Galloway[9] showed that for saturated liquids cavitation threshold was directly proportional to the hydrostatic pressure. The cavitation threshold was 1 atm. peak acoustic pressure at 1 atm. hydrostatic pressure. With undersaturated water the cavitation threshold was independent of the hydrostatic pressure from 1 atm. down to 0.05 atm.

Cavitation Damage

Cavitation damage is one of the phenomena resulting from the motion of a cavitation bubble. Plesset and Ellis[22] studied the cavitation damage on metal surfaces by means of micro-photographs and X-ray diffraction patterns. Both methods showed that plastic deformation occurred whenever there was cavitation damage. The damage to a nickel specimen in water was compared to the damage to a similar nickel

specimen in liquid toluene, free of air and covered by a helium atmosphere. They found that essentially the same type and the same extent of plastic deformation had taken place in both liquids. Specimens with unlike chemical properties showed similar results. It was then postulated that cavitation damage starts with a plastic deformation of the material, which by repeated short stresses leads to work hardening, fatigue, and eventual failure of areas on the specimen. Plesset and Ellis concluded that the cause of cavitation damage was the mechanical stress from rapid collapse of cavitation bubbles. The chemical effects were not of primary significance.

There are at least two different situations in which a collapsing bubble may bring high stresses to a solid surface. In the first case, a bubble which has grown from a nucleus in the liquid is only a few radii from the surface. When it collapses, a shock wave would be emitted and the damage to the surface would arise from an interaction between the shock wave and the surface. Sutton[23] measured the stresses set up by cavitation bubbles collapsing on a photoelastic surface by high-speed photography. The resulting strain waves in the photoelastic solid showed that stresses as high as 13,000 atm. may have been generated by cavitation. Jones and Edwards[24] who measured the stresses set up in a bar by bubbles collapsing on one end of the bar reported the stresses at the point of collapse must have been at least 10,000 atm.

Cavitation bubbles can also grow from certain selective spots on the solid surface which are microscopic imperfections containing

trapped gas. When they collapse, the damage to the surface may be due either to the high pressures and temperatures of the compressed gases and vapors within the contracting bubbles, or to the impact of part of the liquid interface on the surface. The latter mechanism, first proposed by Kornfeld and Suvorov[25] and by Eisenberg[26], involves an unsymmetrical collapse of an attached bubble with liquid jets being formed at the contracting interface. The damage to the solid would then be ascribed to the high-speed liquid jets impinging on the surface. High-speed photographs taken by Naudé and Ellis[27] of bubbles collapsing on photoelastic solids confirmed that this is the controlling mechanism. Their experiments also indicated that surface instabilities leading to the generation of high-speed jets can occur both in pulsating gaseous bubbles as well as in collapsing vaporous bubbles.

Since cavitation damage is directly related to the cavitation phenomena, factors affecting cavitation threshold are expected to affect the cavitation damage as well.

The temperature dependence of cavitation damage was first studied by Bebchuk[28,29] who measured the weight loss from a standard specimen of aluminum plate at a frequency of 8 kcps using a number of liquids, including water, ethyl alcohol and carbon tetrachloride, with temperature ranging from 10° to 90°C. The cavitation damage first increased to a maximum and then decreased with increasing temperature. Similar experiments by Devine and Plesset[30] using various metals also showed that a maximum exists in the damage rate and that it is independent of the material. According to Devine and Plesset, the existence

of a maximum is due to the increase of vapor pressure and the decrease
of the equilibrium concentration of dissolved gas in a liquid as the
temperature is increased. Increase in vapor pressure tends to decrease
the damage while the cavitation bubbles would collapse more violently
as the gas content of the liquid decreases. A maximum would be formed
as the more violent bubble collapse tends to oppose the cushioning
effect of rising vapor pressure. Devine and Plesset reported that the
damage correlated directly with the change in vapor pressure of the
liquid and inversely with the concentration of dissolved air.

The cavitation damage was found by Bebchuk to be much
greater in water than in any organic liquid. For example, the damage
maximum in water is approximately six times that in ethyl alcohol and
carbon tetrachloride. Bebchuk and Rosenberg[29,31] ascribed this dif-
ference to the effect of gas solubility. The solubility of gases in
carbon tetrachloride and ethyl alcohol is almost an order of magnitude
greater than that in water.

The effect of surface tension on cavitation damage was
studied by Antony[32] using liquids of different surface tensions and
approximately the same vapor pressure. His results show cavitation
damage varies almost linearly with the surface tension of the liquid.

Since it is established that cavitation damage is prima-
rily a mechanical process, it might be expected that there is a relation
between the weight loss in a fixed time interval and the intensity of
the sound radiated by the collapsing bubbles. Experiments by Bebchuk
et al.[33] showed that the weight loss increased as the square of the

radiated sound pressure amplitude. This leads to the conjecture that cavitation damage may be used as a measure of cavitation activity at a surface. The findings of Bebchuk[28] that, after an initial nonlinear period, the weight loss is a linear function of time in a steady field of cavitation indicate the reliability of this method. The initial non-linear period reflects the surface inhomogeneities of the specimen. Recently, it has been proposed by Crawford[34] and Antony[32] that this method be used to measure the cavitation activity in a commercial ultra-sonic cleaning tank.

Acoustic Streaming

Acoustic streaming is due to the interaction of sound waves with the fluid and boundary surfaces. In addition to the oscil-lating flow that would be anticipated, a steady, directed flow in the body of irradiated fluid is often observed. There are two types of streaming. When the streaming is caused by the interaction of sound waves with the fluid only, it is called the quartz wind. When the streaming is the result of the interaction of the sound waves with the fluid as well as with boundaries or obstacles, it is called the surface streaming.

When a beam of plane waves radiates into a liquid with a plane absorber some distance from the source, it can be shown experi-mentally that a reaction force acts on the source which is proportional to the energy density of the sound field. This force is called the radiation pressure. Since there is absorption of sound in liquids, an

exponential drop of energy density, and thus the radiation pressure, along the axis of the sound beam would occur. If the sound beam fills the bounding container, there will be no circulation and a static pressure gradient will exist in the liquid. If the source is small so that the sound beam does not fill the container, there will be regions in which absorption does not occur. The resulting forces will cause an acceleration of the liquid until viscous forces maintain an equilibrium flow. The resulting streaming is the quartz wind. Eckert[35] has made a theoretical study of the problem and showed that for water, the streaming will have a negligible velocity at frequencies below 1 mcps. If the medium is air, it is appreciable at frequencies above several hundred cycles per second.

Surface streaming is a more complex phenomenon as it depends on the geometry of the surface or obstacle as well as on the properties of the fluid and the characteristics of the vibratory motion. Andrade[36] was one of the pioneer workers who made a photographic study of surface streaming using tobacco smoke. The first mathematical solution was given by Schlichting[37] who predicts two regions of streaming in each quadrant, a thin layer next to the cylinder, called the D-C boundary layer, with streaming toward the surface along the propagation axis, and an outer streaming with direction away from the surface along this axis. Holtsmark et al.[38] conducted an extensive experimental and theoretical investigation and found two regions of streaming on the pattern of the Schlichting predictions. Good agreement was obtained between the predicted values and the observed values of the streaming velocity.

According to the Schlichting theory, the thickness of the D-C boundary layer (δ_{D-C}) is independent of the amplitude of vibration and directly proportional to the A-C boundary layer thickness (δ_{A-C}) which is defined by $(\mathcal{V}/\omega)^{1/2}$ where $\mathcal{V}$ is the kinematic viscosity and ω is the angular frequency of the vibration. Recently, Raney et al.[39] have shown experimentally that for small amplitudes of vibration, the D-C boundary layer thickness may be correlated with the diameter of the cylinder and the A-C boundary layer thickness as defined by Schlichting. The resulting correlation which includes data obtained by Holtsmark et al. is one in which the D-C boundary layer thins rapidly as the A-C boundary layer is also thinned, that is, when the frequency increases or viscosity decreases. Their experimental work also confirms theoretical predictions that for small amplitudes, the streaming pattern will be the same whether the cylinder oscillates in a quiescent fluid or is fixed in an oscillating fluid. These treatments are based on the assumptions that the radius of the cylinder is small compared to the wave length of the sound and large compared to the displacement amplitude of the sound wave.

III. HEAT TRANSFER LITERATURE

Natural and Forced Convection - Air

Acoustically Vibrated Systems

Kubanskii[41] studied the natural convective heat trans-
fer from the outside of an electrically heated horizontal cylinder in
air subjected to a sound field with frequencies ranging from 8 to 30
kcps and intensities ranging from 0.03 to 0.16 watts/cm^2 (approximately
145 to 152 db re 0.0002 microbar). The direction of sound propagation
was parallel to the axis of the cylinder which had a diameter of 2.4 cm.
An increase up to 75% in the heat transfer coefficient was reported.
He concluded from shadowgraph studies that acoustic streaming was respon-
sible for the increase of heat transfer.

Fand and Kaye[42] also investigated the effects of a
horizontal transverse sound field on free convection from a 3/4 in. dia-
meter, electrically heated, horizontal cylinder. The frequency of vibra-
tion varied from 1100 to 6120 cps and the temperature difference between
the cylinder and the air varied from 0° to 250°F. Their data showed
that a "critical sound pressure level" exists below which the influence
of sound is negligible and above which the rate of heat transfer is
markedly increased by sound. From a flow-visualization study using
smoke as the indicating medium[43], they concluded that the increase of
heat transfer was due to a new type of boundary layer flow called
"thermoacoustic streaming" resulting from the interaction of the trans-
verse sound field with the heated cylinder. This streaming was more
intense than the isothermal streaming and was evidenced by a pair of
vortices above the cylinder but not below. The flow pattern resembled

vortex shedding behind a cylinder in forced flow normal to the axis. For the same temperature difference, the superposition of a sound field increased the heat transfer coefficient by a factor of 3. Recently, Fand and Peebles[44] have observed similar flow patterns around a heated and mechanically vibrating cylinder in otherwise still air at a frequency of 104 cps. For $f \leqslant 1500$ cps and $\ell/D \geqslant 6$ (ℓ is the half wavelength of sound and D is the diameter of the test cylinder), Fand and Kaye[42] proposed the following correlation to evaluate the heat transfer coefficient

$$h_v = 0.722[\Delta t(af)^2]^{1/3} \tag{3}$$

where h_v - heat transfer coefficient with vibration, BTU/hr ft^2 ^oF

Δt - temperature difference, ^oF

f - frequency of vibration, cps

a - sinusoidal displacement amplitude of vibration, ft.

The local heat transfer coefficients for the heated cylinder in a similar experimental set-up used by Fand and Kaye[42] have been measured by Fand et al.[45] in a sound field of 146 db (re 0.0002 microbar) and a frequency of 1500 cps. The results show that the maximum increase in the local heat transfer coefficient on the lower portion of the cylinder is approximately 250% and that on the upper portion of the cylinder is approximately 1,200%. The increase on the upper portion is attributed to the vortex flow which is characteristic of the so-called thermoacoustic streaming, while that on the lower portion is attributed to an increase in laminar boundary layer velocities in this region and a modification of the boundary layer temperature profile due to

acoustically induced oscillation within the boundary layer.

Holman and Mott-Smith[46] measured convective heat transfer coefficients on a 3/4 in. diameter, electrically heated cylinder in air between 2780 and 4710 cps. Wall temperatures of the cylinder ranged from 208° to 270°F. It was observed that increase in the heat transfer coefficient did not occur until the sound pressure level was greater than approximately 135 db (re 0.0002 microbar). A 100% increase was obtained when the sound pressure level was 147 db. For the range of values studied, the effect of frequency was negligible. The increased heat transfer was taken to be the result of the thinning of the D-C boundary layer. No correlation was proposed.

The effects of forced convection in a standing sound field were studied by Kubanskii[50]. The direction of propagation of the sound wave was perpendicular both to the axis of the cylinder and to the direction of the forced flow. The velocities of the forced flow varied from 1.45 to 1.77 m/sec, which corresponded to Reynolds numbers of 1450 to 1770. He was able to either increase or decrease the heat transfer rate by changing the axis of the cylinder with respect to the nodes of the sound field. It was observed that changes in the boundary layer flow and thus the heat transfer rate occurred if the acoustic particle velocity was equal to or greater than the forced flow velocity. A maximum increase of about 50% was observed in the heat transfer rate. The same problem has been studied recently by Fand and Cheng[51]. The ranges of experimental variables are as follows: Reynolds number of the forced flow, 590 - 10,750; temperature difference, 50° - 360°F;

sound pressure level, 130 - 150 db (re 0.0002 microbar); and sound frequency, 1100 and 1500 cps. However, the increase in the heat transfer coefficient did not exceed 25% in all cases.

Jackson et al.[52] studied free and forced convection to air inside a steam-heated vertical tube in the presence of a sound field. The sound field was superimposed from a loudspeaker located near the bottom of the tube. Their results indicated that sound pressure levels below approximately 118 db (re 0.0002 microbar) had little effect on the heat transfer coefficient. The sound pressures, however, were measured at the entrance to the tube and did not reflect conditions within the tube. Increases in the heat transfer coefficient of up to 80% were found for frequencies varying from 250 to 2,400 cps and the Graetz number from 40.2 to 1,633. The following correlation was proposed:

$$Nu(Re)^{1/4}(Gz)^{-1/2}f^{1/8} = 5.7 \ e^{SPL/69.5} \tag{4}$$

where Nu - Nusselt number, dimensionless

     Re - Reynolds number, dimensionless

     Gz - Graetz number, dimensionless

    SPL - sound pressure level, db (re to 0.0002 microbar).

Mathewson and Smith[53] studied the effects of pulsations on forced convective heat transfer by cooling pulsed air in a 1 in, vertical double-pipe heat exchanger. The pulses were generated by a motor-driven, flat-plate siren set in the exchanger inlet line. Pulse frequencies ranged from 50 to 330 cps and pulse amplitudes between 10 and 250 lb/ft^2 were used. It was observed that the improvement in heat

transfer coefficient increased with frequency and that amplitude had no effect. A maximum increase of 44% in heat transfer coefficient at Re = 2,300 was obtained, but the increase became negligible when the Reynolds number exceeded 4,000. The range of Reynolds number covered was from 1,600 to 4,000. Using the same equipment, Mathewson and Smith studied the effects of pulsations on film condensation of isopropanol and observed increases in heat transfer rate by 10 to 60%. The increase depended on the vapor flow rate which varied from 1 to 2.5 lb mole/hr and was almost independent of pulse frequency where the same frequency range was used for air. A critical pulse amplitude was required before any increase in heat transfer rate was observed. At amplitudes just greater than the critical value, the heat transfer coefficient increased rapidly with the amplitude, becoming independent of amplitude at very high pulse amplitudes. No correlation was proposed.

The effect of vibration on forced convective heat transfer was also studied by Lemlich and Hwu[49] who used a 25 in. long, horizontal, double pipe, steam to air heat exchanger. Vibration was induced acoustically with frequencies from 198 to 322 cps and superposed directly onto the air stream at Reynolds numbers of 560 to 5900. Increases in Nusselt number of up to 51% in the normally laminar region and up to 27% in the normally turbulent region were reported. Their data were correlated with the following equations:

For Re < 1500

$$\frac{Nu}{Nu_v} - 1 = 1.3 \times 10^{-6} (\bar{H}_p f)^2 \qquad (5)$$

For Re > 2500

$$\frac{Nu}{Nu_v} - 1 = 0.047 \left(\frac{\overline{H}_p f}{Re^2} \right)^{0.8} \tag{6}$$

$\overline{H}_p$ is the root mean square pressure rise along the heated section resulting from vibration in lb. force/ft^2.

Mechanically Vibrated Systems

Lemlich[40] studied the effect of transverse vibrations on natural convective heat transfer from electrically heated, horizontal wires to air, with wire diameters ranging from 0.0253 to 0.0810 in. The amplitude of vibration ranged from 0.028 to 0.116 in. The frequency varied from 39 to 122 cps and the temperature difference between the wire and the ambient air varied from 7° to 365°F. Up to a 400% increase in the coefficient of heat transfer was observed. Both the amplitude and the frequency of vibration has a positive effect on heat transfer rates. The effect of vibration was correlated in terms of a vibrational Reynolds number in which the velocity term was defined as twice the product of amplitude and frequency of the vibration. The following equation was used to correlate the data:

$$\frac{h_v}{h} = 0.75 + 0.0031 \frac{Re_v^{2.05} (\beta \Delta t)^{0.33}}{Gr^{0.41}} \tag{7}$$

where   h   -   heat transfer coefficient without vibration, BTU/hr ft °F

   h_v -   heat transfer coefficient with vibration, BTU/hr ft^2 °F

   β   -   thermal coefficient of volumetric expansion, °F^{-1}

   Δt   -   temperature difference, °F

Re_v - vibration Reynolds number, dimensionless

$$Re_v = \frac{Dv\rho}{\mu} \quad \text{where } \bar{v} = 2af$$

Gr - Grashof number, dimensionless.

Lemlich reported that the above equation correlated data for vertical vibration as well as for horizontal vibration. In order to account for his observations, the concept of a "stretched film" surrounding the entire path of vibration was proposed. An attempt was made to observe the "stretched film" by placing a lighted cigarette under the heated wire, but the results were inconclusive.

Fand and Kaye[47] studied the effects of vertical mechanical vibrations on natural convective heat transfer from a horizontal 7/8 in. cylinder to air. The frequency range varied from 54 to 225 cps with amplitudes of vibration up to 0.16 in. were used. The range of temperature difference was from 25° to 185°F. It was shown that the effect of vibration becomes appreciable only when the intensity of vibration defined as the product of amplitude and frequency of vibration exceeds a value of 0.3 ft/sec. The flow visualization study using smoke indicates a turbulent type of boundary later flow rather than the vortex type flow which was observed with horizontal vibrations.

Anantanaryanan and Ramachandran[48] investigated the effect of vibration on heat transfer from an electrically heated nichrome wire to parallel air streams. An increase as high as 130% was obtained. It was shown that both frequency and amplitude increased the heat transfer coefficients. The frequencies of vibration ranged from 75 to 120 cps and air flow rates from 34 to 64 ft/sec were used.

Natural and Forced Convection - Liquids

Acoustically Vibrated Systems

Robinson et al.[58] made an experimental study on the effects of ultrasonic vibrations at 400 kcps on heat transfer from water and transformer oil to a solid brass cylinder acting as a heat sink. Their results were shown by a plot of Δt, the temperature difference between the heated oil or water and the cylinder surface, versus the electrical power input to the transducer. A reduction of about 18% in Δt for the transformer oil was obtained when ultrasonic vibration was applied. For water, only a 4% reduction was reported. The sound pressure level involved in the case of water was much lower than that for the oil so that a meaningful comparison of the relative effects in the two liquids is not possible. Whether the increase in heat transfer is due to cavitation is not mentioned by the authors. Since only the electrical power inputs to the transducer are reported, it is impossible to tell if the cavitation threshold for the transformer oil or water had been reached.

Larson and London[57] studied the effects of ultrasonic vibrations on natural convective heat transfer from a 1 in. electrically heated copper sphere to water and toluene. The sphere was located at the center of a 3-inch diameter glass pipe cross with the transducer located at the lower opening. The frequency range varied from 20 to 1,000 kcps. As much as a four-fold increase in heat transfer coefficient could be obtained. At lower frequencies, it was concluded from shadowgraph studies that the increase was due to the ultrasonic

cavitation. The increases in heat transfer coefficient were correlated with the parameter $[(I/I_c)^{0.5}(C_A/C_S)^{1.5}]$ with some success (here I is the sound intensity at the transducer surface, I_c is the cavitation threshold intensity of the gas-saturated liquid, C_A is the actual gas content of the liquid, and C_S is the gas content of the gas-saturated liquid). For frequencies above 100 kcps, the increase was taken to be the result of quartz wind streaming. No attempt was made to correlate these data.

It should be emphasized that the sound intensity values used to correlate the heat transfer data are the intensities at the transducer and not the intensities at the sphere surface which are of prime interest. The sound intensity at the transducer was calculated from the electrical power input to the transducer and would be proportional to the sound intensity at the copper sphere surface. But the exact relationship between these two quantities depends on the geometry of the system, the fluid used, the nature of the sound field, etc. In general, it is impossible to convert one to another.

Larson and London also studied the forced convective heat transfer with the same equipment. It was found that for frequencies below 125 kcps, depending on the sound intensity at the transducer, up to 60% increase in the Nusselt number could be obtained when the flow Reynolds number was 400. The flow Reynolds number was defined as $(W/D\mu)$ where W is the mass flow rate of the liquid, D is the diameter of the sphere and μ is the viscosity. The increase became small as the flow Reynolds number was increased, and was negligible when the flow Reynolds

number was approximately 6,000. For frequencies above 400 kcps, no measurable increase was found for flow Reynolds numbers over 1,000.

Mechanically Vibrated Systems

One of the earliest studies on the effect of vibration on heat transfer to liquids was made by Martinelli and Boelter[54]. A 0.75 in. horizontal cylinder was vibrated in water at frequencies up to 40 cps and amplitude up to 0.1 in. The data were correlated by means of a dimensionless equation relating the Nusselt number with the Grashof number, Prandtl number, and a vibrational Reynolds number in which the velocity term was taken to be the root-mean-square velocity of the vibration of the cylinder. For vibrational Reynolds numbers below 1,000, there was no change in heat transfer. An improvement was observed with higher vibrational Reynolds numbers, and as much as 500% increase in heat transfer coefficient was obtained with Reynolds numbers of about 7,000. However, attempts to reproduce these data have been unsuccessful[40].

West and Taylor[55] studied the effect of pulsation on heat transfer in turbulent flow of water inside tubes. The pulsations were generated by a reciprocating pump. An increase of up to 70% in heat transfer coefficient was reported when a pulsation rate of 1.7 pulses/sec was applied to water flowing at Reynolds numbers of 30,000 to 85,000. No appreciable improvement was observed for other flow rates.

The effects of normal surface vibration on laminar forced convective heat transfer were studied by Scalan[56], who used a system where degassed water flowed by gravity through a chamber which contained the vibrating heat transfer surface. Frequencies up to 600 cps and

amplitudes of vibration up to 0.004 in. were used. A maximum increase
in heat transfer coefficient was observed when the frequency was in the
range of 50 to 80 cps. The increase, however, became almost negligible
at high frequencies when the amplitude of vibration was small. Accor-
ding to Scalan, the decreasing effect of vibration at higher frequencies
was due to cavitation. In the words of Scalan, "the resulting blanketing
effect (from cavitation) would be expected to counteract the increase
in coefficient caused by mixing. Below a certain combination of ampli-
tude and frequency, this blanketing effect will not occur. Above this
point, the blanketing will increase with increased amplitude and fre-
quency as that portion of a cycle during which the critical acceleration
is exceeded becomes larger." The critical frequency was observed to be
about 70 cps for the range of frequency and amplitude studied. If cavi-
tation is responsible, one would expect some variation in the critical
frequency as there was a fourfold increase in amplitude. Larson and
London[57] have proposed that the maximum in the heat transfer coeffi-
cient observed by Scalan at about 70 cps is probably due to the fact
that the resonant frequency of the system is also at about 70 cps. At
higher frequencies and amplitudes, the cavitation which could occur can
satisfactorily explain the increase in heat transfer rate reported by
Scalan.

Deaver, Penney and Jefferson[59] measured heat transfer
rates from an oscillating horizontal wire to water. A platinum wire of
0.007 in. diameter was vibrated mechanically in an otherwise still tank
of water in the frequency range of 0 to 4.25 cps and amplitudes up to

2.76 in. Temperature differences between the wire and the water varied from 0° to $140^{\circ}F$. For large-amplitude vibrations (~ 1 in), the data were correlated by an equation which is almost identical to the equation for heat transfer for flow of liquid normal to single bodies. The velocity term in the Reynolds number, however, is based on the mean velocity of the wire, which is taken as the total distance through which the wire moved per cycle divided by the period of the oscillation. The correlation is as follows:

$$\frac{Nu_v}{(Pr)^{0.3}} = 0.35 + 0.48 \ (Re_v)^{0.52} \tag{8}$$

It is unfortunate that Deaver et al. did not attempt to observe the boundary layer flow around the wire so that it could be compared with that for flow of liquid normal to a heated cylinder.

Raben[60] studied the effects of transverse vibration on forced convective heat transfer. The vibration was induced mechanically to a pipe of 1 in O.D. at frequencies from 32 to 84 cps with water flowing on the outside of the pipe in an annular space. The maximum amplitude of vibration was 0.150 in. The Reynolds number for the water flow ranged from 541 to 23,600. It was shown that increases in heat transfer coefficient varied from 450% at a Reynolds number of 540 to 11% at a Reynolds number of 16,000. For Reynolds numbers greater than 5,000 the data were correlated by the following equation:

$$(\frac{h_v}{h} - 1) = 0.115[\ Re_v/Re \ ]^{1.69} \tag{9}$$

The vibrational Reynolds number was defined to be the same as in Equation (7).

In the laminar region, no single correlation could be obtained.

Recently, Bergles[61] made an experimental study of forced convective heat transfer from an electrically heated stainless steel tube to water flowing inside the tube with vibration applied to degassed water at the downstream end by an electrodynamic vibrator. The frequency of vibration was 80 cps with amplitudes varying from 0.05 to 0.14 in. The velocity of water was 11 ft/sec. It was shown that there was a critical temperature difference between the water and the heating surface, below which the effect of vibration on heat transfer was negligible. As the amplitude of vibration was increased, the critical temperature difference was reduced. An increase of up to 100% was obtained in heat transfer rate. No correlation was proposed.

Boiling Heat Transfer

Acoustically Vibrated Systems

Isakoff[62] studied the effect of vibration at a frequency of 10 kcps on boiling heat transfer. An electrically heated platinum wire of 0.008 in. diameter was suspended horizontally in water at the saturation temperature. The transducer was located at the bottom of a tank measuring 6 in. x 10 in. x 3 in. deep. The sound intensity was estimated to be approximately 2 watts/cm^2 at the transducer surface. The sound pressure or intensity in the boiling water was not measured. It

was concluded that the use of a sound field could increase the burnout heat flux by about 60%. In the nucleate boiling region, at a given Δt, it was found that the effect of acoustic vibration on the heat transfer rate was negligible. Isakoff also observed that film boiling could be made to revert to nucleate boiling by applying the acoustic vibrations. No mechanism was proposed to account for the increase in the burnout heat flux.

A similar pool-boiling experiment at atmospheric pressure was performed by Ornatskii and Shcherbakov[63] who used distilled water and a nichrome wire heater with a diameter of 0.4 mm. The quartz transducer which was vibrating at the frequency of 1000 kcps was also located at the bottom of the glass vessel. It was stated that the intensity of the ultrasound in the water was approximately 1.5 to 2 watts/cm^2. But the method used to obtain these values was not given. Experiments were performed in water temperatures of 20°, 35°, 50°, 70° and 97^oC. It was shown that the value of burnout heat flux with ultrasonic vibrations increased with the increase of the subcooling of the liquid. For example, when the subcooling was 80^oC (water temperature = 20^oC), the increase in burnout heat flux was 80%. It dropped to 30% when the water was at the saturation temperature. The increase was attributed to an increase in the frequency of bubble generation from the wire as the result of ultrasonic vibrations.

Markels, Durfee and Richardson[65] studied the effects of acoustic vibrations on the burnout heat flux of saturated pool boiling of isopropanol. A horizontal, steam heated copper tube with

diameter of 3/8 in. and length of $3\frac{1}{4}$ in. was used as heater. Sound waves were generated by a barium titanate transducer located in the bottom of the tank. The sound pressure was measured by a second transducer placed near the heating surface. Frequencies were varied from 20 to 38,000 cps. It was found that acoustic energy did not affect significantly either the burnout heat flux or the critical temperature difference. No data were taken for nucleate boiling. For the range of frequency used, the effect of frequency was also negligible. It should be noted, however, that except for the case when the frequency was 38,000 cps, which was the resonant frequency of the transducer, the sound pressures measured by the second transducer located near the heating surface were very small. For example, the sound pressure was 7 psi when the frequency was 38,000 cps, but it varied between 2.5×10^{-3} psi and 400×10^{-3} psi for frequencies from 200 to 18,000 cps when the electrical power input to the transducer in each case was about the same. Thus, except when the transducer was operating at its resonant frequency, the acoustic power output from the transducer at any other frequency was so low that one would not expect it to have any effect on heat transfer.

A note of caution concerning the sound pressure data of Markels et al. must be introduced here. As mentioned above, a second transducer was placed near the heating surface to probe the sound pressure. The exact position of this transducer probe as well as its size were not given. Furthermore, there was no mention of the possible variation of sound pressure along the length of the copper tube. Although the dimensions of the tank were not given, it is expected that there

would be a standing wave pattern in the tank with a wide spatial variation of sound pressure. The sound pressure value used for correlating heat transfer data should be the time-space average at the heating surface. Values of sound pressure reported by Markels et al. apparently were those measured at a specific point near the heating surface. While these measurements are useful for comparing data obtained in their equipment, they do not represent the true sound pressure exerted on the entire heating surface.

Romie and Aronson[66] made an experimental investigation of the effects of ultrasonic vibrations on the burnout heat flux for forced convection, subcooled boiling. In their experiment, water flowed at atmospheric pressure through an annulus formed by a 1/4 in. diameter, electrically heated tube and a concentric glass tube of 3/4 in. I.D. The length of the heating element was $5\frac{1}{2}$ in. The ultrasonic transducer, which was operated at 25 kcps and an electrical power input of 300 watts, was located at the inlet end of the annulus. The ultrasonic waves were propagated in the same direction as the flow, and thus were parallel to the heating surface. The velocity of the water varied from 1.61 to 6.25 ft/sec and the degree of subcooling from 16° to 28°F. No measurement of acoustic power at the transducer surface or in the water was made. It was found that the effect of ultrasonic vibrations on burnout heat flux was negligible. Romie and Aronson also reported that at heat fluxes appreciably below the burnout level, the presence of an ultrasonic field did have some effect on the bubble activity surrounding the heating element, provided the flow velocities were low. The

average bubble size appeared to have been decreased and the frequency of bubble generation increased. They also reported that the number of nucleation points for bubble generation did not appear to be influenced by the ultrasonic field. However, it is not clear whether there was cavitation in the water close to the heating element. No quantitative result in this range of heat flux was presented. As the flow velocity increased, the effect of ultrasonic vibrations decreased.

Mechanically Vibrated Systems

Recently, an experimental investigation has been carried out by Nangia and Chon[64] to determine the effects of vibration of the heat transfer surface in saturated pool boiling of water at atmospheric pressure. Platinum wires of 0.01 in. diameter were heated electrically and vibrated electro-magnetically at frequencies between 35 and 115 cps and amplitudes from 0.030 to 0.178 cm. The heat flux with vibration was always higher than the flux from a stationary wire. At frequencies below 35 cps, the heat flux increased with frequency for a constant amplitude and temperature difference. Between 35-45 cps, the heat flux decreased with frequency while the expected increase with frequency was observed for frequencies above 45 cps. The above results were confirmed by varying the amplitude at a fixed frequency. Results from high speed motion pictures taken at 4800 frames/sec showed that the increase was due to a decrease in the average bubble size and an increase in the frequency of bubble generation. The bubble growth rate for a pulsating wire was also lower than that of a stationary wire. No satisfactory explanation was given for the reversing trends in the heat flux

for frequencies between 35 to 45 cps. A more detailed study is currently underway to determine the reason for such behaviour.

The effect of flow vibrations on forced convection, sub-cooling boiling was also studied by Bergles[61] with degassed water flowing in an electrically heated stainless steel tube. Vibrations were applied to the water at the downstream end by an electrodynamic vibrator at 80 cps with amplitudes of 0.08 in. The temperature of water was kept at 50°F and the flow velocities varied from 7 to 28 ft/sec. It was found that vibrations had no detectable effect on burnout heat flux as well as on the heat transfer rates in the region of fully developed surface boiling. However, at lower heat fluxes, increases up to 70% in heat transfer rate were obtained. As it was reported by Romie and Aronson[66], the improvement in heat transfer decreased as flow velocity increased. The pressure amplitude of the vibration which was probed by a diaphragm-type pressure transducer near the vibrator was 15 psi. It was attenuated to 2 psi at the upstream end. Bergles mentioned that he was doubtful there was cavitation in his system at such pressure amplitude levels.

IV. GENERAL COMMENTS

It can be seen that although considerable work has been done on the effects of vibrations on heat transfer, the published data are far from being conclusive as wide discrepancies can be found between them. This is usually due to the different experimental conditions and ranges of variables which have been used.

The effects of vibrations on heat transfer by convection and by boiling have been studied experimentally either by vibrating the fluid or by vibrating the heating surface. The two methods are directly comparable if the wavelength of sound is large relative to the characteristic dimension of the heating surface[44,51]. Another important experimental variable is the ratio of the amplitude of vibration to the characteristic dimension of the heating surface. For isothermal conditions, Raney et al.[39] have observed that the D-C boundary layer thickness is independent of (a/d), the ratio of the amplitude of vibration (a) to the diameter of the test cylinder (d), when (a/d) is about 0.25 or less. At higher values of (a/d), the D-C boundary layer thickness begins to shrink, and decreases to zero at sufficiently high amplitudes of vibration. As a result, the boundary layer flow pattern around a heated cylinder for small values of (a/d) is expected to be different from that for large values of (a/d) and hence the effects of vibrations on heat transfer. For values of (a/d) about 0.017 and less, Fand and Kaye[42,43] have observed the so-called "thermoacoustic streaming" which is characterized by the development of two vortices above the cylinder. Similar flow patterns were obtained by Fand and Peebles[44] with a value of

(a/d) of 0.16. Experiments involving large values of (a/d) have been performed by Lemlich[40] and Deaver et al.[59]. While Lemlich employed values of (a/d) up to 4, Deaver et al. used values of (a/d) almost up to 200. Using smoke, Lemlich observed a stretched film around the entire vibrating path of the heated wire. However, Lemlich mentioned that his observation was not conclusive. Deaver et al.did not attempt any observation of the boundary layer flow around the heated wire.

For systems where the heat transfer surface is vibrating, the measurement of the amplitude of vibration is usually accomplished by means of a calibrated microscope[40,56]. In cases where the heat transfer surface is stationary and the fluid vibrates, the measurement of the amplitude of vibration is also simple provided the fluid is a gas. It is usually measured by a microphone system and the results expressed as sound pressure level (SPL)[42,53]. It should be emphasized here that the effect of vibrations on the heat transfer rate depends very much on the location of the heat transfer surface in the sound field. Thus, Fand and Kaye[42] obtained a 300% increase in heat transfer coefficient when the heated cylinder was located on the plane of pressure antinodes of a stationary sound field. When the heated cylinder was positioned at the node of the same sound field, the resulting heat transfer coefficient had the same value as that for the analogous case without vibration. Kubanskii[50] also reported that he was able to either increase or decrease the convective heat transfer rate by moving the cylinder relative to the nodes of the stationary sound field. As a result, measurements of sound pressure must be made in the vicinity

of the heat transfer surface. It can be seen that the sound pressure data reported by Jackson et al.[52] were not the actual sound pressures exerted on the heat transfer surface as the sound level meter was located beside the loudspeaker at the entrance to the steam heated vertical tube.

For systems where the vibrating fluid is a liquid, depending on the intensity of the sound field, measurement of the sound pressure can be a problem. For sound pressures below the cavitation threshold of the liquid, they can be measured by a pressure sensitive microphone[67,68]. The specific requirements that must be achieved for probes of this type have been discussed[67,69,70]. For sound pressures near the cavitation threshold or above, the microphone cannot be used as it can easily be damaged by the cavitation action. Other methods for measuring the sound field include the calorimetric method where the rate at which the sound energy introduced into the liquid is degraded into heat is measured[69,71] and the radiation pressure float method where the radiation pressure is measured in terms of the buoyancy of a float[69,72,73]. The calorimetric method requires isolation of the system to avoid heat gain or loss from and to its environment. This is very difficult, if not impossible, to achieve in experiments involving heat transfer. The radiation pressure float method is applicable if small probes are used. However, these probes are also subjected to cavitation damage in a high intensity sound field. Because of these difficulties, most investigators[57,58,62] reported only the electrical power input to the transducer(s) or the acoustic power output from the transducer(s). It has been mentioned that standing waves are usually set up with a non-uniform distribution

of pressure and particle velocity in the sound field. This is further complicated by cavitation. The presence of the cavitation bubbles tends to scatter and dissipate a part of the sound energy. The knowledge of the acoustic power output from the transducer(s) does not reflect the conditions of sound pressure in the vessel. Furthermore, it has been pointed out that for the same acoustic power output, depending on the location of the heat transfer surface, the resulting vibration can cause an increase or decrease in the heat transfer rate. As a result, it is difficult to compare the experimental data of various investigators as they are strongly dependent on the geometry of the test. Larson[75] was one of the investigators who realized this limitation of his work and emphasized this point in the following manner:

"It is to be emphasized that this investigation is for a single geometry -- that of a 1 in. diameter sphere located at the center of a 3 in. diameter vertical circular tube 5 in. above the sound source, which is located at the lower end."

In all the works that have been reviewed, an empirical method is used to determine the governing parameters of these systems. The mathematical formulation of coupled sound vibration and convective heat transfer problems is very difficult and has not been attempted even in the simpler case where the fluid is a gas. For systems where a liquid is involved, the problem becomes more complicated because of the cavitation phenomena. For systems where the fluid is a gas, it is apparent that there exists a sound pressure level below which the effect of vibrations on heat transfer is negligible. An attempt, based on the

work of Raney et al[39], has been made by Westervelt[74] to determine
this critical value. Raney et al. have observed under isothermal con-
ditions that acoustical streaming patterns in the vicinity of a cylinder
deviate strikingly from theory when the ratio (a/δ_{AC}) is appreciably
greater than unity. (a = amplitude of vibration, δ_{AC} = A-C boundary
layer thickness). As (a/δ_{AC}) increases beyond the value 1, the thick-
ness of the streaming boundary layer increases slightly for a while and
suddenly, at a critical value of (a/δ_{AC}), the layer appears to collapse
entirely. At the collapsed stage, the regular streaming motion appears
to be replaced by a vigorous and chaotic motion. Westervelt[74] postu-
lated that the effect of sound waves is mainly a result of the alteration
of the streaming configuration. The condition (a/δ_{AC}) = 1 is taken as
a criterion for determining the critical sound pressure level (SPL$_{crit}$).
For air at atmospheric conditions, the criterion has been expressed as
follows:

$$SPL_{crit.} = 136 + 10 \log \left(\frac{f}{1000} \right) \text{ db} \qquad (11)$$

$$(\text{re } 0.0002 \text{ microbar})$$

where f = frequency of the sound wave in cps.

Values of critical SPL predicted by Equation (11) compare favourably
with those reported by Fand and Kaye[42] and Holman and Mott-Smith[46].

When the fluid is a liquid, the mathematical formulation
of the problem becomes more complicated because of the cavitation pheno-
menon. A study of the physical mechanism for such systems has been
made only by Larson and London[57]. They have shown that for frequencies
above 400 kc, the increase in convective heat transfer rates for water

is the result of the quartz wind streaming. At low frequencies, the controlling mechanism is the acoustic cavitation in water near the heat transfer surface. It is apparent that the cavitation threshold of the liquid can be used as a criterion in determining the effects of ultrasonic vibration on heat transfer in liquids. The threshold value, however, should correspond to the liquid at a temperature equal to that of the liquid near the heat transfer surface. It is unfortunate that experimental data of cavitation threshold for liquids near the saturation temperature are very scarce. A value of 1 atm is predicted by Blake[7] for water at its saturation temperature (Table I). The value from Galloway's equation[9] is 4.4 atm, if the threshold value of saturated water at $0^{\circ}C$ is taken to be 6.9 atm as measured by Connolly and Fox[18]. All equations listed in Table I are based on experimental data for the narrow temperature ranges listed. As pointed out by Blake[7], his empirical equation should not be used for temperatures above $50^{\circ}C$, the upper temperature limit of his experiment. One of the limitations of these equations is that the vapor pressure has not been taken into consideration.

The fact that quartz wind streaming is the controlling mechanism at high frequencies is also expected. The cavitation threshold of water has been found to increase rapidly for frequencies above 350 kcps[8]. Before acoustic cavitation can be induced, the streaming velocity as the result of the high intensity ultrasonic waves becomes appreciable and is an important contributor in increasing the heat transfer.

Based on the published data on the effects of ultrasonic

vibrations on boiling heat transfer, the following conclusions can be drawn. First of all, the results on burnout heat flux are rather inconsistent. While Isakoff[62] and Ornatskii et al.[63] reported an increase of 60% and 30% respectively, Markels et al.[65], as well as Romie and Aronson[66], have shown that the effect of ultrasonic vibration on burnout heat flux is negligible. Secondly, the amount of data on nucleate boiling is very limited. Several investigators, however, have discussed the possible effects of ultrasonic vibrations on nucleate boiling. Isakoff suggested that cavitation and microagitation induced by ultrasonic vibrations might accelerate the formation and evolution of vapor bubbles from the heating surface. In other words, there would be an increase in the number of active nuclei on the heating surface for vapor bubbles and in the frequency of bubble generation. Romie and Aronson as well as Ornatskii and Shcherbakov have mentioned that the effect of an ultrasonic field is a reduction in mean bubble size and an increase in frequency of bubble formation. However, these proposed mechanisms cannot be taken as conclusive as they are based on visual observations.

NOMENCLATURE

ROMAN SYMBOLS

a	amplitude of vibration
C	gas content of liquid
C_p	specific heat at constant pressure
D	diameter
$\mathcal{D}$	diffusivity
f	frequency of vibration
h	heat transfer coefficient
$\overline{H}_p$	root mean square pressure rise
I	sound intensity
k	thermal conductivity
L	length of tube
ℓ	half wavelength of sound
P_o	ambient pressure in liquid
P_p	peak acoustic pressure
P_{CV}	cavitation threshold pressure
P_z	P_c evaluated at $0^{o}C$ and atmospheric pressure
R_o	mean bubble radius
SPL	sound pressure level
T	temperature
v	velocity
W	mass flow rate

GREEK SYMBOLS

β	thermal coefficient of volumetric expansion
Δt	temperature difference
δ_{A-C}	A-C boundary layer thickness, $\quad_{A-C} = (\frac{v}{\omega})^{1/2}$
δ_{D-C}	D-C boundary layer thickness
μ	viscosity
ν	kinematic viscosity
ρ	density
σ	surface tension
ω	angular frequency

DIMENSIONLESS GROUPS

Gr	Grashof number, $g\beta \rho^2 D^3 \Delta t / \mu^2$
Gz	Graetz number, WC_p/kL
Nu	Nusselt number, hD/k
Pr	Prandtl number, $\mu C_p/k$
Re	Reynolds number, $Dv\rho/\mu$

SUBSCRIPTS

A	actual
ℓ	liquid
s	saturation condition
v	with vibration
w	based on wall temperature.

REFERENCES

1. Nukiyama, S. J.Soc.Mech.Engrs. (Japan), 37, No. 206, 367 (1934).

2. Gaertner, R.F. General Electric Research Laboratory, Rept. No. 63-RL-3357C. June, 1963.

3. Westwater, J.W. and Kirby, D.B. Paper presented at the 16th National Heat Transfer Conference, Boston, Aug. 1963, AIChE Preprint No. 14.

4. Moisis, R. and P.J. Berenson. J.Heat Transfer, Trans.Am.Soc. Mech. Engrs., 85, 222 (1963).

5. Westwater, J.W. and J.G. Santangelo. Ind.Eng.Chem., 47, 1005 (1955).

6. Frenkel, J. "Kinetic Theory of Liquids" Oxford, The Clarendon Press (1964).

7. Blake, F.G. Jr. Tech.Memo. No. 12, Acoustic Research Lab., Harvard U., September (1949).

8. Barger, J.E. Tech.Memo. No. 57, Acoustic Research Lab. Harvard U., April (1964).

9. Galloway, W.J. J.Acoust.Soc.Am., 26, 849 (1954).

10. Willard, G.W. J.Acoust.Soc.Am., 25, 669 (1953).

11. Rosenberg, R.D. Tech.Memo. No. 26, Acoustic Research Lab., Harvard U. (1953).

12. Hsieh, D.Y. and M.S. Plesset. J.Acoust.Soc.Am., 33, 206 (1961).

13. Pode, L. Rept. No. 854, David W. Taylor Model Basin, Washington, D.C., May (1953).

14. Strasberg, M. J.Acoust.Soc.Am., $\underline{33}$, 359 (1961).

15. Noltingk, B.E. and E.A. Neppiras. Proc.Phys.Soc. (London) B$\underline{63}$, 674 (1950).

16. ibid. B$\underline{64}$, 1032 (1951).

17. Flynn, H.G. "Physics of Acoustic Cavitation in Liquids". Physical Acoustics, Vol. 1B. Academic Press. W.P. Mason,ed. 1964.

18. Connolly, W. and F.E. Fox. J. Acoust.Soc.Am., $\underline{26}$, 843 (1954).

19. Briggs, H.B., J.B. Johnson and W.P. Mason. J.Acoust.Soc.Am., $\underline{19}$, 664 (1947).

20. Esche, R. Akust.Beihefte $\underline{4}$, 208 (1952).

21. Heuter, T.F. and R.H. Bolt. "Sonics" John Wiley, New York, p.230 (1955).

22. Plesset, M.S. and A.T. Ellis, Trans.Am.Soc.Mech.Engrs. $\underline{77}$, 1055 (1955).

23. Sutton, G.W. J.Appl.Mech., $\underline{24}$, 340 (1957).

24. Jones, I.R. and D.H. Edwards. J.Fluid Mech., $\underline{7}$, 596 (1960).

25. Kornfeld, M. and L. Suvorov. J.Appl.Phys. $\underline{15}$, 495 (1944).

26. Eisenberg, P. Rept. 712, David W. Taylor Model Basin, Washington, D.C. (1950).

27. Naudé, C.F. and A.T. Ellis. Trans.Am.Soc.Mech.Engrs. D$\underline{83}$, 648 (1961).

28. Bebchuk, A.S. Soviet Phys. - Acoustics, $\underline{3}$, 95 (1957).

29. ibid. $\underline{3}$, 395 (1957).

30. Devine, R.E. and M.S. Plesset. Rept. No. 85-27. Div.Eng. and App.Sci., California Inst. of Tech., Pasadena, April (1964).

31. Rosenberg, L.D. and A.S. Bebchuk. Soviet Physics - Acoustics, $\underline{6}$, 496 (1961).

32. Antony, O.A. Ultrasonics, $\underline{1}$, 194 (1963).

33. Bebchuk, A.S., In.Ia. Borisov and L.D. Rosenberg, Soviet Physics - Acoustics, $\underline{4}$, 372 (1958).

34. Crawford, A.E. Ultrasonics, $\underline{2}$, 120 (1964).

35. Eckert, C. Phys.Rev., $\underline{73}$ 68 (1948).

36. Andrade, E.N. Proc.Roy.Soc. (London) A$\underline{134}$, 445 (1931).

37. Schlichting, H. Physik Z., $\underline{33}$, 327 (1932).

38. Holtsmark, J., I. Johnson, T. Sikkeland and S. Skavlem, J.Acoust. Soc.Am., $\underline{26}$, 26 (1954).

39. Raney, W.P., J.C. Corelli, P.J. Westervelt. J.Acoust.Soc.Am., $\underline{26}$, 1006 (1954).

40. Lemlich, R. Ind.Eng.Chem. $\underline{47}$, 1175 (1955).

41. Kubanskii, P.N. Trans.USSR Academy of Science, $\underline{82}$, 585 (1952).

42. Fand, R.M. and J. Kaye. J.Heat Transfer, Trans. ASME, $\underline{83}$, 133 (1961).

43. Fand, R.M. and J. Kaye. J.Acoust.Soc.Am., $\underline{32}$, 579 (1960).

44. Fand, R.M. and E.M. Peebles. J.Heat Transfer. Trans. ASME, $\underline{84}$, 268 (1962).

45. Fand, R.M., J. Roos, P. Cheng and J.Kaye. J.Heat Transfer, Trans. ASME, $\underline{84}$, 245 (1962).

46. Holman, J.P. and T.P. Mott-Smith, J.Aero/Space Science, $\underline{26}$, 188 (1959).

47. Fand, R.M. and J. Kaye. International Developments in Heat Transfer. Part I. 490-498 (1961).

48. Anantanaryanan, R. and A. Ramachandran, Trans.ASME, 80, 1426 (1958).

49. Lemlich, R. and Hwu, C.K. Am.I.Ch.E.J. 7, 102 (1961).

50. Kubanskii, P.N. J.Tech.Phys. USSR, 22, 593 (1952).

51. Fand, R.M. and P. Cheng. Int.J.Heat Mass Transfer, 6, 571 (1963).

52. Jackson, T.W., W.B. Harrison and W.C. Boteler. J.Heat Transfer, Trans. ASME, 81, 68 (1959).

53. Mathewson, W.F. and J.C. Smith. Chem.Eng.Prog.Sym.Series, 59, No. 41, 173 (1963).

54. Martinelli, R.C. and L.M.K. Boelter. Proc.5th Int.Congr. of Applied Mechanics, 578 (1938).

55. West , F. and A. Taylor. Chem.Eng.Progr. 48, 39 (1952).

56. Scalan, J.A. Ind.Eng.Chem., 50, 1565 (1958).

57. Larson, M.B. and A.L. London. ASME. Paper 62-HT-44 (1962).

58. Robinson, G.C., C.M. McClure, and R. Hendricks. Bull.Am. Ceramic Soc., 37, 399 (1958).

59. Deaver, F.K., W.R. Penney and T.B. Jefferson. J.Heat Transfer, Trans. ASME, 84, 251 (1962).

60. Raben, I. Proc.Heat Transfer and Fluid Mech.Institute, Stanford University, p. 90 (1961).

61. Bergles, A.E. J.Heat Transfer, Trans. ASME, 86, 559 (1964).

62. Isakoff, S.E. Proc.Heat Transfer and Fluid Mech. Institute, Stanford University, p.15 (1956).

63. Ornatskii, A.P. and V.K. Shcherbakov, Teploenergetika, 6, 84 (1959). Translation appears in (65).

64. Nangia,K.K. and W.Y. Chon. Paper presented at the 15th Canadian
    Chemical Engineering Conference, Quebec City, October,
    1965,

65. Markels, M., R.L. Durfee and R. Richardson. United States Atomic
    Energy Commission, NYO 9500, September, 1960.

66. Romie, F.E. and C.A. Aronson. Advanced Technology Laboratories,
    Report ATL-A-123, July, 1961.

67. Goldman, R. "Ultrasonic Technology", Reinhold, p. 278-280 (1962)

68. Heuter, T.F. and R.H. Bolt. "Sonics". John Wiley, p. 146-152
    (1955).

69. Henry, G.E.   IRE Trans. PGUE 6, 17 (1957).

70. Massa, F.   J.Acoust.Soc.Am., 17, 29 (1945).

71. Goldman, R. "Ultrasonic Technology". Reinhold, p. 277-278 (1962).

72. ibid, p. 276-277 (1962).

73. Fox, F.E. and V. Griffing, J.Acoust.Soc.Am., 20, 352 (1948).

74. Westervelt, P.J.   J.Acoust.Soc.Am., 32, 337 (1960).

75. Larson, M.B.   Tech.Rept. No. 48, Dept. of Mechanical Engineering,
    Stanford University, California, September 30, 1960.

PRESENT INVESTIGATION

INTRODUCTION

This investigation was concerned with the effects of
ultrasonic vibrations on heat transfer to distilled water and methanol
by natural convection and by surface boiling, specifically, a study on
the important variables and the possible mechanisms of these processes.
In addition, a technique to measure a high intensity sound field in a
cavitating liquid was to be developed.

In Part I of this study, a method using cavitation damage
to measure the cavitation activity of a liquid under strong ultrasonic
vibrations was developed.

In Part II, the natural convective heat transfer and sur-
face boiling heat transfer rates from a platinum wire to distilled
water and methanol at three different acoustic intensity levels were
measured. Other variables including the degree of subcooling and fre-
quency were also studied. High speed photography was used to study the
mechanisms of these processes.

In Part III, the effects of ultrasonic vibrations on burn-
out heat flux and critical temperature difference were studied.

PART I

MEASUREMENT OF SOUND FIELD IN LIQUIDS

INTRODUCTION

The method used to measure a liquid sound field depends
on the type of data required. In general, the experimental quantities
that are of interest are sound pressure, sound intensity, and the rate
at which acoustic energy is delivered from the ultrasonic transducer to
the liquid load. These quantities are inter-related where there is a
free sound field. However, the usual laboratory set-up is one in which
a great deal of interference exists, giving rise to various irregular
standing wave patterns. At sound pressures above the cavitation threshold,
the presence of cavitation bubbles further complicates the picture as
they scatter and dissipate a part of the acoustic energy. Consequently,
most investigators reported the acoustic power output from the trans-
ducer. In studying the effects of ultrasonic vibrations on processes
such as heat transfer, it is expected that the boundary layer flow pat-
tern around the heated surface would be changed. The resulting data
could then be correlated with local acoustic variables on the heated
surface. Such information is not available from a knowledge of the
acoustic power output of the transducer.

The difficulty in obtaining local acoustic variables in
a high intensity liquid sound field is primarily due to the erosive
nature of the cavitation phenomena which tends to damage the probes
normally used in non-cavitating liquids. It becomes more practical to

attempt to measure the cavitation activity in the liquid since direct measurement of acoustic variables, such as sound pressure and sound intensity, becomes rather difficult.

Acoustic cavitation bubble fields may be characterized either by the motions of the cavitation bubbles or by the physical effects that such motions bring about. Cavitation damage is one of the phenomena resulting from these effects. It has been mentioned in the Literature Review section of this thesis that the damage on metal surfaces in a cavitating liquid increased as the square of the sound pressure[1]. Further studies by Bebchuk[2] and other investigators[3,4] have shown that the weight loss, or cavitation damage, is a linear function of the time of exposure in a cavitation bubble field. Since cavitation damage has been interpreted as a mechanical process, it seems logical to use the rate of cavitation damage for measuring the cavitation activity of a liquid under strong ultrasonic vibrations.

The objective of the present study was to provide information on the sound field in which heat was being transferred. Measurement of the cavitation activity was directed toward the liquid around the heated surface which was a platinum wire about 1 in. long with diameter of 0.007 and 0.010 in. When the applied acoustic energy was below the cavitation threshold level, the sound pressure on the platinum wire was measured by a probe microphone.

EXPERIMENTAL

Equipment

An overall schematic diagram of the equipment including that for studying heat transfer rates in a sound field is shown in Figure 1. Figure 2 is a photograph of the apparatus. Two ferrite transducers with a resonant frequency of about 20 kcps were cemented directly onto the bottom of an open stainless steel tank ($7\frac{1}{2}$ in. x $4\frac{1}{2}$ in. x 6 in. deep). A glass window was installed on the front of the tank and there was a jacket surrounding the remaining three sides. Three 250-watt strip heaters were placed in the jacket, one in each side, to control the temperature of the liquid in the tank through a powerstat. The remaining space of the jacket was filled with an asbestos slab.

The transducers were driven by a sine-wave form signal generator, whose output was amplified by a custom-built power amplifier. The amplifier had a frequency range of 15 to 500 kcps with a power output rating of 200 watts.

Two types of transducer were used in this study. For the low frequency work, namely for 20 kcps and 44 kcps, magnetostrictive transducers made of ferroxcube 7A2 manufactured by Philips were used. For the higher frequencies, 108 kcps and 306 kcps, ceramic transducers made of lead zirconate and manufactured by Gulton Industries were used. Other information concerning transducers such as the number of transducer used, the cementing procedures, the impedance matching, etc. is given in Appendix A.

FIGURE 1

SCHEMATIC DIAGRAM OF APPARATUS

PRECISION
RESISTOR

DC POWER
SUPPLY

PRECISION
POTENTIOMETER

A

POTENTIAL
TAPS

ULTRASONIC
PROBE

TRAVERSING
MECHANISM

INSULATOR

ELECTRIC
STRIP HEATER

TEST
SECTION

TRUE RMS
VOLTMETER

FERRITE
TRANSDUCERS

CAPACITOR

SIGNAL
GENERATOR

POWER
AMPLIFIER

VTVM
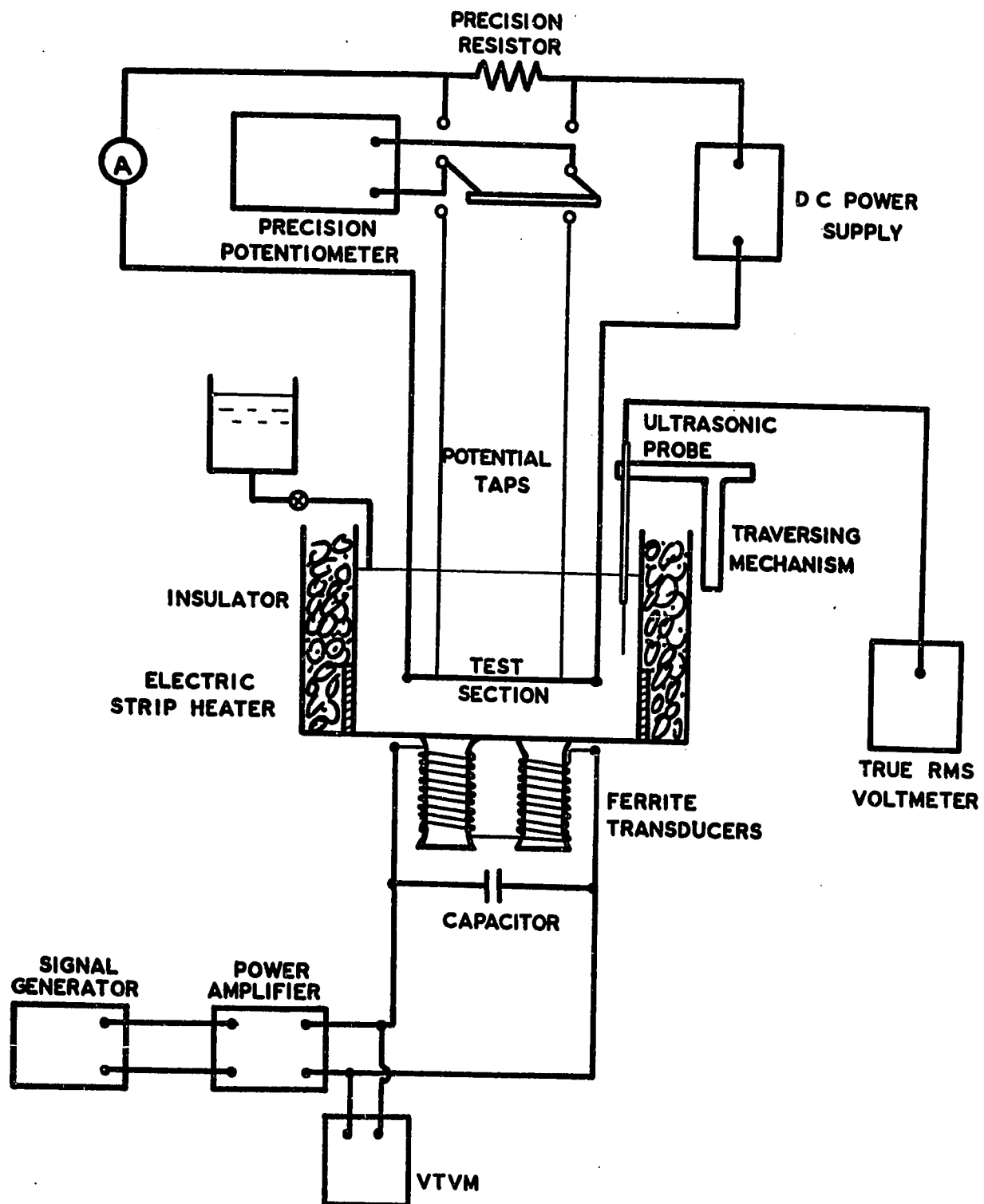
FIGURE 2

PHOTOGRAPH OF THE EXPERIMENTAL APPARATUS
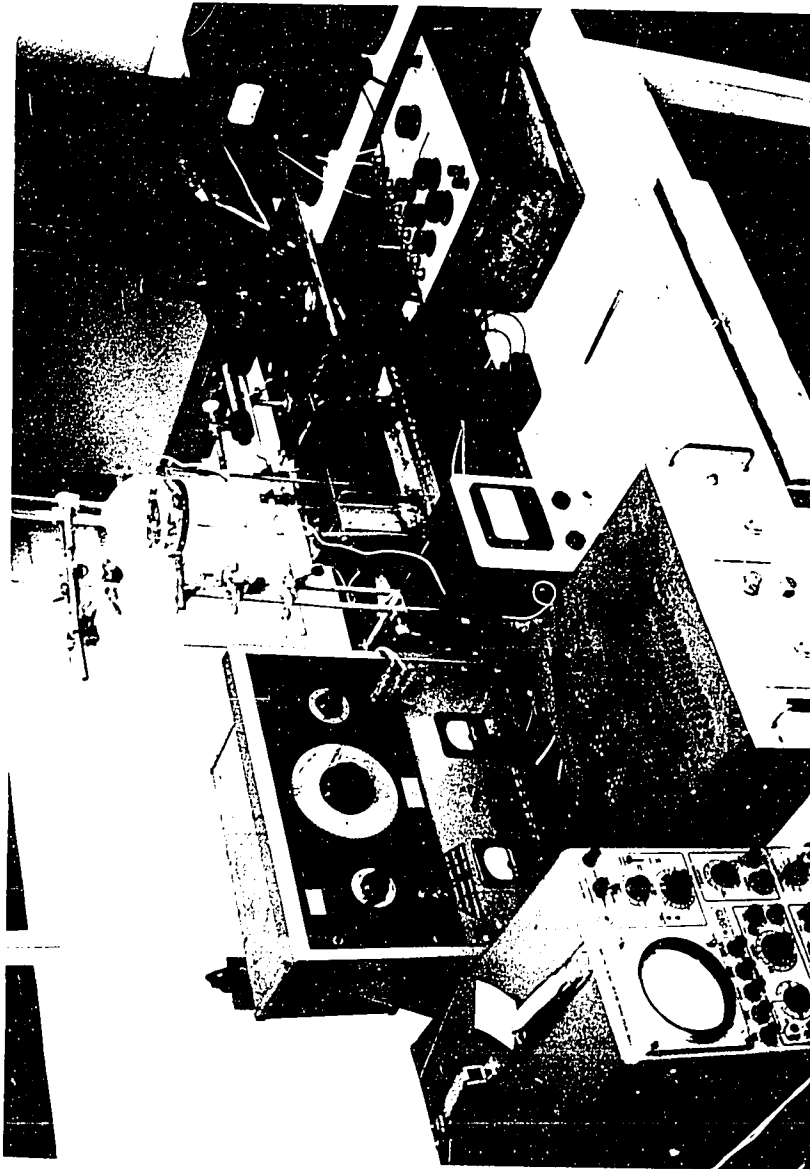
The voltage drop across the transducers was measured by a Hewlett-Packard vacuum-tube voltmeter model 400D. A standard resistor (Type 1682), having a resistance of 0.02 ohm and manufactured by Guild-line Instruments Ltd., was connected in series with the transducers to measure the current. The purpose was to obtain the apparent power (W_A), which is the product of the effective values of voltage and current[5]. No attempt was made to determine the power factor of the circuit.

The cavitation damage specimen was an 18 gauge (D = 0.0403 in.)copper wire, $1\frac{1}{2}$ in. long, and coated with a radioactive soil. It was clamped at each end in a groove between brass blocks, as shown in Figure 3 (the two small brass blocks and the electrical wires in the background of the photograph were for heat transfer experiments). The frame was fastened to a support so that the specimen was $1\frac{1}{2}$ in. from the bottom and midway from the sides of the tank.

The radioactivity of the specimen was measured by a well-type gamma ray scintillation detector (model 810B) manufactured by Baird Atomic Company. A scalar-timer (model 135) manufactured by the same company was used to register the measurement from the scintillation detector. Since the well of the detector is $1\frac{35}{64}$ in. deep and the length of the specimen is $1\frac{1}{2}$ in., the entire specimen could be introduced into the well.

When the applied acoustic energy was below the cavitation threshold level, the sound pressure along the specimen was measured by a Glennite ultrasonic probe (model UP-800C), manufactured by Gulton Industried Ltd. The sensitive element of the probe is a barium titanate

FIGURE 3

SUPPORTING FRAME FOR CAVITATION DAMAGE

SPECIMEN AND PLATINUM WIRE
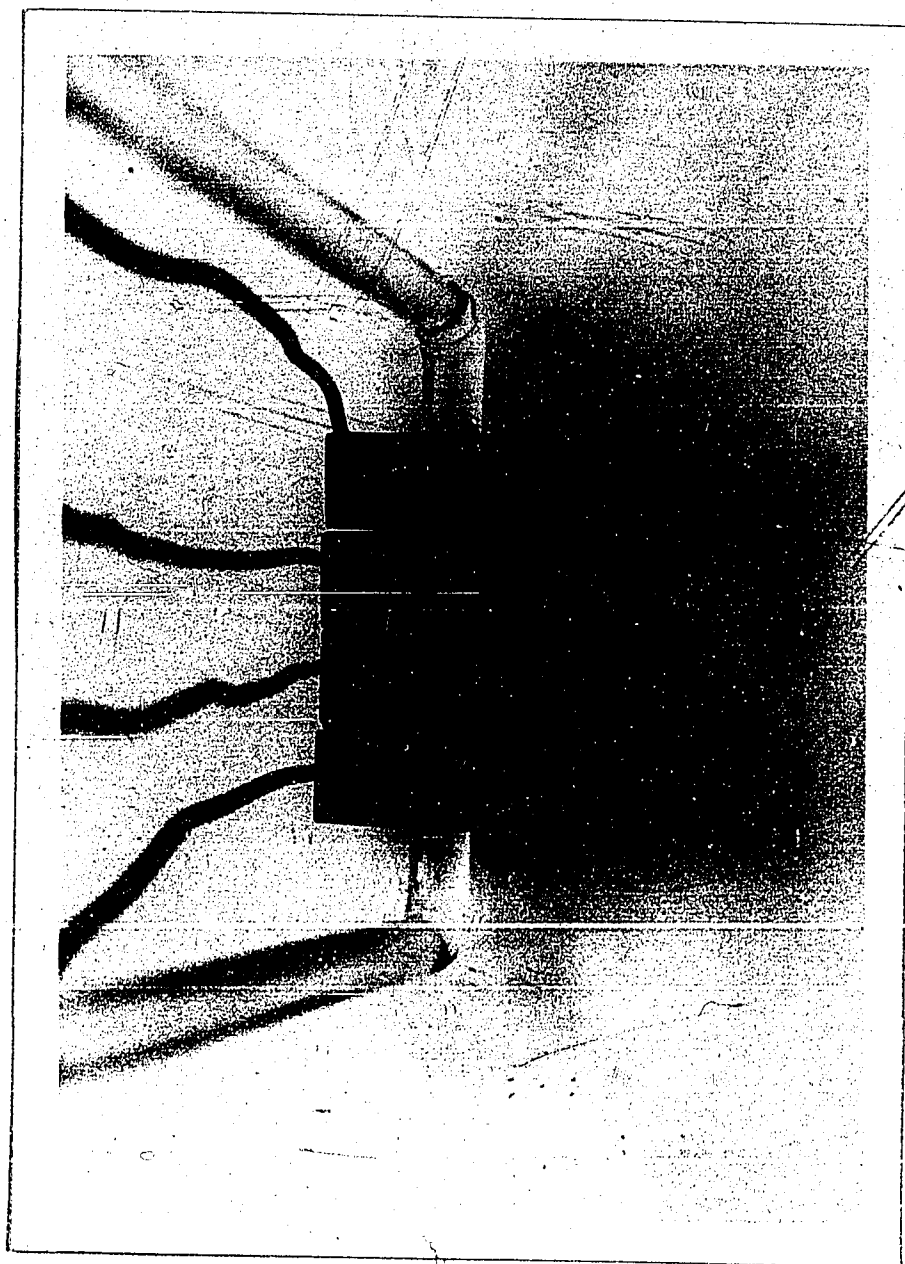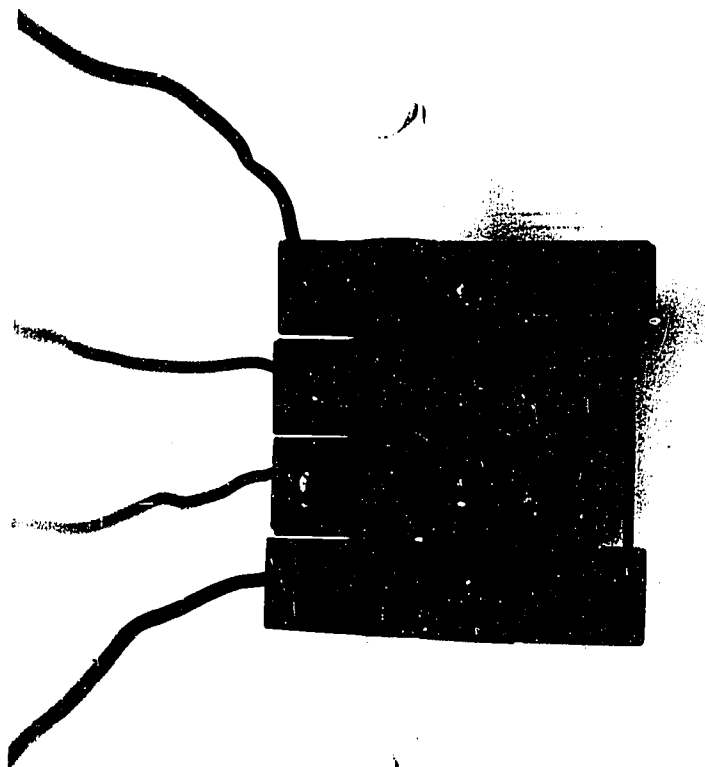
ceramic cylinder 1/16 in. in diameter by 1/16 in. long. The calibration, made at five points between 100 kcps and 1000 kcps, was supplied by the manufacturer. Below 100 kcps, the frequency response curve was assumed to be flat. The probe which was connected to a Brüel and Kjaer vacuum tube voltmeter (type 2409) was mounted in a traversing device capable of giving an accuracy of 1/1000 in. When the frequency of the system was 306 kcps, the Hewlett-Packard voltmeter described earlier was used.

Materials

Cobalt-60 was the tracer material and approximately 10 g. of cobalt oxide was shipped to the Atomic Energy of Canada Ltd. for irradiation. The total activity after irradiation was given as approximately 100 microcurie.

The binder materials for the soil were Esso MP grease H and carbon black.

Distilled water and methanol were used in this study. The absolute methanol was supplied by Anachemia Chemical Ltd.

Preparation of Specimen

After a number of trials, the following procedures were established.

1. Into a Kimax test tube with plastic cap (length x O.D. = 125 x 16 mm), 0.45 g. of carbon black, 4 g. of radioactive cobalt oxide and 2 g. of Esso MP grease H were introduced. Ten ml. of benzene was then added into the test tube.

2. The test tube was capped and placed into a 1 in. pipe jacket, whose purpose was to protect the test tube from breaking and act as a radiation shield. The jacket was picked up by a clamp and it was then shaken vigorously until a smooth mixture was obtained. It was found that a more homogeneous mixture could be obtained if the test tube was exposed to a cavitating liquid for a few minutes to disperse the carbon black.

3. Tinned copper wire, gauge 18, from Birnback Radio Co. was cut into lengths of approximately $6\frac{1}{2}$ in. They were thoroughly cleaned by successively dipping them into test tubes containing dilute HCl, distilled water, acetone and benzene.

4. The clean wire was dipped into the test tube containing the mixture three times. The second and third dippings were made only after fanning the wire in the air for approximately 30 seconds after each dipping so that the benzene would be evaporated. For all dippings, care was taken not to have the wire touch any part of the test tube when it was introduced into the test tube or taken out from it. The mixture was shaken again to ensure its homogeneity after 4 to 6 lengths of wire were prepared.

5. The wire was then clamped horizontally from the portion of the wire that was bare in an oven of 120°F for 20 hr. The length of wire covered with soil was about 4 in., out of which $1\frac{1}{2}$ in. was cut out to make a specimen. Since the specimen would be subsequently clamped at each end in a groove between the two blocks, a protective coating of 1/4 in. in length was put on both ends of the specimen. This procedure is described in 6).

6. Specimens to be used in distilled water were dipped 3 times into a mixture consisting of 3 parts by volume of Ambroid liquid cement to 2 parts of acetone. For specimens to be used in methanol, Armstrong epoxy A12T was used directly.

These coatings were found to be sufficiently strong to resist the stresses due to the brass blocks as well as the damaging action of a cavitating liquid for a short period of time. It was found that the counting rate of a completely damaged specimen, that is, a specimen on which the unprotected portion of the soil was completely eroded away by the cavitation action, was, within experimental error, one third of the original counting rate. The active length of each specimen was then 1 in.

7. The specimen stored in a small polyethylene bag was placed in the well of the scintillation detector to measure its radioactivity. All specimens whose radioactivity did not fall in the range of 35,000 - 50,000 counts per minute were rejected as it was found in preliminary studies that the sensitivity of the test depended very much on the soil thickness.

8. It was found that the results were more reproducible if new specimens were prepared fresh for each test sequence. During the course of the experiment which lasted for 3 months, two batches of soil were made. The soil did not appear to become aged. All specimen preparation work was done in a Fisher isolator. The specimen was handled only with tweezers after it was cut to the length of $1\frac{1}{2}$ in. Figure 4 shows a specimen with the polyethylene bag used to store it.

FIGURE 4

CAVITATION DAMAGE SPECIMEN WITH POLYETHYLENE BAG

Procedure

In all experiments, the tank was filled with distilled water or methanol to a depth of $4\frac{3}{4}$ in. and maintained at this level. The temperature of the liquid was controlled by the powerstat and the three strip heaters. The liquid temperature was always brought up slowly so that the dissolved air content in the test liquid would be at its equilibrium value. The cavitation damage determination was started 1 hr after the liquid attained the desired temperature. No measurements were made of the air content of the liquid at the various test temperatures.

The specimen was clamped in place in the brass block with its active portion properly exposed. The specimen assembly was installed into its place. The ultrasonic probe mounted on the traversing mechanism was used to measure the sound pressure along the specimen at intervals of 0.20 in. at different apparent electrical power input levels until cavitation was observed to be occurring near the probe. The probe was then withdrawn, and the cavitation damage for a finite time interval was measured after the specimen was replaced by a new one.

The time for which a specimen was exposed to the cavitating liquid depended on the electrical power input. The possible error of the final result, that is, the percentage of soil removed, would be very much reduced if the exposed time was selected to give a value of soil removed of 20 to 30% for a specific electrical power input. For reasons which will become obvious later, the exposure time should be kept below a value which would yield a soil removal value of more than 35%.

Before using the scintillation detector for radioactivity measurements, the scintillation plateau region of the detector was first determined using a standard source of cobalt-60 supplied by Baird Atomic Company. The plateau curve is shown in Appendix C. The voltage of the scaler-timer was then set at the voltage corresponding to the plateau region which was 1,400 volts and the background was measured before and after each test. The counting time for all specimens as well as the background was 6 minutes.

The test liquids were distilled water and methanol. When the frequency was 20.6 kcps, the temperatures of distilled water at which measurements were made were 113°F, 149°F, and 180°F. For methanol, they were 95°F and 113°F. Other frequencies at which measurements were made were 44.1, 108, and 306 kcps. The temperature of distilled water was 149°F and that of methanol was 113°F for these frequencies. Little difficulty was encountered in maintaining the temperature at the desired level to within $\pm$ 1°F.

RESULTS

When the applied acoustic energy levels are below the cavitation level, the root-mean-square values of sound pressure along the specimen were measured by the ultrasonic probe. Figure 5 shows some typical sound pressure profiles. The distance between two sound pressure readings was chosen to be 0.02 in. A smaller interval was not used because subsequent heat transfer experiments showed that the motion of the cavitation bubbles on the platinum wire did not appear to be

FIGURE 5

SOME TYPICAL SOUND PRESSURE PROFILES ON THE

CAVITATION DAMAGE SPECIMEN

LIQUID		$T_L, °F$	W_A, WATTS
▲	WATER	113	7.0
△	WATER	149	4.8
●	METHANOL	95	2.0
○	METHANOL	113	1.0
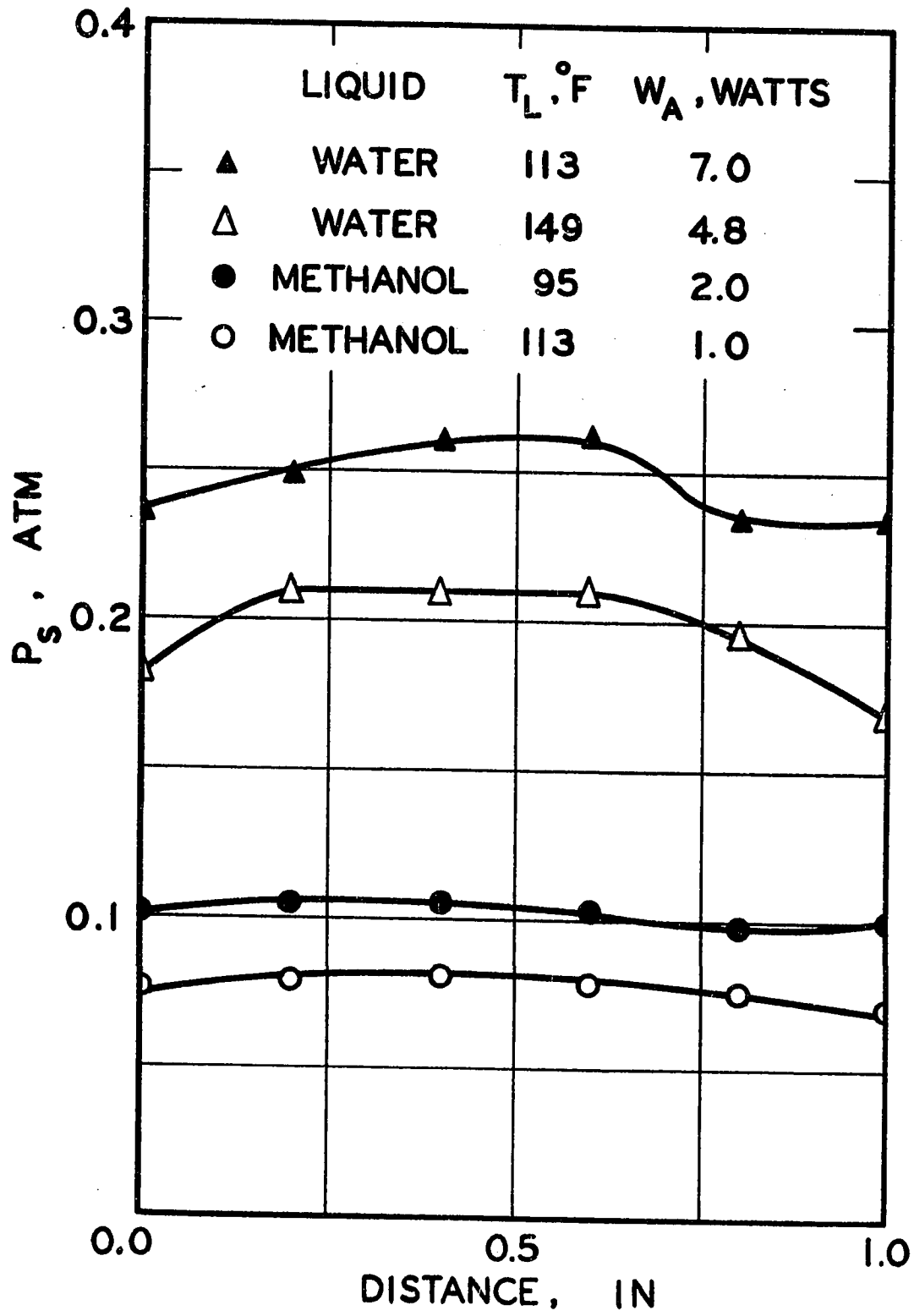
dependent on the sound pressure profile.

The effective value of sound pressure for the active portion of the specimen was calculated by taking the square root of the average of the squares of the individual sound pressure values along the specimen. The calculated results of sound pressure values for experiments at different frequencies are shown in Tables 1, 2, 3 and 4. The value of P_s which is underlined indicates the sound pressure at which cavitation began to occur in the test liquid. Where there are two values underlined, cavitation occurred somewhere between the two values. The criterion used to determine this value was that when the first cavitation bubble was observed to appear anywhere in the test liquid. In Tables B-1 to B-10 in Appendix B where experimental data on sound pressure are shown, the corresponding peak sound pressures are also included. The peak values were measured directly by the Brüel and Kjaer voltmeter and each value represents the maximum peak sound pressure that was recorded on the active portion of the specimen. They should not be taken as the cavitation threshold of the test liquid, as the occurrence of the first cavitation bubble was usually not on or near the specimen surface. In these tables, each value of the voltage signal (E_s) picked up by the ultrasonic probe was the average of three or four readings. The reproducibility was always within 15%.

In measuring the sound pressure, it was assumed that the variation in the radial direction of the specimen was small. The assumption was justified since the sensitive element of the probe was a 1/16 in. by 1/16 in. cylinder, while the diameter of the specimen was approximately

TABLE 1

Effective Value of Sound Pressure on the Specimen

$f = 20.6$ kcps

W_A watts	P_s (atm)			
	Water		Methanol	
	$T_L = 149°F$	$T_L = 113°F$	$T_L = 113°F$	$T_L = 95°F$
1.0	.092	.085	.076	.072
2.0	.16	.14	.11	.10
4.8	.20	.18	.14	.12
7.0	.27	.25	.16	.14
15.6	.34	.34	-	-

TABLE 2

$f = 44.1$ kcps

W_A watts	P_s (atm)	
	Water	Methanol
	$T_L = 149°F$	$T_L = 113°F$
0.5	.13	.090
1.3	.16	.13
3.2	.16	.15
4.6	.19	.17
9.5	.26	.23
23.2	.36	-

TABLE 3

f = 108 kcps

W_A watts	P_s (atm) Water $T_L = 149^\circ F$	P_s (atm) Methanol $T_L = 113^\circ F$
16.0	.35	.34
24.0	.45	.42
34.2	.53	.48
47.0	.63	. -
10.0	-	.25

TABLE 4

f = 306 kcps

W_A watts	P_s (atm) Methanol $T_L = 113^\circ F$
22	-
54	.57
74	.71
92	.83
125	.92
165	. -

0.04 in. In fact, most of the sound pressure measurements were made along the platinum wire whose diameter was even smaller.

The results of experiments on cavitation damage are shown in Figures 6 to 11. The percentage of soil removed (S_R) was based on the amount of soil on the active portion of the specimen before it was exposed to a cavitating liquid. Consequently, the percentage of soil removed was calculated by the following expression:

$$S_R = \frac{CPM_i - CPM_f}{\frac{2}{3}(CPM_i)} \times 100\% \tag{1}$$

where CPM_i - counting rate of the specimen per minute before cavitation damage

CPM_f - counting rate of the specimen per minute after cavitation damage.

It is to be noted that the active portion of the specimen was equal to two-thirds of the total length.

Figure 6 shows the percentage of soil removed for distilled water at 149°F and at various exposure times with apparent electrical power input to the transducers as parameter. Bebchuk[2] and other investigators[3,4] who studied cavitation damage on metal surfaces have shown that the cavitation damage is a linear function of time. The non-linearity of the results of present work was due to the finite thickness of the soil on the tinned copper wire. It was observed that when the percentage of soil removed was about 40, the specimen became partially bare so that one could actually see the tinned copper wire surface.

FIGURE 6

DETERMINATION OF THE TIME OF EXPOSURE OF A SPECIMEN

IN A CAVITATING LIQUID
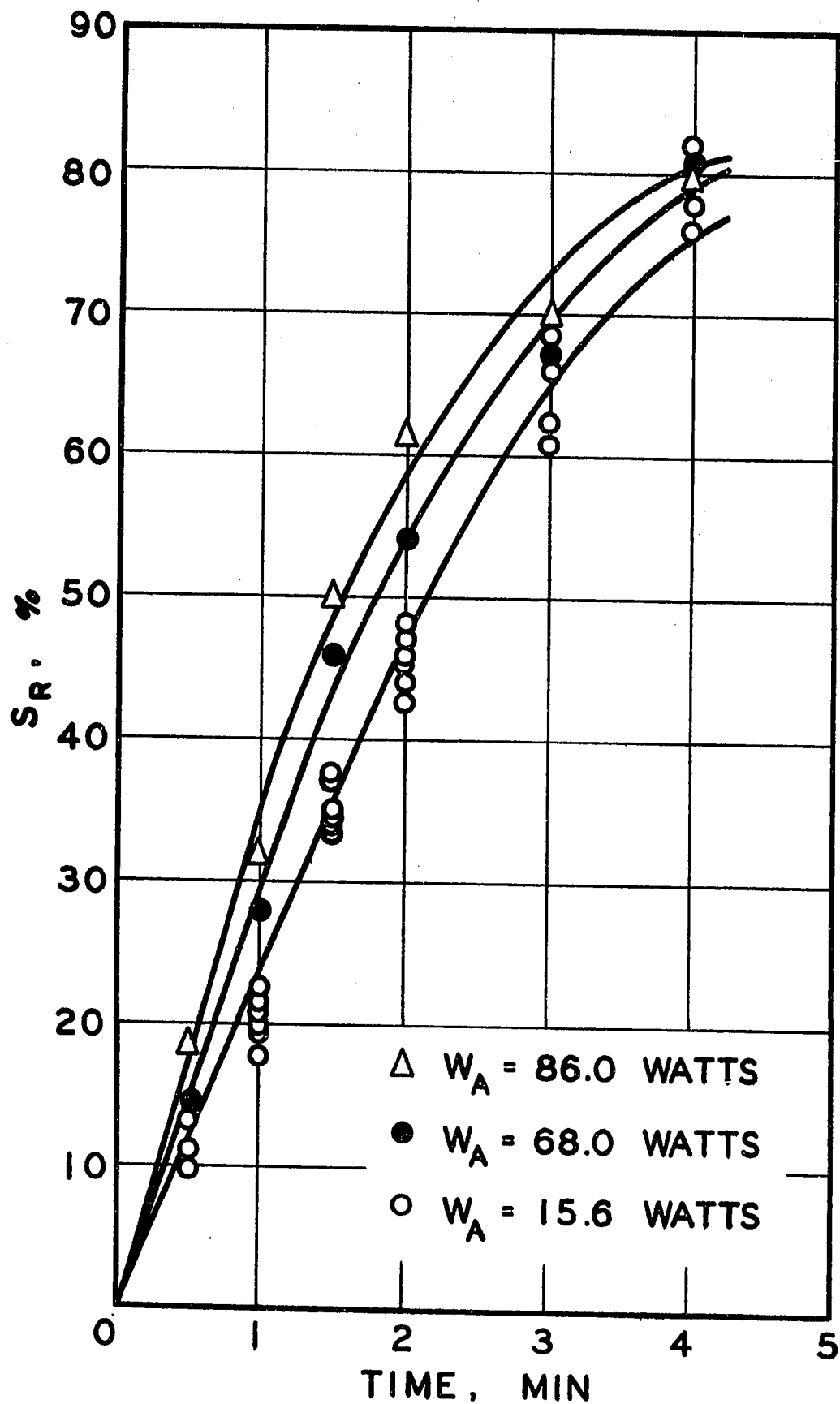
PERCENT SOIL REMOVAL AS A FUNCTION OF APPARENT

ELECTRICAL POWER INPUT TO TRANSDUCERS AT

20.6 kcps WITH AN EXPOSURE TIME OF 1 MINUTE

FIGURE 7   Distilled Water at 113°F, 149°F and 180°F

FIGURE 8   Methanol at 95°F and 113°F
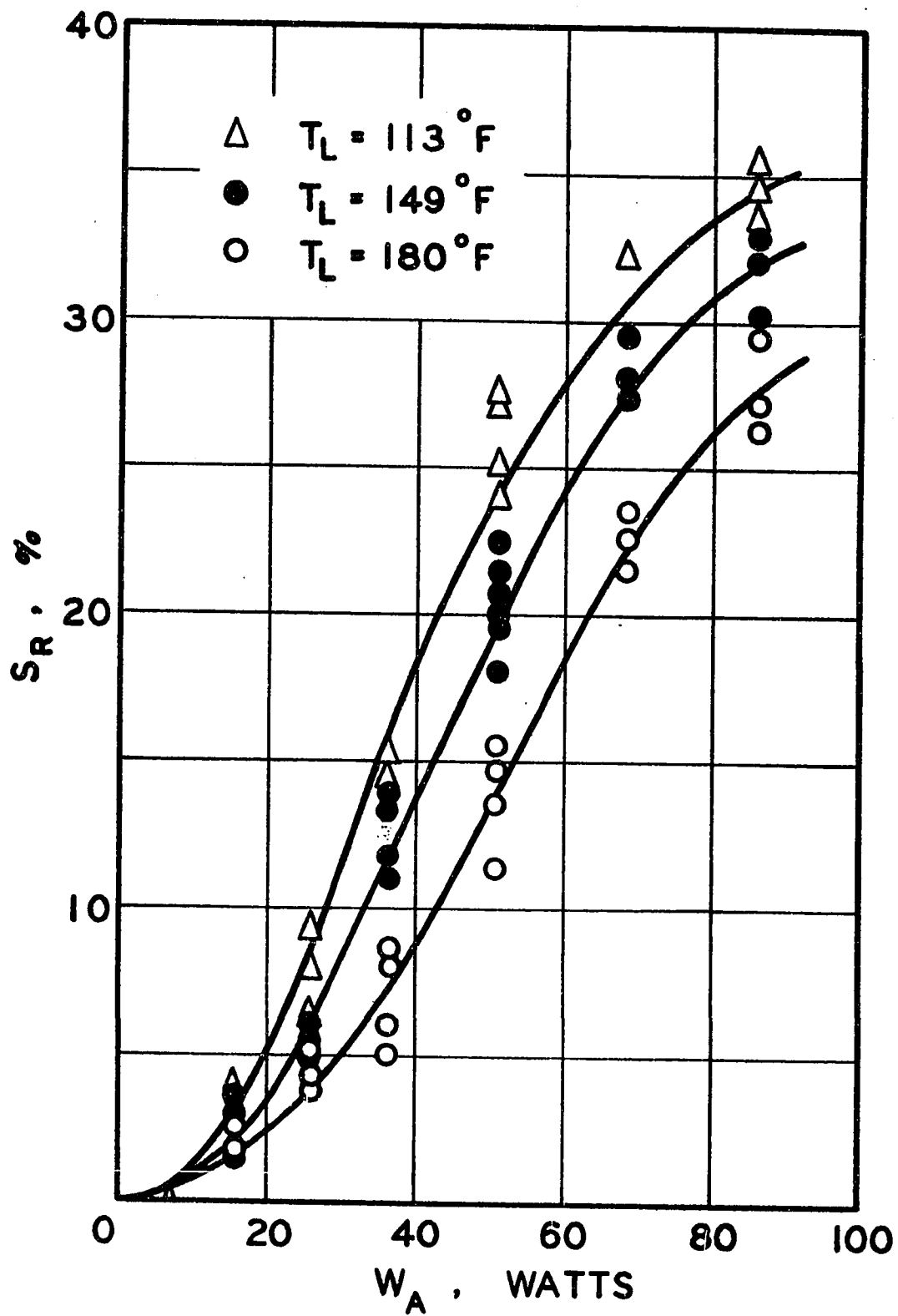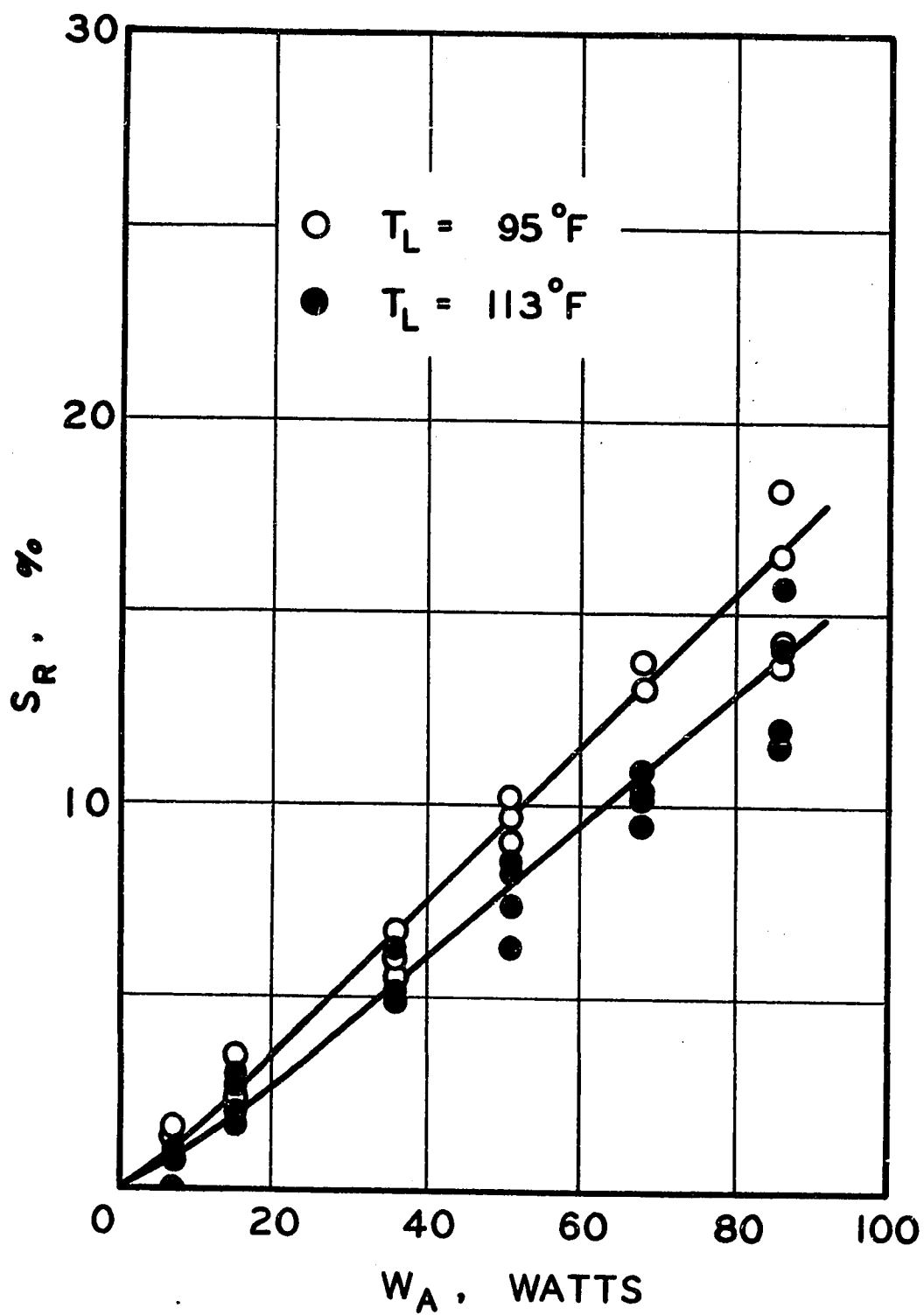
PERCENT SOIL REMOVAL AS A FUNCTION OF APPARENT ELECTRICAL

POWER INPUT TO THE TRANSDUCERS FOR DISTILLED WATER AT

$149^{\circ}F$ AND METHANOL AT $113^{\circ}F$

FIGURE 9   f = 44.1 kcps   Exposure time = 1 min.

FIGURE 10   f = 108 kcps   "   "   "   "

FIGURE 11   f = 306 kcps   "   "   "   "

$T_L = 149°F$ (WATER)

$T_L = 113°F$ (METHANOL)
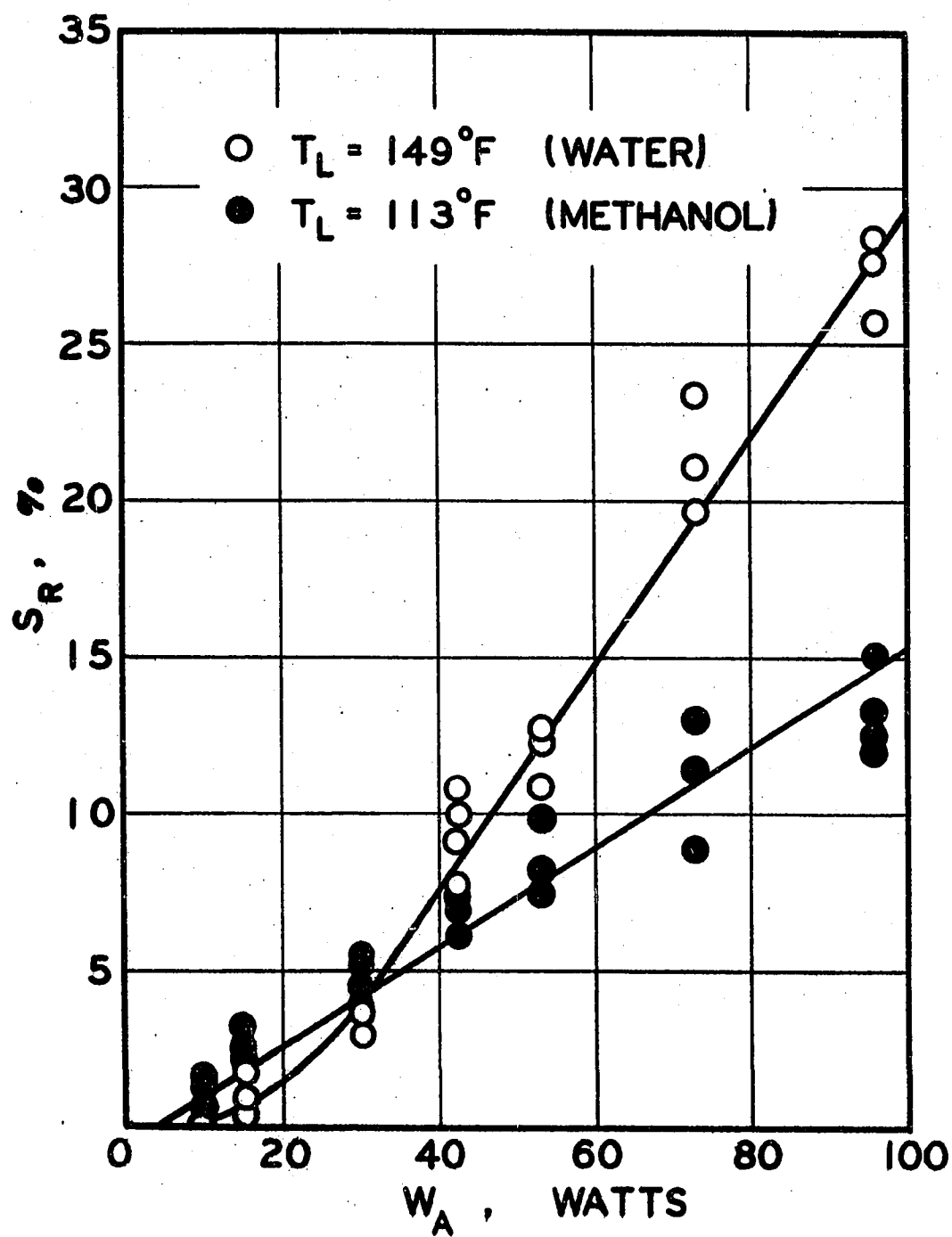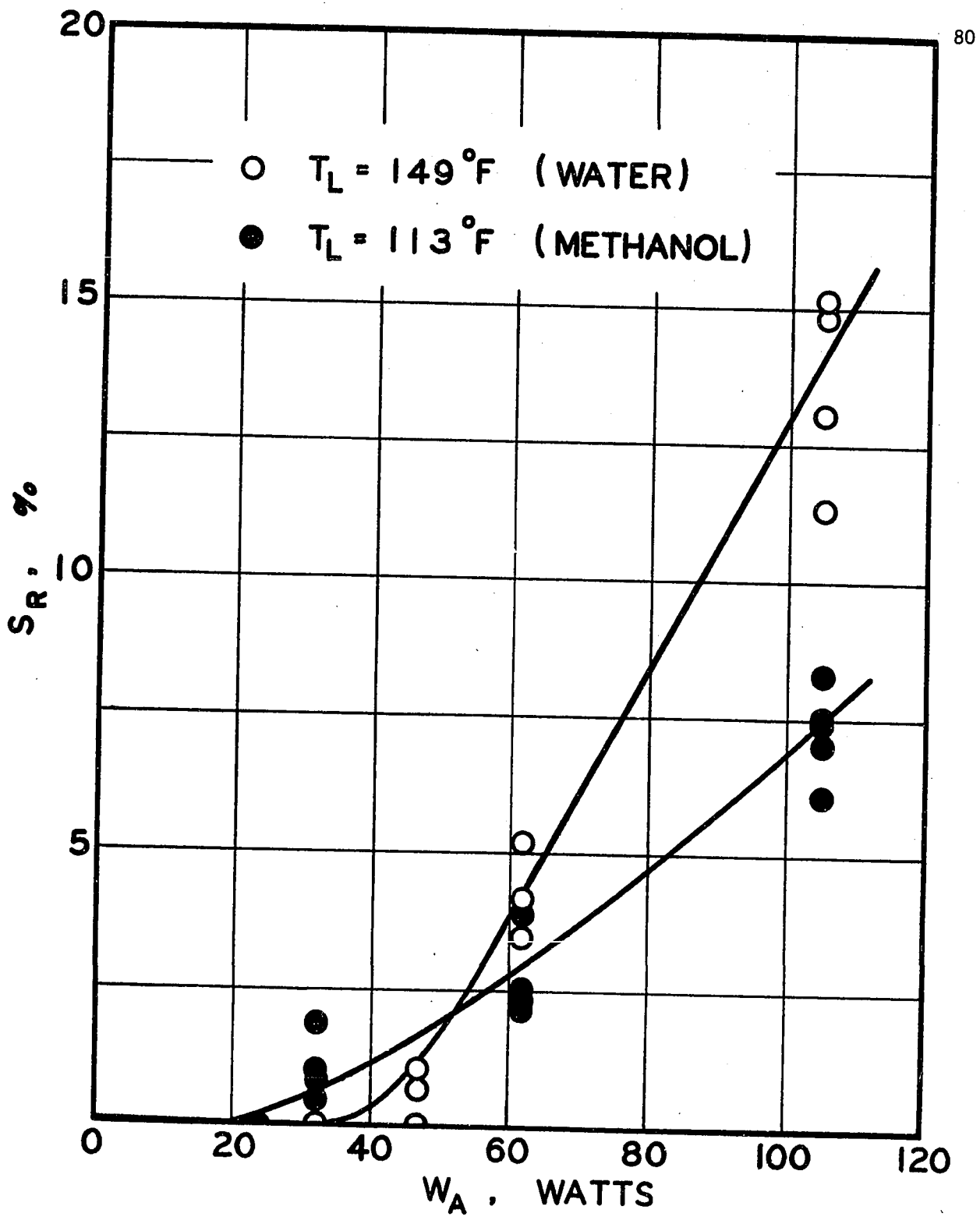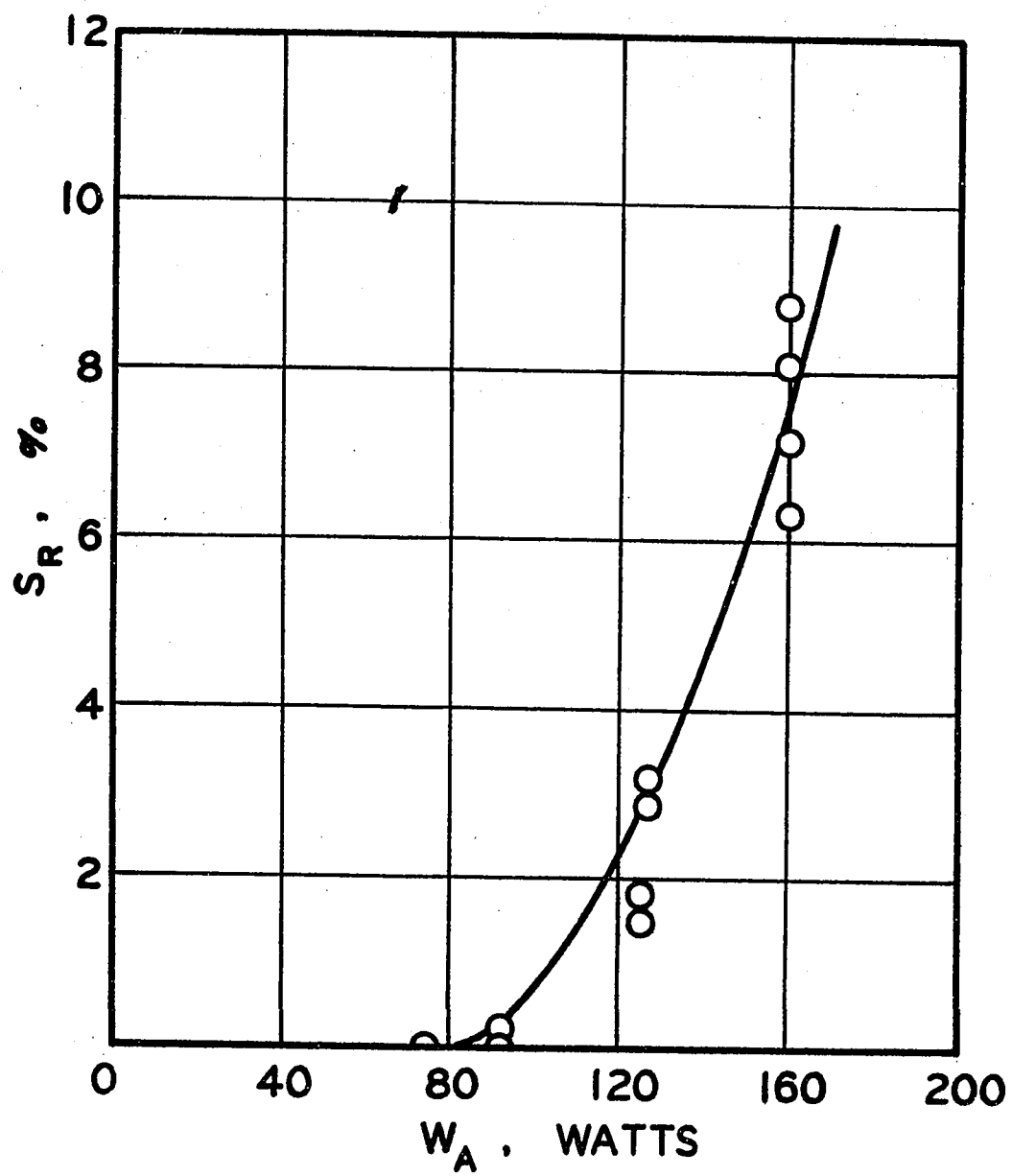
However, when the percentage of soil removed was below 35, a linear relationship was indeed obtained. In order that the results of a cavitation damage experiment should reflect the cavitation activity of the liquid near the specimen, the time of exposure of a specimen in a cavitating liquid should be chosen so that at the maximum value of apparent electrical power input, it would lie within the linear portion of the curve. The exposure time basis of one minute that was used in preparing Figures 7 to 11 was chosen under these considerations. In actual experiments, the exposure time was dependent on the electrical power input to the transducers. A longer exposure time was used for small electrical power inputs as this would decrease the possible error of the final result, provided the value of the percentage of soil removed did not exceed 35. An independent study on exposure time for methanol was not necessary because the cavitation damage was observed to be always lower than that of distilled water.

Figures 7 and 8 summarize the percentage of soil removed at the frequencies of 20.6 kcps for distilled water and methanol respectively at different apparent electrical power inputs with the temperature of the test liquid as parameter. The percentage of soil removed for frequencies of 44.1 kcps, 108 kcps, and 306 kcps are shown in Figures 9, 10 and 11 respectively. In all the figures, each point represents an experimental data point, except in Figure 6 where the average values were plotted when the apparent electrical power inputs were 86 watts and 68 watts. For any run with eight to twelve measurements, the mean deviation of each measurement from its average for the entire run is in the

range $\pm$ 10 to 15%. Individual deviation of more than 30% occurred about once in perhaps twelve measurements.

In Figures 9 and 10 where the cavitation damage for the two test liquids are superimposed on one another, the percentage of soil removed for methanol at 113° was higher than that for distilled water at 149°F at low apparent electrical power input. This is because the cavitation threshold for methanol at 113°F is much lower than the cavitation threshold for distilled water at 149°F. For example, as shown in Figure 9, cavitation took place in methanol and the value of percentage of soil removed was about 1.5% when the apparent electrical power input was 9.6 watts. For the same electrical power input, there was no cavitation in distilled water.

DISCUSSION OF RESULTS

It has been established that the cause of cavitation damage is the mechanical stress arising from the motion of cavitation bubbles[6]. Both the pulsating stable gaseous cavitation bubbles and the collapsing vaporous cavitation bubbles are capable of generating high mechanical stresses. The extent of cavitation damage would then give a measure of the cavitation activity of the cavitating liquid. Attempts have been made in industry to assess the activity of ultrasonic cleaning tanks by using strips of lead or aluminum foil and measuring the weight loss due to erosion. Due to the relatively low rate of erosion on metal surfaces, it would be difficult to obtain accurate results.

In the present work, a soil containing cobalt-60 powder was used. Cobalt-60 was chosen because of its relatively long half-life (5.3 years), its high gamma-energy level (1.2 Mev average) and the low scattering property. It has been mentioned that the reproducibility of data was within 15%. This is quite acceptable taking account of the difficulty in reproducing the position of the specimen in the sound field. For applications below 100 kcps, the use of the specimen has the further advantage that it will not disturb the sound field as the diameter of the specimen is small compared to the value of 0.58 in., which is the wavelength of sound in water at 100 kcps. The radioactivity level involved was sufficiently low so that it would not present much hazard.

In studying the cavitation damage on metal surfaces, a number of investigators[2,3,4,6] have reported that an initial non-linear period is always present as a result of surface inhomogeneities. Although the non-linear period was observed in the present work, the interval was relatively short, indicating the uniformity of the specimen surface.

The diameter of the platinum wire which was used as heater in the heat transfer experiments varied from 0.007 to 0.010 in. The specimen for measuring the cavitation activity of the liquid should have similar diameter size. Preliminary experiments showed that it was extremely difficult to put a uniform coating of soil onto a wire of such diameter. Tinned copper wire, gauge 18 (D = 0.0403 in.) was subsequently used. It has been mentioned that the specimen diameter is small compared

to the wavelength of sound fields used in present work except for the
case of 308 kcps. The cavitation activity measured by the specimen
should be applicable to the platinum wire which was mounted on the same
position as the specimen in the test liquid.

The percentage of soil removed for distilled water, as
seen from Figures 7 to 10, was always higher than that for methanol
except for very low electrical power inputs. This is in accordance with
the findings of Bebchuk and Rosenberg[7,8] who attributed the difference
to the effect of gas solubility. Cavitation bubbles would collapse more
violently when the gas content in the liquid is small and thus increase
the damage. The solubility of gases in methanol is more than an order
of magnitude greater than the solubility of gases in water. The rever-
sing trend at low electrical power input was due to the lower value of
cavitation threshold of methanol.

It should be noted that values of percentage soil removed
at different frequencies should not be compared even when the apparent
electrical power inputs to the transducers were the same. The efficien-
cies of the transducer system were not determined and the effective
sound pressures on the specimen as shown in sound pressure data were
not the same in every case.

The effect of temperature on cavitation damage is shown
in Figures 7 and 8. Bebchuk[2] measured the weight loss from a specimen
of aluminum plate in water at a frequency of 8 kcps with temperature
ranging from 50° to $194^\circ F$. His results show that the cavitation damage
first increases to a maximum which is located at approximately $120^\circ F$

and then decreases with increasing temperature. Similar experiments
carried out by Devine and Plesset[9] have shown that the maximum is in
the temperature range $105°$ to $120°F$, depending on the type of metal sur-
face used. The results shown in Figure 7 are in agreement with these
findings. As mentioned in the Literature Review section, the existence
of the maximum can be explained as the result of the increase in the
vapor pressure and the decrease of the equilibrium concentration of dis-
solved gas in a liquid as the temperature is increased. Increase in
vapor pressure tends to decrease the damage while the cavitation bubbles
would collapse more violently as the gas content of the liquid decreases.
A maximum would be formed as the more violent bubble collapse tends to
oppose the cushioning effect of rising vapor pressure. Devine and
Plesset have shown that the temperature dependence of the cavitation
damage in water is similar to a plot of

$$[1 - \frac{P_v (T)}{P_v (212°F)}][\frac{C_s (32°F)}{C_s (T)}]$$

versus the water temperature with the maximum located at approximately
$120°F$. There are no data available in the literature for methanol.

Recently, Koontz and Amron[10] and Heim [11] have studied
the rate of cavitation damage of a specially prepared soil applied to
a metal surface. Similar work has been reported by Romero and Stern[12]
who used a soil labelled with carbon 14. The purpose of these studies
was primarily to determine the cleaning efficiency of an ultrasonic
cleaning unit as compared to other methods of cleaning. They were con-
cerned with the total time required to clean the specimen completely

and studied it as a function of frequency, temperature of the cleaning
liquid, the electrical energy input to the system as well as the type
of detergent used. This is in contrast to the objective of this investi-
gation which was concerned with the development of a technique using the
rate of cavitation damage to measure the acoustic intensity of a liquid
under strong ultrasonic vibrations. The success of their work, however,
gives further support to the reliability of the present technique.

CONCLUSIONS

The proposed method provides an accurate and reliable
means using cavitation damage to measure the cavitation activity of a
liquid sound field. While smaller specimens may be prepared, the use
of present specimens will not interfere with any sound field at a fre-
quency of 100 kcps or lower. The radiation level involved is sufficiently
low that it does not involve much hazard.

NOMENCLATURE

A surface area, ft

CPM_i initial counting rate per minute

CPM_f final counting rate per minute

C_s equilibrium dissolved gas concentration, cc/lit

D diameter, ft

f frequency, kcps

P_s rms sound pressure, atm

P_p peaks sound pressure, atm

P_r vapor pressure, mm Hg

q heat transfer rate, BTU/hr

S_R soil removal, %

T_L liquid temperature, $^\circ$F

W_A apparent electrical power, watt

REFERENCES

1. Bebchuk, A.S., Iu.Ia. Borisov, and L.D. Rosenberg, Soviet Physics - Acoustics, $\underline{4}$, 372 (1958).

2. Bebchuk, A.S. Soviet Physics - Acoustics, $\underline{3}$, 95 (1957).

3. Crawford, A.E. Ultrasonics, 120, July-September (1964).

4. Antony, O.A. Ultrasonics, 194, October-December (1963).

5. Gray, A. and G.A. Wallace. "Principles and Practice of Electrical Engineering", McGraw-Hill, p. 281 (1955).

6. Plesset, M.S. and A.T. Ellis. Trans.Am.Soc.Mech.Engrs. $\underline{77}$, 1055 (1955).

7. Bebchuk, A.S. Soviet Physics - Acoustics, $\underline{3}$, 395 (1957).

8. Rosenberg, L.D. and A.S. Bebchuk. Soviet Physics - Acoustics, $\underline{6}$, 496 (1961).

9. Devine, R.E. and M.S. Plesset, Rept. No. 85-27, Div.Eng. and Appl. Sci., California Institute of Technology, April (1964).

10. Koontz, D.E. and I. Amron. ASTM Special Technical Publication, No. 246, pp. 22-31 (1958).

11. Heim, R.C. Inst.Radio Engrs.Convention Record, Part 6, 219 (1960).

12. Romero, E.L. and H.A. Stern, ibid, Part 6, 225 (1960).

PART II

EFFECTS OF ULTRASONIC VIBRATIONS ON HEAT TRANSFER TO

LIQUIDS BY NATURAL CONVECTION AND BY BOILING

INTRODUCTION

In Part I of this section, a technique has been developed to measure the cavitation activity of a liquid under intense ultrasonic vibrations. This technique was used to obtain the cavitation activity of the liquid near the heat transfer surface and subsequently, using this information, to correlate the heat transfer results. Applied sound pressure amplitudes below the cavitation threshold level were measured by the ultrasonic probe.

Platinum wires with diameters of 0.007 in. and 0.010 in. were used as heating elements because of the following advantages: 1) Since the diameters of the wire are small compared with the wavelength of the ultrasound, one can assume that there is no variation of sound pressure in the radial direction; 2) Platinum can be used as an accurate resistance thermometer.

To study the mechanism of the heat transfer processes, high speed photography was used.

EXPERIMENTAL

Equipment

The same apparatus described in Part I was used except that the specimen for measuring the cavitation activity was replaced by a platinum wire. In order to minimize the end conduction effects, only the central portion (approximately 3/4 in.) of the heating element was made to serve as the test section by use of platinum potential leads having smaller diameters relative to that of the heating element.

A regulated DC power supply, Model 520A (0-36 V, 0-25A) manufactured by Harrison Laboratories was used to energize the heating circuit. The heating current was obtained by measuring the drop in electric potential across the 0.02 ohm standard resistor described earlier, with a Tinsley Model 3184E precision potentiometer and a Tinsley galvanometer (Type SR-1). The Tinsley potentiometer and galvanometer combination was capable of reading to 0.01 mv at 1 mv. The accuracy of the readings, however, was limited by the stability of the boiling and the cavitation phenomena rather than by the instruments. The voltage drop across the test section was also measured with the same potentiometer and galvanometer.

Materials

All platinum wires including the 0.0045 in. diameter and 0.0002 in. diameter wires used as potential leads were CP platinum wires, reference grade, manufactured by Engelhard Industries.

The liquids used were distilled water and methanol, described earlier.

Procedure and Observations

The platinum potential leads were spot-welded to the heating element which was then annealed at red heat in air for 15 minutes with alternating current. The test section of the heating element was calibrated in water at 212°F by using very low DC current and measuring the voltage drops across the standard resistor and the test section. This was done after the temperature coefficients of resistivity of platinum obtained from a number of calibrations performed at both 32°F and 212°F were in good agreement with the known values. At least ten sets of readings were taken at 212°F for each wire to obtain its average value of resistance. The length of the test section was measured by a scale capable of giving an accuracy of 1/64 in. For the wire diameter, the value given by the manufacturer was used.

The calibrated platinum wire assembly was placed in the same location as the specimen used in Part I. The temperature of the test liquid was brought slowly up to the desired level so that the

dissolved air content in the test liquid would be at its equilibrium value. The liquid level in the tank was the same as before.

Heat Transfer Experiments Without Vibration

The current from the DC power supply was passed through the wire, and readings of voltage drop across the standard resistor and the test section were taken. It was then either increased or decreased, depending on the initial value used, by small steps so that measurements were made in the whole region of natural convection and nucleate boiling. When the test liquid was methanol at 113°F, the amperage of the power supply was sufficient to burnout the wire. Subsequently, the effects of ultrasonic vibrations on burnout heat flux and the critical temperature differences were also studied as described in Part III of this section. With distilled water at 149°F as the liquid, the maximum available current was insufficient to burnout the wire. For reasons which will become obvious later, saturated pool boiling or subcooled pool boiling with smaller values of the degree of subcooling are undesirable. Using smaller diameter wires as the heating element would also require less current to achieve burnout. Preliminary experiments had shown, however, that a heating element made of smaller diameter wires (0.0045 and 0.002 in.) vibrated at high heat fluxes under intense ultrasonic vibrations.

Determination of the Critical Sound Pressure

A small DC current was passed through the wire and the acoustic energy was imposed upon the system, starting with a very low

value of apparent electrical power input to the transducers. The apparent electrical power input was increased in small steps. The voltage drops across the standard resistor and the test section as well as the apparent electrical power input were recorded after each increment. It was observed that the potential across the test section remained the same until at some value of apparent electrical power input a sudden drop was recorded indicating a decrease in the wire temperature. Simultaneously cavitation bubbles appeared on the wire. These cavitation bubbles were very unstable and began to roll on the wire surface soon after they were formed. The root mean square sound pressure on the wire measured at this value of apparent electrical power input to the transducers is then called the critical sound pressure. It can be defined as the sound pressure at which the applied sound pressure field begins to have an effect on the heat transfer rate. For values of sound pressure below the critical value, the heat transfer rate was the same as in the case where there was no vibration.

The following procedure was adopted in determining the critical sound pressure. The voltage drop across the transducers was increased in small steps of 1 minute duration. The actual value of increase in voltage depended on the frequency of the sound field. For example, when the frequency was 20.6 kcps, the voltage increment was 1 volt. At 108 kcps, the increment was increased to 25 volts. When a drop in the potential across the test section was recorded, the voltage drop across the transducers was decreased by one step, that is 1 volt if f = 20.6 kcps. If the potential drop across the test wire returned to

its vibration-free value after a 5-minute interval, the sound pressure measured prior to the decrease in transducer voltage was taken as the critical sound pressure. If the potential across the test section did not return to its value without vibration, the voltage drop across the transducers was further reduced by one step for 5 minutes. In all cases, the lowest sound pressure for which a drop in the voltage across the test section occurred was taken to be the critical sound pressure. The 5-minute interval criterion was checked by waiting for periods of as much as 30 minutes. It was found that the 5-minute interval was sufficient in 10 out of the 11 cases checked. The critical sound pressures were reproducible to within 12%.

Heat Transfer Experiments with Ultrasonic Vibrations

It was found that the critical sound pressure was a function of the wire temperature as well as the frequency of the sound field. In order to be able to compare directly the heat transfer results with ultrasonic vibrations, it was necessary to select values of apparent electrical power input to the transducers so that for the whole range of the wire temperature used, the resulting sound pressures on the wire surface would exceed their corresponding critical values. When the frequency was 20.6 kcps, the three values of voltage drop across the transducers used were 15, 25 and 40 volts, corresponding to values of apparent electrical power input of 15.6, 36.2 and 86.0 watts respectively. After the critical sound pressure was determined, the voltage drops across the transducers were changed to the above values. The DC current

passing through the wire was then increased in small steps. For each new wire temperature, measurements were made first without imposing vibration.

The liquids used and the experimental variables studied were the same as in Part I. When the frequency was 20.6 kcps, two different liquid temperatures were used for both liquids; namely, 113°F and 149°F for distilled water, and 95°F and 113°F for methanol. For the three remaining frequencies (44.1, 108 and 306 kcps), the temperature of distilled water was 149°F and that of methanol was 113°F. A thermometer located near one end of the wire was used to measure the temperature of the liquid. The temperature was always maintained at the desired level to within 1°F.

All platinum wires were used as received. It was found however that, after two or three tests, it became rather difficult to reproduce the heat transfer results using the same wire. Microscopic studies showed that the wire surface conditions had changed considerably after two or three tests. In Appendix G, the change of surface conditions is shown in three photographs taken through a microscope. The change of surface conditions of the platinum wire was taken to be the result of cavitation damage. It has been established that the surface condition is an important variable in the study of nucleate boiling[1,2,3]. Subsequently, each platinum wire was not used for more than three tests.

RESULTS

Critical Sound Pressure

The results of the critical sound pressure measurements are shown in Figures 1 to 5. Figure 1 shows some typical temperature history curves used in the determination of the critical sound pressure. For a given value of heat flux, the temperature difference between the wire and the bulk liquid remained almost constant until the critical sound pressure was reached when it dropped rather abruptly to a lower value. The DC current passing through the wire was maintained at the same value. The heat flux value dropped slightly due to the decrease in platinum wire resistance as the wire temperature decreased. The change, however, was less than 2%, and the values reported in Figure 1 are the mean values.

Figure 2 shows the critical sound pressure for distilled water at two different liquid temperatures at a frequency of 20.6 kcps. The effect of frequency on critical sound pressure is shown in Figures 4 and 5 for distilled water at $149^{o}F$ and for methanol at $113^{o}F$, respectively. Figure 3 gives the same information for methanol at $95^{o}F$ and $113^{o}F$, as Figure 2 does for distilled water. The critical sound pressure shows a minimum in the temperature range of 235° to $245^{o}F$ for distilled water and 170° to $180^{o}F$ for methanol, both corresponding to temperatures for the incipience of boiling of the two liquids.

FIGURE 1

SOME TYPICAL TEMPERATURE HISTORY CURVES DURING THE

DETERMINATION OF CRITICAL SOUND PRESSURE
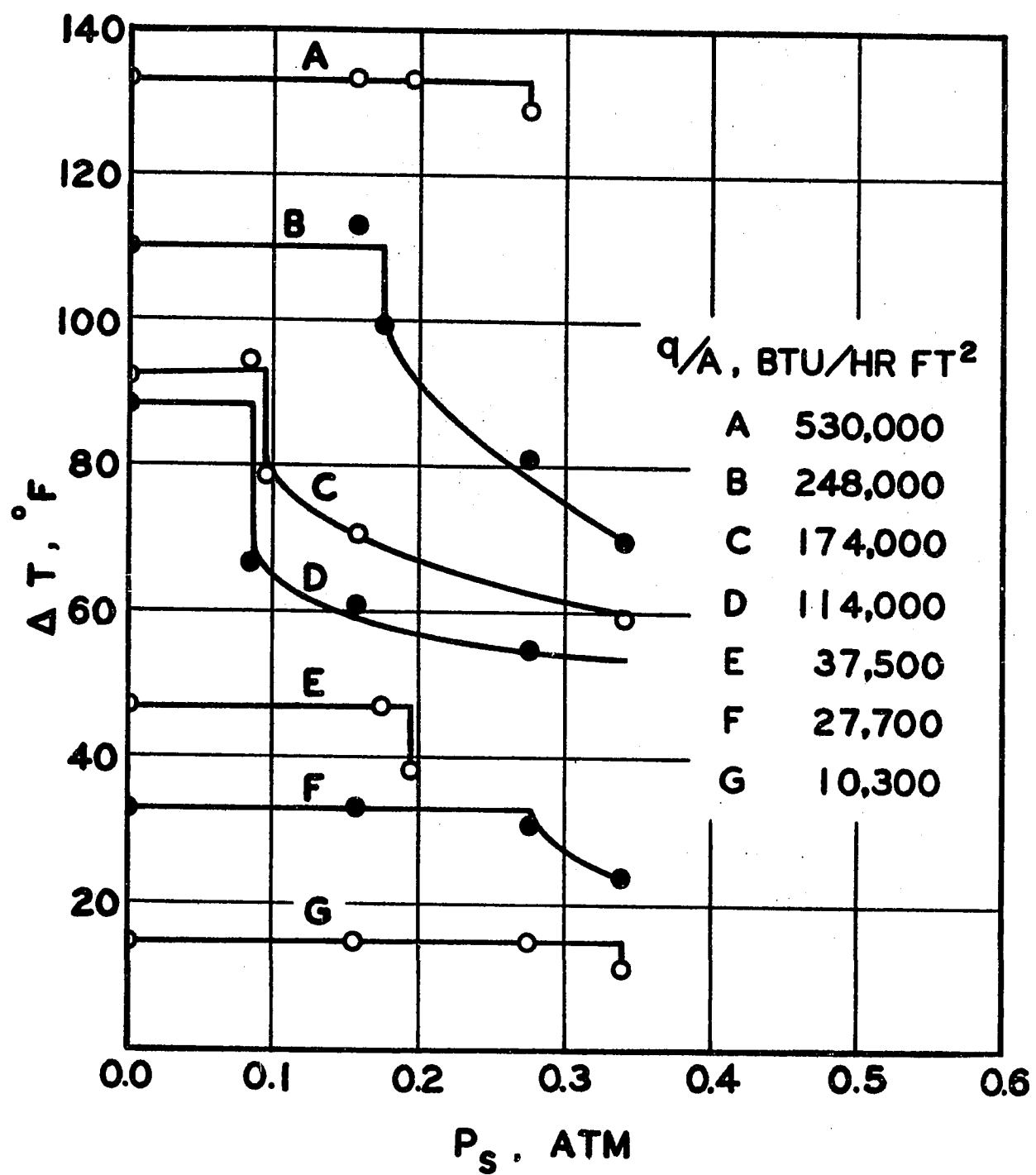
VARIATION OF CRITICAL SOUND PRESSURE AS A FUNCTION

OF THE WIRE TEMPERATURE AT 20.6 kcps

FIGURE 2   DISTILLED WATER AT 113°F AND 149°F

FIGURE 3   METHANOL AT 95°F AND 113°F.
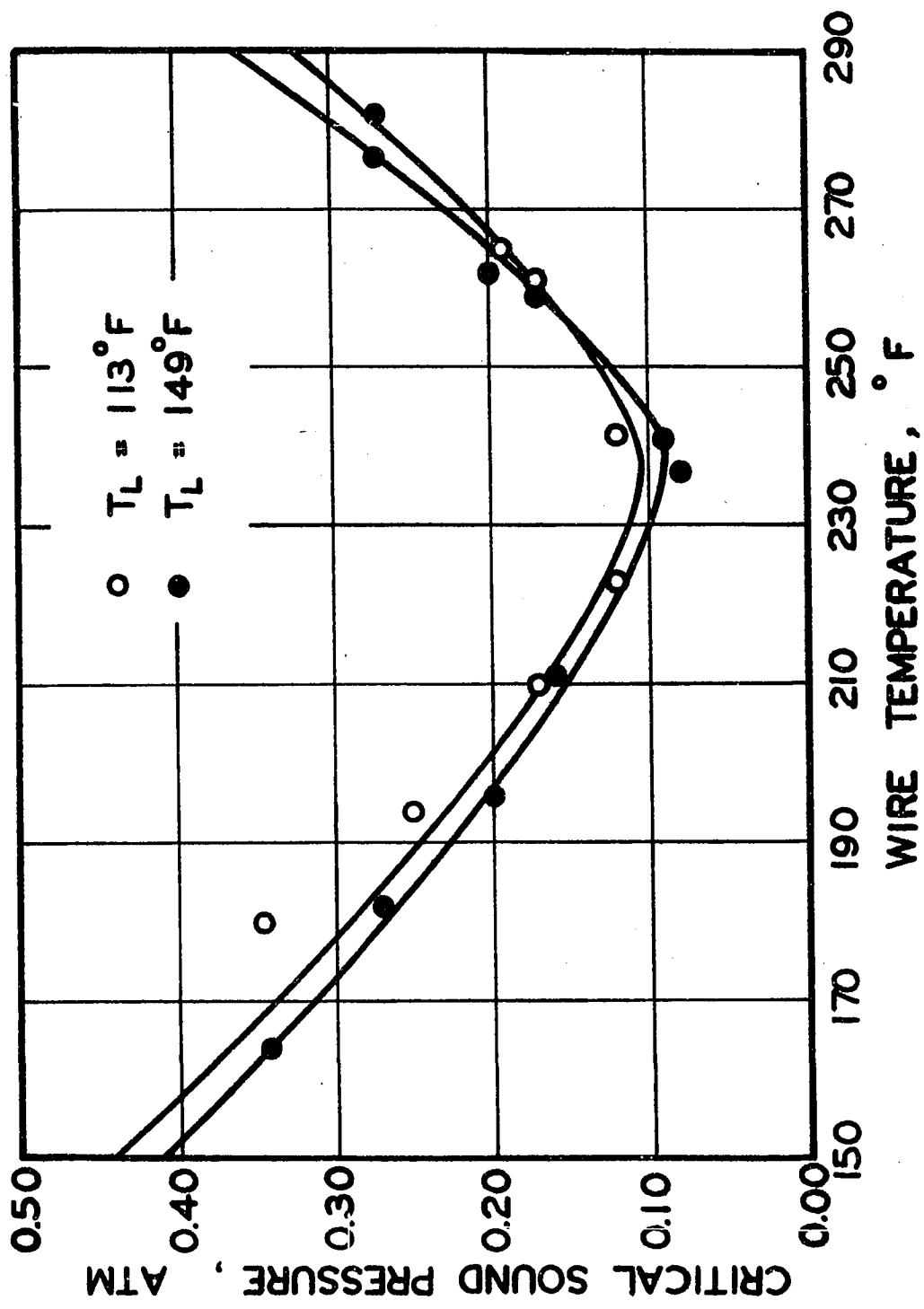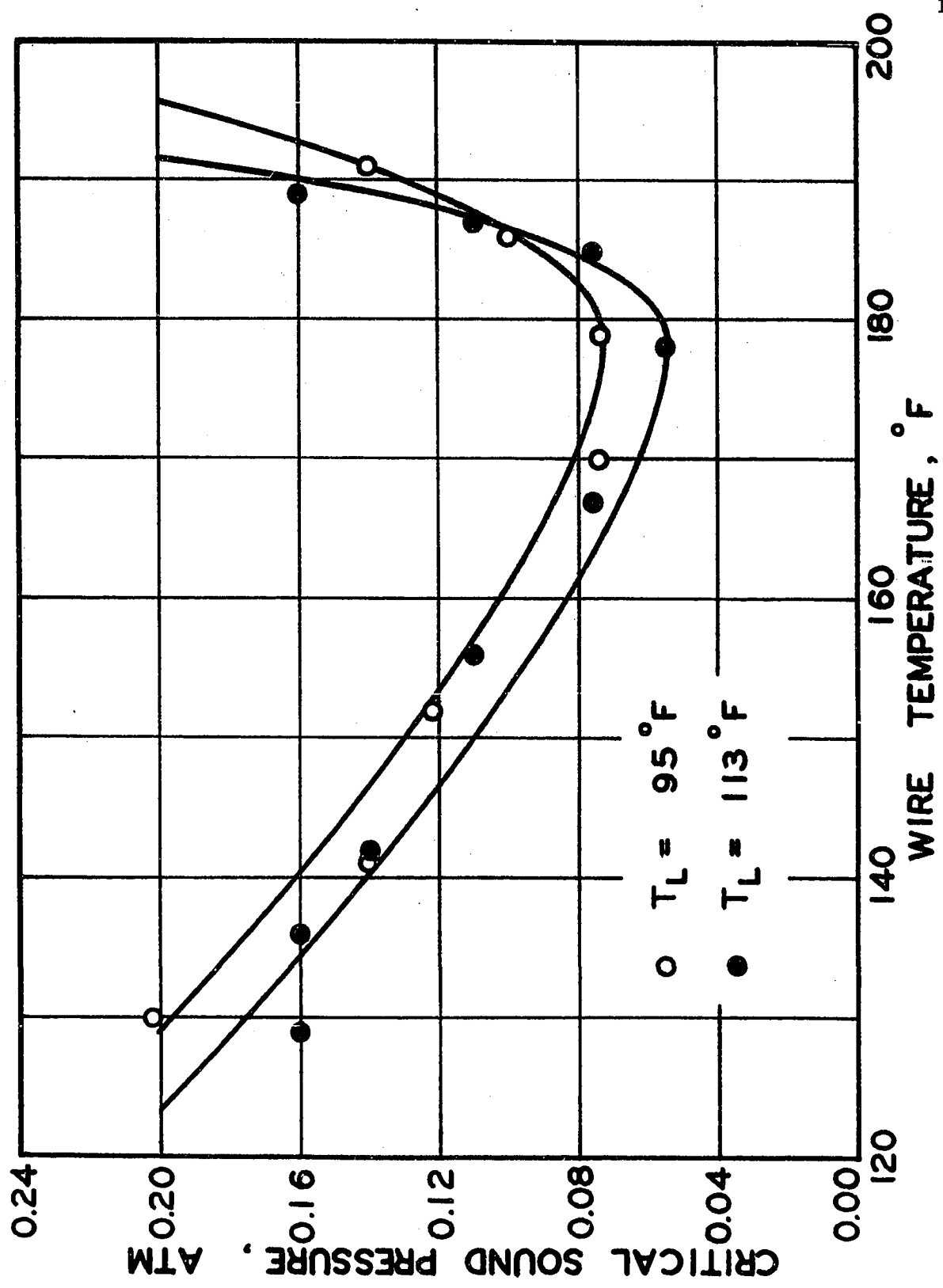
VARIATION OF CRITICAL SOUND PRESSURE AS A FUNCTION

OF THE WIRE TEMPERATURE AT DIFFERENT FREQUENCIES

FIGURE 4   DISTILLED WATER AT 149°F

FIGURE 5   METHANOL AT 113°F.
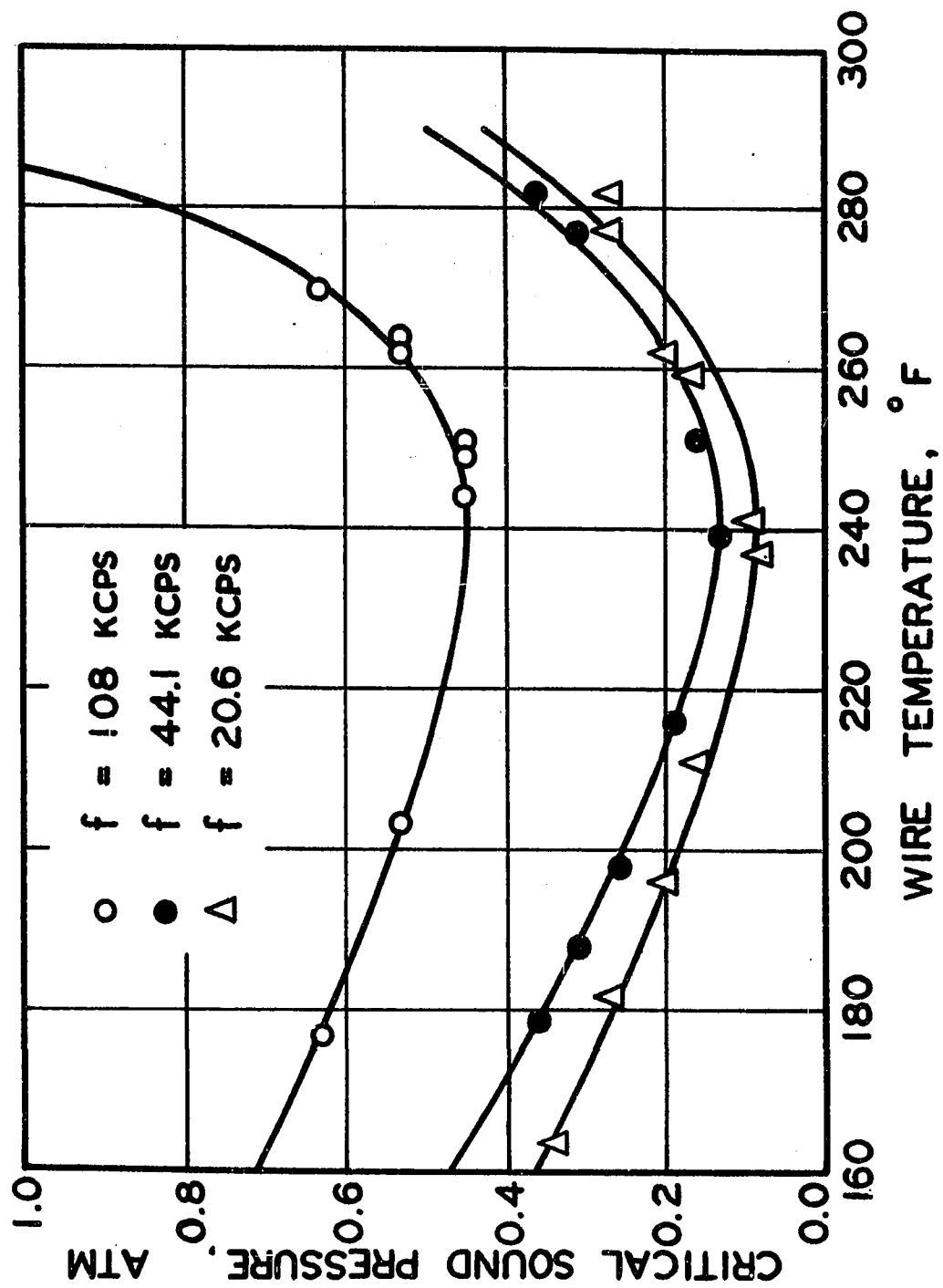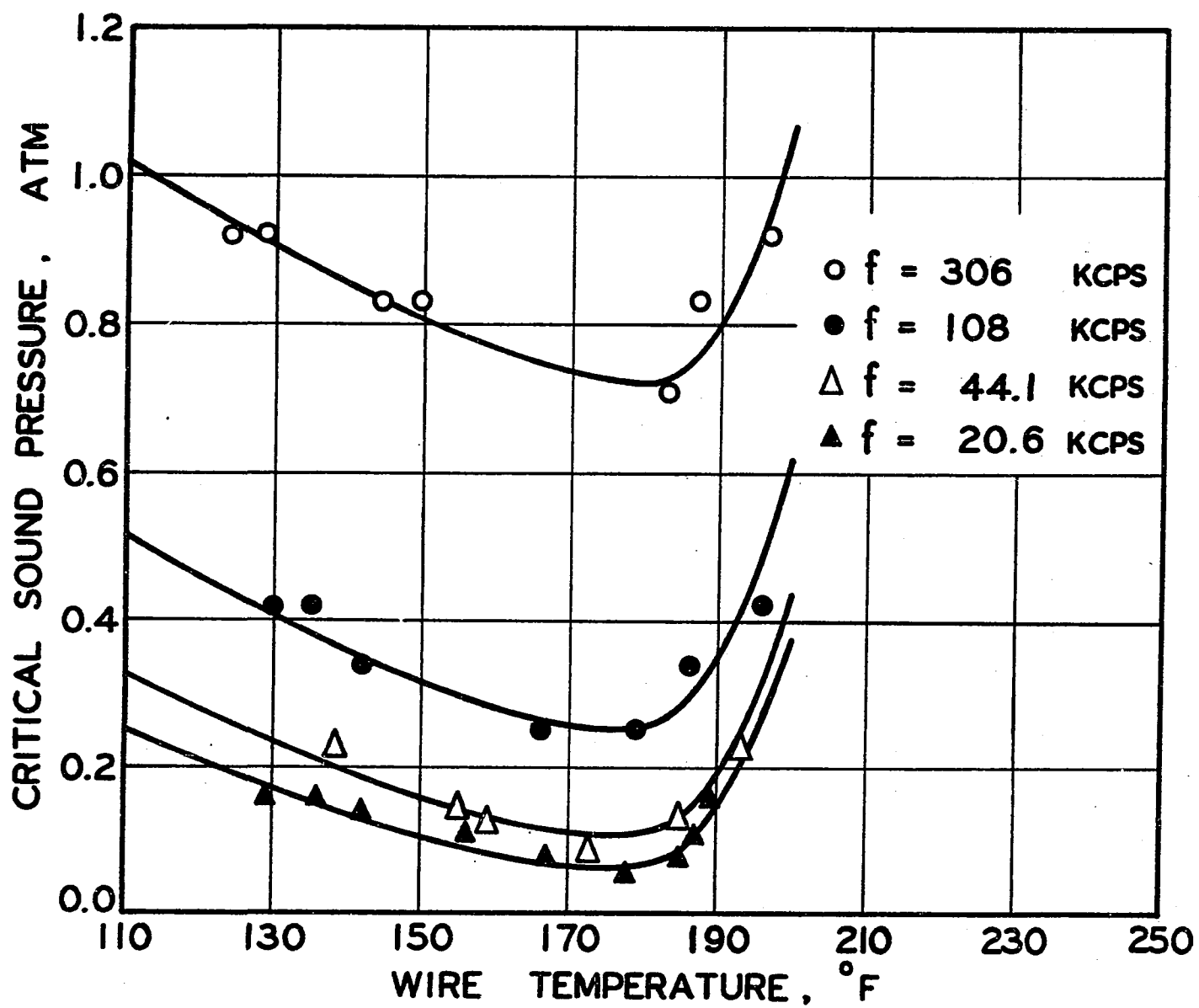
Heat Transfer Data

The results of heat transfer experiments with and without ultrasonic vibrations are presented in Figures 6 to 14. In each figure, the heat fluxes are shown at three different acoustic energy levels except in Figures 11, 13 and 14 for frequencies of 108 and 306 kcps where they were measured at two levels.

Because of the high precision of the potentiometer-galvanometer combination, the values of heat flux were measured to within 1% accuracy. However, the small fluctuations in voltage as the result of the instability of the boiling and cavitation phenomena might have increased the error up to 5%. The errors in Δt caused by these fluctuations were more serious as they were calculated to be as large as $2^{o}F$ in some cases. Subsequently, heat transfer data with Δt smaller than $10^{o}F$ were neglected and less emphasis was put on data with Δt smaller than $20^{o}F$.

The radial temperature gradient within the platinum wire was calculated according to an equation given by McAdams et al.[4]. The correction was not made as the error involved was less than 2% in all cases. The calculations are given in Appendix F. The temperature difference (Δt) in all figures is the temperature difference between the platinum wire and the bulk liquid.

The acoustic energy levels were expressed in terms of the apparent electrical power input to the transducers, which could be translated from the results obtained in Part I to the percentage of soil removed. Table 1 shows the corresponding percentage soil removed for

EFFECT OF 20.6 kcps ULTRASONIC VIBRATIONS ON HEAT

TRANSFER RATES IN DISTILLED WATER

FIGURE 6   DISTILLED WATER AT 149°F

FIGURE 7   DISTILLED WATER AT 113°F
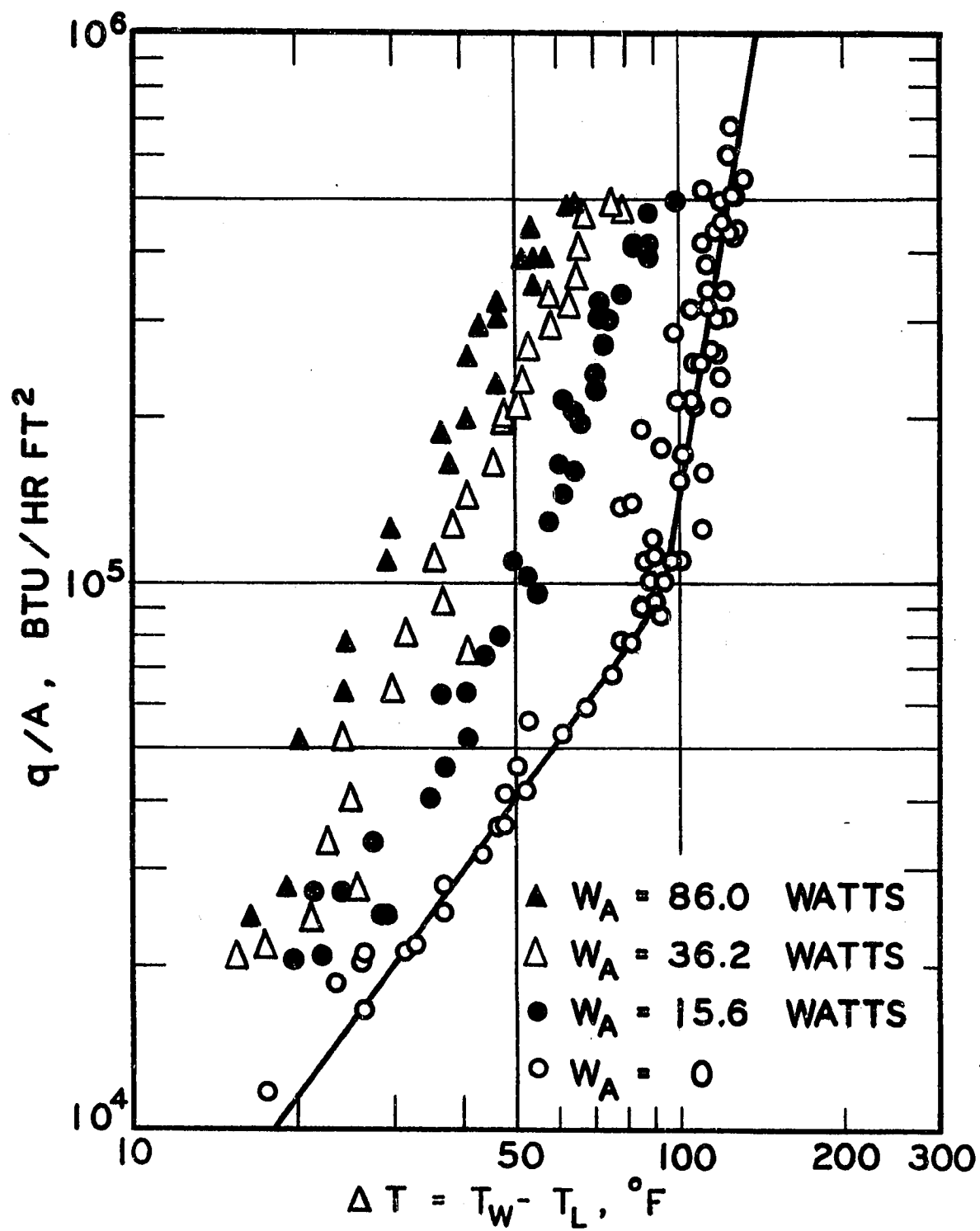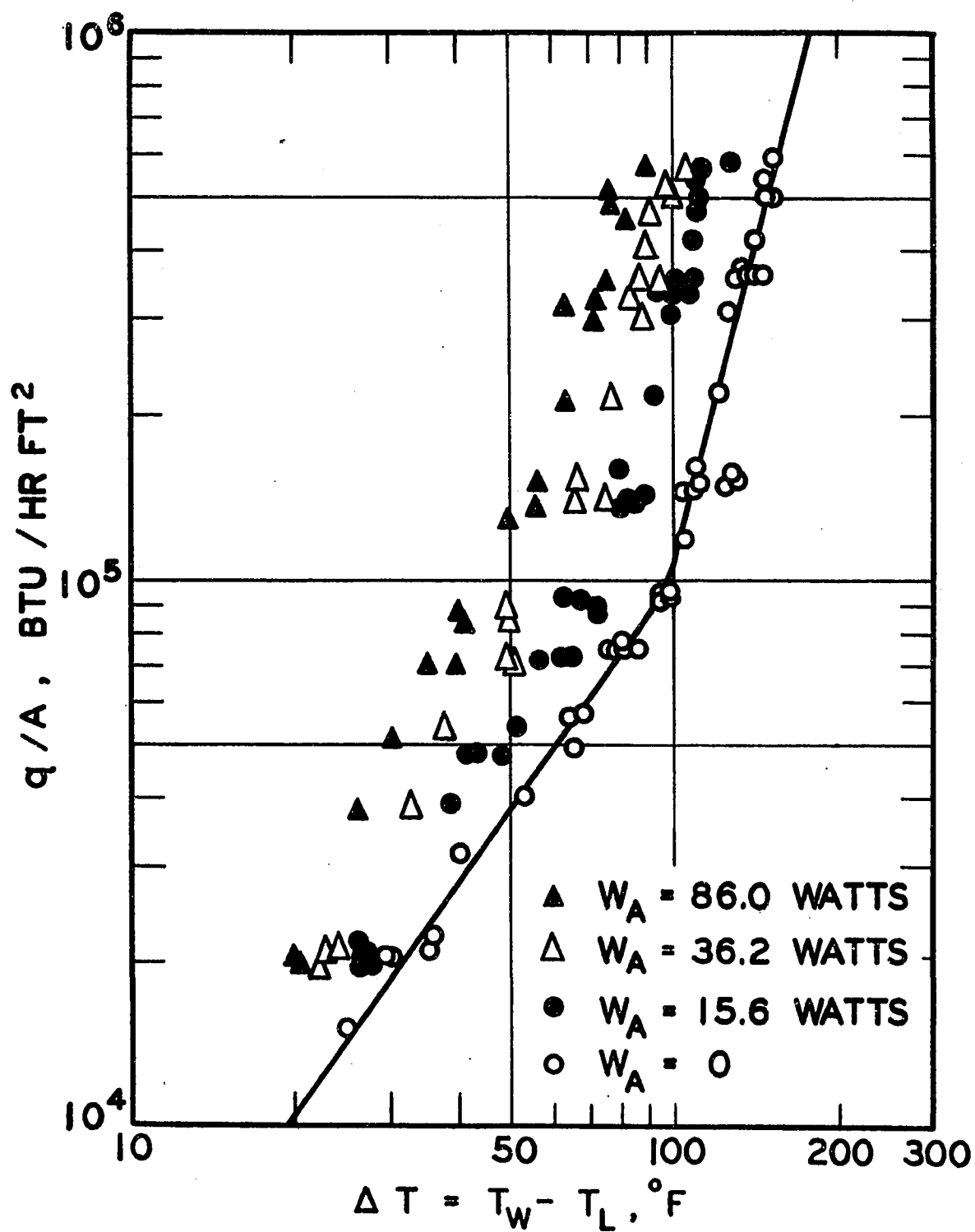
EFFECT OF 20.6 kcps ULTRASONIC VIBRATIONS ON HEAT

TRANSFER RATES IN METHANOL

FIGURE 8   METHANOL AT 113°F

FIGURE 9   METHANOL AT 95°F
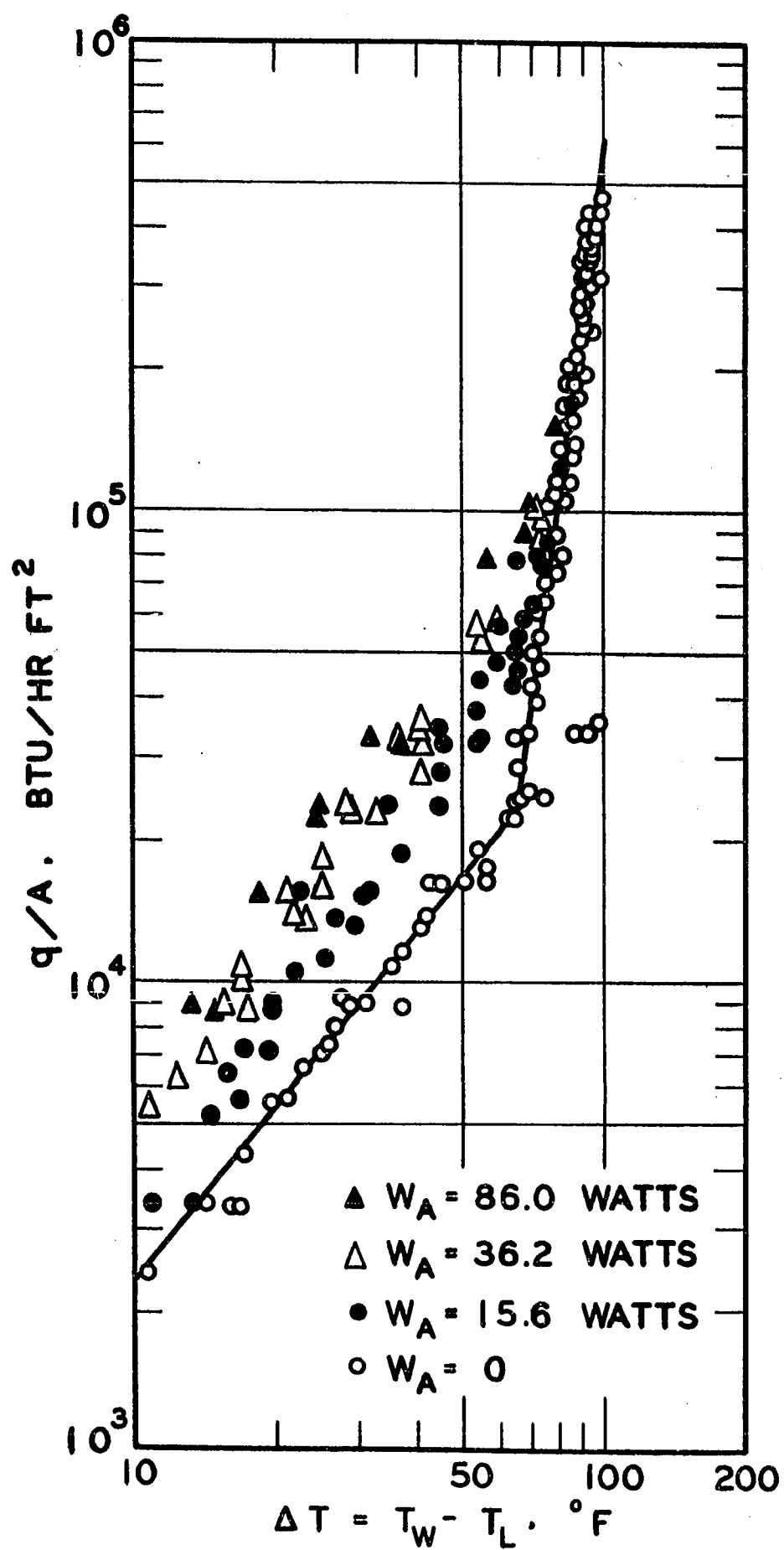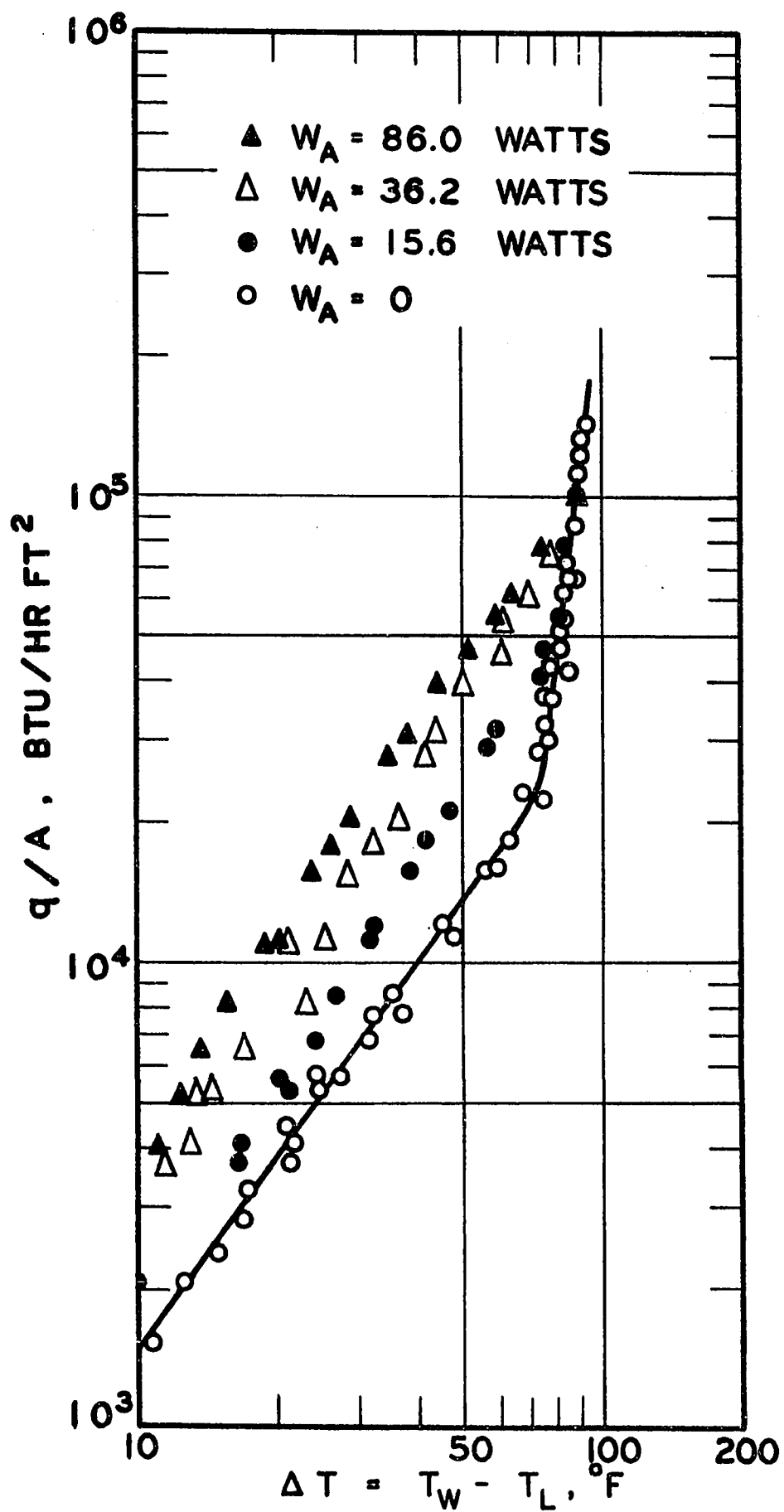
EFFECT OF ULTRASONIC VIBRATIONS ON HEAT TRANSFER

RATES IN DISTILLED WATER AT 149°F

FIGURE 10   FREQUENCY = 44.1 kcps

FIGURE 11   FREQUENCY = 108 kcps

108
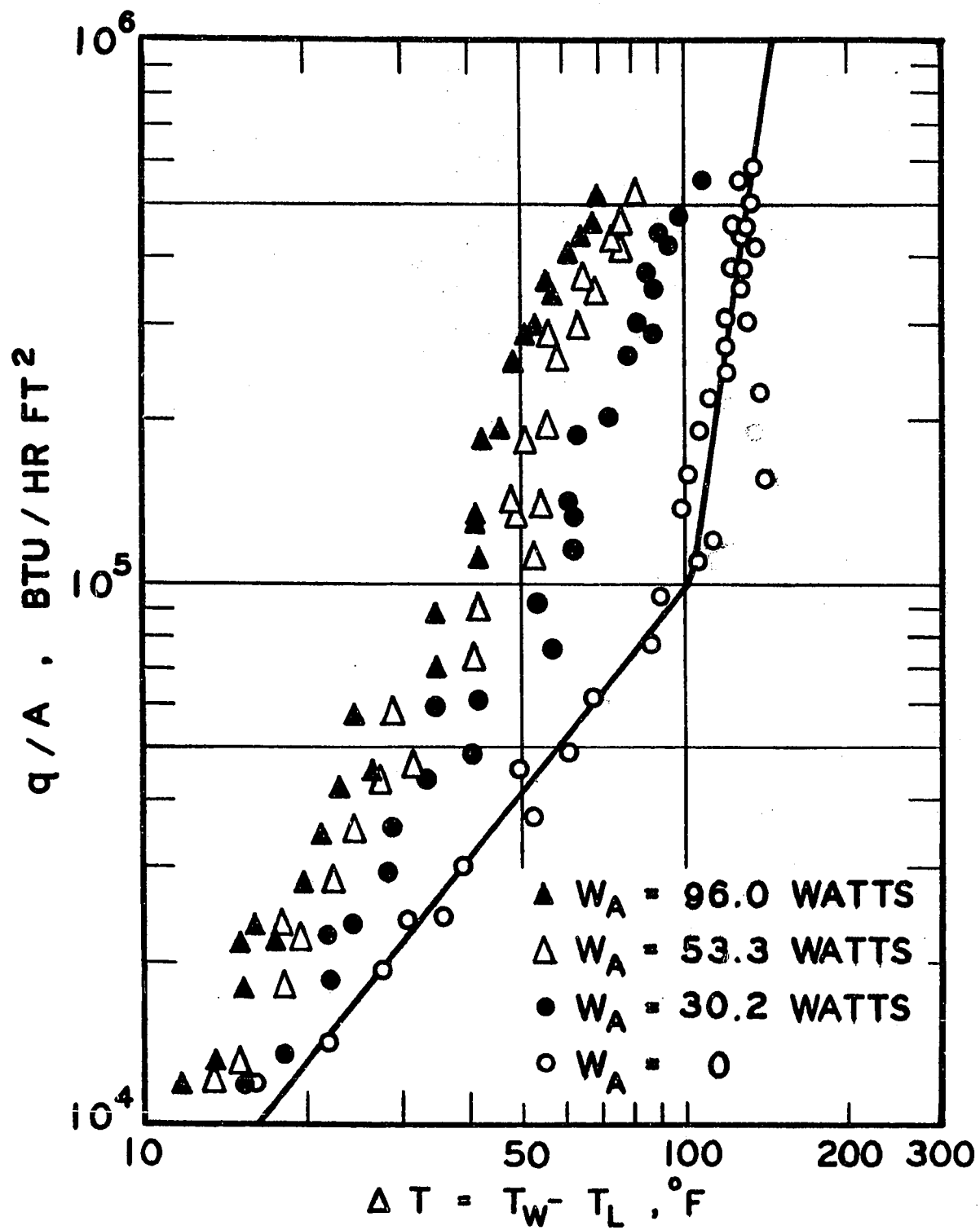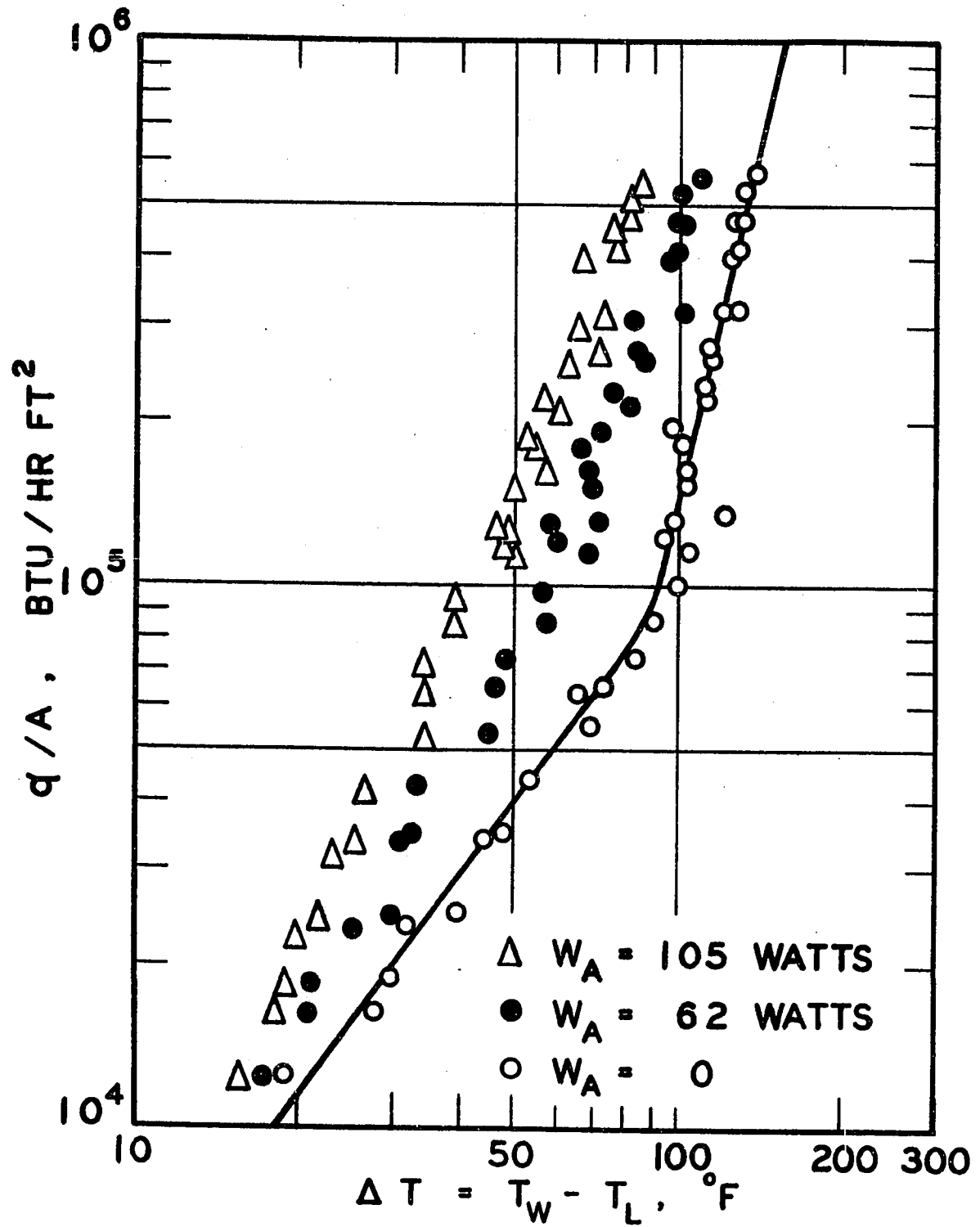
EFFECT OF ULTRASONIC VIBRATIONS ON HEAT TRANSFER

RATES IN METHANOL AT 113°F

FIGURE 12	FREQUENCY = 44.1 kcps
FIGURE 13	FREQUENCY = 108 kcps
FIGURE 14	FREQUENCY = 306 kcps
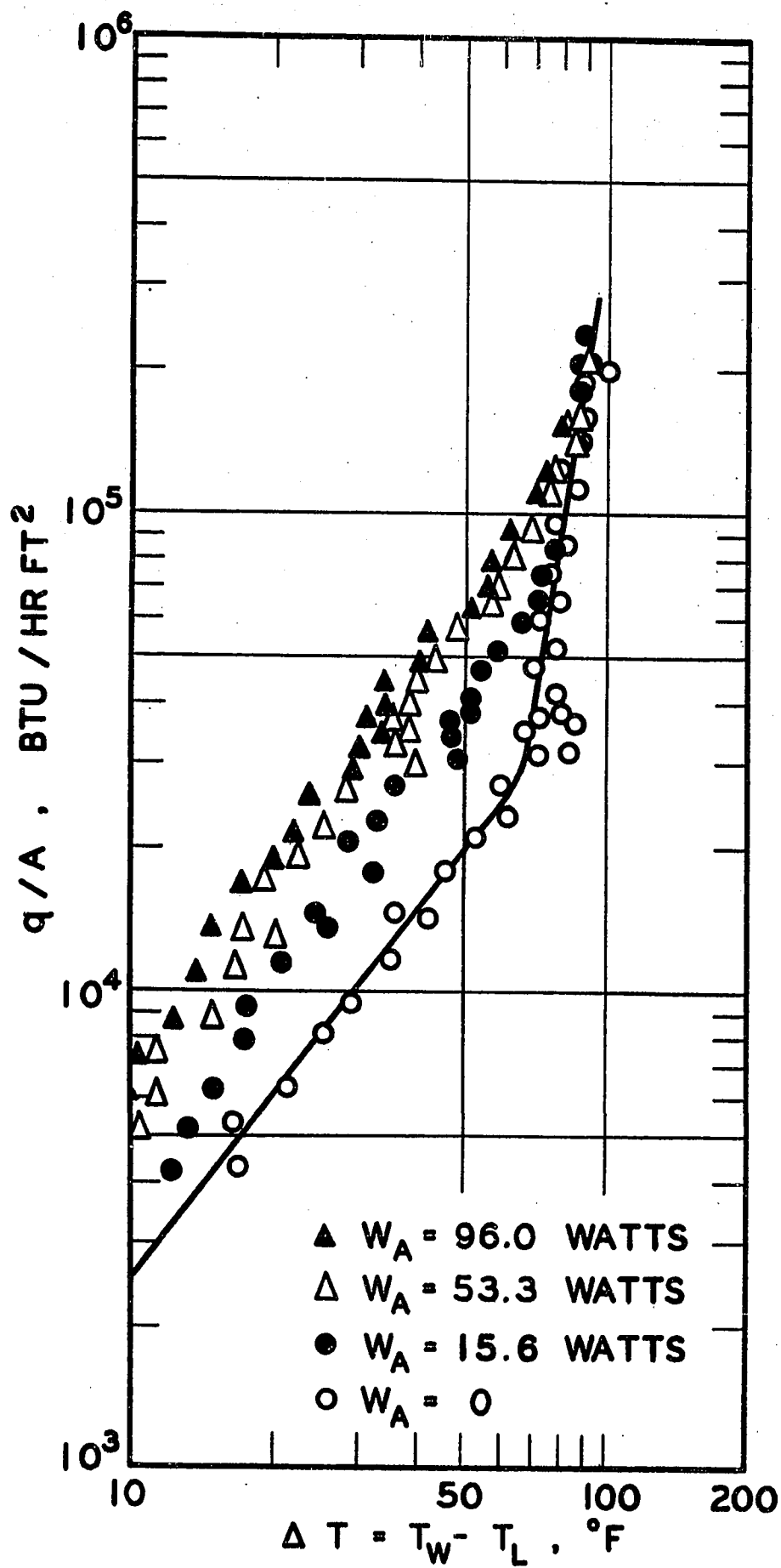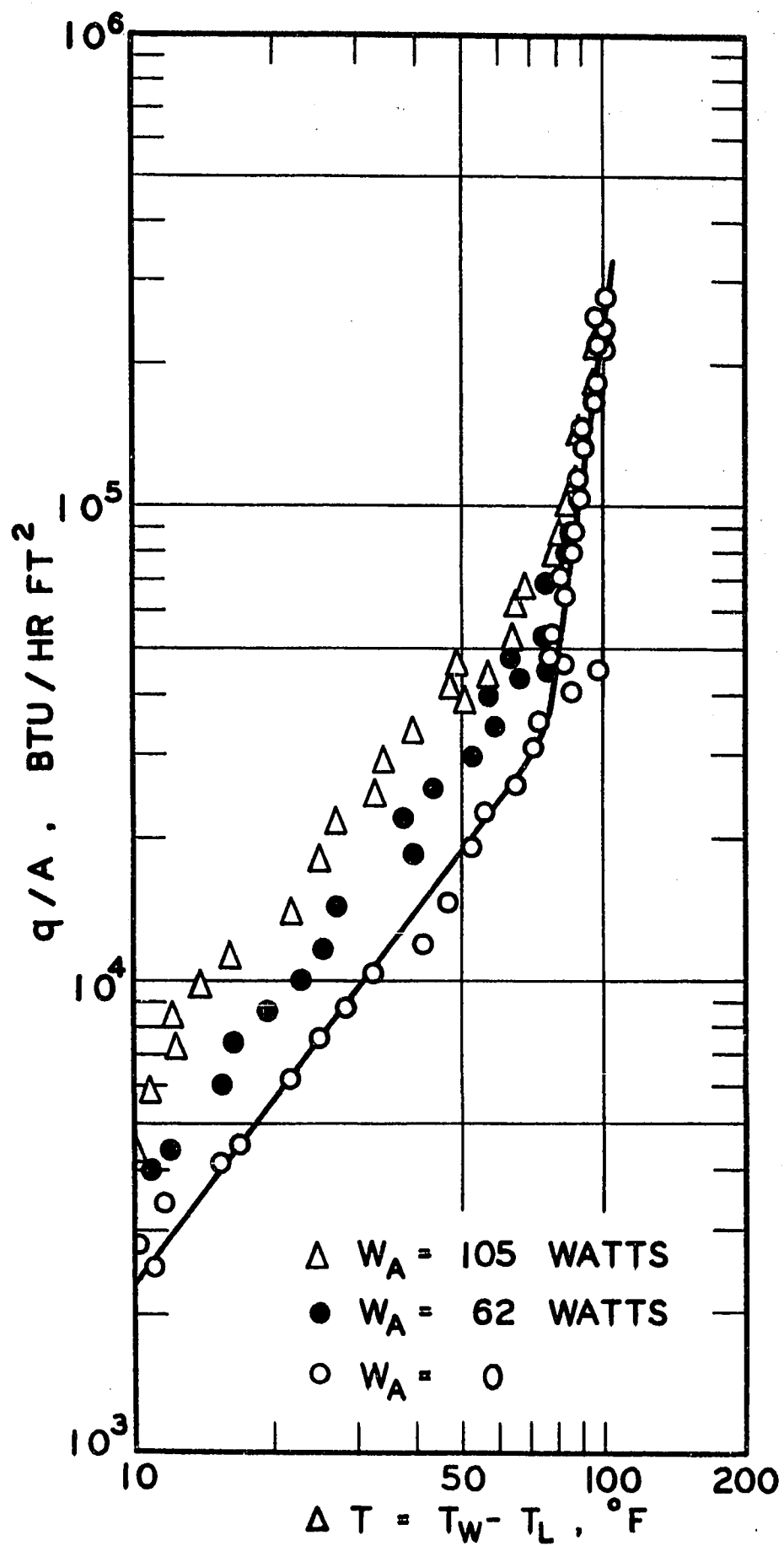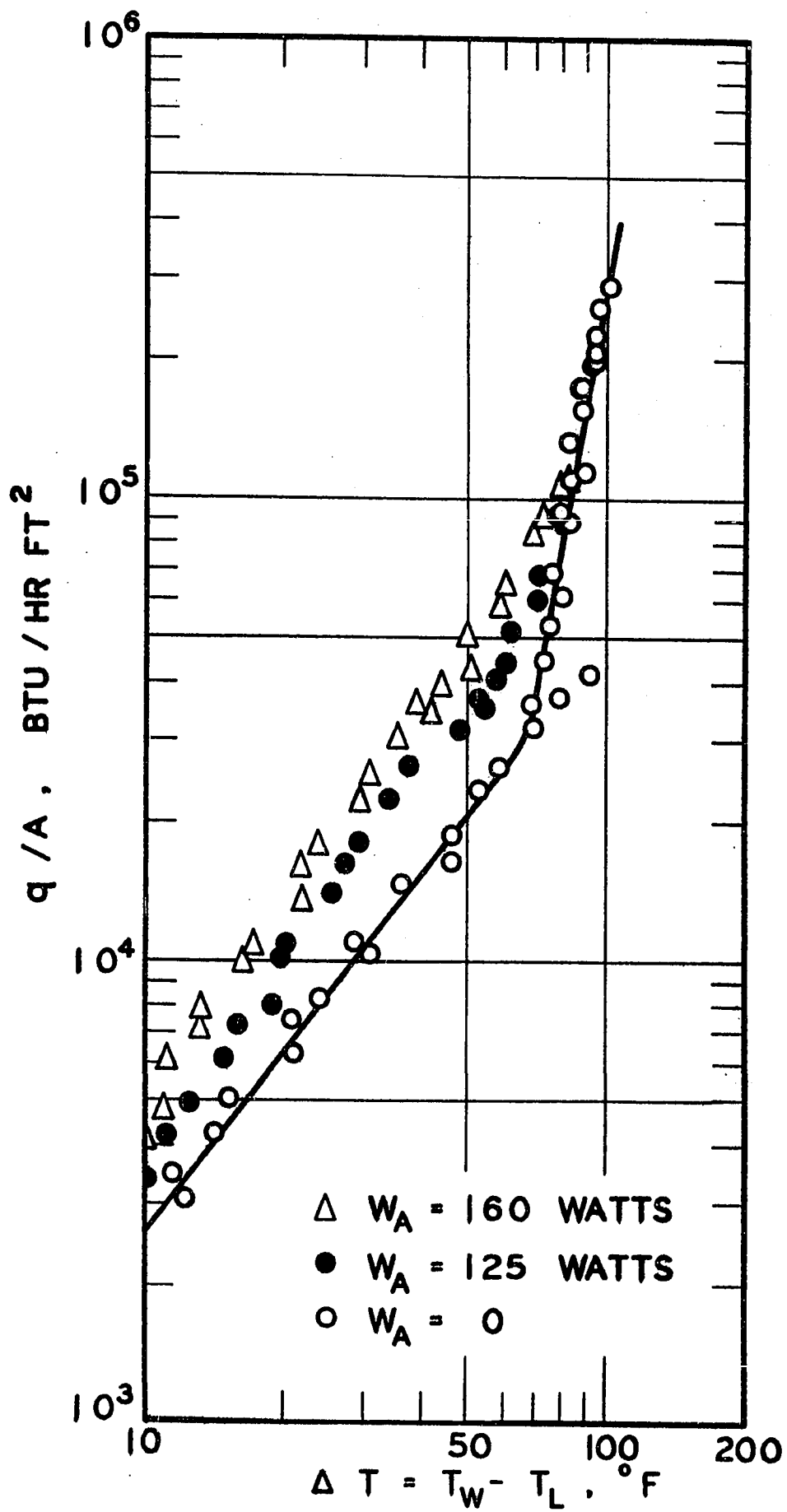
TABLE 1

Values of Percentage Soil Removed at Which

Heat Transfer Data Were Measured

$f = 20.6$ kcps

Figure	Liquid	T_L °F	Percentage Soil Removed		
			$W_A = 15.6$	$W_A = 36.2$	$W_A = 86.0$ watts
6	Distilled Water	149	3.0	12.5	32.0
7	Distilled Water	113	4.0	15.0	34.5
8	Methanol	113	2.3	5.4	13.4
9	Methanol	95	2.7	6.0	14.8

$f = 44.1$ kcps

Figure	Liquid	T_L °F	Percentage Soil Removed			
			$W_A = 15.6$	$W_A = 30.2$	$W_A = 53.3$	$W_A = 96.0$ watts
10	Distilled Water	149	-	3.8	11.9	27.4
12	Methanol	113	2.6	-	6.8	13.3

$f = 108$ kcps

Figure	Liquid	T_L °F	Percentage Soil Removed	
			$W_A = 62$	$W_A = 105$ watts
11	Distilled Water	149	3.9	13.6
13	Methanol	113	3.2	7.4

$f = 306$ kcps

Figure	Liquid	T_L °F	Percentage Soil Removed	
			$W_A = 125$	$W_A = 160$ watts
14	Methanol	113	2.9	7.6

values of apparent electrical power input used in Figures 6 to 14. The experimental data for these figures are given in Appendix D.

Heat transfer experiments without vibration were performed in order to check the experimental techniques and to establish a reference relation with which to compare results when ultrasonic vibrations were used. For data in the natural convection region, the Grashof-Prandtl product and the Nusselt number were calculated and are presented as a plot of Nu versus (Gr x Pr) in Figure 15. The solid line is the best-fitted straight line for the data points and the dashed line is the recommended correlation for single horizontal cylinder in the same range of Grashof-Prandtl product (10 to 150) given by McAdams[5]. The difference in Nusselt numbers from the two lines does not exceed 4%.

The effects of ultrasonic vibrations, as shown in Figures 6 to 14, were to increase the heat transfer rates, and hence the heat transfer coefficients at a given Δt. Depending on the apparent electrical power input as well as the temperature difference, up to 800% increase in heat transfer rates could be obtained. When the test liquid was methanol, regardless of the frequency of the sound field or the liquid temperature, the effects of ultrasonic vibrations diminished as the wire temperature was increased. At wire temperatures corresponding to well-developed nucleate boiling, the effects of ultrasonic vibrations became negligible. It is expected that similar results would be obtained for distilled water if the DC power supply had a larger amperage output. The highest value of heat flux from the wire to distilled water at 149°F was about 6×10^5 BTU/hr ft^2 at a wire current of about 23 amp.

FIGURÉ 15

NATURAL CONVECTIVE HEAT TRANSFER FROM HORIZONTAL

PLATINUM WIRES TO LIQUIDS
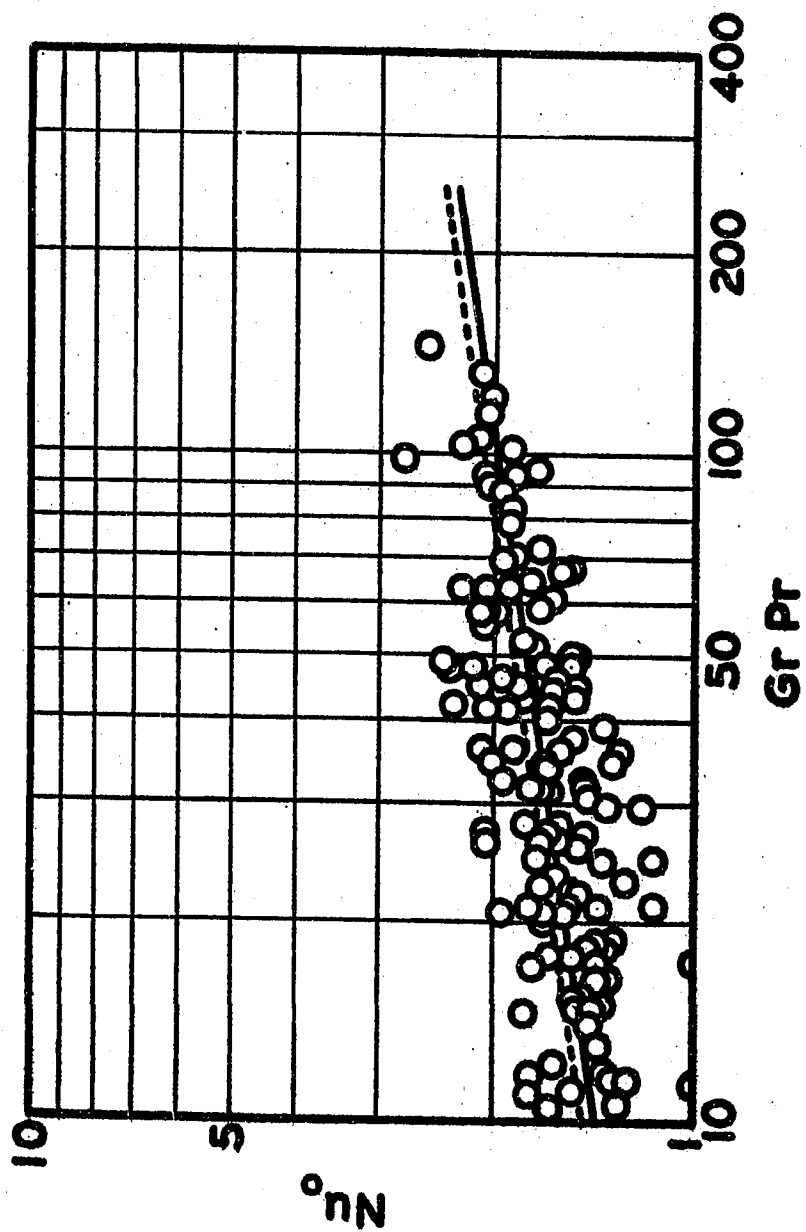
The effect of liquid temperature on heat transfer rates in an ultrasonic field can best be observed by comparing their values in the natural convection region. As shown in Figure 6 where the water temperature was 149°F, the heat flux was increased from 3.0 x 10^4 BTU/hr ft^2, where there was no vibration, to 6.2 x 10^4 BTU/hr ft^2 when the soil removed was 3.0%, both at a temperature difference of 40°F. Namely, the increase was about 100%. For water temperature of 113°F (Figure 7), the heat flux of 2.9 x 10^4 BTU/hr ft^2 without vibration was increased to 4.2 x 10^4 BTU/hr ft^2 with a 4.0% soil removal, resulting in an increase of only 45%. Similar results were obtained for methanol although the increases were lower in the latter case.

The effect of frequency on heat transfer rates in an ultrasonic field cannot be evaluated from the apparent electrical power input to the transducers. The arrangement of transducers at the bottom of the tank was not the same in each case and the efficiency of the transducer system had not been determined. On the basis of cavitation damage, or the percentage of soil removed, higher frequency results in only a slight decrease in heat transfer rates. For the two lower frequencies (20.6 and 44.1 kcps), the effect of frequency was negligible. The increase in heat transfer rate for distilled water at 149°F and at 20.6 kcps with 3.0% soil removal was approximately 100%. At the same liquid temperature and the temperature difference of 40°F, the increase was approximately 70% at 108 kcps with a 3.9% soil removal. Thus, for a fivefold increase in the frequency of the sound field, only a 30% decrease in heat transfer rates resulted for approximately the same value of percentage soil removal. It should be noted, however, that to achieve the

same degree of cavitation damage, more acoustic energy was required at the higher frequency.

High Speed Photography Study

A Fastex High-Speed 16 mm camera (Model WF-3) was used in this study. The framing speed was 4000 frames/sec. The motion picture was taken through the glass window with illumination coming from the top.

In order to make a thorough study on the mechanisms of the heat transfer processes in a sound field, high speed motion pictures were taken at the four different conditions summarized in Table 2. For each set of experimental conditions, motion pictures were taken for both cases, i.e. with and without vibration. Some representative frames from the motion picture are shown in Figures 16 to 19. A 5X enlargement of the image in the motion picture negative which is close to the actual size was made in the printing process. The pictures shown in each figure are from successive frames from the motion picture.

The apparent electrical power input to the transducers was 36.2 watts, in all cases. The resulting sound pressure on the platinum wire therefore exceeded the critical sound pressure. It is to be noted that sound pressure was also much higher than the cavitation threshold of both test liquids so that cavitation bubbles were formed in the bulk liquid as well. The results of the high speed photographic study for methanol will be given first.

TABLE 2

Experimental Conditions Selected for High Speed Photography Study

Apparent electrical power input = 36.2 watts
Frequency of vibration = 20.6 kcps
Filming speed = 4000 frames/sec
Platinum wire diameter = 0.007 in.

	Test Liquid	Liquid Temp. ^{o}F	Without Vibration		Remarks	With Vibration		
			Δt ^{o}F	q/A BTU/hr ft^2		Δt ^{o}F	q/A BTU/hr ft^2	
A	Methanol	113	43	19,400	Natural Convection	22	18,700	(Fig.16)
B	Methanol	113	67	39,200	Nucleate Boiling (Isolated Bubbles)	42	37,700	(Fig.17)
C	Methanol	113	81	167,000	Nucleate Boiling (Well-developed)	81	167,000	(Fig.18)
D	Distilled Water	149	121	229,000	Nucleate Boiling (Isolated Bubbles)	50	209,000	(Fig.19)

FIGURE 16

CAVITATION BUBBLE MOTION ON A HEATED WIRE
WIRE DIAMETER = 0.007 in.

FREQUENCY OF VIBRATION = 20.6 kcps,

W_A = 36.2 watts; METHANOL AT 113°F WITH

Δt = 22°F AND HEAT FLUX = 18,700 BTU/HR FT^2
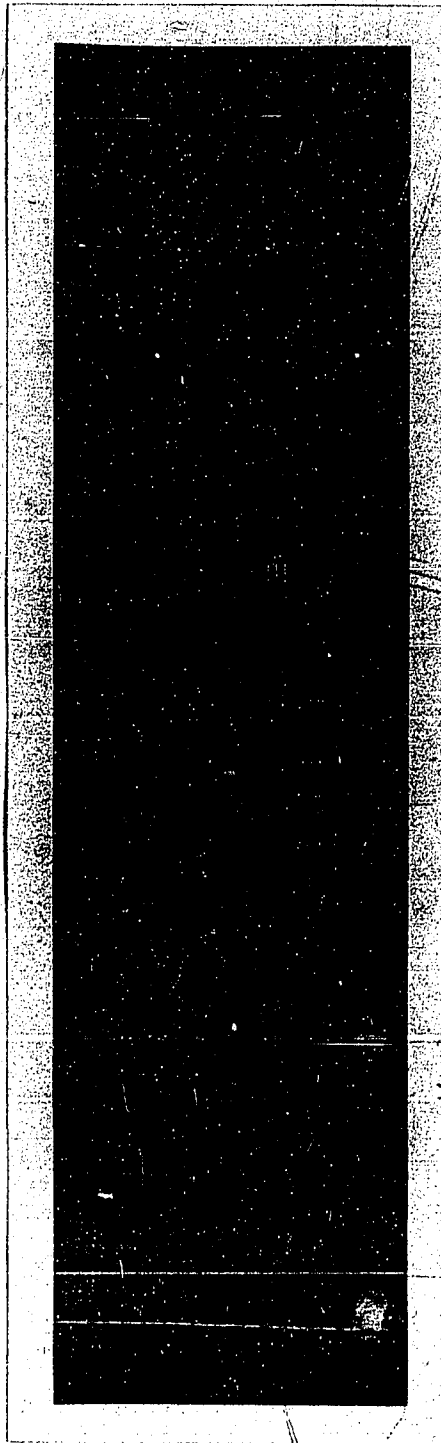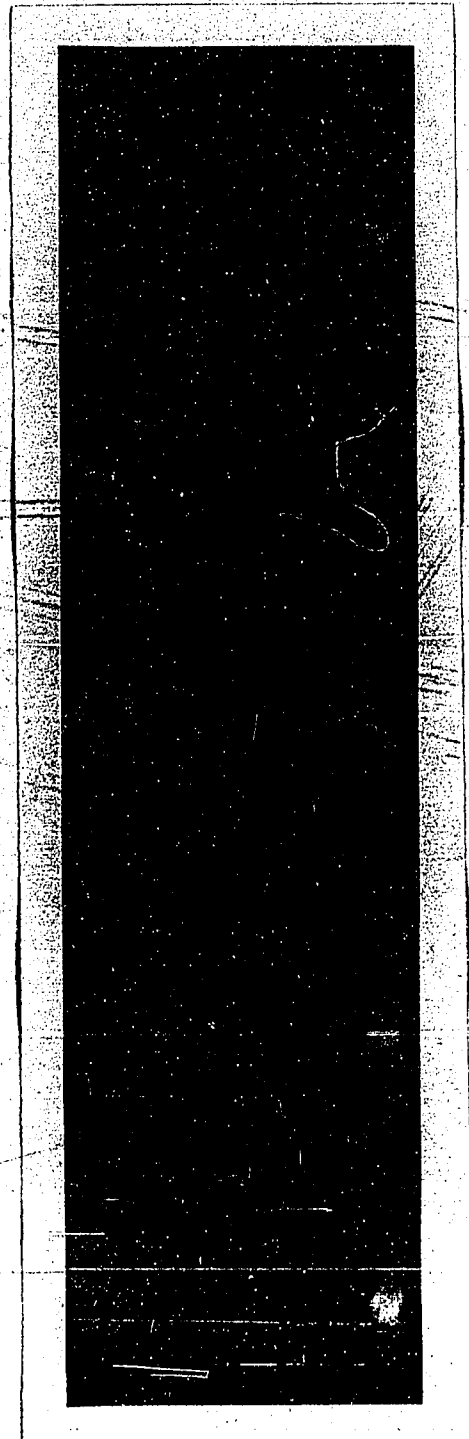
A1   A2

A1
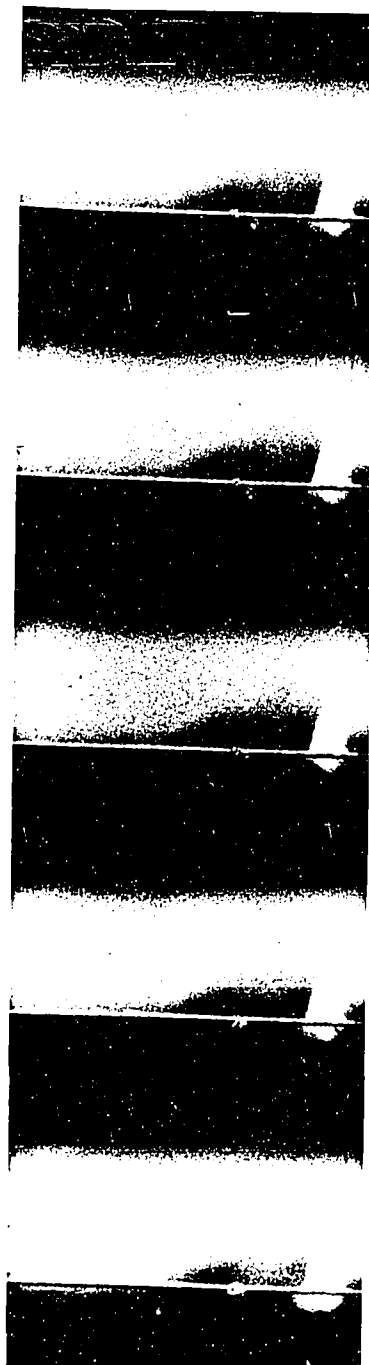
A2
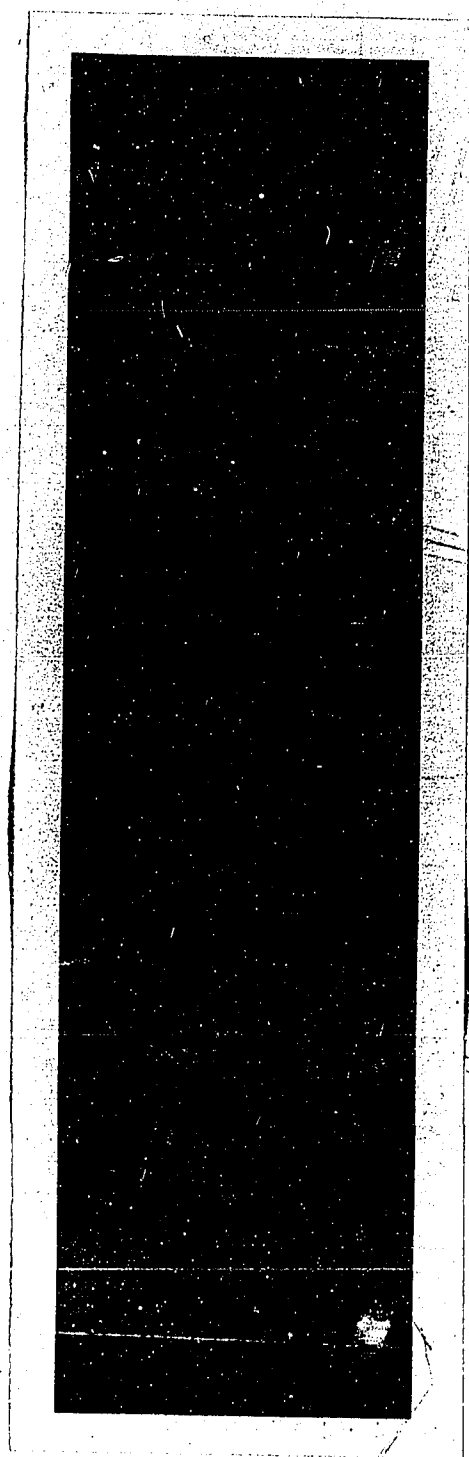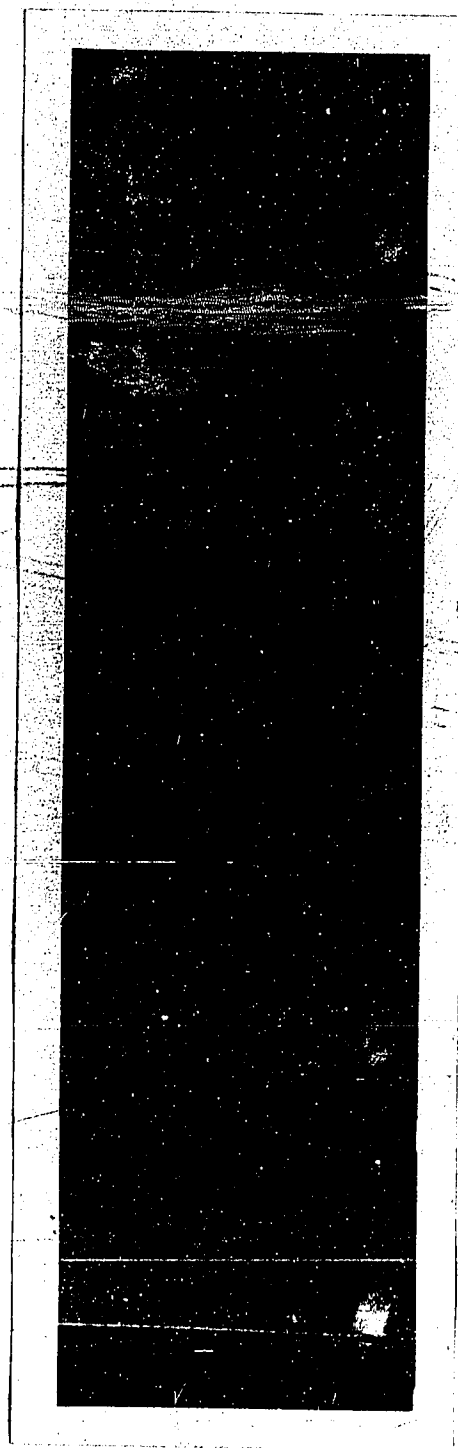
A3   A4
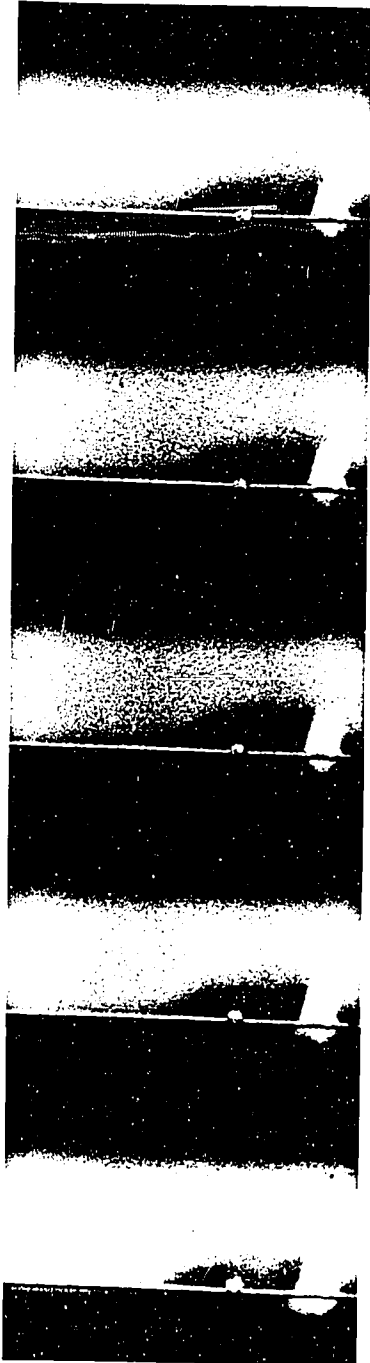
A3
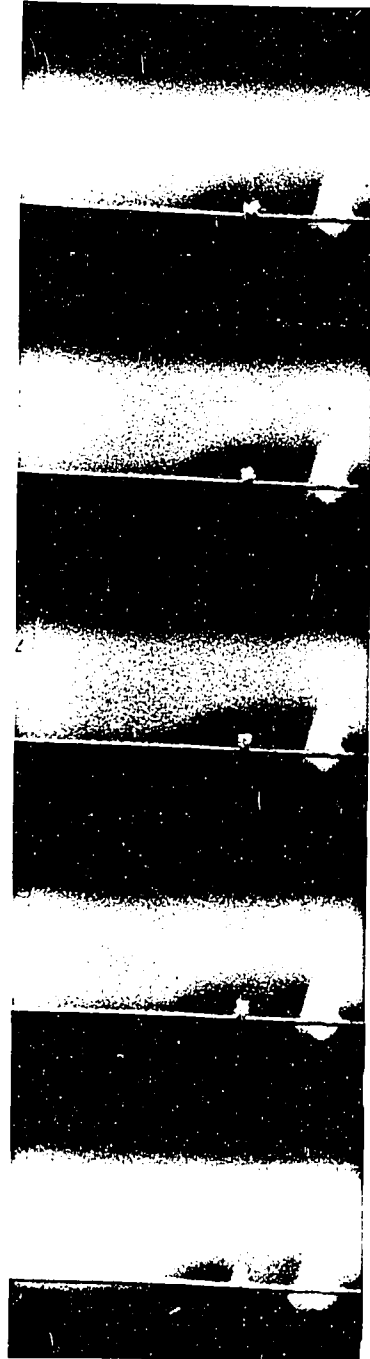
A4

FIGURE 17

CAVITATION BUBBLE MOTION ON A HEATED WIRE

WIRE DIAMETER = 0.007 in.

FREQUENCY OF VIBRATION = 20.6 kcps,

W_A = 36.2 WATTS. METHANOL AT 113°F WITH

$\triangle t$ = 42°F AND HEAT FLUX = 37,700 BTU/HR FT^2

121

B1   B2

123

B1

B2
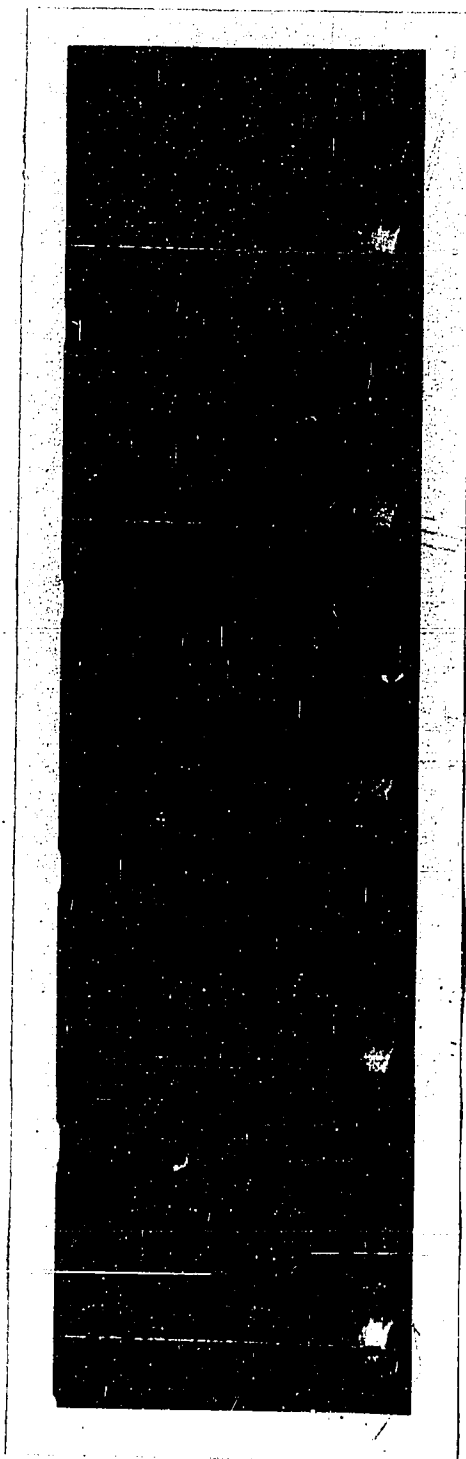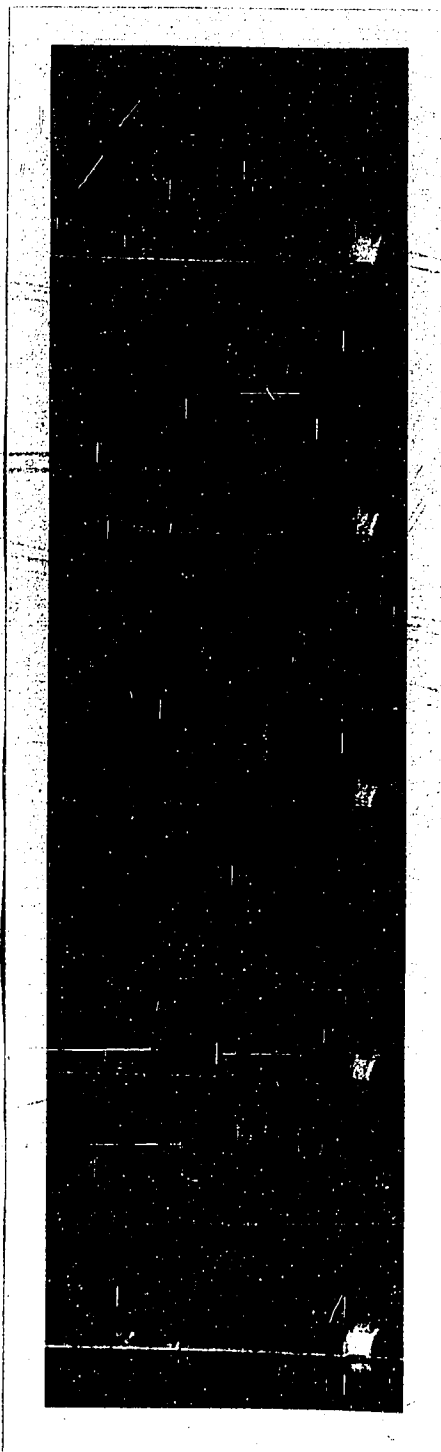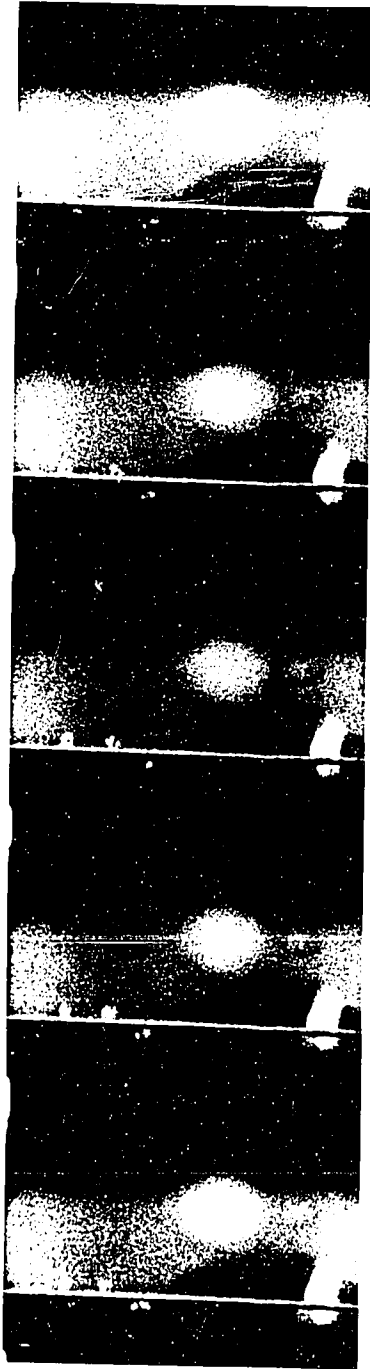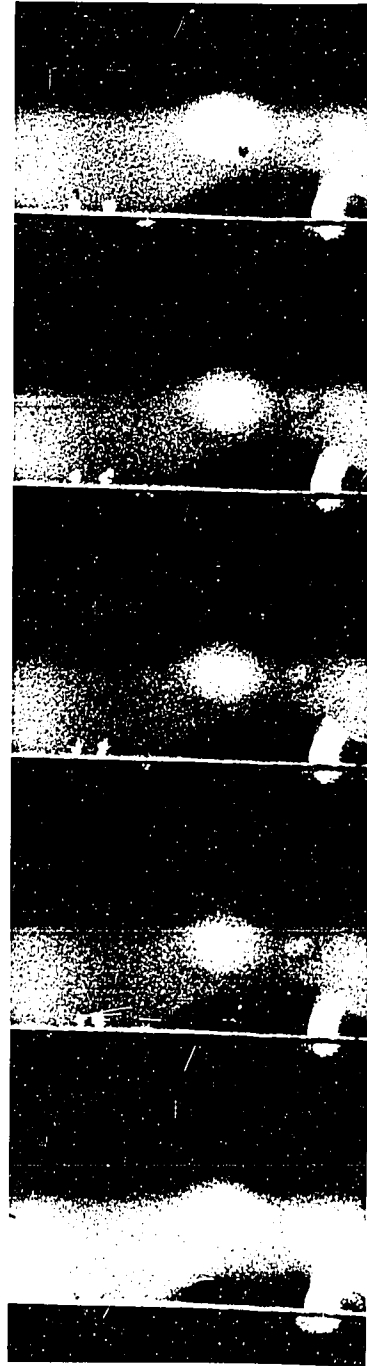
122
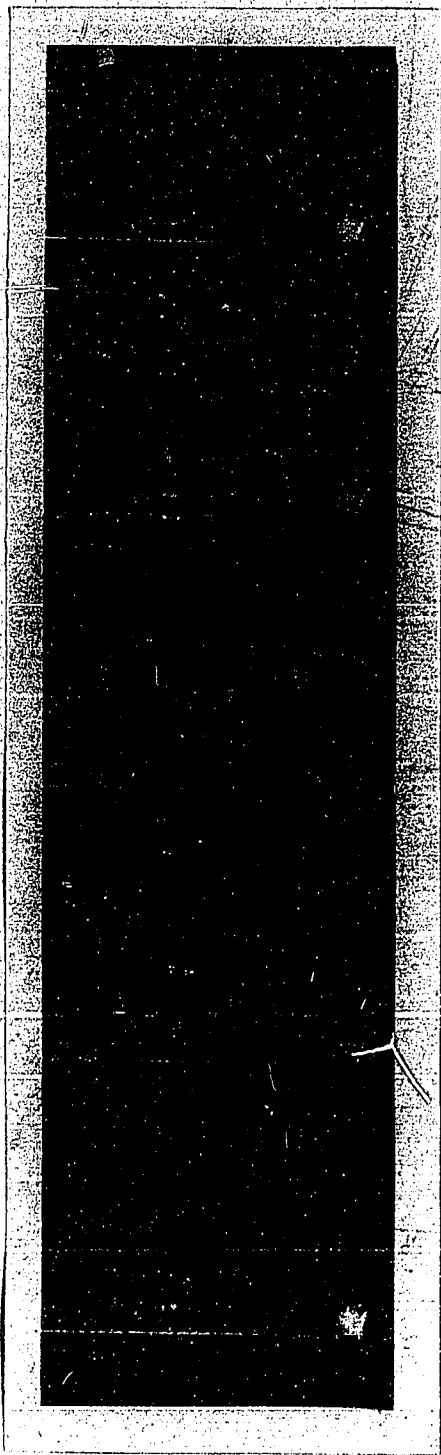
B3
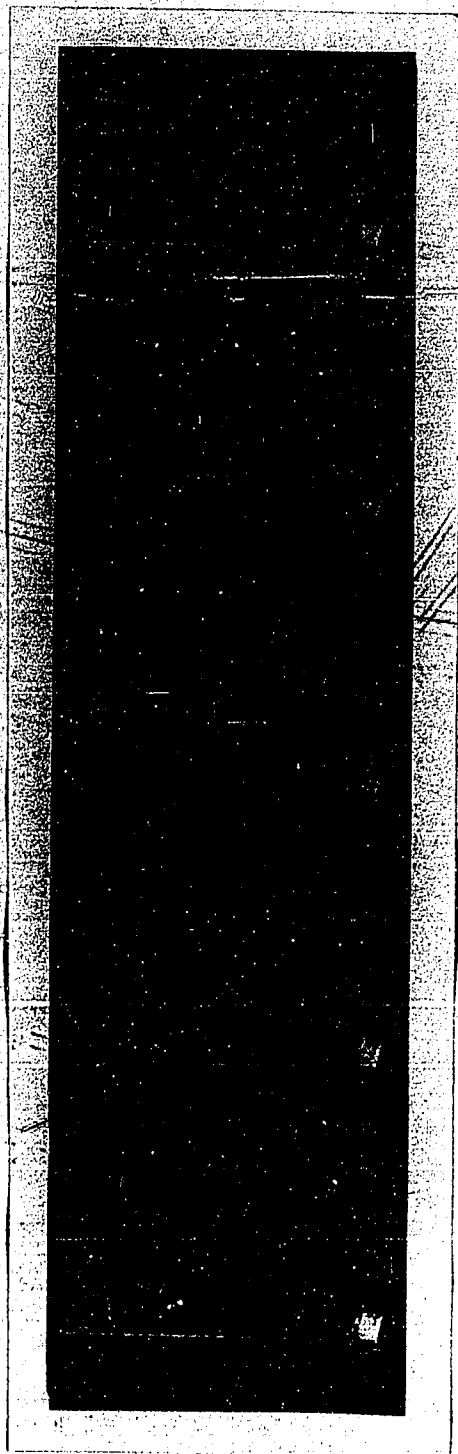
B4
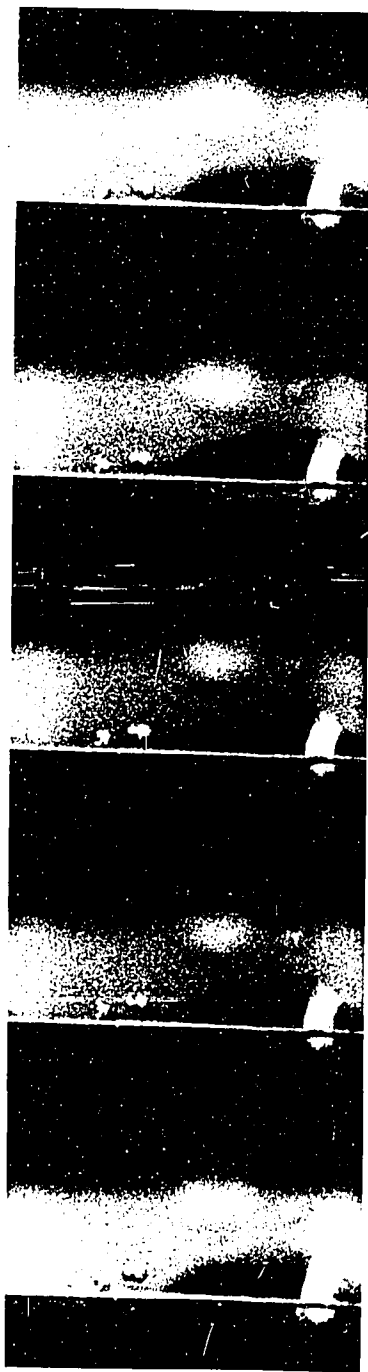
B3
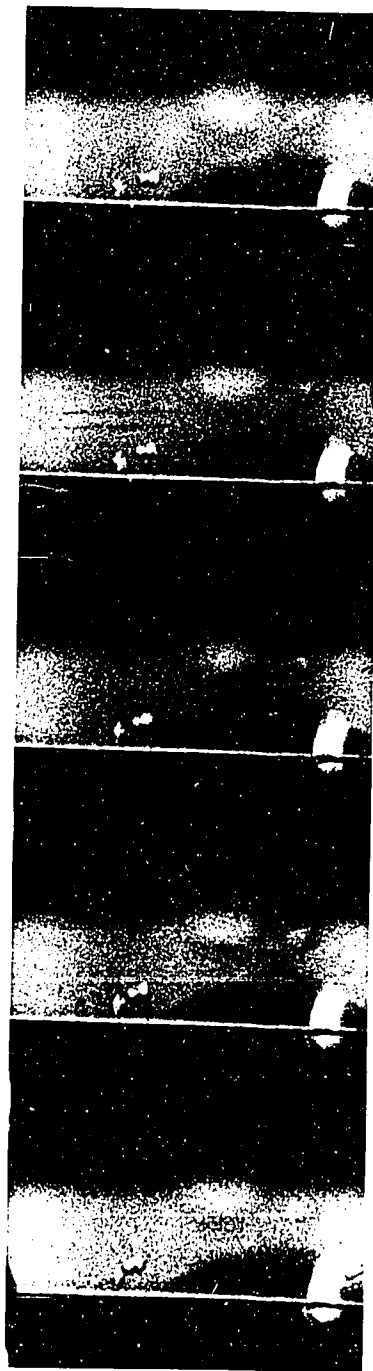
B4

FIGURE 18

CAVITATION BUBBLE MOTION ON A HEATED WIRE

WIRE DIAMETER = 0.007 in.

FREQUENCY OF VIBRATION = 20.6 kcps,

W_A = 36.2 WATTS: METHANOL AT $113^{\circ}F$ WITH

$\triangle t$ = $81^{\circ}F$ AND HEAT FLUX = 167,000 BTU/HR FT^2

C1   C2

C1   C2

124
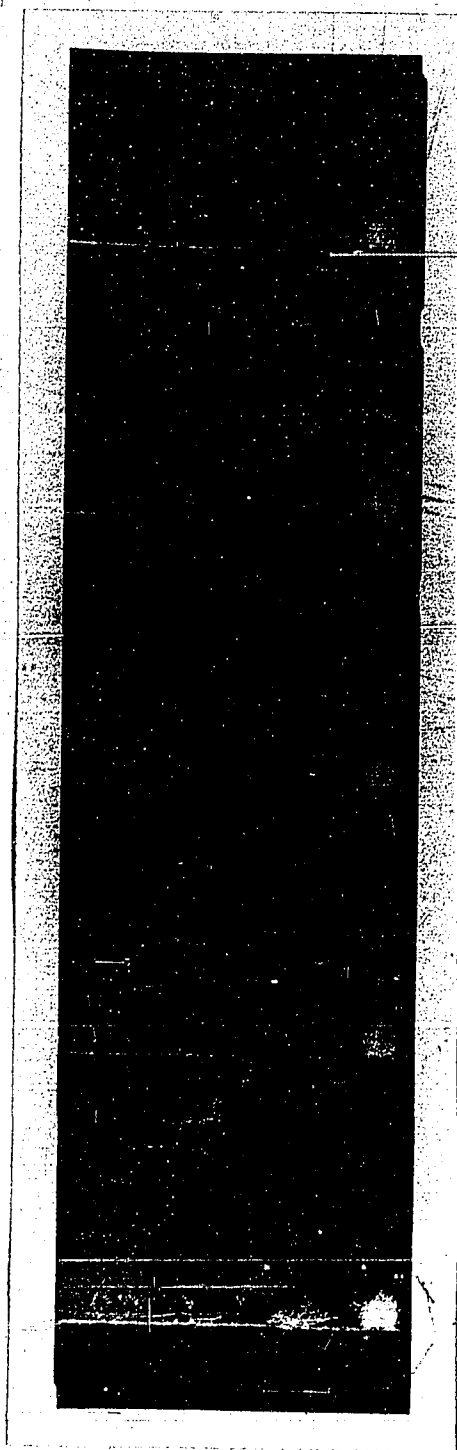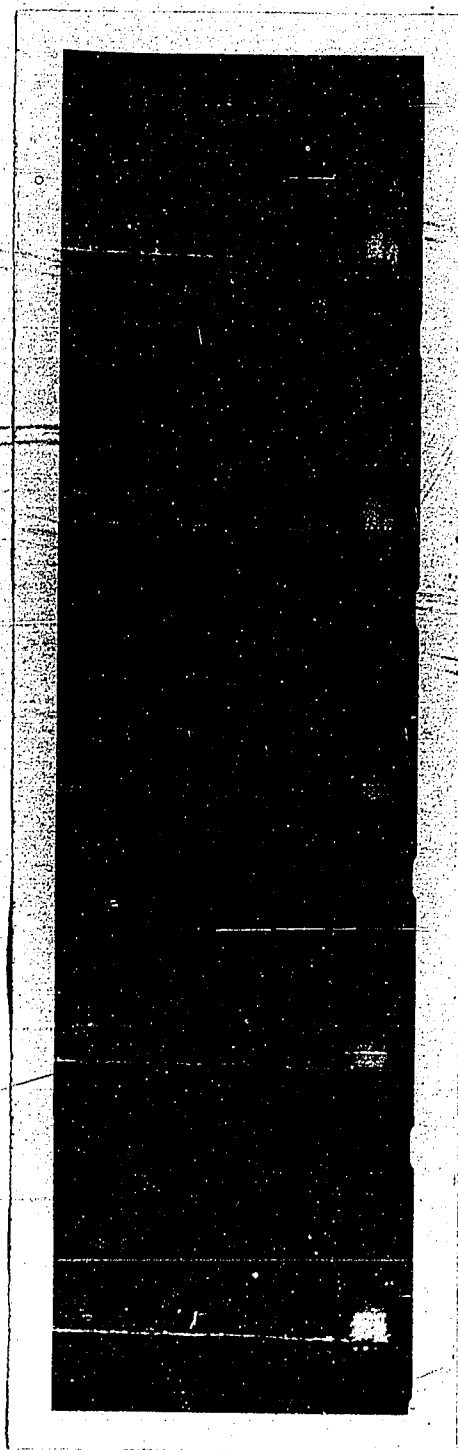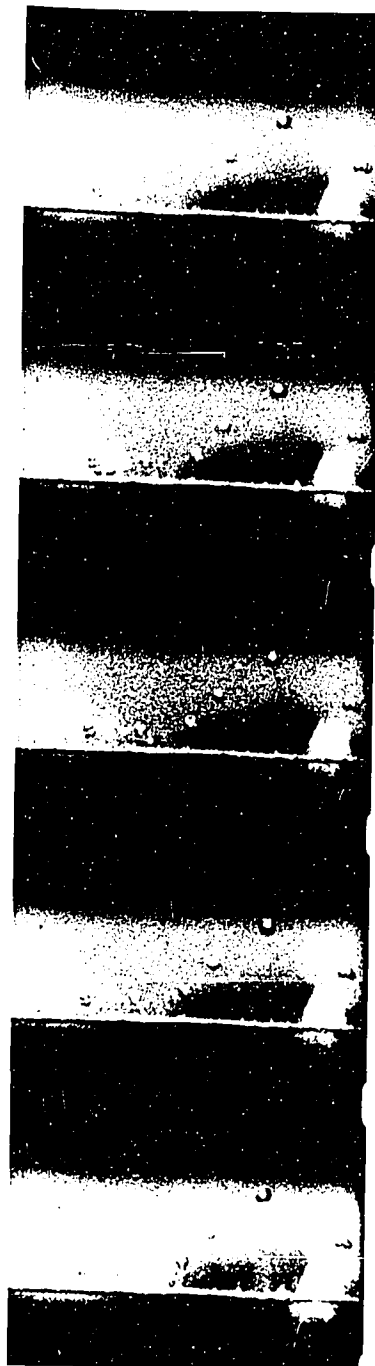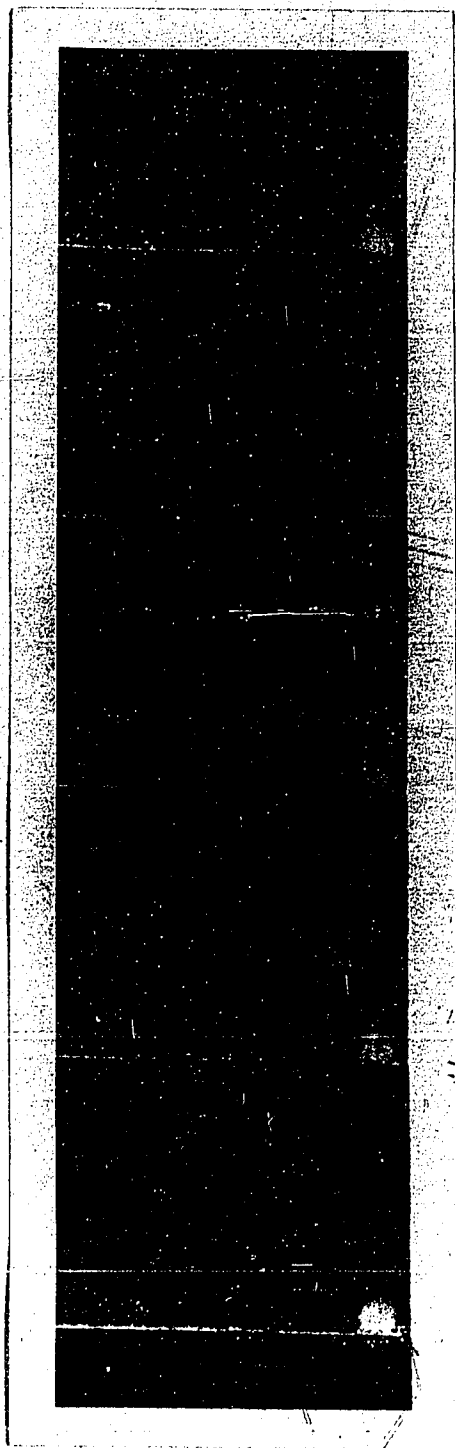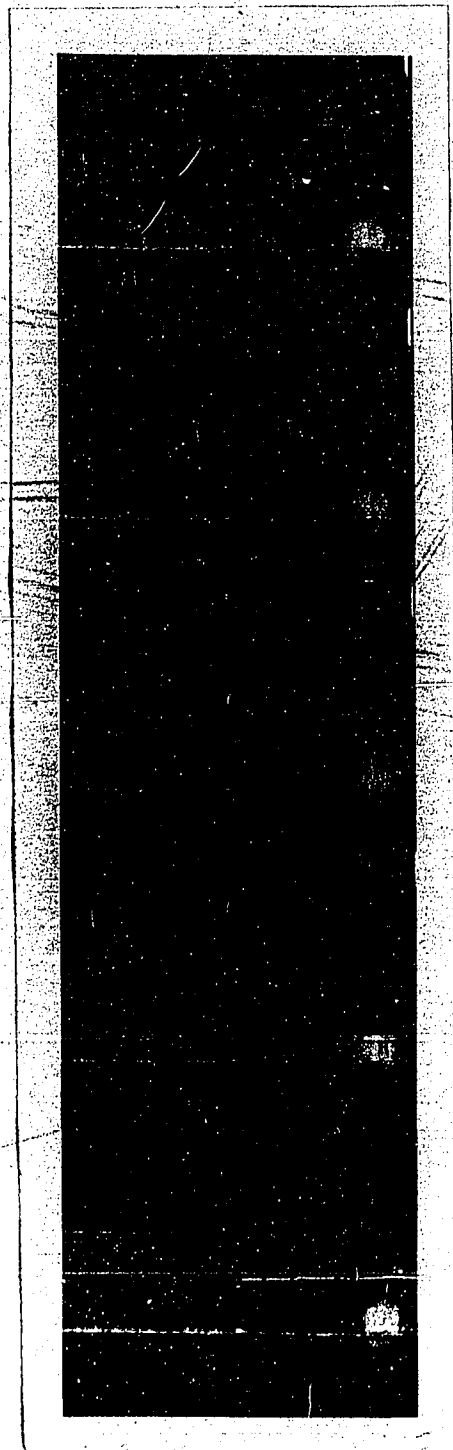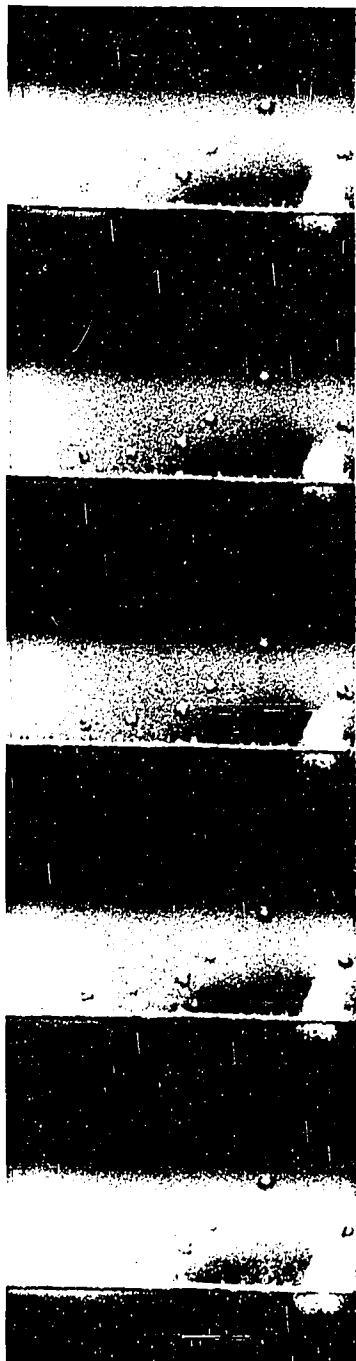
C3   C4
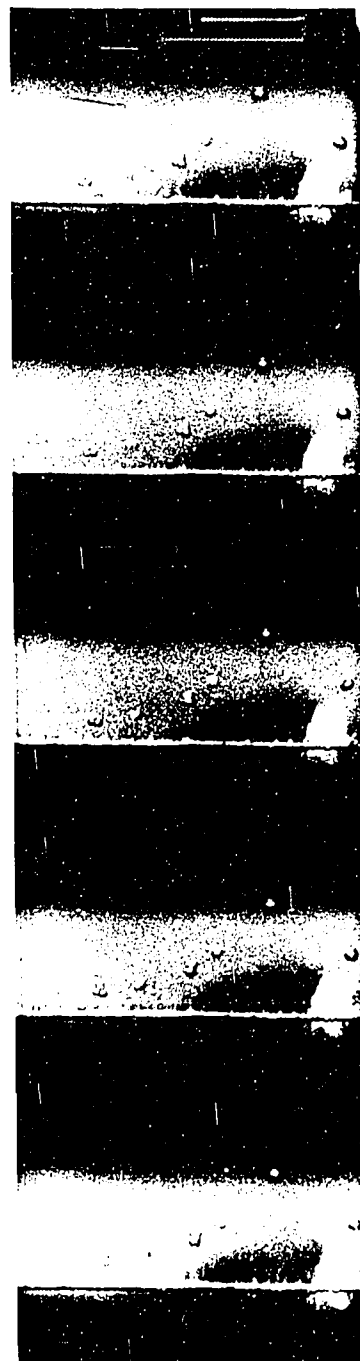
C3   C4

FIGURE 19

CAVITATION BUBBLE MOTION ON A HEATED WIRE

WIRE DIAMETER = 0.007 in.

FREQUENCY OF VIBRATION = 20.6 kcps;

W_A = 36.2 WATTS: DISTILLED WATER AT 149°F

WITH Δt = 50°F AND HEAT FLUX = 20,900

BTU/HR FT^2

D1   D2

D1

D2

126
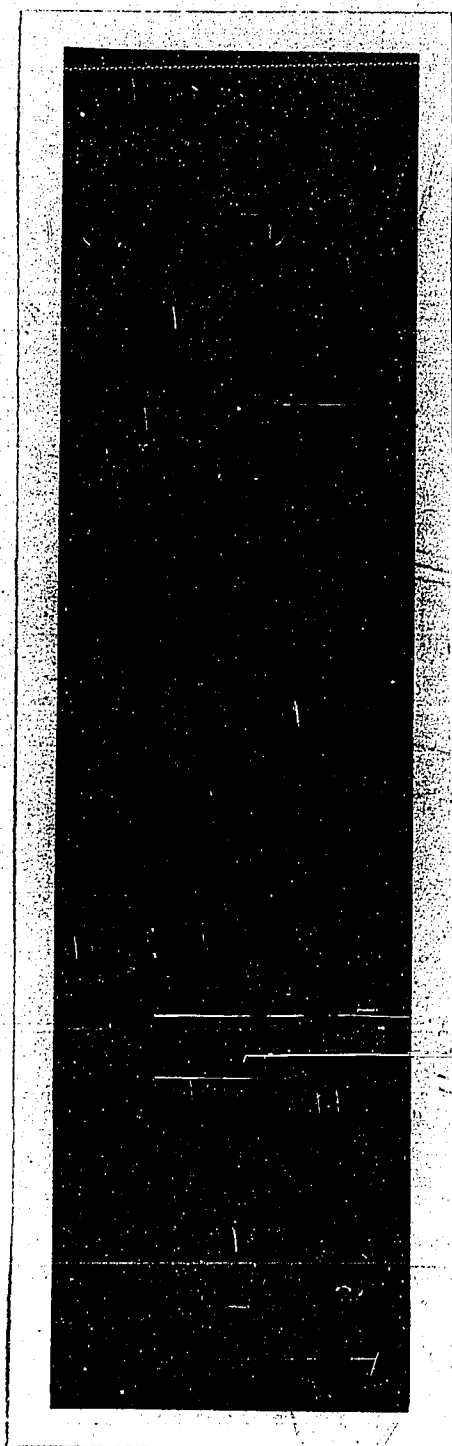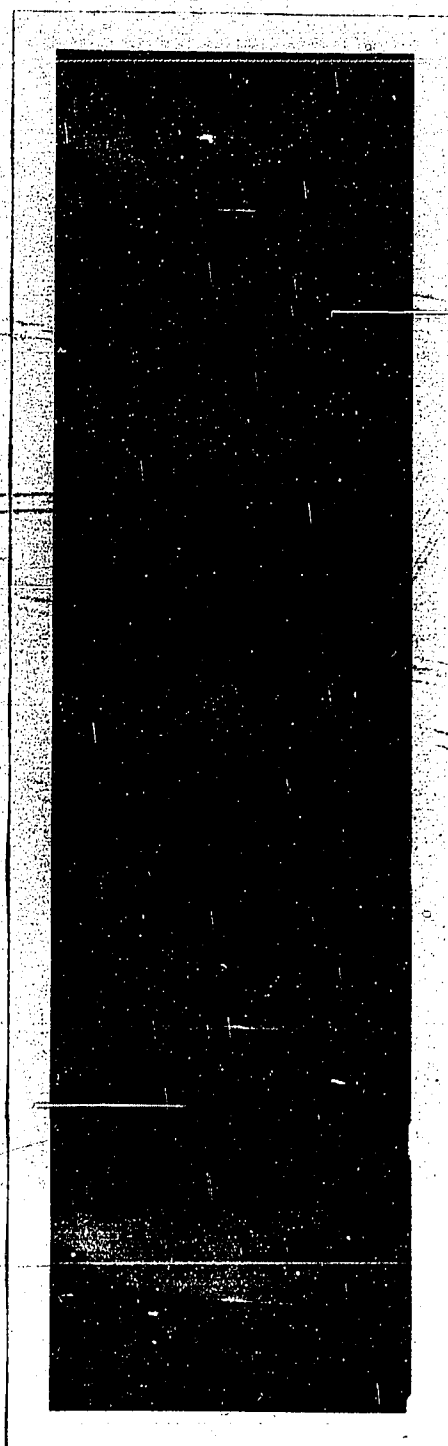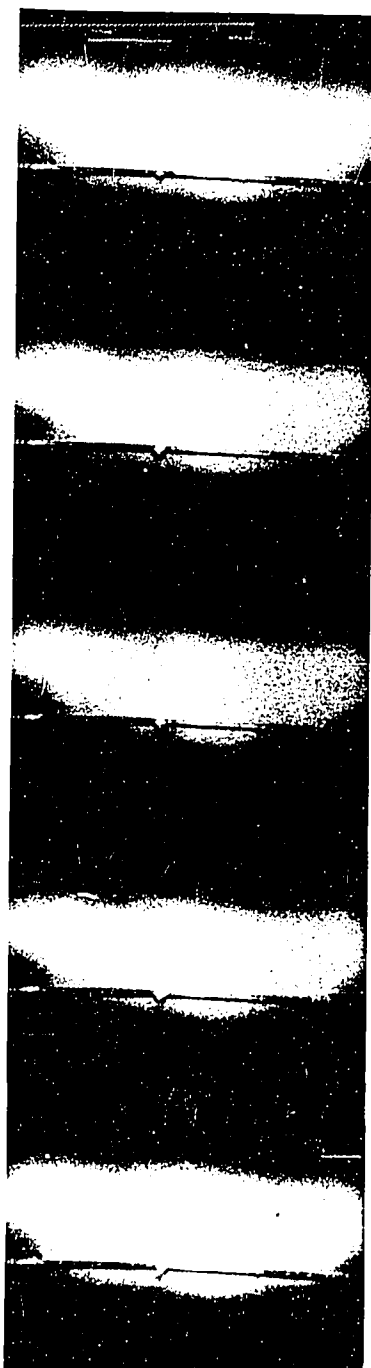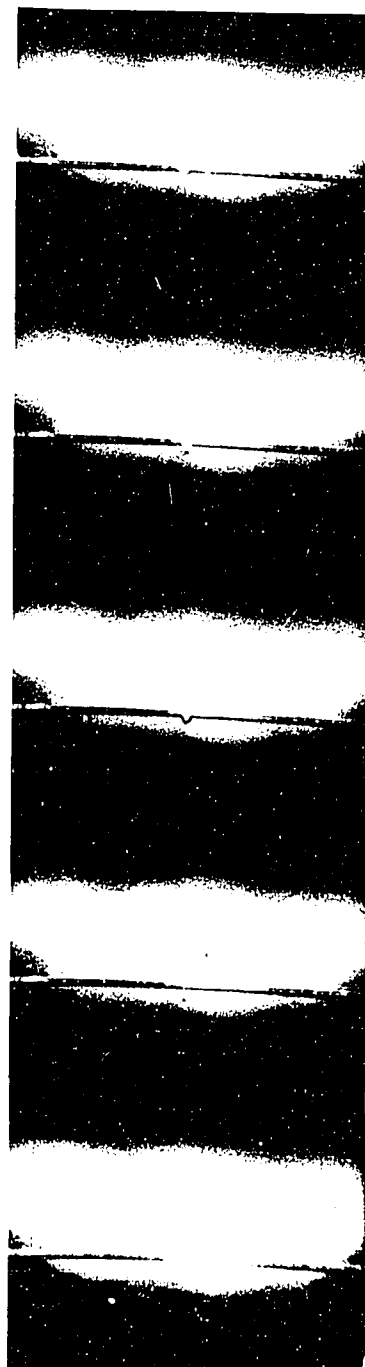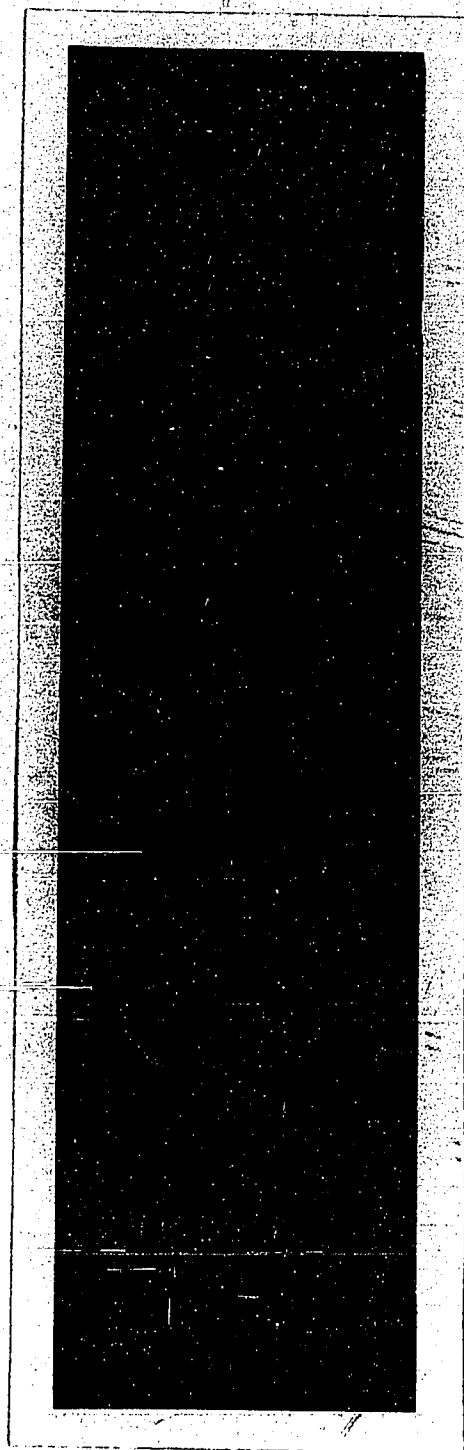
D3   D4
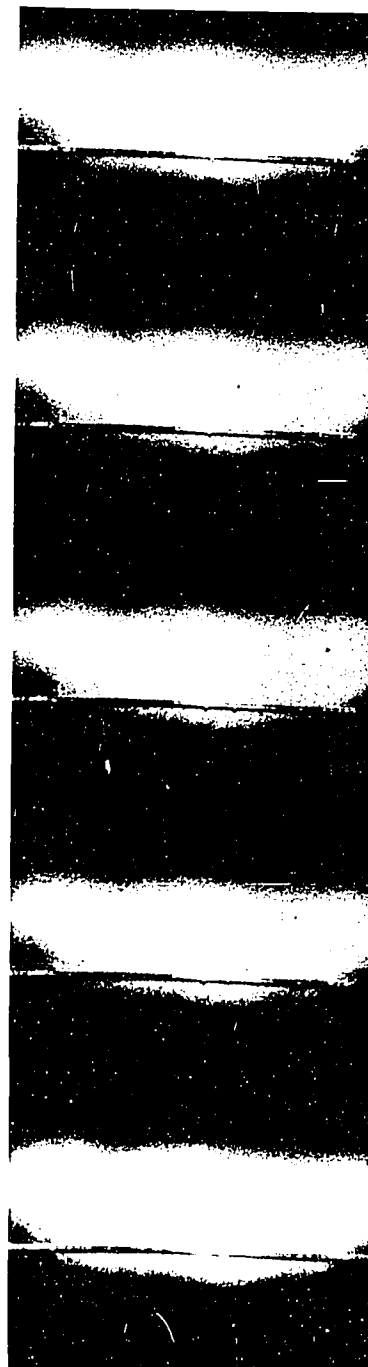
D3   D4

It appeared that there was no particular site from which cavitation bubbles would grow. Small cavitation bubbles usually appeared first on the lower portion of the wire, and as they grew larger, moved to the upper portion of the wire. Small cavitation bubbles usually grew to larger sizes and left the wire by one of the following mechanisms:

(1) They rolled along the wire, grew in size by agglomerating with other smaller cavitation bubbles, and eventually left the wire. This is illustrated in Figure 17. The two cavitation bubbles on the wire in B1 moved toward each other, agglomerated in the last frame of B2, and left the wire surface 3.8 msec later, that is, five frames after the last frame in B4 where the 'big' cavitation bubble - a cluster of cavitation bubbles sticking together - further agglomerated with another cavitation bubble.

(2) While they were rolling along the wire and agglomerating with small cavitation bubbles, a cavitation bubble originated from the bulk liquid migrated to the wire, agglomerated with the cavitation bubble on the wire, and the resulting 'big' cavitation bubble left the wire. This process is illustrated in Figure 16. The lower bubble in the first frame of A1 was a cavitation bubble originating in the bulk liquid. It agglomerated with the cavitation bubble on the wire in the third frame of A2 and left the wire after 4 msec. The same process is also illustrated in Figure 17 where the cavitation bubble which appeared underneath the wire in the first frame of B1 was originated from the bulk liquid.

The motion of cavitation bubbles on the wire surface was rather erratic and rapid. The directions of rolling were not always the same. A cavitation bubble could start rolling in one direction on the wire and then in the opposite direction a moment later, or it could settle on a particular spot after rolling along the wire for a short distance. Consequently, it was impossible to establish any definite pattern of the bubble motion. Also, the cavitation bubble did not necessarily roll on the upper surface of the wire. This can be seen in Figure 16 -A1 where the cavitation bubble was on the lower surface of the wire. It began to move around the wire and was on the upper surface in A4. As the temperature of the wire increased, the population of cavitation bubbles on the wire and their activities also increased. The bubbles were moving at a great speed and their motion was much more erratic. However, at wire temperatures corresponding to the well developed nucleate boiling region, as shown in Figure 18, the growth and collapse of vapor bubbles which was observed when there was no vibration were still occurring on the wire surface. It appears that the formation of cavitation bubbles only took place above the wire which was partially covered with vapor bubbles.

Another point of interest is that there existed a high degree of radial oscillation in all cavitation bubbles as they rolled on the wire surface. This is shown by the frosted appearance and the non-spherical shape of cavitation bubbles in all photographs. It can be seen that 'big' cavitation bubbles were composed of clusters of small bubbles sticking together. The clusters of small cavitation bubbles

would coalesce and become smooth and spherical only after they left the wire surface. This is illustrated in Figure 18. In the first frame of Cl, a 'big' cavitation bubble, whose previous history was similar to the three cavitation bubbles which appeared near the wire in the same frame, can be seen above the wire surface and near the right end of the wire. They did not coalesce together until after the third frame of C3, although partial coalescence did occur somewhere in the last frame of Cl. Unlike vapor bubbles due to boiling, the smooth spherical bubbles so generated did not appear to collapse into the liquid.

Since no preferential site from which a cavitation bubble would grow could be observed, it would be impossible to determine the frequency of generation of the cavitation bubbles. A frame-to-frame analysis showed that, regardless of the wire temperature, the diameter of the cavitation bubbles when leaving the surface was quite constant. The diameters of eight cavitation bubbles which were measured after they had left the wire surface and coalesced to form smooth spheres were all within the range of 0.018 to 0.021 in. They were larger than the diameters of vapor bubbles due to boiling which varied from 0.01 to 0.02 in. The determination of the vapor bubble diameters, however, was much more difficult since most of the vapor bubbles collapsed on the wire surface. An effort was also made to determine the speed of the motion of cavitation bubbles in the natural convection region (Case A). It was found that the smaller the bubble, the higher the speed. When the diameter was approximately 0.02 in., the speed which was measured when the cavitation bubble was moving continuously in one direction only,

varied from 0.8 to 1 ft/sec.

Figure 17 also provides an opportunity of studying the characteristics of the young cavitation bubbles. The first one which was present throughout the twenty frames of Figure 17 was a small bubble which appeared on the lower surface and near the center of the wire. The second one seemed to appear first in the first frame of B3, growing from the lower surface of the wire about midway between the two 'big' cavitation bubbles. It became quite visible in the last frame of B3. In both bubbles, the radial oscillation which was characteristic of the 'big' cavitation bubbles did not seem to exist. However, the lifetimes of these young bubbles were usually very short as they soon agglomerate with other bubbles rolling on the wire.

When distilled water at 149°F was used and there was no vibration, the vapor bubbles due to boiling were larger and they collapsed more rapidly. The average vapor bubble diameter assuming a hemispherical bubble was about 0.03 in. The lifetimes which varied from 0.25 to 0.5 msec were about half of that for vapor bubbles in methanol at 113°F.

The cavitation bubble behaviour in water was radically different from that in methanol as the cavitation bubbles collapsed almost completely on the wire surface. It differed from the case without vibration in that small bubbles with diameters from 0.002 to 0.005 in. were always observed to remain on the wire surface after the collapse of a cavitation bubble, serving as nucleus from which a new cavitation bubble began to grow. It was observed that, before its collapse, the bubble was also travelling on the wire at a relatively high speed. The

result was a local explosion in the superheated liquid layer around the wire. One could see in the high speed motion pictures the turbulence generated in the liquid as the result of such explosions. Occasionally, a cavitation bubble originating in the liquid migrated to the wire and coalesced with a bubble on the wire. The resulting bubble also collapsed. The average size of a cavitation bubble before its collapse was about 0.015 in., but some of them were as large as 0.03 in. The lifetime varied from 0.7 to 2 msec. The speed based on three bubbles varied from 2 to 3 ft/sec.

Figure 19 illustrates some of the phenomena described above. The cavitation bubble which was in the first frame of D1 grew in size and at the same time moved toward the center of the wire until in the third frame of D2 it collapsed. It can be seen, however, that it did not collapse completely. A small bubble was observed in the same location where the big cavitation bubble had collapsed and it migrated to the wire surface almost immediately to form a new nucleus from which another cavitation bubble grew. Consequently, the same process was observed to repeat itself, starting from the last frame of D2 to the last frame of D3. The lifetimes of these cavitation bubbles varied widely as demonstrated by the two cavitation bubbles just mentioned. The distance that the first cavitation bubble travelled between the first frame of D2 to the second frame of D3 was about 0.035 in. The speed was then calculated to be approximately 2 ft/sec. The cavitation bubbles also exhibited radial oscillations although the amplitudes were not as high as the cavitation bubbles in methanol.

The results of the high speed photographic study then show that the formation as well as the motion of the cavitation bubbles on the heated wire surface were random and erratic processes. Under the present experimental conditions, it was difficult to make any statistical study of the cavitation bubble behaviour from the high speed motion picture. The numerical values given for the diameters and the speed of the cavitation bubbles in this section are approximate values and should be regarded as a qualitative indication of magnitudes involved.

DISCUSSION OF EXPERIMENTAL RESULTS

High Speed Photography Study

The cavitation bubble behaviour observed in methanol was radically different from that observed in distilled water. Before discussing some of the details of the results, it will prove convenient to establish first whether the cavitation bubbles generated in each liquid are gaseous or vaporous cavitation bubbles.

Barger[7] studied the acoustic cavitation of water in a focussed standing wave system and described his observations of gaseous cavitation in the following manner:

" The single bubble that was formed at the center (the focal region) gradually increased in size with time. It had a very clear spherical surface. This bubble seemed to grow even when no new small bubbles were being added to it. After a period of time, which could be as long as one minute, this bubble suddenly developed a frosted appearance and began to dance around, executing an erratic and rapid motion about the center of the sphere. This behaviour was observed to begin when the bubble radius was about equal to the resonance size at the driving frequency*. After a few seconds of this behaviour, this bubble was rapidly ejected from the center radially outward. It slowed down and came to rest at the nearest pressure node. As it came to rest its surface became smooth and clear again."

These observations compare favourably with the results obtained here for methanol.

* See Eq. (1), page 134

It was observed that the young bubbles on the wire did exhibit a clear spherical surface. The lifetimes of these young bubbles were very short as they agglomerated with other cavitation bubbles rolling on the wire surface or migrated from the bulk liquid. The 'big' cavitation bubbles also exhibited a frosted appearance and rolled on the wire in a random and erratic manner. After they left the wire surface, coalescence of the bubbles took place and their surface became spherical and smooth again.

According to Barger[7], the erratic behaviour of the bubble was observed when the bubble radius was about equal to the resonance size at the driving frequency. The resonance radius R_o of an air bubble in a liquid is given to the first approximation by[8]

$$R_o = \frac{0.326 \, P_o^{1/2}}{f \, \rho_L^{1/2}} \qquad (1)$$

where R_o equilibrium radius of the bubble, cm

      P_o ambient pressure, atm

      ρ_L density of the liquid, g/cm^3

      f driving frequency, kcps.

Equation (1) involves the assumption of $P_o \gg 2\tau/R_o$ which is valid as all experiments were performed under atmospheric conditions (τ is the surface tension of the liquid).

The resonance diameter based on Equation (1) for methanol at a frequency of 20.6 kcps was calculated to be 0.014 in. It was difficult under the present experimental conditions to determine the bubble size at which the erratic behaviour of the bubble was first observed.

The bubble diameter after leaving the wire surface should be greater than the resonance size and was measured to be approximately 0.02 in. It appears that the cavitation bubbles in methanol are similar to gaseous cavitation bubbles. As they did not collapse in the liquid, the contents of these bubbles must be mainly gas.

The interpretation of the results of the high speed photographic study for methanol becomes straightforward if the cavitation bubble was taken to be a gaseous cavitation bubble. A cavitation bubble is formed from a small surface crack or scratch on the wire surface. It may also have originated in the liquid containing a nucleus such as dust particles near the wire and then migrated to the wire. The latter mechanism seems to be the more important one as most cavitation bubbles appeared to have originated from the lower surface of the wire. This is because the temperature of the liquid near the lower surface of the wire is lower than that above the wire. The result is a higher dissolved gas content in the liquid near the lower wire surface. The bubble is believed to grow by the rectified diffusion mechanism as suggested by Hsieh and Plesset[9], that is, gas will diffuse out of the bubble in the compression period of the acoustic cycle and diffuse into the bubble in the tension period of the acoustic cycle; a net increase of gas in the bubble resulted because the surface area in the tension period is larger than the compression period in an acoustic cycle. Before it grows to the resonance size, it usually agglomerates with other cavitation bubbles. As the bubble approaches the resonance size the amplitude of oscillation will increase. This corresponds to the observation that

The bubble diameter after leaving the wire surface should be greater than the resonance size and was measured to be approximately 0.02 in. It appears that the cavitation bubbles in methanol are similar to gaseous cavitation bubbles. As they did not collapse in the liquid, the contents of these bubbles must be mainly gas.

The interpretation of the results of the high speed photographic study for methanol becomes straightforward if the cavitation bubble was taken to be a gaseous cavitation bubble. A cavitation bubble is formed from a small surface crack or scratch on the wire surface. It may also have originated in the liquid containing a nucleus such as dust particles near the wire and then migrated to the wire. The latter mechanism seems to be the more important one as most cavitation bubbles appeared to have originated from the lower surface of the wire. This is because the temperature of the liquid near the lower surface of the wire is lower than that above the wire. The result is a higher dissolved gas content in the liquid near the lower wire surface. The bubble is believed to grow by the rectified diffusion mechanism as suggested by Hsieh and Plesset[9], that is, gas will diffuse out of the bubble in the compression period of the acoustic cycle and diffuse into the bubble in the tension period of the acoustic cycle; a net increase of gas in the bubble resulted because the surface area in the tension period is larger than the compression period in an acoustic cycle. Before it grows to the resonance size, it usually agglomerates with other cavitation bubbles. As the bubble approaches the resonance size the amplitude of oscillation will increase. This corresponds to the observation that

the bubble surface developed a frosted appearance. The bubble becomes very unstable and starts its erratic and rapid motion on the wire surface. This is further complicated by the local temperature fluctuations as well as the uneven pressure distribution on the wire. Further agglomerations occurred and eventually the bubble leaves the surface. The bubble has now grown to be much larger than its resonance size, the amplitude of its oscillation is smaller, and the bubble becomes spherical and smooth again.

Attempts have been made to establish a pattern of the motion of the cavitation bubbles on the wire and were unsuccessful as the motion was rapid and erratic. The motion did not appear to be related to the sound pressure distribution on the wire although the latter might have affected them.

The cavitation bubbles generated in distilled water collapsed on the wire surface and their lifetimes were much shorter. The collapse of these bubbles indicated that their contents were mainly vapor. Barger[7] also studied vaporous cavitation in water at 27 kcps and described his visual observations of the vaporous cavitation bubble as a small comet whose total length was as long as 1.2 in. with a maximum diameter of 0.4 in. near the tail. Similar descriptions were given by Lieberman[10] for a vaporous cavitation bubble at a frequency of 26.3 kcps. The dimensions of the vaporous cavitation bubbles were observed to be approximately inversely proportional to the square of the driving frequency. The diameters of the cavitation bubbles observed in this work were about 0.010 in. and the length which was calculated from

the product of its lifetime and the speed was about 0.05 in., both of which are more than an order of magnitude smaller. The sound pressure levels employed in this work, although not measured directly, were much lower than the vaporous cavitation threshold reported by other investigators. It is then postulated that a new type of cavitation bubble is generated when it is formed on a heated surface in an acoustic pressure field. It has the characteristics of a gaseous cavitation bubble as was demonstrated by the behaviour of the cavitation bubble in methanol. The content of this new type of cavitation bubble which may be called the gaseous-vaporous cavitation bubble depends on the dissolved gas content as well as the vapor pressure of the liquid. Since both of these properties are temperature dependent, the bubble content becomes dependent on the temperature of the wire. When methanol was used as in cases A and B, because of its high solubility of gas, the bubble content was mainly gas when the wire temperature was relatively low. Consequently, the bubble behaviour was similar to that of a gaseous cavitation bubble. With increasing wire temperature resulting in an increase in the vapor pressure of the liquid at the wire as in case C, it is unlikely that the bubble content continues to be mainly gas. It was observed that the cavitation bubbles did not collapse after they left the wire. The vapor in the bubbles might have been dissolved into the liquid before they left the wire so that the content of the observed bubbles was still mainly gas. On the other hand, when there was no vibration, methanol vapor bubbles were observed to leave the wire surface without collapsing at relatively high heat flux values.

With distilled water and using relatively low wire temperatures as in case D, cavitation bubbles with diameter of about 0.015 in. were observed to have collapsed to less than one tenth of their original volumes. The content of the non-collapsible bubble must be gas. The high vapor content of the bubble can be ascribed to the low gas solubility of water which is about one fourth of that for methanol. With increasing wire temperature, a lower value in the gas content of the cavitation bubble would be expected. It is interesting to note that the resonance diameter of 0.013 in. calculated from Equation (1) compares favourably with the observed bubble diameter of 0.015 in. The results of the high speed photographic study of distilled water can then be interpreted as follows. A new cavitation bubble is formed from a crack containing trapped gas on the wire as in the case of methanol. The bubble grows to the resonance size, becomes unstable, and begins its erratic motion on the wire. When it reaches a certain critical size depending on the temperature of the liquid surrounding the bubble, the bubble collapses. The non-condensable gas in the bubble becomes a small bubble on the surface from which a new cavitation bubble will grow.

The purpose of the high speed photographic study was to establish the mechanisms of the heat transfer processes studied in the present work. At wire temperatures corresponding to the isolated bubble region and below, the increase in heat transfer rates, and thus the heat transfer coefficients, was due to the erratic and rapid motion of the gaseous-vaporous cavitation bubbles which created intense turbulence in the superheated liquid layer on the heat transfer surface. The erratic

and rapid motion of the bubbles was the result of the interaction of the bubbles with the acoustic pressure field, complicated further by the local temperature fluctuations of the liquid around the bubbles. The activity of the cavitation bubbles is a function of the applied sound pressure amplitude as well as the temperature of the heat transfer surface. The activity also depended on the gas solubility of the liquid which determines the content of the cavitation bubbles. As the heat transfer surface temperature increases, the population and the activity of the cavitation bubbles, as well as the vapor content of the cavitation bubbles, also increase. At surface temperatures corresponding to the well-developed nucleate boiling region where intense turbulence is already created by the growth and subsequent detachment (collapse) of the vapor bubbles, the effects of the motion of cavitation bubbles became negligible. This was observed experimentally using methanol at 95°F and 113°F. In fact, the results of the high speed photographic study showed that under these conditions, the formation of cavitation bubbles appeared to be occurring only above the wire surface which was partially covered by vapor bubbles.

Isakoff[11] and Romie and Aronson[12] as well as Ornatskii and Shcherbakov[13] suggested that the effects of ultrasonic vibrations on boiling heat transfer were to increase the frequency of bubble formation and the number of active nuclei on the heat transfer surface. High speed photographic study indicated that with the application of ultrasonic vibrations, the controlling mechanism of the heat transfer process was the rapid and erratic motion and the subsequent collapse of the

cavitation bubbles on the heat transfer surface. It was difficult to determine the active sites for the cavitation bubbles and their frequency of generation because of the agglomeration resulting from the motion of cavitation bubbles on the heat transfer surface.

Critical Sound Pressure

The critical sound pressure, as mentioned earlier, was defined as the sound pressure at which the applied sound pressure field begins to have an effect on heat transfer rates. Experimentally, it is the sound pressure at which the first drop of potential across the test section of the platinum wire was observed, indicating a drop in the wire temperature for the same heat flux density. At wire temperatures corresponding to the isolated bubble region of nucleate boiling or lower, the first appearance of a cavitation bubble on the wire was observed when the sudden drop of potential across the test section of the wire was recorded. The critical sound pressure is, in fact, the

ιtation threshold of the liquid at the wire. At higher wire temperatures, visual observation of the first occurrence of cavitation bubbles became difficult due to the increased vapor bubble activity on the wire. In the well-developed nucleate boiling region where the effect of ultrasonic vibrations was negligible, the determination of critical sound pressure from visual observations of the occurrence of a cavitation bubble was impossible. Subsequently, the criterion based on the potential drop across the wire test section was adopted.

The critical sound pressure, as shown in Figures 2 to 5,

was a function of the wire temperature, the temperature of the liquid and the frequency of the sound field. For both methanol and distilled water, at wire temperatures corresponding to the natural convection region, an increase in wire temperature resulted in a lower value of critical sound pressure. Although the cavitation threshold of the liquid at the wire surface depends on the gas content and the vapor pressure of the liquid, the latter appears to be the controlling variable as decreased gas content resulting from increasing temperature would increase the critical sound pressure instead of decreasing it as observed. The temperatures at which minimum values of critical sound pressure were observed were close to the values for the incipience of boiling. Consequently, little acoustic energy was necessary to induce the formation of cavitation bubbles. At temperatures above the point of incipient boiling, because of the increased vapor bubble activity, more acoustic energy was required to cause an increase in heat transfer rates. Since the vapor bubble density on the wire without vibration was very sensitive to the wire temperature in the nucleate boiling region, a rapid increase in critical sound pressure resulted. The plots of critical sound pressure versus wire temperature became asymptotic to the critical sound pressure in the well-developed nucleate boiling region where the effect of ultrasonic vibrations on heat transfer rates was negligible.

The effect of liquid temperature on critical sound pressure is shown in Figures 2 and 3 for distilled water and methanol, respectively. At the same wire temperature, the critical sound pressures

decreased with increased liquid temperature. This can be ascribed, again, to the higher value of vapor pressure of the liquid at a higher temperature. The minimum critical sound pressure, however, was constant for all liquid temperatures as it was observed to occur at the temperature of incipient boiling. The discrepancy in the values of minimum critical sound pressure was within the experimental error of $\pm$ 12%.

At wire temperatures above the incipience of boiling, the curves for two liquid temperatures crossed over in both Figures 2 and 3. The critical sound pressure for the liquid at lower temperature was lower because the vapor bubble activity at the same wire temperature when there was no vibration was lower. This was opposite to the results for wire temperatures below the point of incipient boiling and subsequently a reversing trend was obtained.

The critical sound pressure increased with frequency as expected, since it has been established by Esche[14] and Barger[7] that the cavitation threshold of a liquid increases directly with frequency. Quantitative comparison of their results with those obtained in this work cannot be made as the temperature and the state of liquid were different.

A comparison of the sound pressure data in Tables 1 to 4 in Part I and the critical sound pressure data in Figures 2 to 5 shows that depending on the wire temperature, the critical sound pressure could be higher than the value of sound pressure at which a cavitation bubble would be generated in the bulk liquid. For example, the critical sound pressure for methanol at 113°F, as shown in Figure 3, varied from

0.17 to 0.06 atm. for wire temperatures between $130^{\circ}F$ and $170^{\circ}F$. The sound pressure at which cavitation bubble was observed to occur in the bulk liquid for methanol at $113^{\circ}F$ was 0.11 atm (rms) as shown in Table 1 in Part I. This suggests that it was easier to induce cavitation in the bulk liquid than in the liquid at the wire surface which was at a higher temperature. It should be noted that the value of 0.11 atm was the sound pressure measured on the wire. The element of liquid in the bulk liquid where cavitation was first observed (owing to the interaction of sound waves with the container walls), might have a higher sound pressure, but this was not measured. It was also possible that there existed an active nucleus such as a dust particle which required much lower sound pressure to induce cavitation. When the critical sound pressure was below the value at which cavitation would occur in the bulk liquid, cavitation bubbles were observed only on the wire.

It may be recalled that there were two mechanisms through which a small cavitation bubble could grow to larger size. The first mechanism was agglomeration resulting from the motion of cavitation bubbles which originated on the wire only, while the second one involved agglomeration on the wire of cavitation bubbles which originated in the bulk liquid and migrated to the wire. Consequently, it is possible that only the first mechanism is taking place if the applied sound pressure is sufficient to induce cavitation on the wire but not in the bulk liquid. In order to be able to compare the heat transfer results directly, the apparent electrical power input to the transducers was selected so that cavitation occurred in the test liquid as well as

0.17 to 0.06 atm. for wire temperatures between 130°F and 170°F. The sound pressure at which cavitation bubble was observed to occur in the bulk liquid for methanol at 113°F was 0.11 atm (rms) as shown in Table 1 in Part I. This suggests that it was easier to induce cavitation in the bulk liquid than in the liquid at the wire surface which was at a higher temperature. It should be noted that the value of 0.11 atm was the sound pressure measured on the wire. The element of liquid in the bulk liquid where cavitation was first observed (owing to the interaction of sound waves with the container walls), might have a higher sound pressure, but this was not measured. It was also possible that there existed an active nucleus such as a dust particle which required much lower sound pressure to induce cavitation. When the critical sound pressure was below the value at which cavitation would occur in the bulk liquid, cavitation bubbles were observed only on the wire.

It may be recalled that there were two mechanisms through which a small cavitation bubble could grow to larger size. The first mechanism was agglomeration resulting from the motion of cavitation bubbles which originated on the wire only, while the second one involved agglomeration on the wire of cavitation bubbles which originated in the bulk liquid and migrated to the wire. Consequently, it is possible that only the first mechanism is taking place if the applied sound pressure is sufficient to induce cavitation on the wire but not in the bulk liquid. In order to be able to compare the heat transfer results directly, the apparent electrical power input to the transducers was selected so that cavitation occurred in the test liquid as well as

on the wire for the whole range of wire temperature used.

Heat Transfer Results

The effects of ultrasonic vibrations on heat transfer rates have been found to be dependent on the liquid used and its temperature. The higher heat transfer rates obtained in distilled water appeared to be the result of its low value of gas solubility which controlled the cavitation bubble content. The cavitation bubbles in water were observed to have collapsed on the wire surface as the bubble content was mainly vapor. The turbulence so generated was much more intense than that by the motion of the non-condensable cavitation bubbles generated in methanol.

A change in water temperature from 149°F to 113°F resulted in a change in the increase in heat transfer rates from 100% to 45% for approximately the same value of soil removal. It may be recalled that the increase in heat transfer rates was evaluated at a temperature difference of 40°F in both cases. The critical sound pressures, as shown in Figure 2, were 0.23 atm for a water temperature of 149°F and 0.42 atm for 113°F. At the same value of the percentage of soil removal, the liquid with a lower critical sound pressure showed an increased cavitation bubble activity on the wire surface. This explains the dependence of the increase in heat transfer rates on wire temperature at the same value of the percentage of soil removal. It is advantageous to use a liquid at its saturated condition since its cavitation threshold will be low and the critical sound pressure is close to the minimum value.

The effects of ultrasonic vibrations on saturated pool boiling were not studied because the motion of vapor bubbles generated on the walls of the stainless tank from the strip heaters interfered with the sound field and rendered the measurements of sound pressure on the wire surface very difficult. In preliminary experiments using methanol at its boiling point, more than a 100% fluctuation was obtained in sound pressure measurements by the ultrasonic probe. The liquid temperatures used in this work were selected so that the strip heaters maintained the temperature at the desired level without formation of vapor bubbles on the tank walls. Since the ultrasonic probe depolarizes at a temperature of $170^\circ F$, the temperature could not exceed this value.

Since only platinum wires of diameters 0.007 and 0.010 in. were used in this study, the range was too small to determine the effect of wire diameter.

The effect of frequency based on the percentage of soil removed has been shown to be relatively unimportant. The increase in heat transfer rates based on the same liquid temperature, the same temperature difference and approximately the same value of the percentage of soil removed was only lowered from 100% to 70% for a fivefold increase in frequency. According to Equation (1), the resonance size of the cavitation bubble was decreased by a factor of five as the frequency increased from 20.6 kcps to 108 kcps. In order to have the observed effect on heat transfer rates, the small cavitation bubbles must be as efficient as the larger cavitation bubbles in creating turbulence in the liquid at the wire surface.

CORRELATION OF EXPERIMENTAL DATA

The mathematical formulation of the effects of coupled acoustic or ultrasonic vibrations and heat transfer in fluids is very difficult and has not been attempted. If the fluid is a liquid, the analysis is further complicated by cavitation phenomena. It does not appear possible to write an appropriate differential equation which could be used to search out the important non-dimensional parameters of the problem. Consequently, the parameters used to correlate the data have been based on proposed mechanisms and tested empirically.

The experimental variables studied in this work were the liquid temperature, acoustic energy input to the system, and frequency. The acoustic energy input to the system was expressed in terms of sound pressure when the levels were below the cavitation threshold of the liquid and in terms of the percentage of soil removed when the levels were above. The latter quantity has been shown to give a measure of the cavitation activity at the heater surface. It should be noted that both the sound pressure and the soil removal measurements were conducted in liquids under isothermal conditions.

The heat transfer coefficient was first calculated by the following equation

$$h = \frac{q}{A \Delta t} \tag{2}$$

where h - heat transfer coefficient, BTU/hr ft^2 $^{\circ}$F

q/A - heat flux, BTU/hr ft^2

Δt - temperature difference between the wire and the bulk liquid, $^{\circ}$F.

An equation of the form shown as follows was used to correlate the heat transfer data at 20.6 kcps

$$Nu_w = \emptyset \ (Gr, \ Pr, \ S_R, \ P_{CR}) \qquad (3)$$

where Nu_w -   Nusselt number based on the wire diameter, dimensionless

      Gr -   Grashof number, dimensionless

      Pr -   Prandtl number, dimensionless

      S_R -   percentage soil removed, %

      P_{CR} -   critical sound pressure, atm.

In determining the dimensionless groups, all liquid properties were evaluated at the arithmetic mean temperature of the wire and the bulk liquid. A plot of Nu_w versus $(Gr \ Pr)^{0.65}(S_R)^{0.5}/P_{CR}$ yielded a reasonably good correlation except for the data points taken at wire temperatures above the temperature for incipient boiling which were above the correlation. It was decided that at high values of wire temperature, different dimensionless groups (reflecting the boiling mechanism) should be used to correlate the heat transfer results.

The results from the high speed photographic study showed that the cavitation bubble activity and its content depended on the wire temperature. Since the percentage of soil removed indicated only the cavitation activity of the liquid at the wire when it was not heated, the wire temperature effect was included in the critical sound pressure term and partially in the Grashof number which explains the high exponent for the latter. As the wire temperature increased, the frequency of formation and the activity of cavitation bubbles were increased, the

bubble content changing gradually from mainly gas to mainly vapor. The mechanism of heat transfer became similar to that in nucleate boiling without vibration. The wire temperature effect can no longer be accounted for by the critical sound pressure and the Grashof number. A Reynolds number for the cavitation bubbles was then postulated similar to that in nucleate boiling. The question which arises here is what criterion should be used to separate the heat transfer results into two groups. A convenient basis would be the cavitation bubble content which consists of 50% gas and 50% vapor. Since it was difficult to measure the actual bubble content, the heat flux value at the incipience of boiling was chosen. The choice was purely an arbitrary one and, in fact, data points with heat flux values 50% higher than the incipient boiling heat flux were included in the correlation for the low heat flux region.

After the data were divided into two parts, the data of the graphs of heat flux (q/A) versus temperature difference (Δt) in a log-log plot for the low heat flux region could be better correlated using lines with smaller slope. Subsequently, a new exponent of 0.5 was obtained for the product of Grashof number and Prandtl number. Satisfactory correlations were also obtained when the same dimensionless groups were used to correlate data in the low heat flux region at other frequencies. The final correlation takes the form of

$$Nu_w = C_1 \frac{(Gr\ Pr)^{1/2} (S_R)^{1/2}}{P_{CR}} + C_2 \tag{4}$$

where C_1 and C_2 are constants.

The results are shown in Figures 20 to 23. The slope and the intercept

of the straight line in each figure were obtained by the least squares method and are shown in Table 3 together with the 95% confidence limits based on the t test. For each frequency, there was a set of constants. It was impossible to correlate heat transfer results from different frequencies with a single equation, because the exact relationship between the critical sound pressure and frequency of the sound field has not been found.

The plots of Nu_w/Nu_o where Nu_o is the Nusselt number for the wire when there was no vibration, versus $(Gr\ Pr)^{1/2}(S_R)^{1/2}/P_{CR}$ were also prepared for the four frequencies and are shown in Figures 24 to 27. Although the degree of scatter was about the same, the data points from one test liquid temperature mixed better with data points from a different test liquid temperature. The slope and intercept are also summarized in Table 3.

To correlate the heat transfer results with vibrations in the high heat flux region, that is, the data points with heat flux values greater than that at the incipient boiling, a Reynolds number for cavitation bubbles would be used to account for the high cavitation bubble activity on the wire surface.

In nucleate pool boiling the volumetric flow rate of the vapor away from the surface is given by

$$Q = \frac{q}{\rho_v \lambda} \tag{5}$$

where   Q - volumetric flow rate of the vapor, ft^3/hr

      q - heat transfer rate, BTU/hr

CORRELATION OF HEAT TRANSFER DATA IN THE

LOW HEAT FLUX REGION

FIGURE 20   FREQUENCY = 20.6 kcps

FIGURE 21   FREQUENCY = 44.1 kcps

FIGURE 22   FREQUENCY = 108 kcps

FIGURE 23   FREQUENCY = 306 kcps

△ METHANOL, $T_L = 113\,°F$

○ WATER, $T_L = 149\,°F$

Nu_{nN}

$Gr^{\frac{1}{2}} Pr^{\frac{1}{2}} S_R^{\frac{1}{2}} / P_{CR}$

METHANOL, $T_L = 113 \ ^\circ F$

$Gr^{\frac{1}{2}} Pr^{\frac{1}{2}} Sr^{\frac{1}{2}} / P_{CR}$

Nu_W
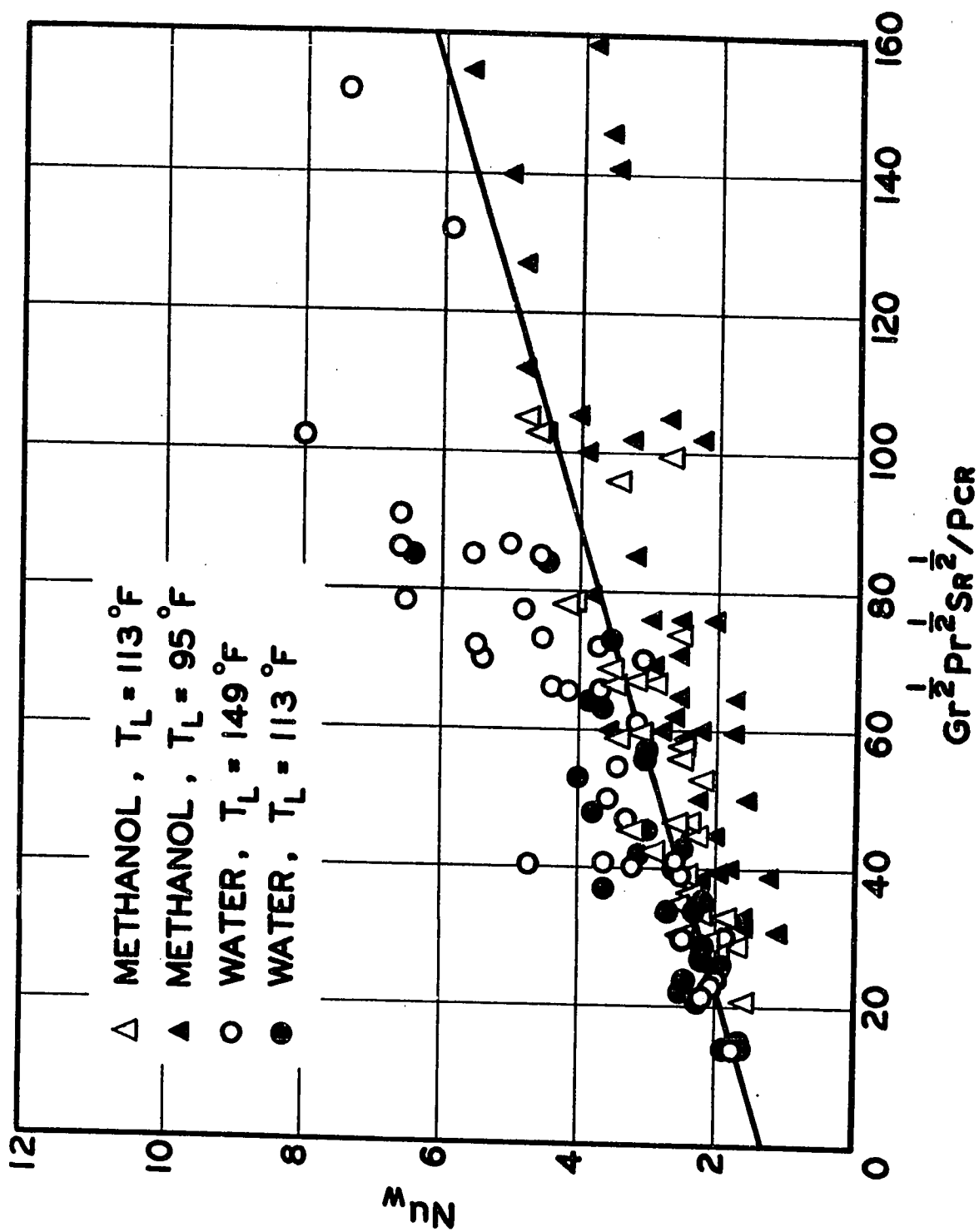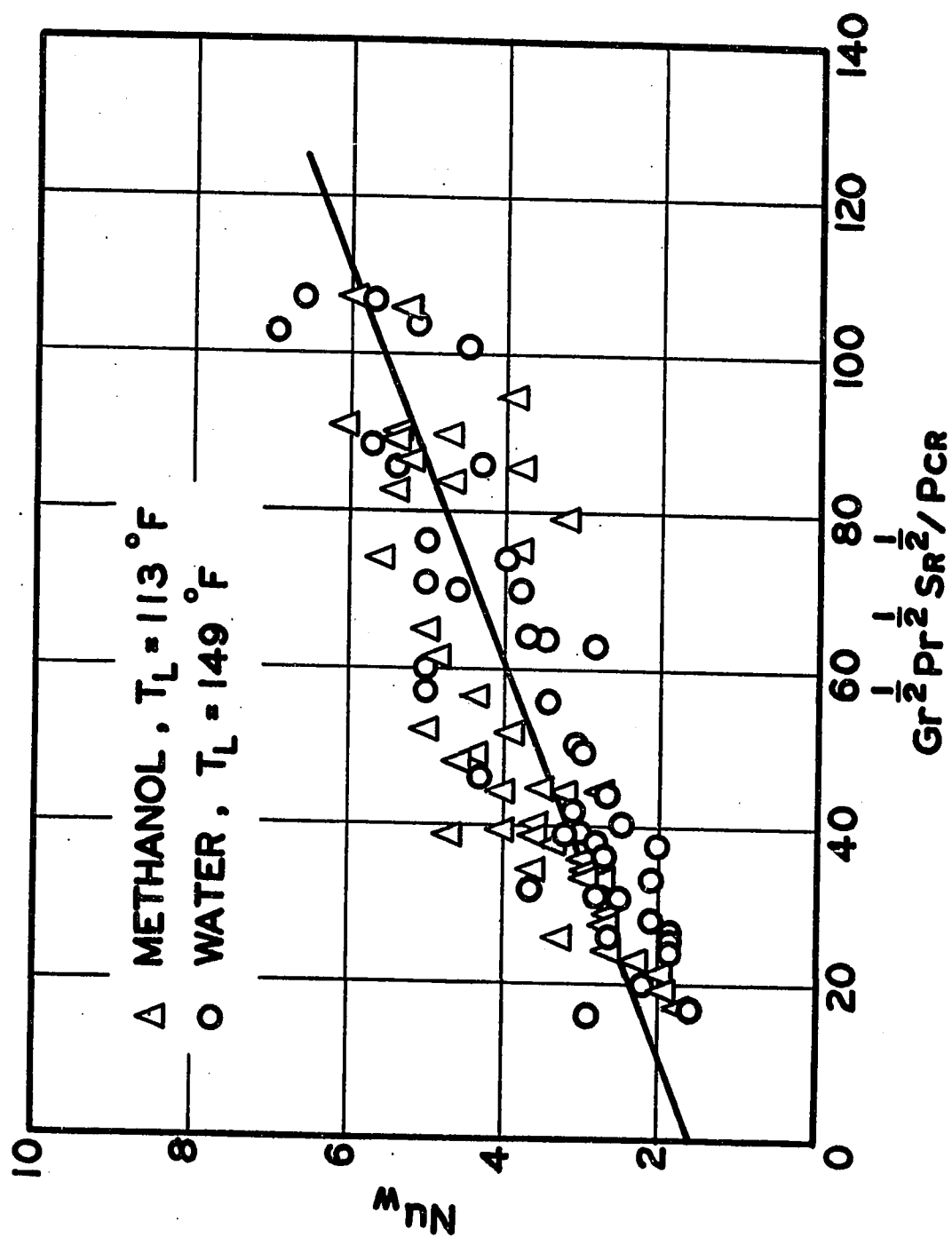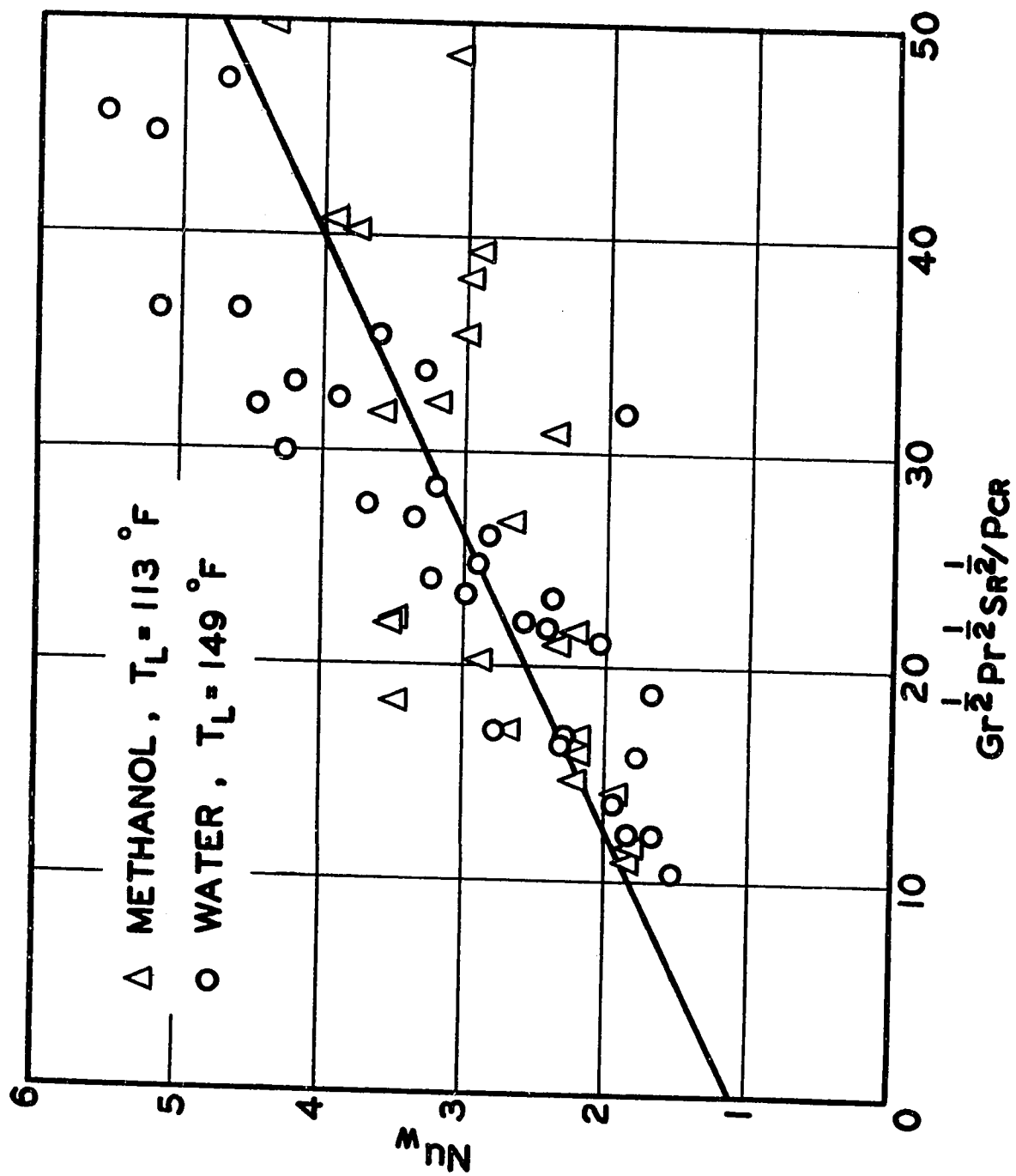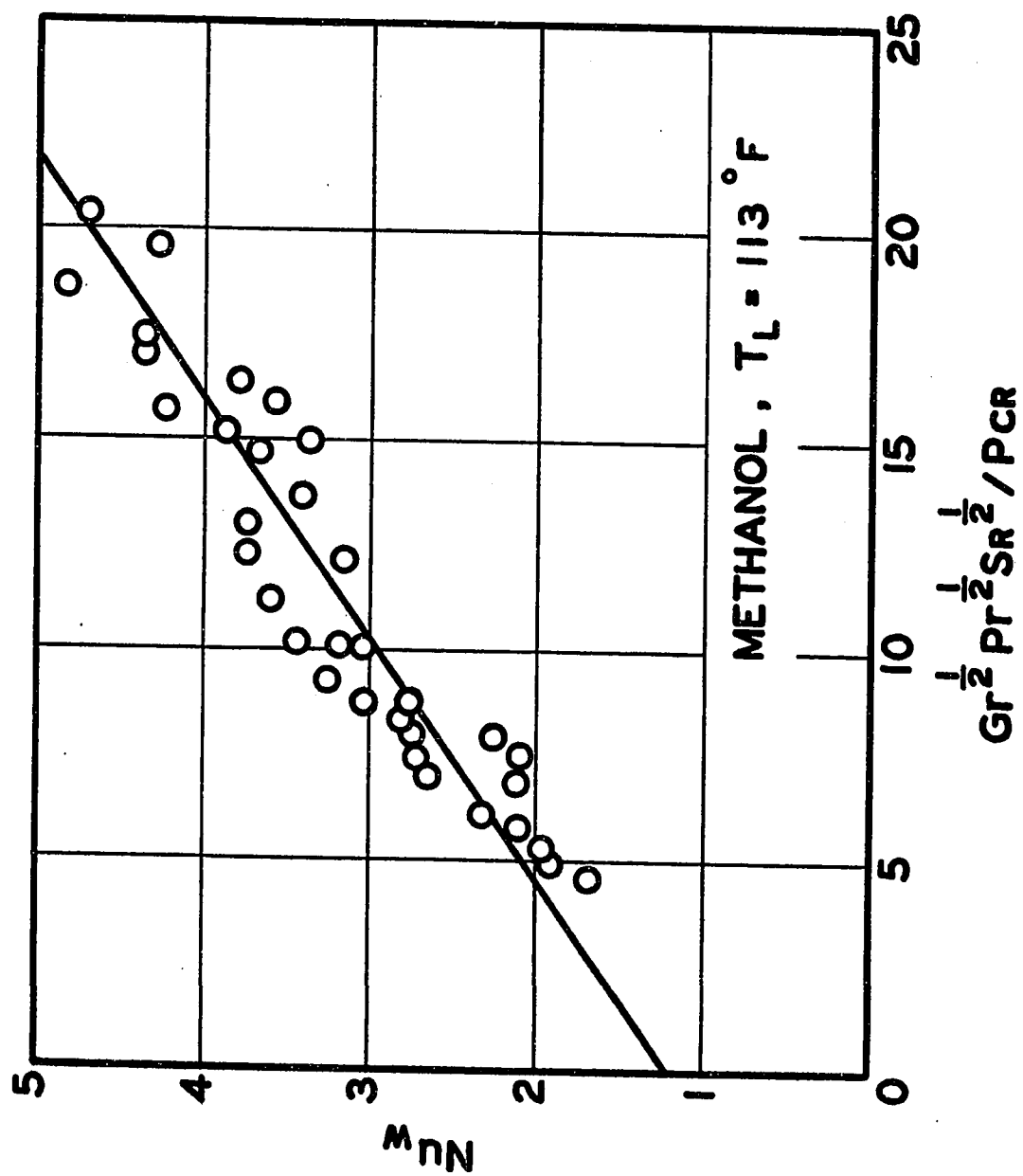
TABLE 3

Summary of Slope and Intercept of Correlations

FREQUENCY kcps	FIGURE NUMBER	SLOPE	INTERCEPT	THE 95% CONFIDENCE LIMITES	
				SLOPE	INTERCEPT
20.6	20	0.0305	1.34	$\pm$ 0.0048	$\pm$ 0.17
44.1	21	0.0402	1.56	$\pm$ 0.0055	$\pm$ 0.16
108	22	0.0732	1.09	$\pm$ 0.015	$\pm$ 0.22
306	23	0.174	1.22	$\pm$ 0.022	$\pm$ 0.13
20.6	24	0.0139	1.20	$\pm$ 0.0030	$\pm$ 0.093
44.1	25	0.0191	1.48	$\pm$ 0.0047	$\pm$ 0.14
108	26	0.0303	1.21	$\pm$ 0.011	$\pm$ 0.16
306	27	0.0573	1.49	$\pm$ 0.020	$\pm$ 0.17
20.6	28	0.00470	5.84	$\pm$ 0.00089	$\pm$ 0.63
44.1	29	0.00471	2.96	$\pm$ 0.00058	$\pm$ 0.21
108	30	0.00881	0.745	$\pm$ 0.0026	$\pm$ 0.19

CORRELATION OF HEAT TRANSFER DATA IN THE LOW HEAT

FLUX REGION IN TERMS OF A NORMALIZED NUSSELT NUMBER

FIGURE 24	FREQUENCY	=	20.6 kcps
FIGURE 25	FREQUENCY	=	44.1 kcps
FIGURE 26	FREQUENCY	=	108 kcps
FIGURE 27	FREQUENCY	=	306 kcps

157

METHANOL, $T_L = 113 °F$

Nu_w/Nu_o (vertical axis)

$\frac{1}{2} Gr^2 Pr^2 Sr^2/Pcr$ (horizontal axis)
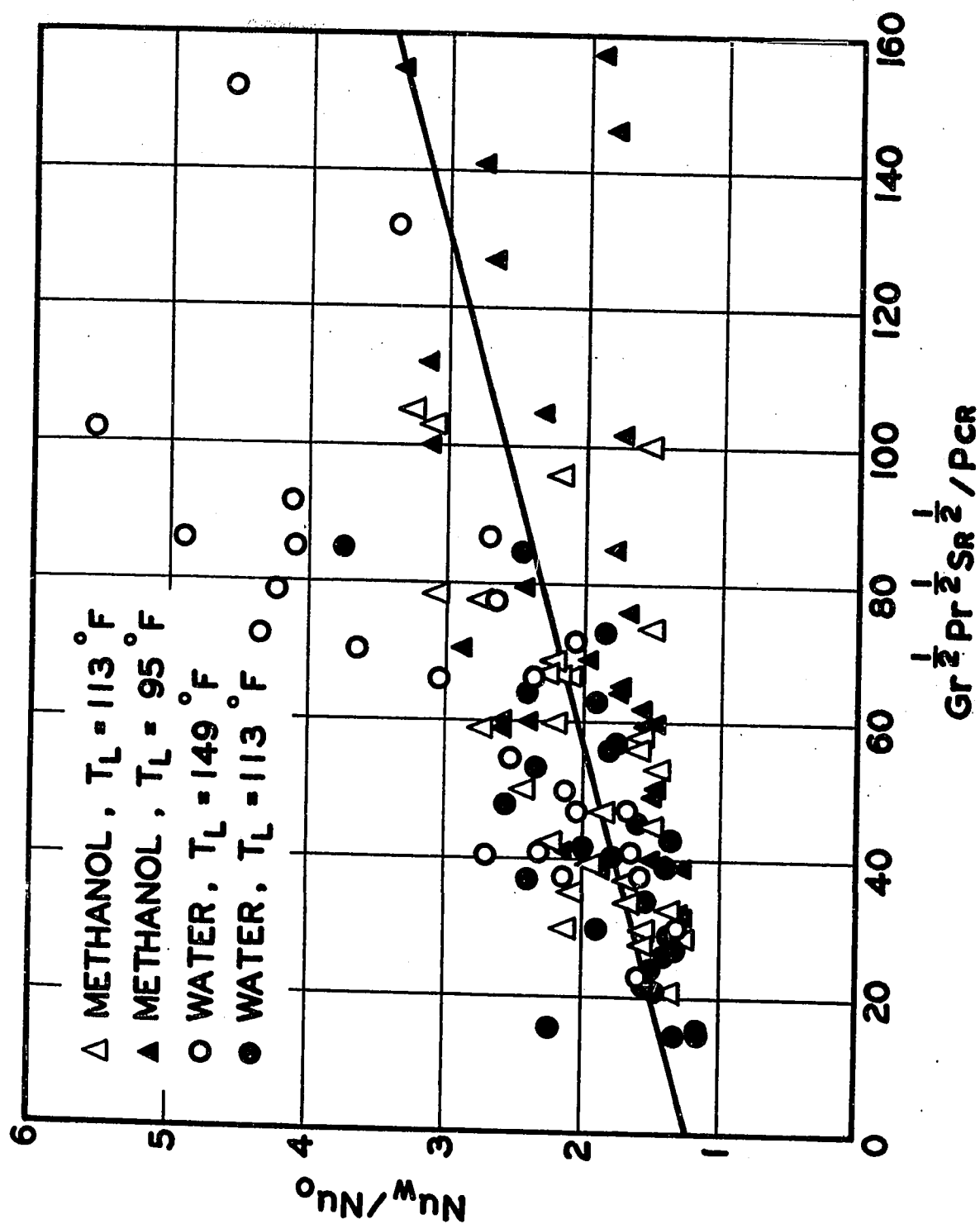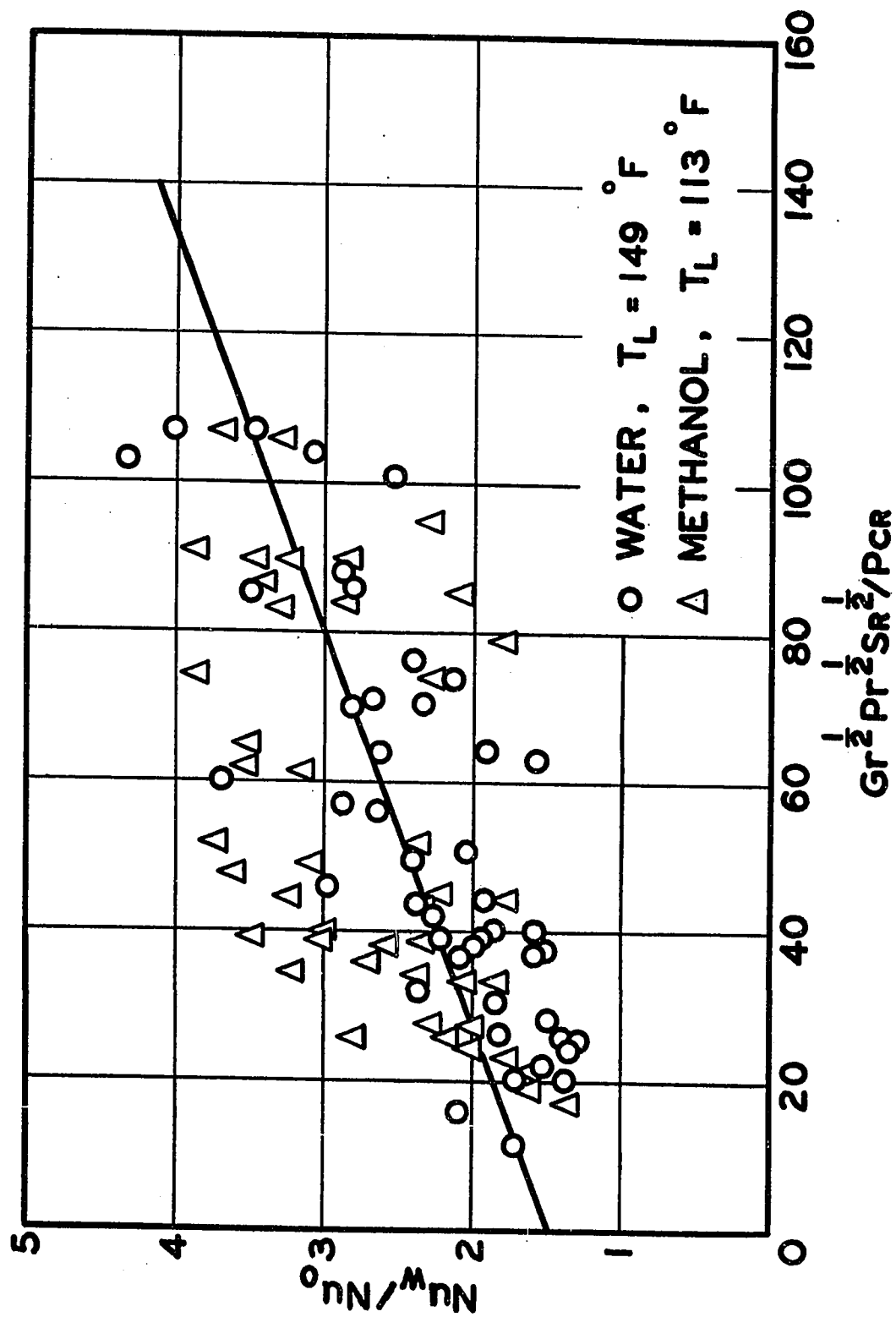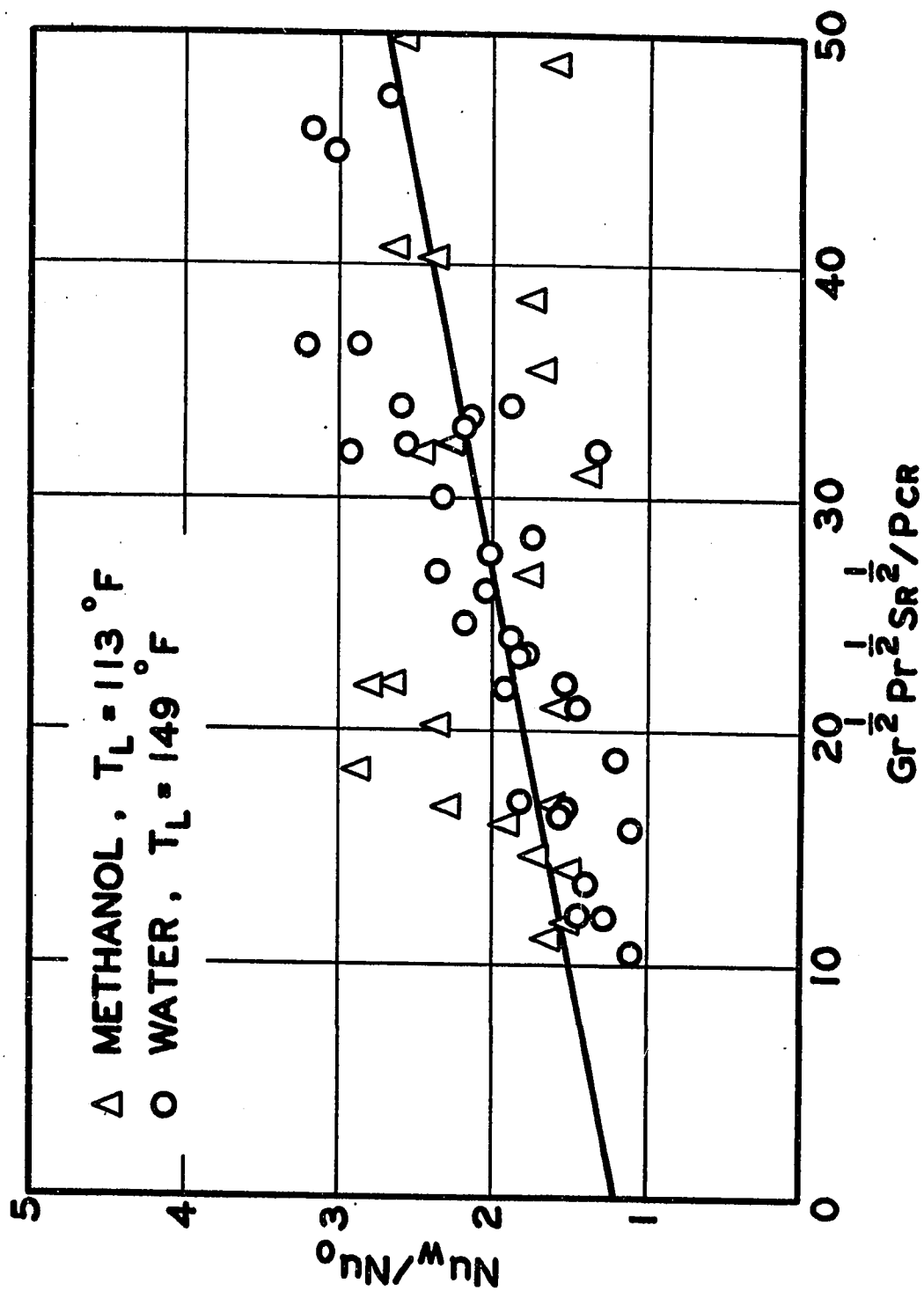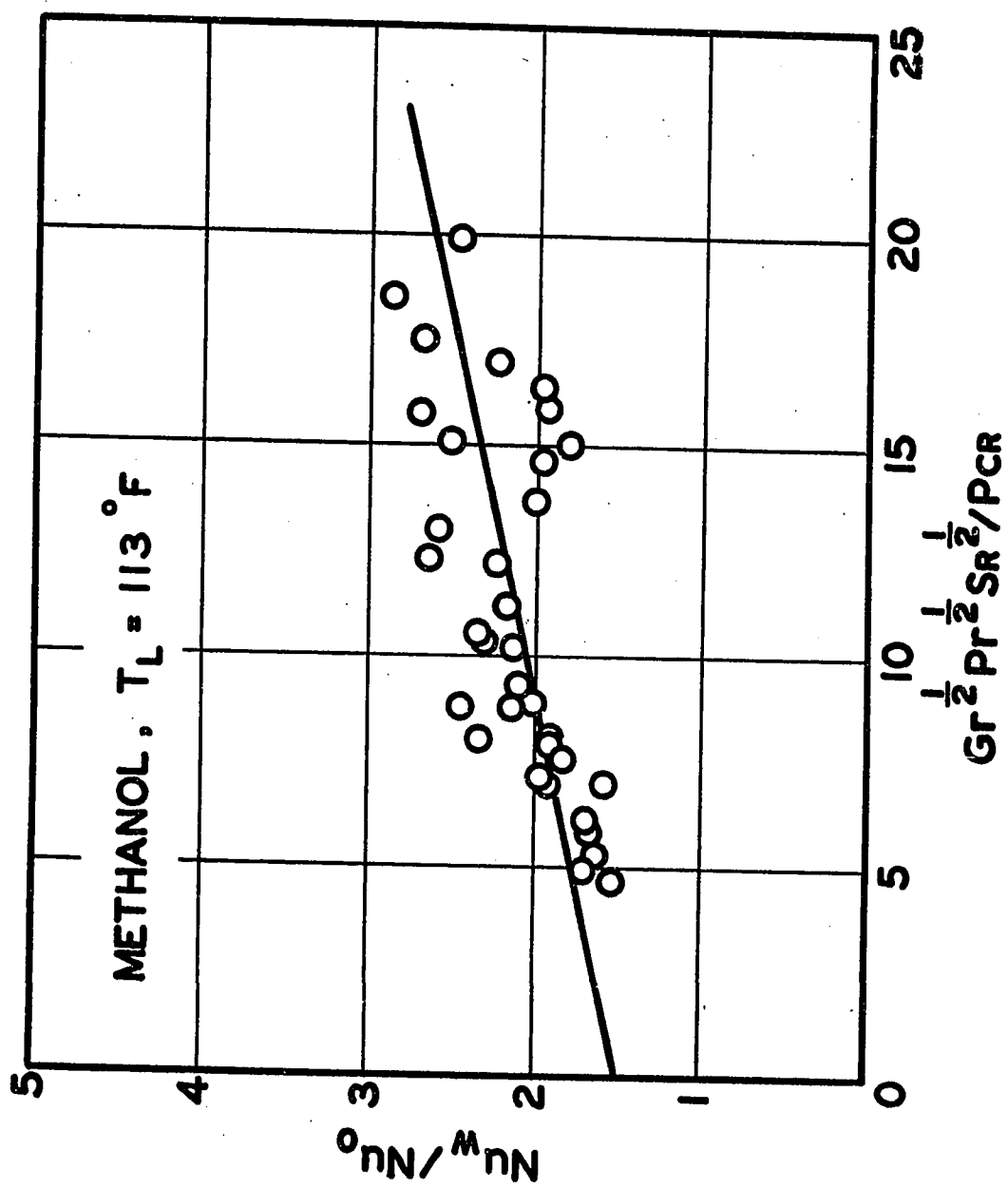
ρ_v - density of the vapor, lb/ft^3

λ - latent heat of vaporization, BTU/lb.

The superficial vapor velocity (V_{SV}), that is, the velocity based on the total available cross section, is

$$V_{SV} = \frac{q}{A \rho_v \lambda} \tag{6}$$

where A - total available surface area, ft.

If it is assumed that the flow of the liquid toward the surface is determined by simple volumetric exchange, the superficial velocities of the liquid and the vapor are equal. Equation (6) has been used by a number of investigators as the velocity term in the Reynolds number for correlation of nucleate boiling data[15,16,22].

Before defining the characteristic length in the Reynolds number, it may be recalled that the cavitation bubble size at which the erratic behaviour of the bubble was first observed, could be approximated by Equation (1) which relates the resonance size of an air bubble in a liquid to the frequency of the sound field. Comparison of the observed cavitation bubble size with the value predicted by Equation (1) for both methanol and distilled water at heat flux values in the region of isolated bubbles of nucleate boiling showed good agreement. It is likely that Equation (1) can be used to approximate the cavitation bubble diameter formed on the wire at increased temperatures. At higher frequencies, visual observations also showed that the cavitation bubble sizes were much smaller than that at 20.6 kcps. The Reynolds number is then defined as

$$Re = \frac{D_B q \, \rho_L}{A \, \rho_v \, \lambda / \mu_L} \tag{7}$$

where Re - Reynolds number for cavitation bubble, dimensionless

D_B - Diameter of cavitation bubble, ft. $D_B = 2R_o$

where R_o is the resonance radius defined in Equation (1)

ρ_L - density of liquid, lb/ft^3

μ_L - viscosity of liquid, lb/ft hr.

Using a Nusselt number based on the cavitation bubble diameter (from Equation (1)), the data in the high heat flux region were correlated and the results are shown in Figures 28 to 30. Because of the dependence of the critical sound pressure on the frequency of the sound field, a different correlation was obtained for each frequency. The final correlation is given as follows

$$Nu_B = C_3 \frac{Re^{1/2} Pr^{2/3} S_R^{1/2}}{P_{CR}} + C_4 \tag{8}$$

where C_3 and C_4 are constants. The slope and the intercepts of the correlation for each frequency are given in Table 3 together with the 95% confidence limits.

The results at 306 kcps were not correlated because few data points were available. The normalized plots of Nu_B/Nu_o versus $Re^{1/2} Pr^{2/3} S_R^{1/2}/P_{CR}$ were not prepared because an accurate determination of heat transfer coefficients in the nucleate boiling region without vibration was extremely difficult. While the normalized plots in the low heat flux region showed an increase in heat transfer coefficient

CORRELATION OF HEAT TRANSFER DATA IN THE

HIGH HEAT FLUX REGION

FIGURE 28   FREQUENCY = 20.6 kcps

FIGURE 29   FREQUENCY = 44.1 kcps

FIGURE 30   FREQUENCY = 108 kcps
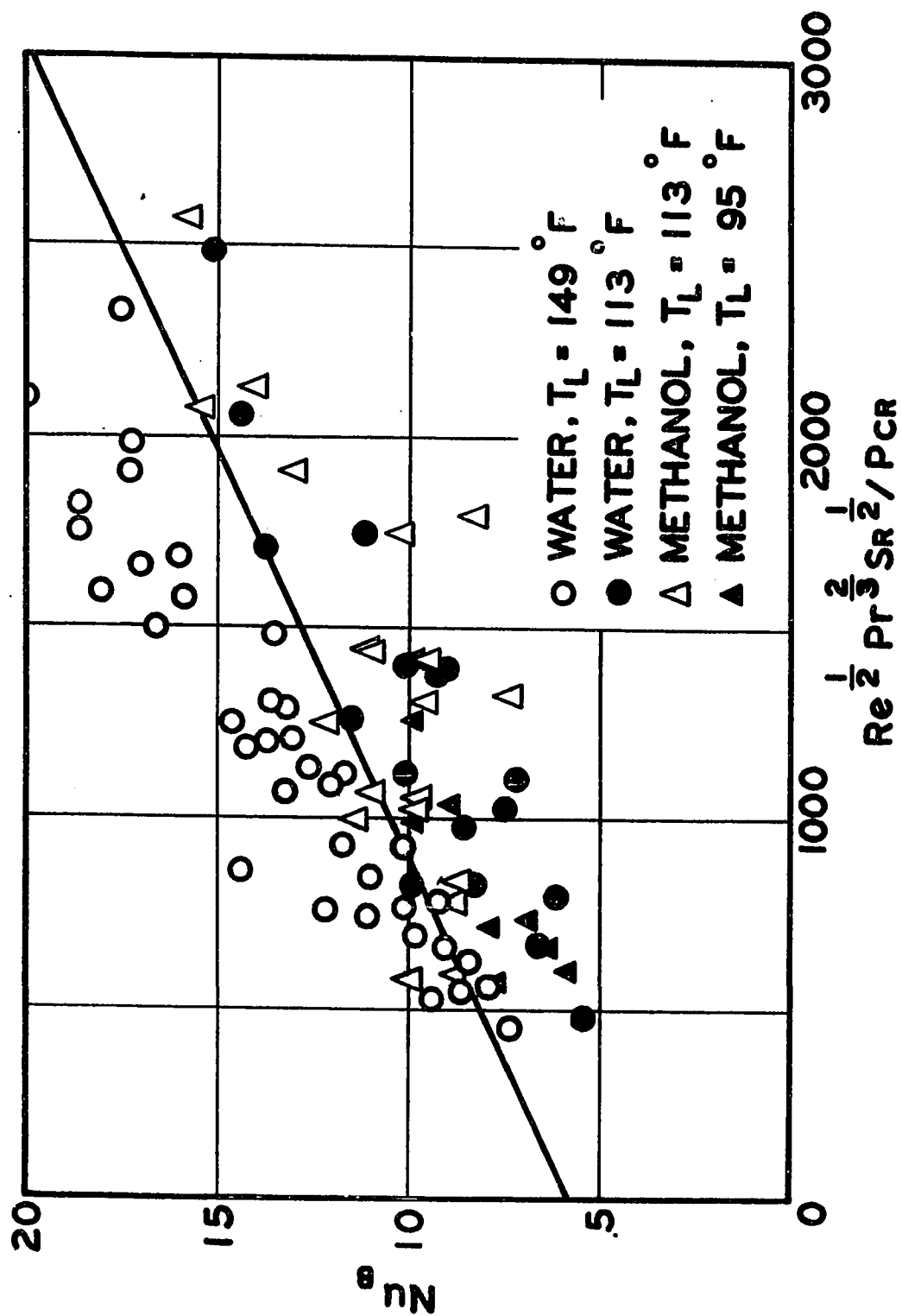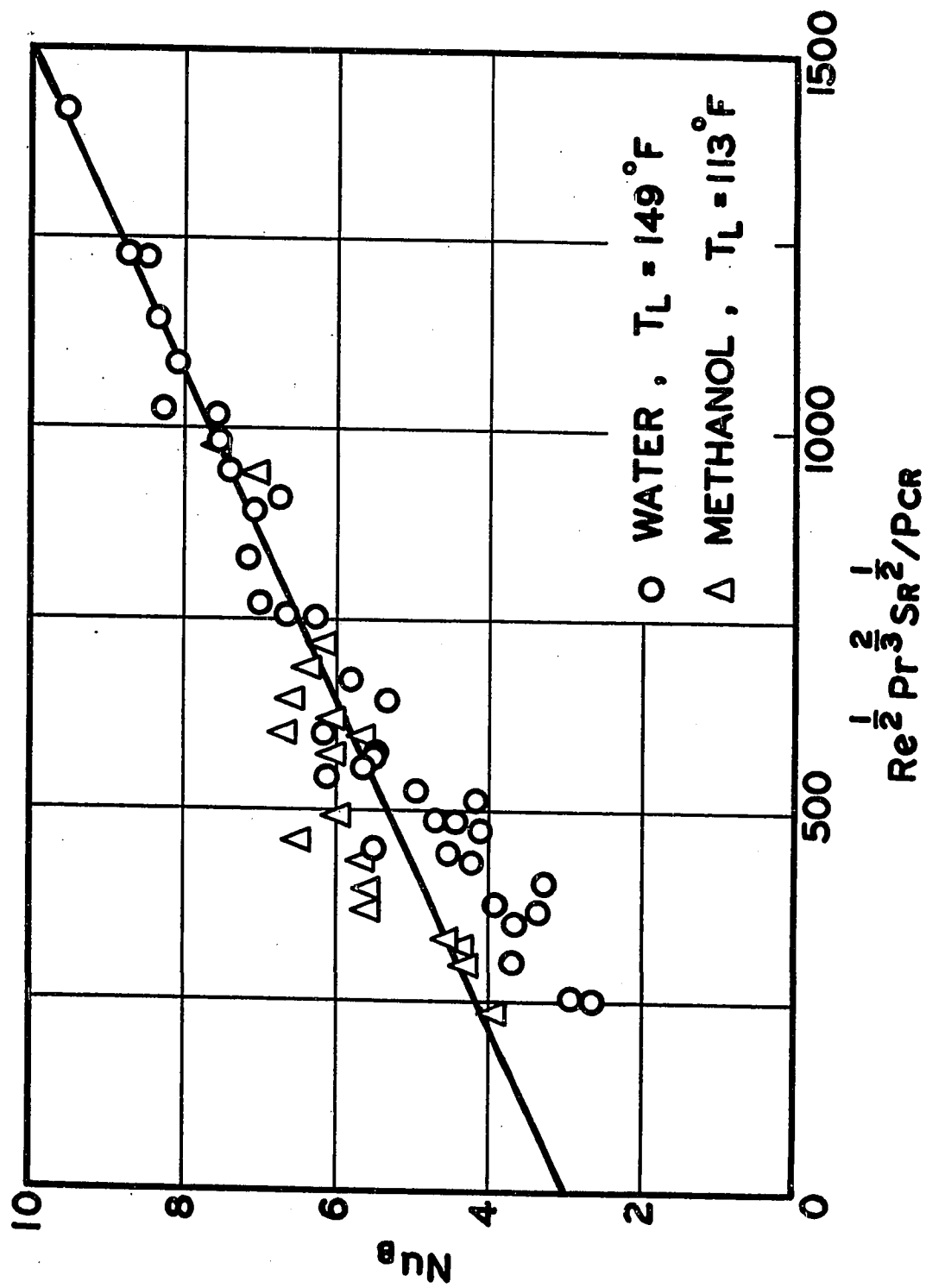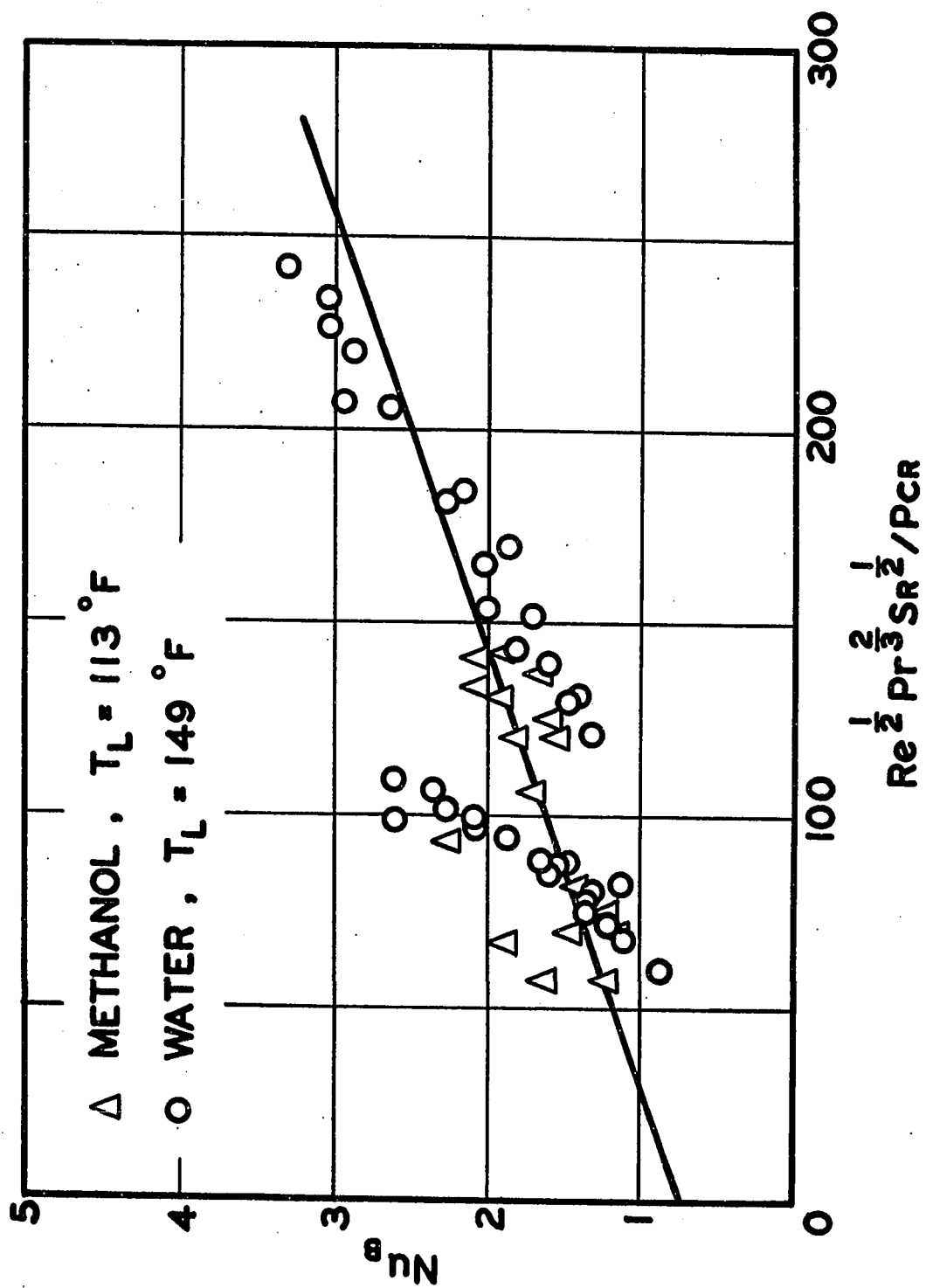
as wire temperature increased, the reverse would be expected in the high heat flux region.

DISCUSSION OF CALCULATED RESULTS

As mentioned earlier, attempts have been made to correlate the heat transfer results at different frequencies with a single equation. They were unsuccessful because the exact relationship between the critical sound pressure and the frequency of the sound field has not been established. The values of the slope and intercept of the correlations for different frequencies, in fact, reflect the dependence of the critical sound pressure on the frequency of the sound field. The critical sound pressure values for distilled water and methanol at 44.1 kcps, as shown in Figures 4 and 5, were only slightly higher than those for 20.6 kcps. Subsequently, a comparison of the slopes and intercepts at different frequencies shows that the values at 20.6 and 44.1 kcps are much closer to each other than those at other frequencies.

The exponent of the Grashof number in the final correlation for heat transfer results in the low heat flux region is 0.5 which is unusually high compared with the value of 0.17, the exponent of the Grashof number found when there was no vibration (Figure 15). It has been mentioned that both the soil removal and the critical sound pressure measurements were made in a liquid, whose temperature was the same as that in the bulk liquid. In heat transfer experiments, the cavitation bubble activity on the wire was observed to increase directly with the wire temperature. The increase in cavitation bubble activity would cause an increase in the turbulence of the liquid at the wire, resulting in higher values of heat transfer coefficient. In correlating the heat transfer results in the low heat flux region, since this temperature

effect was not accounted for in the cavitation damage data, that is, percentage of soil removed, it was combined with the temperature effect which produced the buoyancy force usually represented by the Grashof number in natural convective heat transfer. The result was the large value of the exponent of the Grashof number.

It should be pointed out that the critical sound pressure and the percentage of soil removed measured under isothermal conditions might not represent the actual values when the radioactive specimen was replaced by a heated platinum wire. The thermal gradient in the liquid near the wire, the formation and the motion of the cavitation bubbles on the wire would scatter sound waves. Since the ultrasonic probe cannot be used at temperatures above $170^\circ F$ and since it was impossible to simulate the thermal gradient of the liquid near the specimen when the percentage of soil removed was measured, this represents one of the limitations of the present work.

The heat transfer coefficients in both the low and high heat flux regions were found to be directly proportional to the square root of the percentage of soil removed which is a measure of the cavitation activity of the liquid at the heat transfer surface. In the penetration theory proposed by Danckwerts[17,18], it is shown that the mass transfer coefficient is inversely proportional to the square root of the time of contact between the liquid and the gas phase. The penetration theory assumes that the interface is continuously replaced by eddies so that fresh surface will be formed continuously at a constant rate. The reciprocal of the contact time is then shown to be the

fractional rate of surface renewal. Consequently, the mass transfer

coefficient is proportional to the square root of the fractional rate

of surface renewal, which depends on the degree of turbulence in the

liquid. From the analogy of heat and mass transfer, it appears that

the percentage of soil removed is directly related to the intensity of

turbulence resulting from cavitation in a liquid under ultrasonic vibra-

tions. The mechanism of cavitation damage, as mentioned earlier, is

mainly due to the collapse of cavitation bubbles near and on a solid

surface. The percentage of soil removed can then be interpreted as a

measure of the rate of formation (collapse) of cavitation bubbles which

becomes a measure of the turbulent intensity in the liquid.

The cavitation damage has been shown to increase directly

with the square of the sound pressure amplitude[19]. This renders the

term $(Gr\ Pr)^{1/2}(S_R)^{1/2}/P_{CR}$ in the correlation for the low heat flux

region and the term $Re^{1/2}Pr^{1/2}S_R^{1/2}/P_{CR}$ in the correlation for the

high heat flux region dimensionless as the percentage of soil removed

becomes directly proportional to the square of the sound pressure ampli-

tude. The dimensionless term $S_R^{1/2}/P_{CR}$ gives a measure of the cavita-

tion bubble activity for different liquids at different temperatures.

The effects of quartz wind streaming and the surface

streaming have been neglected in correlating the heat transfer results.

Eckert[20] has shown that the quartz wind streaming which is a volume

effect resulting from sound absorption in a liquid will have a negligible

velocity at frequencies below 1000 kcps. The frequency range of the

present work is well below this value.

Surface streaming is a local effect resulting from the interaction of the sound waves with a surface. Westervelt[21] suggested a Reynolds number (Re_s) for correlating heat transfer results due to surface streaming. It is given as follows

$$Re_s = \frac{u^2}{\omega \nu} = \left(\frac{a}{\delta_{AC}} \right)^2 \qquad (9)$$

where u - particle velocity amplitude, ft/hr

ω - angular frequency, rad/hr

ν - kinematic viscosity, ft^2/hr

a - particle displacement amplitude, ft

δ_{AC} - A-C boundary layer thickness, $\left(\frac{\nu}{\omega} \right)^{1/2}$, ft.

Westervelt predicted that the heat transfer will increase for values of $Re_s > 1$, but below unity no effect will be observed. As mentioned in the Literature Review section, Equation (9) has been successfully used to determine the critical sound pressure level - the sound pressure level at which the effect of sound on heat transfer becomes appreciable - when the fluid is air.

For progressive waves, Equation (9) may be written as

$$Re_s = \frac{2P_s^2}{\rho c^2 \omega \mu} \qquad (10)$$

where P_s - effective sound pressure, atm

c - velocity of sound in the fluid, ft/hr

μ - viscosity of the fluid, lb/ft hr.

In the present work, the Reynolds numbers were calculated

to be 0.07 for water at 20.6 kcps and 0.0048 at 306 kcps, taking the
sound pressure to be 1 atm. The success of the correlation of data also
indicates that the effects of quartz wind and surface streaming were
negligible.

CONCLUSIONS

1. There existed a critical sound pressure, depending on the liquid used and its temperature, the acoustic frequency and the heat transfer surface temperature, below which the effects of ultrasonic vibrations on heat transfer were negligible.

2. Above the critical sound pressure, the effects of ultrasonic vibrations on heat transfer to liquids varied from a 800% increase in heat transfer coefficient in the natural convection region to a negligible increase in the well-developed nucleate boiling.

3. The increase in heat transfer coefficient was due to the intense turbulence resulting from the radial oscillations as well as the rapid and erratic motion of the cavitation bubbles on the heat transfer surface. The characteristics of these cavitation bubbles resembled that of a gaseous cavitation bubble with content varied from mainly gas to mainly vapor, depending on the gas solubility of the liquid at the heat transfer surface temperature. An increase in the surface temperature also increased the population and the activity of the cavitation bubbles. Under the present experimental conditions, it was impossible to determine the frequency of generation of the cavitation bubbles and the number of active sites (if there was any) on the heat transfer surface.

4. The cavitation damage results (percentage of soil removed) obtained in Part I were used successfully to correlate the heat transfer results. The dependence of the population and the activity of

cavitation bubbles on the heat transfer surface temperature, however, was not accounted for by the cavitation damage measurements. Subsequently, it was necessary to separate the heat transfer results into two regions using the heat flux value at the incipience of boiling as the criterion. In the low heat flux region, the wire temperature effect was reflected in the high exponent of the Grashof number while a cavitation bubble Reynolds number was defined to account for the wire temperature effect in the high heat flux region. The correlations for $f = 20.6$ kcps are given as follows with the slopes and intercepts for all frequencies summarized in Table 4.

Low Heat Flux Region

$$Nu_w = 0.0305 \ \frac{(Gr\ Pr)^{1/2} (S_R)^{1/2}}{P_{CR}} + 1.34$$

$$\frac{Nu_w}{Nu_o} = 0.0139 \ \frac{(Gr\ Pr)^{1/2} (S_R)^{1/2}}{P_{CR}} + 1.20$$

High Heat Flux Region

$$Nu_B = 0.00470 \ \frac{Re^{1/2}\ Pr^{2/3}\ S_R^{1/2}}{P_{CR}} + 5.84$$

Since the relationship between the critical sound pressure and the frequency of the sound field has not been established, it was impossible to combine the correlations at different frequencies into a single one.

TABLE 4

Summary of Slope and Intercept for Correlations

at Different Frequencies

Frequency (kcps)	$Nu_w(Nu_B)$ plot		Nu_w/Nu_o plot	
	Slope	Intercept	Slope	Intercept
Low Heat Flux Region				
20.6	0.0305	1.34	0.0139	1.20
44.1	0.0402	1.56	0.0191	1.48
108	0.0732	1.09	0.0303	1.21
306	0.174	1.22	0.0573	1.49
High Heat Flux Region				
20.6	0.00470	5.84	-	-
44.1	0.00471	2.96	-	-
108	0.00881	0.745	-	-

The exponent of 0.5 for the percentage of soil removed in all cor-
relations, when viewed in the light of penetration theory, indicates
that the percentage of soil removed is related to the turbulent in-
tensity of the liquid resulting from cavitation.

5. The increase in heat transfer coefficient resulting from ultrasonic
   vibrations depended on the liquid used as well as its temperature.
   Liquid with low gas solubility would yield higher heat transfer co-
   efficients and higher heat transfer rates would be obtained in
   liquid at a higher temperature.

6. For the range of frequency of sound field studied, the effect of
   frequency was negligible if the cavitation activity of the liquid
   was the same. In order to have the same cavitation activity in a
   liquid, higher frequency means that more acoustic energy is required.

NOMENCLATURE

ROMAN SYMBOLS

a	particle displacement amplitude, ft
A	surface area, ft
c	velocity of sound in the fluid, ft/hr
c_p	specific heat, BTU/lb ^{o}F
C_1, C_2, C_3, C_4	constants
D_w	wire diameter, ft
D_B	cavitation bubble diameter, ft
f	frequency of the sound field, kcps
g	acceleration due to gravity, ft/hr^2
h	heat transfer coefficient, BTU/hr ft^2 ^{o}F
k	thermal conductivity, BTU/ft hr ^{o}F
P_{CR}	critical sound pressure, atm
P_o	ambient pressure, atm
Q	volumetric vapor flow rate, ft^3/hr
q	heat transfer rate, BTU/hr
R_o	resonance radius, cm
S_R	percentage of soil removed, %
T_W	wire temperature, ^{o}F
V_{SV}	superficial vapor velocity, ft/hr
W_A	apparent electrical power input to transducers, watts

GREEK SYMBOLS

β	coefficient of thermal expansion of fluid, ^{o}F^{-1}

Δt temperature difference ($\Delta t = t_w - t_L$), ^{o}F

Δt_{CR} critical temperature difference, ^{o}F

δ_{A-C} A-C boundary layer thickness, ft

λ latent heat of vaporization, BTU/lb

μ viscosity, lb/ft hr

ν kinematic viscosity, ft^2/hr

ρ density, lb/ft^3

σ surface tension, dyne/cm

ω angular frequency, rad/hr

DIMENSIONLESS GROUPS

Gr   Grashof number, $g\beta \rho^2 D^3 \Delta t / \mu^2$

Nu   Nusselt number, hD/k

Nu_B Nusselt number, hD_B/k

Nu_o Nusselt number without vibration

Nu_w Nusselt number, hD_w/k

Pr   Prandtl number, $\mu c_p/k$

Re   Reynolds number, $D V \rho/\mu$

Re_s Reynolds number - surface streaming, $(a/\delta_{A-C})^2$

SUBSCRIPTS

B   cavitation bubble

L   liquid

v   vapor

w   wire

REFERENCES

1. Westwater, J.W., paper presented at the 1960 Annual ASME Meeting, New York.

2. Courty, C. and A. Foust. Chem.Eng. Progr. Symp. Ser., 51, 1 (1955).

3. Clark, H.B., P.S. Strenge, and J.W. Westwater. Chem.Eng.Progr. Symp.Ser., 55, 103 (1959).

4. McAdams, W.H., J.N. Addoms, R.M. Rinaldo and R.S. Day. Chem.Eng. Progr. 44, 639 (1948).

5. McAdams, W.H. "Heat Transmission", McGraw-Hill, p. 176,(1954).

6. Gunther, F.C. and F. Kreith, Heat Transfer and Fluid Mechanics Institute, p. 113 (1949).

7. Barger, J.E. Tech.Memo. No. 57, Acoustic Research Lab., Harvard University, April (1964).

8. Heuter, T.F. and R.H. Bolt. "Sonics". John Wiley. p. 229 (1955).

9. Hsieh, D.Y. and M.S. Plesset, J.Acoust.Soc.Am., 33, 206 (1961).

10. Lieberman, D. Phys.Fluids, 2, 466 (1959).

11. Isakoff, S.E. Proc.Heat Transfer and Fluid Mechanics Inst., Stanford University Press, Stanford, Calif., 15 (1956).

12. Romie, F.E. and C.A. Aronson, ATL-A-123, Joint U.S.-Euratom Research and Development Report, July (1961).

13. Ornatskii, A.P. and V.K. Shcherbakov. Teploenergetika, 6, 84 (1959). Translation appears in Ref. (65) in the Literature Review Section.

14. Esche, R. Akust. Beihefte, 4, 208 (1952).

15. Kutateladze, S.S.   J.Heat Mass Transfer, $\underline{4}$, 31 (1961).

16. Jakob, M.   Mech.Eng., $\underline{58}$, 643, 729 (1936).

17. Danckwerts, P.V.   Ind.Eng.Chem. $\underline{43}$, 1460 (1951).

18. Danckwerts, P.V.   A.I.Ch.E. Journal, $\underline{1}$, 456 (1955).

19. Bebchuk, A.S.   In.Ia. Borisov, and L.D. Rosenberg. Soviet Physics
     - Acoustics, $\underline{4}$, 372 (1958).

20. Eckert, C.   Phys.Rev., $\underline{73}$, 68 (1948).

21. Westervelt, P.J.   J.Acoust.Soc.Am., $\underline{32}$, 337 (1960).

22. Rohsenow, W.   Trans.Am.Soc.Mech.Engrs., $\underline{74}$, 969 (1952).

PART III

EFFECTS OF ULTRASONIC VIBRATIONS ON BURNOUT HEAT

FLUX AND CRITICAL TEMPERATURE DIFFERENCE

INTRODUCTION

The critical temperature difference is the temperature
difference which produces a maximum heat flux value, or the burnout
heat flux. It is desirable to operate steam-heated evaporators, vapo-
rizers, and reboilers as closely as possible to the critical temperature
difference. On the other hand, it is necessary to operate electrically
heated boilers and nuclear reactors, in both of which the energy -
generation rates are relatively independent of material temperatures,
at a temperature difference which is safely below the critical value.
At temperature differences above the critical value, the mechanism of
heat transfer changes from nucleate boiling to film boiling resulting
in a sudden increase in the heater temperature which usually exceeds the
melting point of the heating element. Information on the factors which
determine the critical temperature difference or which can change the
critical value is useful in the design of these systems.

The objective of this study was to determine the effects
of ultrasonic vibrations at a frequency of 20.6 kcps on the critical
temperature difference and the burnout heat flux in methanol at $119^{\circ}F$
with platinum wire of 0.007 in. diameter as the heating element.

EXPERIMENTAL

The same apparatus and procedure used to study the effects of ultrasonic vibrations on heat transfer to liquids in Part II were used. A platinum wire of 0.007 in. diameter was used as the heating element, and the diameter of the potential leads was 0.002 in. The test section of the heating element was approximately 3/4 in. long. The liquid was methanol maintained at a temperature of $113^{\circ}F \pm 1^{\circ}F$ in all experiments.

The burnout heat flux and the critical temperature difference were measured both with and without vibrations. When there was no vibration, the DC current passing through the heating element was increased by small increments until the wire burned out. The burnout heat flux and the critical temperature difference were calculated from the last set of data taken on the voltage drops across the test section and the standard resistor.

The burnout heat flux and the critical temperature difference with ultrasonic vibrations were measured only at a frequency of 20.6 kcps. The voltage drop across the transducers was adjusted to 40 volts so that the apparent electrical power input to the transducers was 86 watts which was the highest acoustic energy level used in Part II. The corresponding percentage of soil removed for methanol at $113^{\circ}F$ was 13.4%. The procedure for measuring the burnout heat flux and the critical temperature difference with ultrasonic vibrations was the same as that when there was no vibration.

RESULTS AND DISCUSSION

The burnout heat flux together with the critical temperature difference both with and without vibrations are summarized in Table 1 and Figure 1. The experimental data are given in Table D-5 in Appendix D.

As mentioned earlier, distilled water was not used in this study because the amperage output of the existing regulated DC power supply was too low to cause burnout.

The experimental error for the results shown in Table 1 was the same as that given for the heat transfer results for natural convection and surface boiling, namely 5% in the heat flux values and about $2^\circ F$ in the temperature difference. The mean value and its standard deviation for the critical temperature difference were calculated to be $96^\circ F \pm 3\%$ for the case without vibration and $96^\circ F \pm 4\%$ for the case with vibrations. The corresponding values for burnout heat flux were 412,000 BTU/hr $ft^2 \pm 8\%$ and 369,000 BTU/hr $ft^2 \pm 7\%$. The scatter was mainly due to the instability of the burnout phenomenon. The data on burnout heat flux reported by Morozov[1] show a maximum variation about the mean of $\pm 11\%$, while the results of Howell and Bell[2] scatter $\pm 19\%$ (vs. $\pm 6\%$ stated experimental error).

It can be seen that ultrasonic vibrations did not have any effect on the critical temperature difference at the frequency studied. The 10% decrease in the value of burnout heat flux when ultrasonic vibrations were applied was also too small to justify a conclusion on the

TABLE 1

Effects of Ultrasonic Vibrations on Burnout Heat Flux

and Critical Temperature Difference

Platinum Wire Diameter $\quad$ = 0.007 in.

Test Liquid $\quad$ = Methanol (B.P. = 148°F)

Temperature of the Liquid = 113°F

Frequency of Vibration $\quad$ = 20.6 kcps

Run No.	W_A^* watts	$(\Delta t)_{CR}$ $^{\circ}$F	(q/A) Burnout BTU/hr ft^2
R41	0	93	431,000
R41a	0	93	380,000
R40	0	99	461,000
R43	0	96	402,000
R46	0	97	387,000
R42	86	99	335,000
R44	86	91	383,000
R45	86	97	361,000
R48	86	92	349,000
R49	86	95	396,000
R47	86	100	387,000

* W_A = apparent electrical power input to the transducers.

FIGURE 1

EFFECT OF 20.6 kcps ULTRASONIC VIBRATIONS ON

BURNOUT HEAT FLUX AND CRITICAL TEMPERATURE

DIFFERENCE IN METHANOL AT $113^{\circ}F$
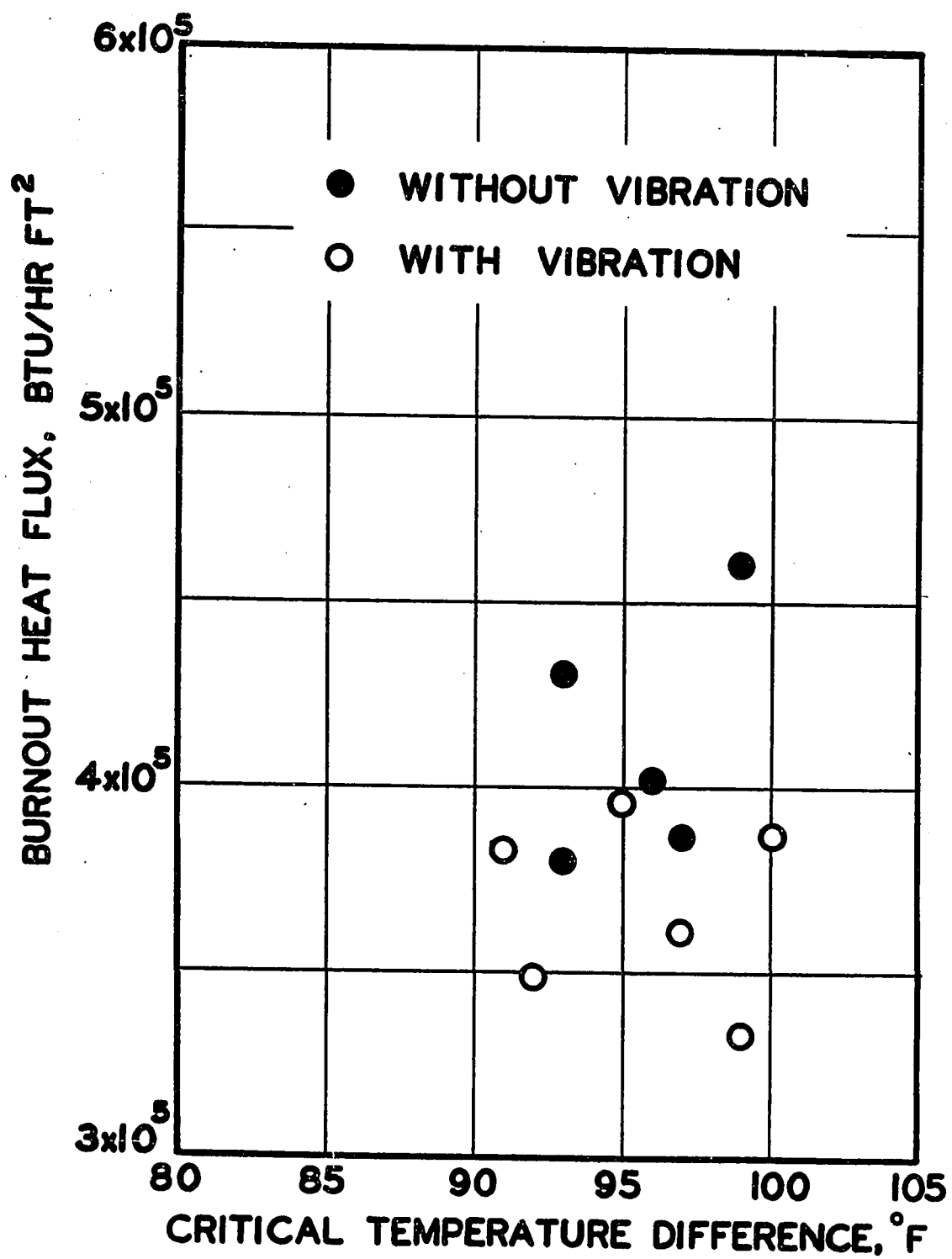
effects of ultrasonic vibrations on burnout heat flux.

In Part II of this investigation, the increase in heat transfer rates resulting from ultrasonic vibrations in the low heat flux region was due to the motion of cavitation bubbles on the wire surface. The effects diminished in the high heat flux region and finally became negligible in the well-developed nucleate boiling region, where the turbulence generated by the motion of the cavitation bubbles was overshadowed by the turbulence resulting from the growth and detachment of vapor bubbles. It is expected that ultrasonic vibration would not have any effect on both the burnout heat flux and the critical temperature difference.

As mentioned earlier, platinum wires with diameter of 0.0045 in. were used in preliminary experiments as heating elements. It was observed that they began to vibrate at heat flux values near the burnout point with the test liquid under intense ultrasonic vibrations (W_A = 86 watts). While no visible vibration was observed when the diameter of the wire was changed to 0.007 in., it is doubtful whether vibration was eliminated completely.

One of the reasons that the present work was undertaken was due to the wide discrepancy in the published data on the effects of ultrasonic vibrations on burnout heat flux. Isakoff[3] reported a 60% increase in the burnout heat flux and the data of Ornatskii and Shcherbakov[4] showed that up to 80% increase could be obtained depending on the degree of subcooling. Markels et al.[5] and Romie and Aronson[6], however, reported that the effect of ultrasonic vibrations was negligible.

The results of this work support the findings of the latter.

Measurements at a higher frequency were not made as the same results were expected.

CONCLUSIONS

Ultrasonic vibrations had a negligible effect on the burnout heat flux and the critical temperature difference.

REFERENCES

1. Morozov, V.G.   Int.J.Heat Mass Transfer, 5, 661 (1962).

2. Howell, J.R. and K.J. Bell.   Chem.Eng.Progr.Symp.Ser., No. 41, 59, 88 (1963).

3. Isakoff, S.E.   Proc.Heat Transfer and Fluid Mechanics Inst., Stanford University Press, Stanford, Calif., 15 (1956).

4. Ornatskii, A.P. and V.K. Shcherbakov. Teploenergetika, 6, 84 (1959). Translation appears in (5).

5. Markels, M., R.L. Durfee, and R. Richardson. USAEC, NYO-9500, September (1960).

6. Romie, F.E. and C.A. Aronson. ATL-A-123, Joint U.S. - Euratom Research and Development Report, July (1961).

SUMMARY AND CONTRIBUTION TO KNOWLEDGE

The effects of ultrasonic vibrations on natural convection and surface boiling heat transfer from electrically heated, horizontal, platinum wires of diameters 0.007 and 0.010 in. were measured. Two liquids, distilled water and methanol were used at three different acoustic intensity levels with frequency varying from 20.6 to 306 kcps. The temperatures of the distilled water were 113°F and 149°F and of methanol, 95°F and 113°F, when the frequency was 20.6 kcps. For other frequencies, namely 44.1, 108 and 306 kcps, the temperature was 149°F and 113°F for distilled water and methanol, respectively.

1. When compared with the heat transfer rates without vibration, the effects of ultrasonic vibrations varied from an 800% increase in the natural convection region to no effect in the well-developed nucleate boiling region. In all cases, however, no increase in heat transfer rates was observed until the critical sound pressure was applied. The critical sound pressure was a function of the liquid used and its temperature, the frequency of the sound field, as well as the heat transfer surface temperature. At surface temperatures corresponding to the natural convection region, the critical sound pressure was equivalent to the cavitation threshold of the liquid at the heat transfer surface.

2. The increase in heat transfer was due to the intense turbulence resulting from the radial oscillations as well as the rapid and erratic motion of the cavitation bubbles on the heat transfer

surface, as shown by the results of high speed photographic study. The characteristics of the cavitation bubbles resembled those of a gaseous cavitation bubble with content varying from mainly gas to mainly vapor depending on the surface temperature and the gas solubility in the liquid . An increase in the surface temperature also increased the population and the activity of the cavitation bubbles. At sufficiently high surface temperatures, the turbulence generated by the motion of the cavitation bubbles could not exceed that resulting from the growth and detachment (collapse) of vapor bubbles as in the well-developed nucleate boiling when there was no vibration and no increase in heat transfer rate was observed.

3. A technique using cavitation damage to measure the cavitation activity of the liquid at the unheated platinum wire surface was developed and the results used to correlate the heat transfer data. This quantity, the percentage of soil removed, however, did not take into account the thermal gradient in the liquid near a heated wire. Consequently, it was necessary to separate the heat transfer results into two regions, using the heat flux value at the incipience of boiling as the criterion. In the low heat flux region (natural convection), the wire temperature effect was reflected in the high exponent of the Grashof number while a cavitation bubble Reynolds number was defined to account for the wire temperature effect in the high heat flux region (nucleate boiling region). The final correlations for the two heat flux regions take the form of

Low Heat Flux Region

$$Nu_w = C_1 \frac{(Gr\ Pr)^{1/2} (S_R)^{1/2}}{P_{CR}} + C_2$$

High Heat Flux Region

$$Nu_B = C_3 \frac{Re^{1/2}\ Pr^{2/3}\ S_R^{1/2}}{P_{CR}} + C_4$$

C_1, C_2, C_3 and C_4 are constants. For each frequency, there was one set of constants. These constants are given in the following table.

Frequency (kcps)	C_1	C_2	C_3	C_4
20.6	0.0305	1.34	0.00470	5.84
44.1	0.0402	1.56	0.00471	2.96
108	0.0732	1.09	0.00881	0.745
306	0.174	1.22	-	-

The correlations for different frequencies could not be combined because the relation between the frequency and the critical sound pressure has not been established.

The exponent of 0.5 for the percentage of soil removed, when viewed in the light of penetration theory, indicates that the percentage of soil removed is related to the contact time which measures the turbulent intensity of the liquid resulting from cavitation.

4. The effect of liquid as well as the liquid temperature on heat transfer in a sound field was studied. Since a cavitation bubble

with high vapor content would collapse on the heat transfer surface and thus generate more turbulence, the liquid with lower gas solubility gave higher increase in heat transfer rates. High heat rates were also obtained at a higher temperature where both the cavitation threshold and the critical sound pressure were lowered. With the same electrical power input to the system, the result was an increase in the cavitation activity in the bulk liquid and on the heat transfer surface.

5. The effect of the frequency of the sound field was negligible if the same cavitation activity in the liquid was used. In order to achieve the same cavitation activity, more acoustic energy was required when the frequency was increased.

6. The effect of ultrasonic vibrations on the burnout heat flux and the critical temperature difference in methanol was studied at a frequency of 20.6 kcps. The bulk liquid temperature was 113°F and the wire was platinum with 0.007 in. diameter. No effect of vibration was found.

SUGGESTIONS FOR FUTURE WORK

1. The critical sound pressure appears to be the most important variable in the heat transfer processes being studied. In the low heat flux region, the critical sound pressure is equivalent to the cavitation threshold of the liquid at the heat transfer surface. Since little information is available on the cavitation thresholds of liquids at high temperatures, it is suggested that this information should be obtained, for example, for water at temperatures up to its boiling point. The cavitation thresholds of liquids at high temperatures can best be measured in a focussed standing wave system where the damage to the pressure probe by the cavitation process can be avoided by placing the probe at the secondary pressure maximum of the sound field. The pressure probe should be made of a piezoelectric material such as lead zirconate having a high curie point.

2. Although it has been established that the increase in heat transfer rate is the result of the motion of cavitation bubbles on the heat transfer surface, the mechanisms through which a cavitation bubble is formed and by which it grows and becomes unstable are not fully understood. Using the focussed standing wave system mentioned above and a point heat source located at the pressure maximum, the mechanism can be established much more easily. In fact, this should be a better system for studying the effects of ultrasonic vibrations on heat transfer since the sound pressures above the cavitation

threshold level can be measured with a pressure probe, and thus eliminates the cavitation damage measurement completely.

3. One subject on which almost no quantitative information exists is the mechanism by which a foreign body in a liquid can become a cavitation nucleus. Such information is useful as it may be possible to generate artificial cavitation nuclei on or near the heat transfer surface to affect the heat transfer rates. Specifically, the problem involves a study of the dependence of wetting angle and boundary geometry on liquid-gas interfacial motion under ultrasonic vibration. This problem can also be studied by using the focussed standing wave system and by creating artificial nucleus of known geometry on a solid surface located at the pressure maximum of the sound field.

4. A regulated DC power supply with increased amperage output could be used so that more data can be obtained for distilled water in the high heat flux region. With a large DC power supply, larger platinum wire diameters can be used as heating elements in measuring the heat transfer rate at burnout point so that vibration of the heating element may be eliminated.

5. It is suggested that heat transfer data should be obtained using a forced convective system as it may have more industrial significance.

APPENDIX A

INFORMATION ON TRANSDUCERS USED IN THIS WORK

The magnetostrictive transducers used for low frequency work, namely for 20.6 and 44.1 kcps were ferroxcube 7A2, double-dumb-bell transducers with ferroxcube biasing slabs, and manufactured by Philips. For higher frequencies, Glennite High Temperature ceramic transducers made of lead zirconate and manufactured by Gulton Industries were used. They were 1.5 in. diameter discs with electrodes and leads and vibrated in thickness mode. The Body No. was 41 for the frequency of 108 kcps and 31 for 306 kcps. Three transducers were used for all frequencies except in the case of 20.6 kcps where only two transducers were used.

Cementing Procedure

All transducers were cemented onto the bottom of the stainless steel tank (7 1/2 in. x 4 1/2 in. x 6 in. deep). Before they were cemented, the surfaces of the transducers and metal walls were sanded with a fine emery cloth and then degreased for four minutes in a mixture of one part by volume of concentrated sulphuric acid, one part of concentrated nitric acid and eight parts of water. The ceramic transducer surfaces, however, were not prepared since the process might damage the electrodes and leads.

To cement two pieces, the surfaces were carefully covered with a thin, homogeneous layer of Armstrong epoxy A12T and then pressed lightly together. The joint was hardened for 24 hours at room temperature.

Arrangement of Transducers

The arrangements of transducers on the bottom of the stainless steel tank for various frequencies are shown in Figures A-1 to A-3. The length or the thickness of the transducers which depends on the frequency is also given.

Impedance Matching of Transducers

A magnetostrictive transducer is inductive because of the inductance of its coil while a piezoelectric transducer is capacitive due to the capacitance of the ceramics. In order to get the maximum acoustic energy output from a transducer, the inductance or the capacitance should be tuned out. For the magnetostrictive transducers used in this work, the required capacitance was calculated by an empirical equation given by the manufacturer. For the ceramic transducers the matching component was calculated from the equation
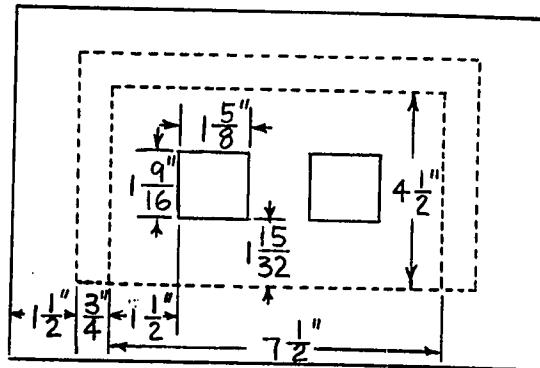
FIGURE A-1

f = 20.6 kcps

Length of transducer = 3.8 in.
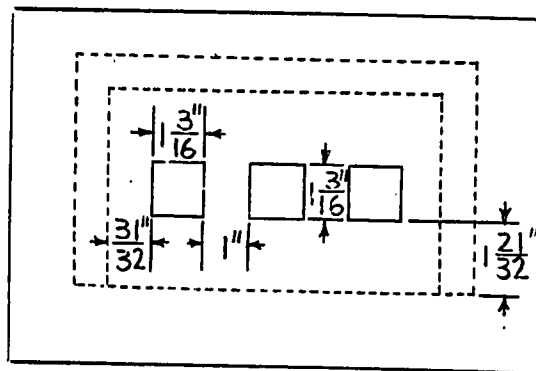
FIGURE A-2

f = 44.1 kcps

Length of transducer = 1.98 in.

DIAMETER = 1½"
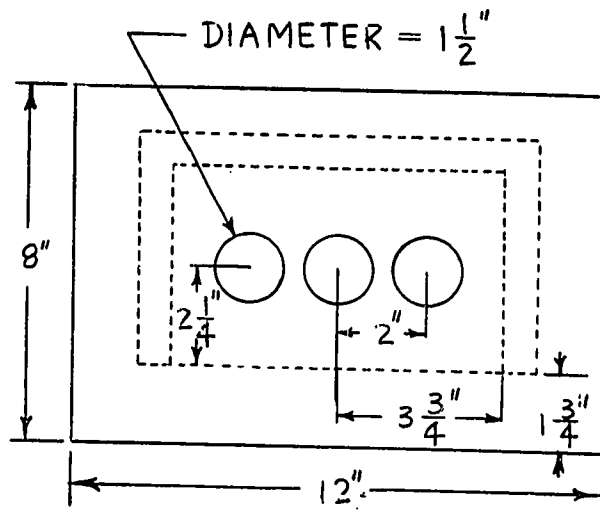
FIGURE A-3

Frequency kcps	Transducer Thickness in.
108	0.75
306	0.25

$$L = \frac{1}{\omega^2 C}$$

where L - inductance

   ω - angular frequency

   C - capacitance.

In both cases, minor adjustments in the matching component in the vicinity of the calculated value were required so that a satisfactory match was achieved. The acoustic energy output from a transducer was very sensitive to the driving frequency. After the determination of the matching component, the frequency of the system was varied in the vicinity of its previous value until the maximum acoustic energy output was obtained.

The following table lists the matching components used for the various transducers. A satisfactory energy output was obtained in the case of 306 kcps transducers without using a matching component, so none was used.

Transducer	Matching Component
20.6 kcps (two in parallel)	1.6 μF in parallel
44.1 kcps (three in series)	0.35 μF in parallel
108 kcps (three in parallel)	1.7 mh in parallel
306 kcps (three in parallel)	-

Relationship Between the Apparent Electrical Power Input to the Transducers and the Voltage Drop Across the Transducers

The relationships between the apparent electrical power input to the transducers (W_A) and the voltage drop across the transducers for

various frequencies are shown in Figures A-4 and A-5.
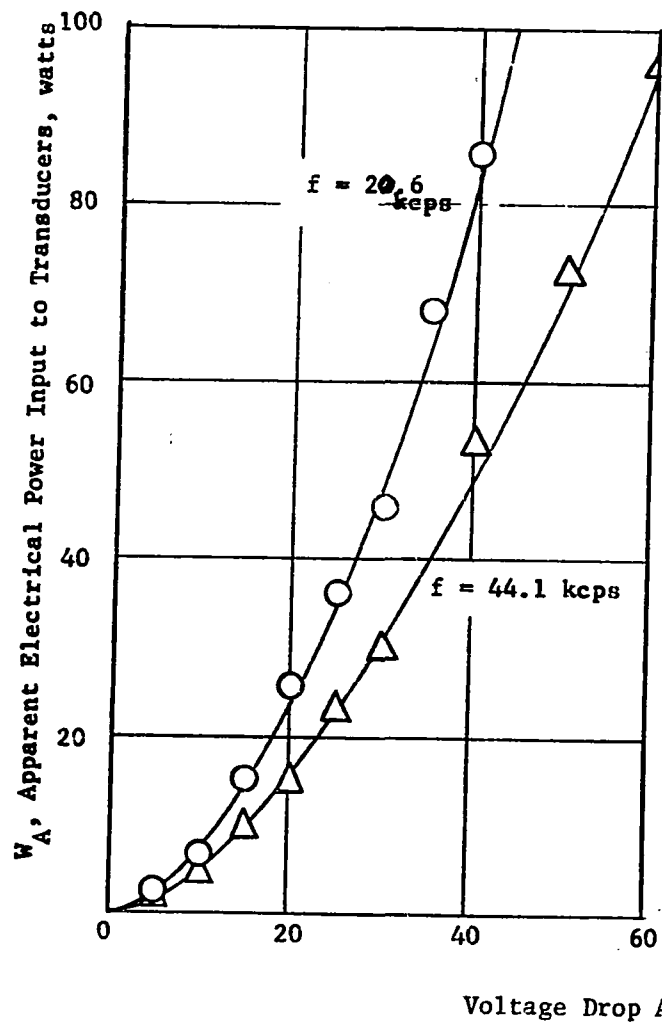
FIGURE A-4
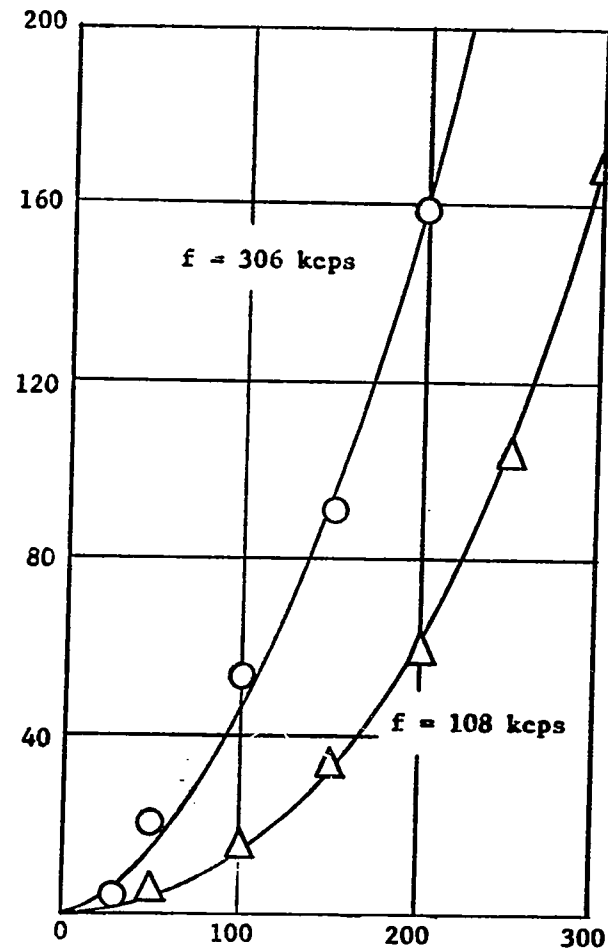
FIGURE A-5

APPENDIX B

SOUND PRESSURE DATA

TABLE B-1

LIQUID: Methanol   TEMPERATURE: 113°F   FREQUENCY: 20.6 kcps

W_A (watts)	E_{rms} (volts) 0.0	0.2"	0.4"	0.6"	0.8"	1.0" (distance along wire)	E_s (rms)	P_s atm.	(P_p)
1.0	.0058	.0060	.0062	.0060	.0058	.0054	.0058	.076	(.12)
2.0	.0082	.0083	.0084	.0083	.0080	.0080	.0082	.11	(.17)
4.8	.0106	.0110	.0110	.0110	.0107	.0105	.0108	.14	(.25)
7.0	.012	.013	.013	.012	.011	.011	.012	.16	(.30)

TABLE B-2

LIQUID: Methanol   TEMPERATURE: 95°F   FREQUENCY: 20.6 kcps

W_A (watts)	E_{rms} (volts) 0.0	0.2"	0.4"	0.6"	0.8"	1.0" (distance along wire)	E_s (rms)	P_s atm.	(P_p)
1.0	.0055	.0056	.0057	.0056	.0054	.0053	.0055	.072	(.11)
2.0	.0078	.0080	.0080	.0079	.0075	.0076	.0078	.10	(.16)
4.8	.0093	.0094	.0095	.0093	.0093	.0090	.0093	.12	(.23)
7.0	.011	.012	.013	.011	.010	.009	.011	.14	(.27)

TABLE B-3

LIQUID: Distilled Water   TEMPERATURE: 149°F   FREQUENCY: 20.6 kcps

W_A (watts)	E_{rms} (volts) 0.0	0.2"	0.4"	0.6"	0.8"	1.0" (distance along wire)	E_s (rms)	P_s atm.	(P_p)
1.0	.0065	.0074	.0076	.0074	.0067	.0063	.0070	.092	(.14)
2.0	.0115	.0125	.0125	.0120	.0115	.0110	.0120	.16	(.24)
4.8	.014	.016	.016	.016	.015	.013	.015	.20	(.34)
7.0	.020	.022	.022	.021	.021	.020	.021	.27	(.50)
15.6	.026	.027	.028	.026	.025	.024	.026	.34	(.60)

TABLE B-4

LIQUID: Distilled Water   TEMPERATURE: 113°F   FREQUENCY: 20.6 kcps

W_A (watts)	E_{rms} (volts)						E_s (rms)	P_s atm.	(P_p)
	0.0	0.2"	0.4"	0.6"	0.8"	1.0"			
			(distance along wire)						
1.0	.0065	.0066	.0067	.0066	.0064	.0062	.0065	.085	(.13)
2.0	.0110	.0115	.0120	.0110	.0105	.0100	.011	.14	(.24)
4.8	.014	.015	.015	.014	.014	.012	.0145	.19	(.34)
7.0	.018	.019	.020	.020	.018	.018	.019	.25	(.44)
15.6	.025	.027	.027	.027	.026	.024	.026	.34	(.58)

TABLE B-5

LIQUID: Distilled Water   TEMPERATURE: 149°F   FREQUENCY: 44.1 kcps

W_A (watts)	E_{rms} (volts)						E_s (rms)	P_s atm.	(P_p)
	0.0	0.2"	0.4"	0.6"	0.8"	1.0"			
			(distance along wire)						
0.5	.080	.0100	.0110	.0110	.0110	.090	.0100	.13	(.20)
1.3	.0100	.0110	.0130	.0130	.0130	.0120	.0120	.16	(.24)
3.2	.0110	.0125	.0135	.0135	.0125	.0120	.0125	.16	(.25)
4.6	.0130	.0140	.0155	.0155	.0155	.0130	.0145	.19	(.33)
9.5	.018	.020	.022	.022	.019	.019	.020	.26	(.51)
23.2	.026	.029	.028	.029	.029	.027	.028	.36	(.62)

TABLE B-6

LIQUID: Methanol   TEMPERATURE: 113°F   FREQUENCY: 44.1 kcps

W_A (watts)	E_{rms} (volts)						E_s (rms)	P_s atm.	(P_p)
	0.0	0.2"	0.4"	0.6"	0.8"	1.0"			
			(distance along wire)						
0.5	.0067	.0068	.0071	.0071	.0070	.0067	.0069	.090	(.13)
1.3	.0096	.0098	.0100	.0100	.0098	.0097	.0098	.13	(.20)
3.2	.0100	.0110	.0130	.0130	.0115	.0105	.0115	.15	(.24)
4.6	.011	.013	.014	.015	.013	.012	.013	.17	(.31)
9.5	.016	.018	.019	.019	.018	.017	.018	.23	(.47)

TABLE B-7

LIQUID: Distilled Water   TEMPERATURE: 149°F   FREQUENCY: 108 kcps

W_A (watts)	E_{rms} (volts)						E_s (rms)	P_s atm.	(P_p)
	0.0	0.2"	0.4"	0.6"	0.8"	1.0"			
			(distance along wire)						
16.0	.026	.027	.029	.029	.026	.025	.027	.35	(.53)
24.0	.032	.035	.037	.036	.032	.032	.034	.45	(.66)
34.2	.039	.040	.043	.043	.042	.039	.041	.53	(.89)
47.0	.047	.048	.049	.049	.047	.047	.048	.63	(1.1)

TABLE B-8

LIQUID: Methanol   TEMPERATURE: 113°F   FREQUENCY: 108 kcps

W_A (watts)	E_{rms} (volts)						E_s (rms)	P_s atm.	(P_p)
	0.0	0.2"	0.4"	0.6"	0.8"	1.0"			
			(distance along wire)						
10.0	.017	.020	.022	.021	.017	.016	.019	.25	(.38)
16.0	.025	.027	.027	.028	.025	.024	.026	.34	(.58)
24.0	.031	.033	.033	.033	.032	.030	.032	.42	(.76)
34.2	.037	.038	.038	.038	.036	.035	.031	.48	(.87)

TABLE B-9

LIQUID: Distilled Water   TEMPERATURE: 149°F   FREQUENCY: 306 kcps

W_A (watts)	E_{rms} (volts)						E_s (rms)	P_s atm.
	0.0	0.2"	0.4"	0.6"	0.8"	1.0"		
			(distance along wire)					
22	.035	.036	.038	.039	.035	.033	.036	.36
54	.062	.062	.064	.066	.060	.058	.062	.62
92	.09	.11	.11	.12	.09	.08	.100	1.0
165	.12	.14	.13	.15	.12	.12	.13	1.3

(No cavitation)

TABLE B-10

LIQUID: Methanol   TEMPERATURE: 113°F   FREQUENCY: 306 kcps

W_A (watts)	E_{rms} (volts)						E_s (rms)	P_s atm.
	0.0	0.2"	0.4"	0.6"	0.8"	1.0"		
			(distance along wire)					
54	.057	.057	.058	.060	.057	.055	.057	.57
74	.069	.071	.073	.074	.070	.069	.071	.71
92	.082	.083	.084	.085	.082	.082	.083	.83
125	.091	.092	.093	.093	.091	.092	.092	.92

APPENDIX C

CAVITATION DAMAGE DATA

TABLE C-1[*]

Frequency : 20.6 kcps

Liquid   : Distilled Water   Temperature: 149°F

W_A (watts)	CPM_i	CPM_f	TIME (min)	S_R (%)
RUN A1		BACKGROUND = 486 CPM		
86.0	36200	32500	0.5	15.5
86.0	37800	30100	1.0	30.8
86.0	42300	29200	1.5	47.0
86.0	41400	24600	2.0	61.4
86.0	37200	21700	3.0	63.4
86.0	35300	17600	4.0	76.1
86.0	44400	38200	0.5	21.0
86.0	42300	34700	1.0	27.1
86.0	50100	35000	1.5	45.7
86.0	49800	32000	2.0	53.8
86.0	37700	20100	3.0	71.0
86.0	36100	18500	4.0	74.1
RUN A2		BACKGROUND = 772 CPM		
68.2	38800	34700	0.5	16.2
68.2	36200	28600	1.0	32.2
68.2	46100	28800	2.0	57.2
68.2	42100	29100	1.5	47.1
68.2	44300	23300	3.0	72.3
68.2	41900	18600	4.0	85.0
86.0	47900	41300	0.5	21.0
86.0	49200	40400	1.0	27.1
86.0	35200	24700	1.5	45.7
86.0	39900	25900	2.0	53.8
86.0	39300	21000	3.0	71.0
86.0	39400	20300	4.0	74.1

[*] In Table C-1 and subsequent tables TIME is the time that a specimen was exposed to the cavitation liquid, CPM_i and CPM_f are the count rate per minute of a specimen before and after being exposed to cavitation, W_A and S_R are defined as before.

TABLE C-1, continued

W_A (watts)	CPM_i	CPM_f	TIME (min)	S_R (%)
RUN A3		BACKGROUND = 486 CPM		
68.2	44100	39700	0.5	15.2
68.2	40800	34600	1.0	23.1
68.2	35700	23800	1.5	50.8
68.2	36600	26400	2.0	42.4
68.2	36200	21000	3.0	64.0
68.2	39200	19900	4.0	74.6
68.2	39500	36300	0.5	12.1
68.2	50712	40600	1.0	30.2
68.2	37700	24300	2.0	54.0
68.2	37900	25800	1.5	48.3
68.2	35600	20700	3.0	63.5
68.2	36200	16300	4.0	83.7
RUN A5		BACKGROUND = 641 CPM		
51.0	36500	31700	1.0	20.0
51.0	44000	37800	1.0	21.4
51.0	36000	33400	0.5	11.1
51.0	37100	34800	0.5	9.6
51.0	38300	26500	2.0	47.1
51.0	42100	30300	2.0	42.6
51.0	47100	33100	2.0	45.2
51.0	38100	21000	3.0	68.6
51.0	39200	23200	3.0	62.4
51.0	39800	18900	4.0	80.2
51.0	40300	18600	4.0	82.0
51.0	50200	37900	1.5	37.1
51.0	35100	32000	0.5	13.1
51.1	37100	32300	0.5	19.7
51.0	48900	42600	1.0	19.5
51.0	44600	28900	2.0	53.5
51.0	47200	40200	1.0	22.5
51.0	43500	33900	1.5	33.4
51.0	36800	28600	1.5	33.9
RUN A6		BACKGROUND = 647 CPM		
51.0	37100	26000	2.0	45.8
51.0	39200	24800	2.5	55.8
51.0	40300	24900	2.5	58.4
51.0	40100	19600	4.0	77.8
51.0	49200	24400	4.0	76.5
51.0	44100	40800	0.5	11.3

TABLE C-1, continued

W_A (watts)	CPM_i	CPM_f	TIME (min)	S_R (%)
RUN A6 - continued				
51.0	37600	33200	1.0	18.0
51.0	38900	33600	1.0	20.7
51.0	41400	31900	1.5	35.0
51.0	43700	32900	1.5	37.6
51.0	46600	31900	2.0	48.0
51.0	37800	21400	3.0	66.0
51.0	47700	23600	4.0	76.8
51.0	47200	24700	4.0	72.5
RUN A7		BACKGROUND = 482 CPM		
36.2	38100	34900	1.0	12.6
36.2	37900	35200	1.0	11.0
36.2	35200	32500	1.0	11.7
26.0	40700	39100	1.0	6.0
26.0	44800	43200	1.0	5.4
15.6	42100	41300	1.0	3.0
15.6	43100	42100	1.0	3.5
15.6	37100	36700	1.0	1.5
RUN A8		BACKGROUND = 738 CPM		
36.2	44500	40400	1.0	13.9
36.2	47800	43600	1.0	13.3
26.0	37900	36700	1.0	5.0
26.0	36200	35300	1.0	3.7
15.6	49200	48400	1.0	2.5
68.2	36800	30200	1.0	27.3
68.2	38900	31400	1.0	29.5
86.0	38100	30600	1.0	30.2
86.0	42100	33600	1.0	30.7
86.0	44400	34800	1.0	32.8

TABLE C-2

FREQUENCY: 20.6 kcps

LIQUID : Distilled Water   TEMPERATURE: $113^{\circ}F$

W_A (watts)	CPM_i	CPM_f	TIME (min)	S_R (%)
RUN A9		BACKGROUND = 742 CPM		
86.0	42300	33000	1.0	33.5
51.0	43900	36100	1.0	27.1
51.0	37800	31500	1.0	25.2
36.2	37600	33800	1.0	15.3
36.2	35300	32000	1.0	14.5
26.0	39500	36200	1.0	12.8
26.0	48600	46000	1.0	8.1
15.6	48100	46000	1.0	6.2
15.6	47800	47000	1.0	2.0
86.0	47700	36500	1.0	35.6
RUN A10		BACKGROUND = 768 CPM		
7.0	37200	37200	1.0	0.0
15.6	48100	46800	1.0	4.1
26.0	48900	46700	1.0	6.7
26.0	50300	47200	1.0	9.5
51.0	36200	30500	1.0	24.0
51.0	37700	30900	1.0	27.6
68.2	38100	30000	1.0	32.4
86.0	38900	30100	1.0	34.7

TABLE C-3

FREQUENCY: 20.6 kcps

LIQUID   : Distilled Water   TEMPERATURE: 180°F

W_A (watts)	CPM_i	CPM_f	TIME (min)	S_R (%)
RUN A12		BACKGROUND = 629 CPM		
26.0	38800	37700	1.0	4.3
26.0	37200	35900	1.0	5.2
36.2	37900	35700	1.0	8.7
36.2	39200	37600	1.0	6.0
51.0	40100	36200	1.0	14.8
51.0	44800	41500	1.0	11.2
68.2	37600	32300	1.0	21.5
68.2	37100	31300	1.0	23.6
86.0	47800	38500	1.0	29.5
15.6	44200	43400	1.0	2.6
15.6	45100	44600	1.0	1.8
RUN A13		BACKGROUND = 819 CPM		
26.0	39800	39700	1.0	0.5
36.2	37900	35900	1.0	8.0
36.2	46800	45200	1.0	5.1
51.0	46100	41400	1.0	15.6
51.0	44100	40200	1.0	13.6
68.2	35800	30500	1.0	22.6
86.0	34800	28600	1.0	27.3
86.0	37900	31400	1.0	26.3

TABLE C-4

FREQUENCY: 20.6 kcps

LIQUID   :   Methanol   TEMPERATURE: 113°F

W_A (watts)	CPM_i	CPM_f	TIME (min)	S_R (%)
RUN A14		BACKGROUND = 623 CPM		
7.0	35800	35800	1.0	0.0
7.0	41000	40700	1.0	1.0
15.6	42800	42300	1.0	1.7
15.6	37900	37200	1.0	2.7
36.2	37000	35800	1.0	5.0
36.2	36600	35400	1.0	5.1
51.0	45400	43200	1.0	7.2
51.0	47700	45700	1.0	6.4
68.2	48000	45000	1.0	9.5
68.2	42200	39400	1.0	10.2
86.0	35500	32200	1.0	14.1
86.0	36700	33800	1.0	12.0
RUN A15		BACKGROUND = 634 CPM		
86.0	47200	42300	1.0	15.7
86.0	41100	37900	1.0	11.7
68.2	42000	38300	1.0	13.5
68.2	46100	42900	1.0	10.4
51.0	37800	35700	1.0	8.5
51.0	35400	33900	1.0	6.3
36.2	42200	40400	1.0	6.3
36.2	45900	44400	1.0	5.1
15.6	47300	46400	1.0	3.0
15.6	36600	36100	1.0	1.9
7.0	38200	38000	1.0	0.8
7.0	39400	39400	1.0	0.0

TABLE C-5

FREQUENCY: 20.6 kcps

LIQUID   : Methanol

TEMPERATURE: $95^{\circ}F$

W_A (watts)	CPM_i	CPM_f	TIME (min)	S_R (%)
RUN A16		BACKGROUND	= 654 CPM	
86.0	39100	35500	1.0	14.2
86.0	39000	34900	1.0	16.5
68.2	44000	40500	1.0	12.0
68.2	41100	37400	1.0	13.7
36.2	37200	35700	1.0	6.0
15.6	38400	37900	1.0	2.0
15.6	36500	35700	1.0	3.3
7.0	47200	47200	1.0	0.0
7.0	49300	48900	1.0	1.2
RUN A17		BACKGROUND	= 650 CPM	
7.0	37900	37500	1.0	1.6
15.6	42900	42100	1.0	2.9
36.2	43800	42200	1.0	5.4
36.2	44400	42500	1.0	6.6
51.0	45600	42500	1.0	10.2
51.0	47300	44500	1.0	9.0
51.0	45800	42900	1.0	9.7
68.2	36800	33600	1.0	13.3
86.0	36100	32900	1.0	13.7

TABLE C-6

FREQUENCY: 44.1 kcps

LIQUID   : Distilled Water   TEMPERATURE: 149°F

W_A (watts)	CPM_i	CPM_f	TIME (min)	S_R (%)
RUN A18		BACKGROUND	= 819 CPM	
9.5	37900	37900	1.0	0.0
9.5	38100	38100	1.0	0.0
15.6	42800	42600	1.0	0.6
15.6	44100	43800	1.0	0.9
30.2	46800	45700	1.0	3.5
30.2	44400	42900	1.0	5.0
42.7	40200	38100	1.0	7.9
42.7	36800	34900	1.0	7.7
53.3	39100	35900	1.0	12.5
53.3	47100	43800	1.0	10.7
42.7	49200	46000	1.0	10.0
73.0	49800	42900	1.0	21.1
96.0	39200	31800	1.0	25.7
RUN A19		BACKGROUND	= 808 CPM	
96.0	36600	29800	1.0	28.4
96.0	37400	30600	1.0	27.6
42.7	38800	36000	1.0	10.7
73.0	41100	35800	1.0	19.7
73.0	47200	39900	1.0	23.4
53.3	46600	42800	1.0	12.4
42.7	43100	40600	1.0	9.0
30.2	39300	38600	1.0	2.9
9.5	42200	42200	1.0	0.0
15.6	41800	41300	1.0	1.8

TABLE C-7

FREQUENCY: 44.1 kcps

LIQUID   : Methanol

TEMPERATURE: 113°F

W_A (watts)	CPM_i	CPM_f	TIME (min)	S_R (%)
RUN A20		BACKGROUND = 802 CPM		
4.6	34900	34900	1.0	0.0
9.5	39900	39600	1.0	1.3
9.5	41100	40900	1.0	0.7
15.6	41700	41000	1.0	2.5
15.6	36300	35500	1.0	3.2
30.2	37700	36400	1.0	5.1
30.2	38200	37100	1.0	4.4
42.7	44300	42600	1.0	6.0
42.7	41400	39400	1.0	7.5
53.0	39700	37600	1.0	8.2
73.0	46700	43200	1.0	11.4
96.0	43400	39900	1.0	12.2
RUN A21		BACKGROUND = 654 CPM		
73.0	36600	33500	1.0	13.0
73.0	35800	33700	1.0	8.9
53.3	41900	39800	1.0	7.5
53.3	42600	39900	1.0	9.8
96.0	41500	37400	1.0	15.0
96.0	43500	39900	1.0	12.6
96.0	37500	34200	1.0	13.2
42.7	37900	36200	1.0	6.8
30.2	36600	35300	1.0	5.3
30.2	47800	46200	1.0	4.9
9.5	49100	48600	1.0	1.6
15.6	50300	49600	1.0	2.2
4.6	38800	38800	1.0	0.0
4.6	36800	36800	1.0	0.0

TABLE C-8

FREQUENCY: 108 kcps

LIQUID : Distilled water   TEMPERATURE: 149°F

W_A (watts)	CPM_i	CPM_f	TIME (min)	S_R (%)
RUN A22		BACKGROUND $=$ 629 CPM		
105.0	37700	33900	1.0	15.2
105.0	38900	35600	1.0	13.1
62.0	42800	41300	1.0	5.2
62.0	47900	46800	1.0	3.5
62.0	42100	41100	1.0	3.8
47.0	48100	48100	1.0	0.0
47.0	44700	44500	1.0	0.7
32.2	46500	46500	1.0	0.0
32.2	35800	35800	1.0	0.0
RUN A23		BACKGROUND $=$ 618 CPM		
24.0	37100	37100	1.0	0.0
24.0	48800	48800	1.0	0.0
32.2	49200	49000	1.0	0.5
32.2	36600	36200	1.0	1.8
62.0	39100	38100	1.0	3.9
62.0	38400	37800	1.0	2.5
105.0	42400	40700	1.0	6.1
105.0	45300	43100	1.0	7.5
105.0	45900	43600	1.0	7.4

TABLE C-9

FREQUENCY: 108 kcps

LIQUID   : Methanol

TEMPERATURE: 113°F

W_A (watts)	CPM_i	CPM_f	TIME (min)	S_R (%)
RUN A24		BACKGROUND = 522 CPM		
32.2	36600	36600	1.0	0.0
47.0	35800	35800	1.0	0.0
47.0	47200	46900	1.0	1.0
62.0	49200	47800	1.0	4.2
62.0	48900	48000	1.0	2.8
105.0	47200	42600	1.0	14.8
105.0	41400	38300	1.0	11.3
62.0	42100	41000	1.0	3.9
RUN A25		BACKGROUND = 654 CPM		
105.0	35500	33600	1.0	8.3
105.0	41900	40000	1.0	7.0
62.0	42300	41700	1.0	2.2
62.0	45400	44100	1.0	4.3
62.0	45900	45000	1.0	3.1
32.2	38800	38600	1.0	0.8
32.2	39100	38800	1.0	1.0
24.0	36200	36200	1.0	0.0
24.0	37700	37700	1.0	0.0

TABLE C-10

FREQUENCY: 306 kcps

LIQUID : Methanol   TEMPERATURE: 113°F

W_A (watts)	CPM_i	CPM_f	TIME (min)	S_R (%)
RUN A26		BACKGROUND = 802 CPM		
74.0	37900	37900	1.0	0.0
74.0	34800	34800	1.0	0.0
92.0	44100	44100	1.0	0.0
92.0	49100	48900	1.0	0.5
92.0	48200	48200	1.0	0.0
92.0	48800	48700	1.0	0.2
125.0	46300	45800	1.0	1.5
125.0	36600	35800	1.0	3.2
125.0	35500	35000	1.0	1.8
125.0	47800	46900	1.0	2.9
160.0	42900	40900	1.0	7.2
160.0	37400	35000	1.0	8.8
160.0	48200	45600	1.0	8.1
160.0	46900	45000	1.0	6.3
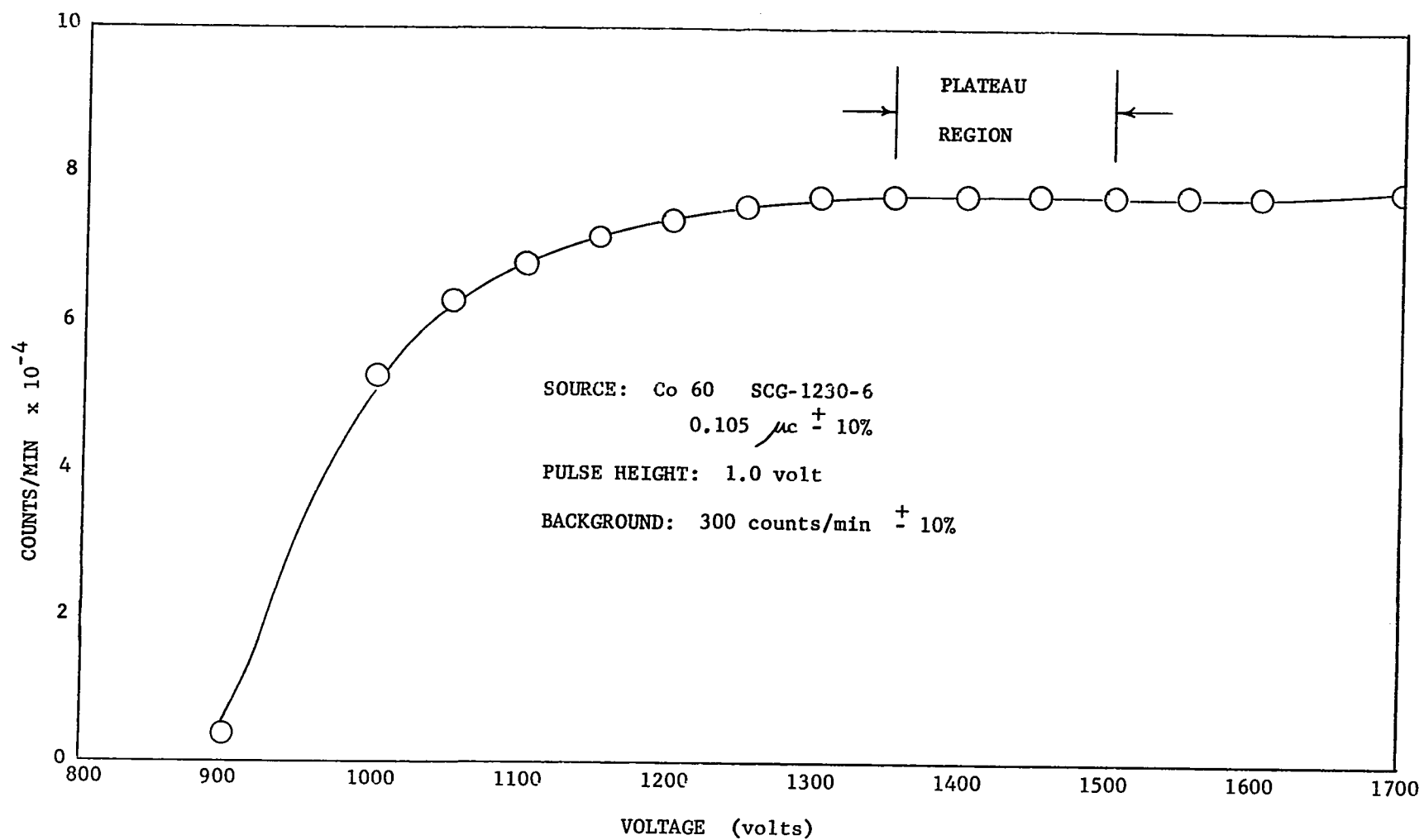
FIGURE C-1   DETERMINATION OF SCINTILLATION PLATEAU REGION

APPENDIX D

HEAT TRANSFER DATA

TABLE D-1

LIQUID: Methanol   TEMPERATURE: 95°F   FREQUENCY: 20.6 kcps

WIRE DIAMETER: 0.010"

W_A watts	E_{SR} Volts	E_{PT} Volts	q/A BTU/HR FT^2	Δt °F	Nu	Y_1*	Y_2*
RUN 30			L = 48/64 in.	R_{100} = .05021 Ω			
0.0	0.0585	0.1285	7,850	36.6	1.55	-	-
0.0	0.0826	0.1879	16,200	57.2	2.07	-	-
0.0	0.0986	0.2291	23,600	69.0	2.53	-	-
0.0	0.1221	0.2886	36,800	79.5	-	-	-
0.0	0.1444	0.3436	51,800	82.6	-	-	-
0.0	0.1657	0.3965	68,600	85.9	-	-	-
0.0	0.1885	0.4523	89,000	87.7	-	-	-
0.0	0.0703	0.1579	11,600	48.4	1.74	-	-
4.8	0.0703	0.1539	11,300	34.8	-	-	-
15.6	0.0705	0.1535	11,300	31.6	2.55	59.5	-
36.2	0.0706	0.1507	11,100	21.3	3.64	59.5	-
86.0	0.0707	0.1504	11,100	19.3	4.07	85.0	-
0.0	0.0951	0.2236	22,200	76.2	-	-	-
1.0	0.0950	0.2158	21,400	56.1	-	-	-
15.6	0.0951	0.2125	21,100	46.4	3.25	102	-
36.2	0.0950	0.2087	20,700	37.0	4.00	105	-
86.0	0.0947	0.2053	20,300	29.4	5.02	102	-
0.0	0.1162	0.2729	33,100	75.7	-	-	-
1.0	0.1162	0.2711	32,900	71.4	-	-	-
15.6	0.1162	0.2613	31,700	50.2	3.85	159	-
36.2	0.1162	0.2586	31,400	43.9	5.07	140.5	-
86.0	0.1162	0.2564	31,100	39.4	5.74	179	
0.0	0.1496	0.3553	55,500	83.2	-	-	-
2.0	0.1499	0.3547	55,500	81.1	-	-	-
15.6	0.1496	0.3529	55,100	79.2	6.94	-	746
36.2	0.1496	0.3438	53,700	62.9	-	-	-
0.0	0.1761	0.4216	77,500	87.1	-	-	-
2.0	0.1761	0.4194	77,100	84.1	-	-	-
15.6	0.1761	0.4178	76,800	81.9	9.6	-	884

* $$Y_1 = \frac{[Gr\,Pr]^{1/2}\,S_R^{1/2}}{P_{CR}} \qquad\qquad Y_2 = \frac{Re^{1/2}\,Pr^{2/3}\,S_R^{1/2}}{P_{CR}}$$

TABLE D-1 continued

W_A watts	E_{SR} Volts	E_{PT} Volts	q/A BTU/HR FT^2	Δt ^{o}F	N u	Y_1	Y_2
RUN 30 - continued							
36.2	0.1760	0.4157	76,400	78.9	-	-	-
86.0	0.1761	0.4140	76,100	76.3	-	-	-
0.0	0.2009	0.4815	101,000	87.8	-	-	-
36.2	0.2015	0.4849	102,000	90.4	-	-	-
86.0	0.2009	0.4814	101,000	87.6	-	-	-
RUN 31			L = 48/64 in.	R_{100} = .05040 Ω			
0.0	0.0506	0.1091	5,760	24.9	1.67	-	-
0.0	0.0332	0.0702	2,430	14.9	1.15	-	-
0.0	0.0263	0.5534	1,520	10.8	1.0	-	-
0.0	0.0212	0.0445	986	8.8	.78	-	-
0.0	0.0384	0.0816	3,270	17.7	1.77	-	-
0.0	0.0445	0.0951	4,420	21.2	1.52	-	-
0.0	0.0584	0.1277	7,790	32.4	1.72	-	-
0.0	0.1212	0.2877	36,400	78.4	-	-	-
0.0	0.1649	0.3962	68,200	86.6	-	-	-
0.0	0.0309	0.0652	2,100	12.9	1.15	-	-
0.0	0.0409	0.0877	3,740	21.4	1.28	-	-
15.6	0.0408	0.0868	3,700	16.6	1.61	31.5	-
36.2	0.0408	0.0861	3,670	11.8	2.27	-	-
0.0	0.0486	0.1049	5,320	25.1	1.54	-	-
15.6	0.0486	0.1041	5,280	21.0	1.75	40	-
36.2	0.0485	0.1026	5,200	13.6	2.72	-	-
86.0	0.0485	0.1024	5,190	12.3	2.94	-	-
0.0	0.0613	0.1348	8,630	35.1	1.77	-	-
15.6	0.0613	0.1329	8,500	27.1	2.25	50	-
36.2	0.0613	0.1321	8,460	23.9	2.55	65	-
86.0	0.0613	0.1302	8,330	15.8	3.67	70.5	-
0.0	0.0830	0.1905	16,500	59.7	2.02	-	-
15.6	0.0829	0.1837	15,900	39.5	2.92	76	-
36.2	0.0829	0.1802	15,600	28.4	3.83	79.5	-
86.0	0.0830	0.1789	15,500	24.1	4.55	103	-
0.0	0.1292	0.3092	41,700	84.4	-	-	-
15.6	0.1290	0.3044	41,000	73.7	5.85	-	600
36.2	0.1290	0.2925	39,400	50.6	7.89	-	567
86.0	0.1288	0.2893	38,900	45.2	-	-	-

TABLE D-1 continued

W_A watts	E_{SR} Volts	E_{PT} Volts	q/A BTU/HR FT^2	Δt °F	Nu	Y_1	Y_2
RUN 32			L = 48/64 in.	R_{100} = .05021 Ω			
0.0	0.0357	0.0756	2,812	17.2	1.20	-	-
0.0	0.0436	0.0932	4,236	22.4	1.38	-	-
15.6	0.0433	0.0917	4,140	17.3	1.67	32.3	-
36.2	0.0430	0.0907	4,072	13.2	2.21	38.5	-
86.0	0.0428	0.0899	4,023	11.4	2.58	-	-
0.0	0.0502	0.1088	5,708	27.5	1.51	-	-
15.6	0.0503	0.1076	5,648	20.5	1.95	39.5	-
0.0	0.0549	0.1193	6,837	31.4	.77	-	-
15.6	0.0550	0.1180	6,774	24.5	1.97	45.0	-
36.2	0.0549	0.1159	6,629	17.2	2.73	48.2	-
86.0	0.0546	0.1148	6,538	14.1	3.28	64.1	-
0.0	0.0730	0.1628	12,410	46.2	1.95	-	-
15.6	0.0717	0.1564	11,708	33.3	2.61	62.0	-
36.2	0.0684	0.1473	10,523	25.5	2.93	69.1	-
86.0	0.0713	0.1520	11,313	20.5	3.92	81.6	-
0.0	0.0871	0.2006	18,245	64.1	2.1	-	-
15.6	0.0894	0.1983	18,512	42.0	3.19	85.4	-
36.2	0.0892	0.1943	18,082	32.5	3.97	90.5	-
86.0	0.0889	0.1917	17,793	26.5	4.78	112	-
0.0	0.1093	0.2557	29,172	73.4	-	-	-
15.6	0.1093	0.2489	28,411	57.2	3.59	146	-
36.2	0.1094	0.2427	27,731	42.4	4.82	127	-
86.0	0.1096	0.2403	27,493	35.1	5.65	155	-
36.2	0.0494	0.1043	5,382	14.5	2.62	41.4	-
86.0	0.0488	0.1028	5,238	13.3	2.83	60.2	-
0.0	0.1395	0.3318	48,321	82.2	-	-	-
15.6	0.1392	0.3282	47,700	76.2	6.40	-	666
36.2	0.1401	0.3221	47,124	61.2	7.89	-	734
86.0	0.1405	0.3179	46,628	51.8	9.21	-	990
0.0	0.1593	0.3798	63,178	83.7	-	-	-
36.2	0.1587	0.3707	61,423	71.3	8.90	-	1040
86.0	0.1603	0.3697	61,881	63.8	9.95	-	1420
0.0	0.1702	0.4068	72,300	85.2	-	-	-
0.0	0.2046	0.4916	105,000	88.6	-	-	-
0.0	0.2212	0.5327	123,000	90.8	-	-	-
0.0	0.2288	0.5526	132,000	92.5	-	-	-
0.0	0.2372	0.5735	142,000	93.3	-	-	-

TABLE D-2

LIQUID: Methanol　　　　TEMPERATURE: 113°F　　　　FREQUENCY: 20.6 kcps

WIRE DIAMETER: 0.007"

W_A watts	E_{SR} Volts	E_{PT} Volts	q/A BTU/HR FT^2	Δt °F	Nu	Y_1	Y_2
RUN 28			L = 49.5/64 in.		R_{100} = 0.1049 Ω		
0.0	0.0294	0.1354	5,750	21.5	1.37	-	-
15.6	0.0289	0.1324	5,540	17.2	1.67	29.2	-
36.2	0.0288	0.1305	5,440	11.3	2.50	30.4	-
0.0	0.0328	0.1526	7,240	26.6	1.4	-	-
15.6	0.0325	0.1497	7,040	19.7	1.84	33.4	-
15.6	0.0327	0.1500	7,100	17.4	2.08	29.8	-
36.2	0.0325	0.1480	6,960	14.5	2.47	39.4	-
0.0	0.0436	0.2084	13,150	41.8	1.64	-	-
15.6	0.0435	0.2038	12,820	30.1	2.22	53.1	-
15.6	0.0470	0.2206	15,000	31.2	2.50	55.8	-
0.0	0.0659	0.3276	31,210	65.3	2.5	-	-
15.6	0.0579	0.2783	23,300	45.0	2.69	99.6	-
0.0	0.0745	0.3733	40,200	70.3	-	-	-
15.6	0.0738	0.3608	38,500	55.2	7.46	-.	1340
36.2	0.0759	0.3599	39,500	37.4	11.22	-	1440
15.6	0.0835	0.4149	50,100	64.8	8.4	-	1790
0.0	0.0938	0.4740	64,300	75.2	-	-	-
15.6	0.0938	0.4706	63,800	71.1	9.74	-	1310
RUN 36							
0.0	0.0312	0.1444	6,500	23.5	1.4	-	-
15.6	0.0312	0.1425	6,420	16.0	2.08	27.7	-
36.2	0.0308	0.1402	6,250	12.6	2.51	35.4	-
0.0	0.0397	0.1880	10,800	36.0	1.6	-	-
15.6	0.0393	0.1814	10,300	22.3	2.38	37.4	-
36.2	0.0387	0.1772	9,910	17.5	2.91	42.8	-
0.0	0.0409	0.1943	11,500	38.0	1.6	-	-
15.6	0.0407	0.1889	11,100	26.0	2.20	44.8	-
36.2	0.0404	0.1850	10,800	17.2	3.22	45.4	-
0.0	0.0497	0.2438	17,500	57.0	1.6	-	-
0.0	0.0515	0.2519	18,750	55.0	1.8	-	-
15.6	0.0519	0.2465	18,500	37.5	2.54	74.1	-
36.2	0.0516	0.2400	17,910	26.1	3.56	68.8	-

TABLE D-2   continued

W_A watts	E_{SR} Volts	E_{PT} Volts	q/A BTU/HR FT^2	Δt $^\circ$F	Nu	Y_1	Y_2
RUN 36 continued							
86.0	0.0574	0.2663	22,100	25.0	4.56	103.0	-
0.0	0.0798	0.4015	46,300	73.0	-	-	-
36.2	0.0790	0.3767	43,000	42.0	11.24	-	1451
0.0	0.0911	0.4557	60,000	70.2	-	-	-
15.6	0.0896	0.4409	57,100	60.3	10.34	-	1750
0.0	0.1037	0.5283	79,200	80.4	-	-	-
15.6	0.1031	0.5197	77,430	74.1	11.46	-	999
0.0	0.1108	0.5635	90,200	79.6	-	-	-
15.6	0.1057	0.5320	81,300	72.8	12.28	-	1254
0.0	0.1245	0.6400	115,000	85.0	-	-	-
15.6	0.1222	0.6229	110,000	81.8	-	-	-
36.2	0.1197	0.6009	104,000	72.0	15.79	-	2559
0.0	0.1330	0.6817	131,000	86.2	-	-	-
0.0	0.1524	0.7809	172,000	85.9	-	-	-
15.6	0.1524	0.7810	172,000	86.1	-	-	-
0.0	0.1616	0.8350	195,000	91.2	-	-	-
RUN 22		L = 48/64 in.		R_{100} = .09915 Ω			
0.0	0.0533	0.2256	16,200	56.4	1.51	-	-
0.0	0.0810	0.3842	46,400	73.2	-	-	-
0.0	0.1087	0.5191	84,100	76.5	-	-	-
0.0	0.1286	0.6189	119,000	81.2	-	-	-
0.0	0.1547	0.7496	173,000	84.6	-	-	-
0.0	0.1785	0.8701	232,000	87.4	-	-	-
0.0	0.1930	0.9444	272,000	88.9	-	-	-
0.0	0.0397	0.1778	10,500	37.3	1.46	-	-
0.0	0.0643	0.3067	29,400	75.7	2.08	-	-
15.6	0.0643	0.2664	22,900	35.1	2.10	66.5	-
36.2	0.0643	0.2643	22,500	33.5	3.47	96.0	-
86.0	0.0643	0.2616	22,100	25.4	4.56	103	-
0.0	0.0908	0.4263	57,700	66.1	4.64	-	-
15.6	0.0908	0.4221	57,200	61.0	10.3	-	1750
36.2	0.0911	0.4191	56,900	54.8	11.3	-	1070
0.0	0.1205	0.5754	103,000	75.5	-	-	-
15.6	0.1205	0.5756	103,000	74.8	-	-	-
36.2	0.1205	0.5757	103,000	74.9	-	-	-
86.0	0.1205	0.5757	104,000	74.9	-	-	-
0.0	0.1504	0.7245	162,000	80.9	-	-	-
36.2	0.1504	0.7267	163,000	82.8	-	-	-
86.0	0.1504	0.7256	163,000	81.9	-	-	-

TABLE D-2 continued

W_A watts	E_{SR} Volts	E_{PT} Volts	q/A BTU/HR FT^2	Δt $^{\circ}F$	Nu	Y_1	Y_2
RUN 22 continued							
0.0	0.1260	0.6046	114,000	79.4	-	-	-
0.0	0.1564	0.7572	177,000	84.1	-	-	-
RUN 26			L = 49.5/64 in.		R_{100} = .10513 Ω		
0.0	0.1794	0.9210	239,000	84.1	-	-	-
0.0	0.2016	1.0446	304,000	89.9	-	-	-
0.0	0.497	0.2191	143,000	44.9	1.66	-	-
15.6	0.0497	0.2119	139,000	27.3	2.58	47.1	-
36.2	0.0497	0.2104	138,000	22.6	3.14	60.2	-
0.0	0.0767	0.3814	42,300	60.9	3.69	-	-
15.6	0.0767	0.3714	41,200	45.1	9.66	-	1040
36.2	0.0767	0.3690	40,900	41.3	10.3	-	681
86.0	0.0767	0.3634	40,300	32.4	13.1	-	1913
0.0	0.1052	0.5261	80,000	66.2	6.43	-	-
36.2	0.1052	0.5180	78,800	58.6	14.2	-	2997
86.0	0.1052	0.5174	78,700	57.9	14.6	-	2130
0.0	0.1197	0.6011	104,000	72.3	-	-	-
15.6	0.1197	0.6000	104,000	70.3	-	-	-
86.0	0.1197	0.5980	103,000	67.3	-	-	-
15.6	0.1464	0.7458	158,000	79.3	-	-	-
36.2	0.1464	0.7453	158,000	78.9	-	-	-
86.0	0.1464	0.7450	158,000	78.6	-	-	-
RUN 38			L = 48/64 in.		R_{100} = 0.1030 Ω		
0.0	0.0321	0.1463	7,000	25.1	1.44	-	-
0.0	0.0443	0.2079	13,700	42.4	1.69	-	-
0.0	0.5510	0.2690	22,100	65.6	1.76	-	-
0.0	0.728	0.3688	40,000	87.7	-	-	-
0.0	0.827	0.4076	50,300	71.6	-	-	-
0.0	0.1001	0.4994	74,500	79.0	-	-	-
0.0	0.1196	0.6004	107,000	82.9	-	-	-
0.0	0.1372	0.6931	142,000	86.8	-	-	-
0.0	0.1596	0.8112	193,000	90.7	-	-	-
0.0	0.1792	0.9159	245,000	94.2	-	-	-
0.0	0.2016	1.0373	312,000	98.4	-	-	-
0.0	0.0191	0.0849	2,420	10.7	1.15	-	-
0.0	0.0223	0.0999	3,320	16.9	1.00	-	-
0.0	0.0226	0.1012	3,420	14.4	1.21	-	-
15.6	0.0226	0.1011	3,410	11.9	1.58	20.8	-

TABLE D-2 continued

W_A watts	E_{SR} Volts	E_{PT} Volts	q/A BTU/HR FT^2	Δt $^\circ F$	Nu	Y_1	Y_2
RUN 38 continued							
0.0	0.0362	0.1669	9,010	31.2	1.49	-	-
2.0	0.0362	0.1666	9,000	29.4	-	-	-
15.6	0.0361	0.1628	8,750	21.0	2.20	33.7	-
36.2	0.0361	0.1625	8,750	18.1	2.49	47.1	-
86.0	0.0319	0.1622	8,750	15.9	2.89	66.8	-
0.0	0.0479	0.2284	16,300	51.5	1.67	-	-
15.6	0.0479	0.2206	15,800	31.2	2.52	58.2	-
36.2	0.0479	0.2184	15,600	25.3	3.18	67.2	-
0.0	0.0608	0.2989	27,100	69.8	2.07	-	-
36.2	0.05844	0.2686	23,400	29.3	4.23	78.3	-
86.0	0.05844	0.2665	23,200	24.9	4.81	105	-
0.0	0.0726	0.3704	40,100	93.9	-	-	-
0.0	0.0863	0.4259	54,800	73.3	-	-	-
1.0	0.0863	0.4250	54,700	72.0	-	-	-
2.0	0.0863	0.4226	54,400	68.5	-	-	-
7.0	0.0863	0.4214	54,200	66.8	-	-	-
15.6	0.0863	0.4213	54,200	65.7	8.70	-	870
36.2	0.0863	0.4140	53,300	55.3	14.1	-	1060
0.0	0.1088	0.5419	87,900	77.1	-	-	-
7.0	0.1088	0.5410	87,700	76.1	-	-	-
15.6	0.1088	0.5402	87,600	75.2	-	-	-
36.2	0.1088	0.5394	87,500	74.3	-	-	-
0.0	0.1209	0.6037	109,000	78.7	-	-	-
15.6	0.1209	0.6023	109,000	77.2	-	-	-
36.2	0.1209	0.6017	108,000	76.6	-	-	-
86.0	0.1209	0.6011	108,000	76.0	-	-	-
0.0	0.1308	0.6566	128,000	82.0	-	-	-
15.6	0.1308	0.6561	128,000	81.5	-	-	-
36.2	0.1308	0.6554	128,000	80.8	-	-	-
86.0	0.1308	0.6554	128,000	80.8	-	-	-
0.0	0.1506	0.7599	171,000	85.2	-	-	-
15.6	0.1500	0.7576	169,000	85.8	-	-	-
36.2	0.1500	0.7575	169,000	85.7	-	-	-
86.0	0.1500	0.7575	169,000	85.7	-	-	-
0.0	0.0254	0.1143	4,330	17.5	1.26	-	-
0.0	0.0286	0.1292	5,500	20.0	1.41	-	-
RUN 39			L = 48/64 in.	R_{100} = 0.1030 Ω			
0.0	0.0342	0.1568	8,000	27.2	1.54	-	-
0.0	0.0536	0.2603	20,800	62.9	1.75	-	-

TABLE D-2 continued

W_A watts	E_{SR} Volts	E_{PT} Volts	q/A BTU/HR FT^2	Δt $^\circ F$	Nu	Y_1	Y_2
RUN 39 continued							
0.0	0.0740	0.3810	42,000	98.8	-	-	-
0.0	0.0935	0.4611	64,300	71.9	-	-	-
0.0	0.1198	0.5975	107,000	78.8	-	-	-
0.0	0.1446	0.7282	157,000	84.9	-	-	-
0.0	0.1694	0.8576	217,000	87.3	-	-	-
0.0	0.2011	1.0289	308,000	93.9	-	-	-
0.0	0.0370	0.1696	9,350	28.8	1.68	-	-
4.8	0.0370	0.1682	9,260	23.9	-	-	-
15.6	0.0369	0.1668	9,100	20.8	2.30	33.7	-
36.2	0.0368	0.1657	9,080	16.5	2.91	42.8	-
86.0	0.0369	0.1651	9,080	13.2	3.41	58.8	-
0.0	0.0479	0.2261	16,200	43.4	1.94	-	-
1.6	0.0479	0.2261	16,200	43.4	-	-	-
2.0	0.0478	0.2232	15,900	37.2	-	-	-
15.6	0.0479	0.2218	15,800	33.0	2.52	58.2	-
36.2	0.0480	0.2178	15,600	25.5	3.18	67.2	-
86.0	0.0480	0.2167	15,500	19.3	4.15	.78.6	-
0.0	0.0577	0.2834	24,400	68.2	1.88	-	-
15.6	0.0576	0.2678	23,000	35.7	3.49	66.5	-
36.2	0.0576	0.2667	22,900	33.3	3.47	96.0	-
0.0	0.0733	0.3583	39,200	66.5	3.08	-	-
0.6	0.0733	0.3544	38,700	59.9	-	-	-
15.6	0.0733	0.3477	38,000	46.6	8.87	-	1040
36.2	0.0733	0.3438	37,600	42.0	9.57	-	1420
86.0	0.0733	0.3416	37,300	38.3	10.2	-	945
0.0	0.0905	0.4467	60,300	72.5	4.45	-	-
2.0	0.0905	0.4443	59,900	69.2	-	-	-
15.6	0.0905	0.4422	59,700	67.3	9.22	-	784
0.0	0.1106	0.5483	90,400	75.1	6.45	-	-
15.6	0.1106	0.5456	90,000	72.1	-	-	-
36.2	0.1106	0.5444	89,800	70.8	-	-	-
86.0	0.1106	0.5434	89,600	69.6	-	-	-
0.0	0.1251	0.6238	116,000	78.7	-	-	-
15.6	0.1251	0.6236	116,000	78.5	-	-	-
36.2	0.1251	0.6228	116,000	77.7	-	-	-
86.0	0.1251	0.6226	116,000	77.5	-	-	-
0.0	0.1356	0.6758	137,000	79.3	-	-	-
15.6	0.1356	0.6753	137,000	78.8	-	-	-
36.2	0.1356	0.6749	136,000	78.5	-	-	-
86.0	0.1356	0.6748	136,000	78.4	-	-	-
0.0	0.1497	0.7502	167,000	82.7	-	-	-

TABLE D-2 continued

W_A watts	E_{SR} Volts	E_{PT} Volts	q/A BTU/HR FT^2	Δt $^\circ F$	Nu	Y_1	Y_2
RUN 39 continued							
15.6	0.1497	0.7498	167,000	82.4	-	-	-
36.2	0.1497	0.7491	167,000	81.8	-	-	-
86.0	0.1497	0.7490	167,000	81.7	-	-	-
0.0	0.1644	0.8261	202,000	84.4	-	-	-
15.6	0.1644	0.8260	202,000	84.3	-	-	-
36.2	0.1644	0.8258	202,000	84.2	-	-	-
86.0	0.1644	0.8260	202,000	84.3	-	-	-

TABLE D-3

LIQUID: Distilled Water   TEMPERATURE: 113°F   FREQUENCY: 20.6 kcps

WIRE DIAMETER: 0.010"

W_A watts	E_{SR} Volts	E_{PT} Volts	q/a BTU/HR FT^2	Δt °F	N_u	Y_1	Y_2
RUN 7			L = 47/64 in.	R_{100}	= 0.04928 Ω		
0.0	0.4394	1.1632	545,000	146.2	–	–	–
15.6	0.4495	1.1288	541,000	111.0	–	–	–
36.2	0.4456	1.0967	521,000	98.1	14.39	–	2073
86.0	0.4489	1.0698	512,000	76.9	18.11	–	2486
0.0	0.3595	0.9392	360,000	136.3	–	–	–
15.6	0.3617	0.8843	341,000	92.9	9.92	–	822
36.2	0.3547	0.8540	323,000	83.2	10.50	–	1440
86.0	0.3589	0.8390	321,000	64.3	13.7	–	1715
0.0	0.2327	0.6005	149,000	129.0	–	–	–
15.6	0.2318	0.5543	137,000	79.8	3.65	62.9	–
36.2	0.2353	0.5500	138,000	65.9	4.55	84.6	–
86.0	0.2321	0.5294	131,000	50.5	6.43	85.0	–
0.0	0.1740	0.4168	77,300	80.3	2.08	–	–
86.0	0.1740	0.3867	71,700	35.6	4.36	56.0	–
0.0	0.0939	0.2069	20,700	30.5	1.50	–	–
15.6	0.0921	0.2026	19,900	28.4	1.64	14.8	–
36.2	0.0922	0.2005	19,700	22.2	2.00	23.9	–
86.0	0.0920	0.1997	19,600	20.9	2.20	34.7	–
RUN 53			L = 47/64 in.	R_{100}	= 0.04928 Ω		
0.0	0.0811	0.1768	15,300	25.0	1.36	–	–
0.0	0.1171	0.2626	32,800	41.2	1.76	–	–
0.0	0.1671	0.3934	70,100	70.3	2.17	–	–
0.0	0.2109	0.5247	118,000	104.9	–	–	–
0.0	0.0972	0.2162	22,400	36.1	1.37	–	–
15.6	0.0971	0.2125	22,000	26.2	1.86	14.4	–
0.0	0.1284	0.2943	40,300	53.3	1.67	–	–
15.6	0.1281	0.2862	39,100	38.3	2.27	21.3	–
36.2	0.1276	0.2829	38,500	33.0	3.57	37.3	–
86.0	0.1273	0.2792	37,900	26.8	3.16	42.5	–
0.0	0.1406	0.3289	49,300	65.6	1.63	–	–
15.6	0.1418	0.3196	48,300	43.5	2.43	24.2	–

TABLE D-3 continued

W_A watts	E_{SR} Volts	E_{PT} Volts	q/a BTU/HR FT^2	Δt °F	Nu	Y_1	Y_2
RUN 53 continued							
15.6	0.1411	0.3205	48,200	48.2	2.19	27.0	-
15.6	0.1420	0.3185	48,200	41.6	2.52	22.4	-
0.0	0.1511	0.3539	57,000	67.3	1.84	-	-
15.6	0.1493	0.3405	54,200	51.2	2.21	29.24	-
36.2	0.1490	0.3322	52,800	37.8	3.10	42.10	-
86.0	0.1484	0.3262	51,600	30.8	3.83	47.8	-
0.0	0.1728	0.4135	76,200	81.1	2.03	-	-
7.0	0.1719	0.4027	73,800	69.3	-	-	-
15.6	0.1711	0.3959	72,200	61.8	2.51	43.0	-
0.0	0.1876	0.4614	92,300	97.4	-	-	-
3.0	0.1903	0.4545	92,200	78.3	-	-	-
15.6	0.1917	0.4506	92,100	67.5	3.00	45.5	-
15.6	0.1922	0.4490	92,000	62.9	3.23	40.4	-
36.2	0.1912	0.4366	89,000	49.2	3.98	53.3	-
86.0	0.1919	0.4325	88,500	41.6	4.70	66.1	-
0.0	0.2468	0.6196	163,000	110.0	-	-	-
1.5	0.2487	0.6035	160,000	88.3	-	-	-
15.6	0.2496	0.5976	159,000	79.9	5.45	-	482.0
36.2	0.2474	0.5799	153,000	67.6	6.16	-	796.0
86.0	0.2463	0.5674	149,000	57.2	7.23	-	1110.0
0.0	0.2835	0.7244	219,000	122.3	-	-	-
15.6	0.2883	0.7028	216,000	92.1	-	-	-
36.2	0.2882	0.6867	211,000	77.8	7.52	-	1030.0
86.0	0.2908	0.6772	210,000	63.7	9.27	-	1381.0
0.0	0.3367	0.8690	312,000	128.1	-	-	-
15.6	0.3412	0.8413	306,000	98.4	-	-	-
36.2	0.3392	0.8240	298,000	88.8	9.02	-	1396.0
86.0	0.3404	0.8046	292,000	71.9	11.20	-	1750.0
0.0	0.3614	0.9342	360,000	128.2	-	-	-
1.5	0.3648	0.9178	357,000	110.3	-	-	-
15.6	0.3661	0.9096	355,000	102.3	-	-	-
0.0	0.3904	1.0138	422,000	132.3	-	-	-
15.6	0.3953	0.9893	417,000	107.8	-	-	-
0.0	0.4205	1.1176	501,000	149.0	-	-	-
3.0	0.4276	1.0945	499,000	123.5	-	-	-
15.6	0.4308	1.0841	498,000	112.3	-	-	-
36.2	0.4342	1.0715	496,000	99.8	-	-	-
86.0	0.4339	1.0354	479,000	78.6	16.60	-	2360.0
0.0	0.4550	1.2163	590,000	152.1	-	-	-
4.8	0.4588	1.1940	584,000	133.8	-	-	-
15.6	0.4590	1.1830	579,000	127.2	-	-	-
36.2	0.4627	1.1553	570,000	106.3	-	-	-

TABLE D-3 continued

W_A watts	E_{SR} Volts	E_{PT} Volts	q/a BTU/HR FT^2	Δt °F	Nu	Y_1	Y_2

RUN 5   L = 47/64 in. R_{100} = 0.04832 Ω

W_A watts	E_{SR} Volts	E_{PT} Volts	q/a BTU/HR FT^2	Δt °F	Nu	Y_1	Y_2
0.0	0.09646	0.2098	21,600	25.3	1.35	–	–
36.2	0.0974	0.2081	21,600	24.2	1.94	26.1	–
86.0	0.0955	0.2030	20,700	20.5	2.26	34.0	–
0.0	0.1720	0.4040	74,100	77.6	2.07	–	–
15.6	0.1711	0.3937	71,800	65.0	2.48	43.0	–
36.2	0.1711	0.3877	70,700	51.0	3.01	56.7	–
86.0	0.1711	0.3845	70,000	40.0	3.85	63.9	–
0.0	0.2369	0.6066	153,000	133.6	–	–	–
15.6	0.2361	0.5611	141,000	85.0	4.55	72.8	–
86.0	0.2361	0.5441	137,000	55.9	5.22	101	–
0.0	0.3618	0.9464	365,000	148.4	–	–	–
2.0	0.3618	0.9408	363,000	127.1	–	–	–
15.6	0.3594	0.8845	339,000	107.3	8.47	–	979
15.6	0.4243	1.0545	477,000	110.0	11.5	–	1260
36.2	0.4243	1.0248	464,000	91.6	13.6	–	1830
86.0	0.4243	1.0106	457,000	82.8	15.1	–	2410
0.0	0.0938	0.2014	20,000	24.6	1.77	–	–
15.6	0.09311	0.1988	19,700	25.8	1.63	14.4	–
36.2	0.0927	0.1971	19,500	22.0	1.92	24.3	–
86.0	0.0931	0.1966	19,500	17.0	2.49	30.3	–
0.0	0.1723	0.4038	74,200	79.9	2.01	–	–
15.6	0.1722	0.3882	70,300	56.3	2.70	34.1	–
36.2	0.1722	0.3841	70,500	50.0	3.04	55.7	–
15.6	0.0941	0.2026	20,300	28.7	1.64	14.8	–
15.6	0.1724	0.3938	72,400	62.4	2.51	39.3	–
15.6	0.2369	0.5556	140,000	82.1	3.70	65.5	–
15.6	0.2360	0.5600	141,000	85.0	3.56	72.8	–

TABLE D-4

LIQUID: Distilled Water   TEMPERATURE: 149°F   FREQUENCY: 20.6 kcps

WIRE DIAMETER: 0.010"

W_A watts	E_{SR} Volts	E_{PT} Volts	q/A BTU/HR FT^2	Δt °F	Nu	Y_1	Y_2
RUN 20			L = 48/64 in.	R_{100} = 0.04989 Ω			
0.0	0.2023	0.5304	112,000	95.5	-	-	-
0.0	0.1072	0.2520	28,200	26.2	1.60	-	-
0.0	0.2352	0.6231	153,000	102.3	-	-	-
0.0	0.2791	0.7448	217,000	107.4	-	-	-
0.0	0.3478	0.9365	340,000	113.5	-	-	-
0.0	0.4034	1.0922	460,000	117.2	-	-	-
0.0	0.4591	1.2497	599,000	121.0	-	-	-
0.0	0.4845	1.3227	669,000	123.1	-	-	-
RUN 23			L = 48/64 in.	R_{100} = 0.04989 Ω			
0.0	0.1343	0.3288	46,100	50.9	1.36	-	-
4.8	0.1346	0.3245	45,600	41.2	-	-	-
15.6	0.1343	0.3217	45,100	37.3	2.60	41.0	-
0.0	0.1934	0.5052	102,000	92.9	1.63	-	-
1.0	0.1932	0.4830	97,400	64.2	-	-	-
15.6	0.1932	0.4760	96,000	55.0	3.70	71.7	-
36.2	0.1951	0.4675	95,200	37.7	-	-	-
0.0	0.2864	0.7794	233,000	120.9	-	-	-
7.0	0.2861	0.7265	217,000	74.2	-	-	-
15.6	0.2864	0.7125	213,000	61.1	9.4	-	527
36.2	0.2861	0.6997	209,000	50.2	11.1	-	934
0.0	0.3524	0.9540	351,000	117.2	-	-	-
15.6	0.3494	0.8827	322,000	70.8	12.2	-	763
36.2	0.3499	0.8732	319,000	63.0	13.6	-	1310
RUN 6			L = 47/64 in.	R_{100} = 0.04832 Ω			
0.0	0.09362	0.2131	21,300	26.1	1.76	-	-
2.0	0.09345	0.2134	21,300	27.9	-	-	-
7.0	0.09345	0.2134	21,300	27.9	-	-	-
15.6	0.09354	0.2105	20,500	19.6	2.24	21.5	-
0.0	0.1718	0.4265	78,100	78.8	2.10	-	-
0.8	0.1718	0.4164	76,300	63.2	-	-	-

TABLE D-4 continued

W_A watts	E_{SR} Volts	E_{PT} Volts	q/A BTU/HR FT^2	Δt °F	Nu	Y_1	Y_2
RUN 6 continued							
2.0	0.1718	0.4093	74,900	53.1	-	-	-
7.0	0.1716	0.4053	74,100	46.4	-	-	-
15.6	0.1716	0.4036	73,800	44.3	3.56	50.0	-
0.0	0.2367	0.6178	156,000	111.6	-	-	-
2.0	0.2367	0.5943	150,000	86.5	-	-	-
7.0	0.2366	0.5754	145,000	65.4	-	-	-
15.6	0.2366	0.5709	144,000	60.4	5.00	86.6	-
36.2	0.2366	0.5631	142,000	51.5	5.90	132	-
86.0	0.2366	0.5541	142,000	41.0	7.41	152	-
0.0	0.3695	0.9637	380,000	112.9	-	-	-
2.0	0.3695	0.9515	375,000	104.2	-	-	-
7.0	0.3695	0.9414	371,000	96.0	-	-	-
15.6	0.3695	0.9294	393,000	87.0	12.4	-	1090
36.2	0.3695	0.8990	354,000	65.7	14.4	-	860
86.0	0.3695	0.8833	348,000	54.5	17.2	-	1981
0.0	0.4315	1.1268	518,000	112.8	-	-	-
4.8	0.4315	1.1140	513,000	104.9	-	-	-
36.2	0.4315	1.0670	491,000	76.2	17.3	-	1908
86.0	0.4315	1.0478	482,000	20.5	-	-	2840
RUN 50			L = 49.5/64 in.		R_{100} = 0.05033 Ω		
0.0	0.0709	0.1658	11,900	17.8	1.44	-	-
0.0	0.0956	0.2291	22,200	32.5	1.47	-	-
0.0	0.1202	0.2946	35,800	46.4	1.65	-	-
0.0	0.1516	0.3848	59,100	67.6	1.86	-	-
0.0	0.1812	0.4770	87,500	91.5	2.03	-	-
0.0	0.2053	0.5360	111,000	86.0	2.74	-	-
0.0	0.2316	0.5997	141,000	80.6	-	-	-
0.0	0.2704	0.7043	193,000	84.5	-	-	-
0.0	0.3044	0.8200	253,000	107.1	-	-	-
0.0	0.3314	0.9036	303,000	115.4	-	-	-
0.0	0.4244	1.1720	503,000	123.4	-	-	-
0.0	0.0626	0.1450	9,200	14.0	-	-	-
7.0	0.0626	0.1450	9,200	14.0	-	-	-
15.6	0.0626	0.1441	9,100	10.3	-	-	-
0.0	0.0947	0.2265	21,700	31.3	1.49	-	-
2.0	0.0947	0.2265	21,700	31.3	-	-	-
7.0	0.0947	0.2183	21,000	25.0	-	-	-
15.6	0.0947	0.2078	20,700	21.7	2.06	23.2	-
36.2	0.0947	0.2011	21,200	17.5	2.61	40.3	-

TABLE D-4   continued

W_A watts	E_{SR} Volts	E_{PT} Volts	q/A BTU/HR FT^2	Δt $^\circ F$	Nu	Y_1	Y_2
RUN 50 continued							
0.0	0.1296	0.3178	41,700	48.5	1.84	-	-
2.0	0.1296	0.3165	41,500	45.9	-	-	-
4.8	0.1296	0.3138	41,200	40.6	-	-	-
15.6	0.1296	0.3110	41,000	35.2	2.52	37.5	-
36.2	0.1296	0.3011	40,700	25.0	3.45	54.6	-
0.0	0.1613	0.4124	67,000	75.0	1.89	-	-
2.0	0.1613	0.4030	65,800	60.2	-	-	-
15.6	0.1613	0.3910	63,800	41.3	3.30	47.1	-
0.0	0.2032	0.5407	111,000	99.7	-	-	-
1.0	0.2032	0.5407	111,000	99.7	-	-	-
2.0	0.2032	0.5104	105,000	61.8	-	-	-
15.6	0.2032	0.5037	104,000	52.4	4.15	66.6	-
0.0	0.2026	0.5420	111,000	103.3	-	-	-
2.0	0.2026	0.5074	107,000	75.3	-	-	-
0.0	0.2957	0.8068	241,000	118.6	-	-	-
2.0	0.2957	0.8068	241,000	118.6	-	-	-
4.8	0.2957	0.8080	242,000	119.6	-	-	-
7.0	0.2957	0.7616	228,000	79.8	-	-	-
15.6	0.2957	0.7505	225,000	70.3	8.49	-	635
0.0	0.3417	0.9385	325,000	121.4	-	-	-
15.6	0.3417	0.8770	303,000	74.7	10.8	-	773
36.2	0.3417	0.8548	296,000	59.2	13.1	-	1210
0.0	0.3925	1.0843	431,000	123.6	-	-	-
2.0	0.3925	1.0830	430,000	122.8	-	-	-
7.0	0.3925	1.0564	420,000	105.6	-	-	-
15.6	0.3925	1.0206	405,000	82.5	13.1	-	1071
36.2	0.3925	0.9940	395,000	65.3	15.9	-	1581
0.0	0.4215	1.1583	494,000	121.8	-	-	-
15.6	0.4215	1.1017	470,000	87.7	-	-	-
36.2	0.4215	1.0179	456,000	67.3	18.6	-	1817
86.0	0.4215	1.0464	446,000	54.4	22.2	-	2250
0.0	0.2847	0.7550	218,000	99.2	-	-	-
15.6	0.2847	0.7152	206,000	63.7	8.61	-	547
36.2	0.2847	0.6968	201,000	47.3	11.5	-	868
86.0	0.2847	0.6897	199,000	41.0	13.2	-	1290
0.0	0.3421	0.9238	320,000	111.5	-	-	-
15.6	0.3421	0.8748	303,000	75.1	10.8	-	773
86.0	0.3421	0.8326	288,000	43.8	18.0	-	1596

TABLE D-4   continued

W_A watts	E_{SR} Volts	E_{PT} Volts	q/A BTU/HR FT^2	Δt $^\circ F$	Nu	Y_1	Y_2
RUN 51			L = 49.5/64 in.	R_{100} = 0.05033 Ω			
0.0	0.0520	0.1201	6,300	11.4	1.20	-	-
0.0	0.0838	0.1981	16,800	26.1	1.40	-	-
0.0	0.1206	0.2952	36,000	47.4	1.63	-	-
0.0	0.1747	0.4518	79,900	81.6	2.08	-	-
0.0	0.3942	1.0634	424,000	108.1	-	-	-
15.6	0.3942	1.0324	412,000	88.1	12.6	-	1126
36.2	0.3942	0.9968	398,000	65.2	16.0	-	1685
86.0	0.3942	0.9767	390,000	52.2	20.2	-	2100
0.0	0.3590	0.9610	349,000	102.9	-	-	-
15.6	0.3590	0.9270	337,000	78.2	11.4	-	898
36.2	0.3590	0.8990	327,000	59.0	14.6	-	1248
86.0	0.3590	0.8881	320,000	46.5	18.6	-	1754
0.0	0.3256	0.8627	284,000	96.8	-	-	-
15.6	0.3256	0.8333	275,000	73.9	9.80	-	690
36.2	0.3256	0.8080	266,000	54.1	13.2	-	1070
86.0	0.3256	0.7920	261,000	41.7	16.6	-	1500
15.6	0.2771	0.7002	196,000	65.6	7.95	-	558
36.2	0.2771	0.6806	191,000	47.7	11.0	-	850
86.0	0.2771	0.6692	188,000	37.2	13.7	-	1200
15.6	.2276	0.5684	131,000	58.1	4.81	77.4	-
36.2	0.2276	0.5512	127,000	39.0	6.62	91.5	-
86.0	0.2276	0.5424	125,000	29.2	9.14	104	-
15.6	0.1809	0.4435	81,000	46.5	3.64	37.4	-
36.2	0.1809	0.4333	79,300	32.2	5.39	70.0	-
86.0	0.1809	0.4275	77,300	24.7	6.66	86.2	-
0.0	0.1462	0.3670	54,300	61.4	1.89	-	-
15.6	0.1462	0.3554	52,000	41.3	2.70	47.1	-
86.0	0.1462	0.3432	50,800	20.7	5.51	71.8	-
0.0	0.1018	0.2454	25,300	37.0	1.47	-	-
15.6	0.1018	0.2420	24,900	28.6	1.87	30.2	-
86.0	0.1018	0.2372	24,400	16.6	3.18	61.2	-
RUN 52			L = 48/64 in.	R_{100} = 0.05063 Ω			
0.0	0.0589	0.1314	8,500	11.1	1.66	-	-
0.0	0.0908	0.2173	20,600	26.3	1.69	-	-
0.0	0.1329	0.3324	46,100	54.4	1.81	-	-
0.0	0.1821	0.4813	91,500	90.2	2.15	-	-
0.0	0.2262	0.5860	138,000	77.0	-	-	-
0.0	0.2694	0.7600	214,000	105.2	-	-	-
0.0	0.3033	0.8317	263,00	115.2	-	-	-
0.0	0.3426	0.9514	340,000	124.0	-	-	-
0.0	0.3815	1.0634	424,000	126.7	-	-	-

TABLE D-4 continued

W_A watts	E_{SR} Volts	E_{PT} Volts	q/A BTU/HR FT^2	Δt $^{\circ}F$	Nu	Y_1	Y_2
RUN 52 continued							
0.0	0.4134	1.1560	499,000	128.9	-	-	-
0.0	0.4572	1.2828	612,000	131.3	-	-	-
0.0	0.4256	1.1972	532,000	133.1	-	-	-
2.0	0.4256	1.1972	532,000	133.1	-	-	-
4.8	0.4256	1.1972	532,000	133.1	-	-	-
7.0	0.4256	1.1902	529,000	129.0	-	-	-
15.6	0.4256	1.1388	506,000	98.5	-	-	-
36.2	0.4256	1.1088	493,000	80.7	-	-	-
86.0	0.4256	1.0798	480,000	63.5	20.5	-	2717
0.0	0.3877	1.0832	438,000	128.3	-	-	-
2.0	0.3877	1.0832	438,000	128.3	-	-	-
7.0	0.3877	1.0608	429,000	113.7	-	-	-
0.0	0.3359	0.9207	323,000	113.1	-	-	-
2.0	0.3359	0.9227	324,000	114.6	-	-	-
4.8	0.3359	0.8862	311,000	87.2	-	-	-
15.6	0.3359	0.8662	304,000	72.2	11.4	-	737
86.0	0.3359	0.8317	292,000	47.2	17.0	-	1660
0.0	0.2994	0.8219	254,000	110.2	-	-	-
2.0	0.2994	0.8200	255,000	117.1	-	-	-
3.0	0.2994	0.8001	250,000	99.4	-	-	-
7.0	0.2994	0.7787	243,000	81.4	-	-	-
15.6	0.2994	0.7648	239,000	69.7	9.05	-	662
36.2	0.2994	0.7440	233,000	52.1	11.7	-	916
86.0	0.2994	0.7376	231,000	46.2	13.5	-	1480
0.0	0.2527	0.6680	176,000	92.1	-	-	-
0.8	0.2527	0.6725	180,000	94.6	-	-	-
1.0	0.2527	0.6539	173,000	78.1	-	-	-
2.0	0.2527	0.6469	171,000	71.1	-	-	-
15.6	0.2527	0.6355	168,000	59.7	7.36	-	452
36.2	0.2527	0.6225	164,000	46.7	9.26	-	780
86.0	0.2527	0.6140	162,000	38.2	11.8	-	1120
0.0	0.2082	0.5480	119,000	88.4	-	-	-
0.8	0.2082	0.5296	115,000	66.1	-	-	-
2.0	0.2082	0.5248	113,000	61.3	-	-	-
7.0	0.2082	0.5199	112,000	55.0	-	-	-
15.6	0.2082	0.5158	112,000	49.4	4.71	40.5	-
36.2	0.2082	0.5054	110,000	36.0	6.52	78.4	-
86.0	0.2082	0.4991	108,000	29.1	8.00	102	-
0.0	0.1586	0.4008	66,400	62.8	2.25	-	-
0.8	0.1586	0.4008	66,400	62.8	-	-	-
2.0	0.1586	0.3995	66,100	60.7	-	-	-

TABLE D-4 continued

W_A watts	E_{SR} Volts	E_{PT} Volts	q/A BTU/HR FT^2	Δt $^\circ F$	Nu	Y_1	Y_2
RUN 52 continued							
4.8	0.1586	0.3964	65,600	55.8	-	-	-
15.6	0.1586	0.3847	63,000	37.2	3.63	40.8	-
36.2	0.1586	0.3805	62,500	30.5	4.44	65.8	-
86.0	0.1586	0.3770	62,400	24.9	5.54	85.0	-
0.0	0.1288	0.3078	38,000	47.0	1.73	-	-
4.8	0.1288	0.3013	37,100	38.0	-	-	-
7.0	0.1288	0.2926	36,500	33.0	-	-	-
0.0	0.1052	0.2556	28,100	33.3	1.81	-	-
2.0	0.1052	0.2558	28,100	33.3	-	-	-
7.0	0.1052	0.2527	27,800	30.4	-	-	-
15.6	0.1052	0.2500	27,200	23.9	2.41	25.3	-
86.0	0.1052	0.2484	27,300	20.0	3.07	70.0	-
0.0	0.0651	0.1526	10,400	14.8	1.52	-	-
7.0	0.0651	0.1526	10,400	14.8	-	-	-
15.6	0.0651	0.1517	10,300	11.3	-	-	-
36.2	0.0651	0.1513	10,300	9.8	-	-	-
86.0	0.0651	0.1503	10,200	5.9	-	-	-

TABLE D-5

LIQUID: Methanol   TEMPERATURE: $113^\circ F$ FREQUENCY: 20.6 kcps

WIRE DIAMETER: 0.007"

W_A watts	E_{SR} Volts	E_{PT} Volts	q/A BTU/HR FT^2	Δt $^\circ F$	
RUN 40			L = 47.5/64 in.	R_{100} = 0.09874 Ω	
0.0	0.0989	0.4703	70,100	74.9	
0.0	0.1444	0.6944	151,000	82.4	
0.0	0.1889	0.9206	262,000	90.5	
0.0	0.2095	1.023	323,000	91.8	
0.0	0.2145	1.049	339,000	93.0	
0.0	0.2187	1.0714	353,000	93.8	
0.0	0.2263	1.1116	379,000	95.5	
0.0	0.2340	1.1517	406,000	96.8	
0.0	0.2414	1.1908	433,000	98.3	
0.0	0.2489	1.2297	461,000	99.3	(BURNOUT)
RUN 41			L = 48/64 in.	R_{100} = 0.09935 Ω	
0.0	0.1216	0.5848	106,000	79.5	
0.0	0.1610	0.7792	187,000	83.3	
0.0	0.2005	0.9801	293,000	88.5	
0.0	0.2105	1.0293	323,000	88.8	
0.0	0.2203	1.0808	355,000	90.8	
0.0	0.2275	1.1174	379,000	91.5	
0.0	0.2347	1.1544	404,000	92.4	
0.0	0.2423	1.1931	431,000	93.1	(BURNOUT)
RUN 41a			L = 47/64 in.	R_{100} = 0.09811 Ω	
0.0	0.1118	0.5375	91,500	84.1	
0.0	0.1857	0.8985	254,000	88.3	
0.0	0.1991	0.9665	293,000	90.2	
0.0	0.2145	1.0439	341,000	91.8	
0.0	0.2262	1.1032	380,000	93.2	(BURNOUT)

TABLE D-5 continued

W_A watts	E_{SR} Volts	E_{PT} Volts	q/A BTU/HR FT^2	Δt $°F$	
RUN 42			L = 48.5/64 in.	R_{100} = 0.1052 Ω	
0.0	0.0530	0.2615	20,400	57.6	
0.0	0.1097	0.5652	91,500	84.1	
0.0	0.1649	0.8617	210,000	92.1	
0.0	0.2134	1.1258	354,000	99.1	
86.0	0.1086	0.5512	88,000	75.7	
86.0	0.1526	0.7890	178,000	87.2	
86.0	0.1952	1.0236	295,000	96.1	
86.0	0.2078	1.0924	335,000	98.6	(BURNOUT)
RUN 45			L = 46.5/64 in.	R_{100} = 0.09548 Ω	
86.0	0.1133	0.5602	93,600	76.2	
86.0	0.1612	0.8113	193,000	86.8	
86.0	0.1935	0.9844	281,000	93.9	
86.0	0.2090	1.0671	329,000	96.2	
86.0	0.2187	1.1186	361,000	97.1	(BURNOUT)
RUN 44			L = 49/64 in.	R_{100} = 0.1000 Ω	
0.0	0.1070	0.5194	81,200	82.2	
0.0	0.1567	0.7690	176,000	87.2	
0.0	0.1909	0.9433	263,000	91.5	
0.0	0.2109	1.0462	322,000	94.0	
86.0	0.1265	0.6088	112,000	74.2	
86.0	0.1663	0.8111	197,000	82.4	
86.0	0.1932	0.9515	268,000	88.5	
86.0	0.2077	1.0280	312,000	91.6	
86.0	0.2150	1.0662	335,000	92.0	
86.0	0.2248	1.1164	367,000	92.9	
86.0	0.2302	1.1396	383,000	90.0	(BURNOUT)
RUN 43			L = 48.5/64 in.	R_{100} = 0.1024 Ω	
0.0	0.1594	0.7470	185,000	87.2	
0.0	0.1829	0.8619	245,000	90.4	
0.0	0.1959	0.9230	281,000	90.3	
0.0	0.2226	1.0552	365,000	94.2	
0.0	0.2333	1.1090	402,000	96.1	(BURNOUT)

TABLE D-5 continued

W_A watts	E_{SR} Volts	E_{PT} Volts	q/A BTU/HR FT^2	Δt $^\circ F$	
RUN 46			L = 47/64 in.	R_{100} = 0.09789 Ω	
0.0	0.1808	0.8717	240,000	88.2	
0.0	0.1991	0.9631	292,000	90.3	
0.0	0.2091	1.0176	324,000	94.1	
0.0	0.2281	1.1144	387,000	96.7	(BURNOUT)
RUN 47			L = 48/64 in.	R_{100} = 0.09993 Ω	
86.0	0.1854	0.9119	252,000	89.8	
86.0	0.2122	1.0526	333,000	95.1	
86.0	0.2256	1.1239	378,000	97.8	
86.0	0.2279	1.1389	387,000	99.7	(BURNOUT)
RUN 48			L = 49.5/64 in.	R_{100} = 0.1033 Ω	
0.0	0.0914	0.4512	59,600	69.8	
0.0	0.1794	0.9082	236,000	86.3	
0.0	0.2063	1.0490	313,000	89.1	
86.0	0.1069	0.5290	81,700	73.1	
86.0	0.1445	0.7228	151,000	80.7	
86.0	0.2034	1.0328	304,000	90.0	
86.0	0.2178	1.1080	349,000	92.1	(BURNOUT)
RUN 49			L = 48/64 in.	R_{100} = 0.1009 Ω	
0.0	0.0867	0.4231	54,700	77.8	
0.0	0.1847	0.9189	253,000	90.0	
86.0	0.1086	0.5261	85,200	93.3	
86.0	0.1416	0.6963	147,000	82.5	
86.0	0.2031	1.0170	308,000	93.9	
86.0	0.2158	1.0817	348,000	94.6	
86.0	0.2301	1.1542	396,000	95.0	(BURNOUT)

TABLE D-6

LIQUID: Distilled Water   TEMPERATURE: 149°F   FREQUENCY: 44.1 kcps

WIRE DIAMETER: 0.010"

W_A watts	E_{SR} Volts	E_{PT} Volts	q/A BTU/HR FT^2	Δt °F	Nu	Y_1	Y_2
RUN 59			L = 48/64 in.		R_{100} = 0.05021 Ω		
0.0	0.0704	0.1646	12,100	16.0	1.63	-	-
15.6	0.0704	0.1646	12,100	16.2	-	-	-
23.2	0.0701	0.1639	12,000	16.2	-	-	-
30.2	0.0699	0.1632	11,900	15.5	2.89	15.8	-
53.3	0.0697	0.1622	11,800	13.6	1.86	24.3	-
96.0	0.0692	0.1606	11,600	11.8	2.11	33.5	-
0.0	0.0980	0.2347	24,000	30.0	1.72	-	-
23.2	0.0962	0.2291	23,000	26.3	-	-	-
30.2	0.0955	0.2257	22,500	22.0	2.20	20.2	-
53.3	0.0952	0.2244	22,300	19.1	2.52	30.9	-
96.0	0.0938	0.2195	21,500	15.0	3.08	40.0	-
0.0	0.1092	0.2649	30,200	38.5	1.68	-	-
4.5	0.1095	0.2659	30,400	38.8	-	-	-
9.5	0.1088	0.2640	30,000	38.3	-	-	-
15.6	0.1085	0.2621	29,700	35.6	-	-	-
53.3	0.1074	0.2542	28,500	22.5	2.72	36.4	-
96.0	0.1069	0.2509	28,000	17.5	3.00	49.5	-
0.0	0.1322	0.3267	45,100	49.0	1.97	-	-
9.5	0.1317	0.3220	44,300	42.3	-	-	-
23.2	0.1317	0.3201	44,000	38.7	-	-	-
30.2	0.1316	0.3173	43,600	33.5	2.79	30.8	-
53.2	0.1316	0.3137	43,100	27.6	3.35	43.5	-
96.0	0.1304	0.3086	42,000	23.5	5.00	57.0	-
0.0	0.1521	0.3855	61,200	67.0	1.95	-	-
4.6	0.1529	0.3823	61,000	58.3	-	-	-
30.2	0.1550	0.3769	61,000	41.5	3.16	39.2	-
53.3	0.1527	0.3637	58,000	29.0	4.29	46.0	-
96.0	0.1519	0.3589	56,900	24.5	5.00	60.1	-
0.0	0.1861	0.4894	95,100	90.0	2.24	-	-
1.0	0.1861	0.4829	93,800	81.3	-	-	-
30.2	0.1878	0.4693	92,000	57.1	3.47	63.6	-
53.3	0.1882	0.4595	90,300	42.2	4.62	69.6	-
96.0	0.1870	0.4512	88,100	35.0	5.40	85.6	-
0.0	0.2297	0.6506	156,000	141.4	-	-	-
0.0	0.2376	0.6369	158,000	101.9	-	-	-

TABLE D-6 continued

W_A watts	E_{SR} Volts	E_{PT} Volts	q/A BTU/HR FT^2	Δt $^\circ$F	Nu	Y_1	Y_2

RUN 59 continued

W_A watts	E_{SR} Volts	E_{PT} Volts	q/A BTU/HR FT^2	Δt $^\circ$F	Nu	Y_1	Y_2
3.2	0.2367	0.6192	153,000	85.7	-	-	-
30.2	0.2324	0.5853	142,000	61.0	5.00	71.2	-
53.3	0.2319	0.5782	140,000	54.5	5.15	104.2	-
96.0	0.2301	0.5621	135,000	41.0	6.95	102.7	-
0.0	0.2783	0.7847	228,000	136.2	-	-	-
0.0	0.2764	0.7521	217,000	112.4	-	-	-
4.6	0.2782	0.7368	214,000	93.8	-	-	-
30.2	0.2802	0.7180	210,000	72.2	3.65	-	350
53.3	0.2748	0.6867	197,000	56.0	4.42	-	486
96.0	0.2755	0.6779	195,000	46.3	5.34	-	644
0.0	0.2932	0.8069	247,000	120.9	-	-	-
0.0	0.3226	0.9028	304,000	132.8	-	-	-
30.2	0.3272	0.8579	293,000	88.1	4.11	-	477
96.0	0.3323	0.8214	285,000	50.0	7.16	-	830
0.0	0.3480	0.9689	352,000	128.3	-	-	-
9.5	0.3483	0.9709	353,000	129.1	-	-	-
15.6	0.3551	0.9494	352,000	99.3	-	-	-
30.2	0.3571	0.9388	350,000	88.0	4.96	-	524
53.3	0.3596	0.9189	345,000	68.5	6.26	-	754
96.0	0.3627	0.9111	345,000	57.5	7.54	-	1020
0.0	0.3635	1.0119	384,000	128.2	-	-	-
0.0	0.3764	1.0613	417,000	137.3	-	-	-
0.0	0.3885	1.0823	439,000	129.5	-	-	-
30.2	0.3922	1.0379	425,000	94.2	5.62	-	555
53.3	0.3904	1.0058	410,000	75.5	6.79	-	910
96.0	0.3929	0.9897	406,000	61.0	8.36	-	1150
0.0	0.4156	1.1639	505,000	133.2	-	-	-
23.2	0.4191	1.1359	497,000	110.4	-	-	-
30.2	0.4153	1.1070	480,000	98.1	6.09	-	542
53.3	0.4145	1.0701	463,000	77.0	7.52	-	985
96.0	0.4194	1.0667	467,000	67.3	8.71	-	1230
0.0	0.4471	1.2555	586,000	134.3	-	-	-
30.2	0.4420	1.1966	552,000	108.0	-	-	-
53.3	0.4414	1.1502	530,000	82.2	8.06	-	1090
96.0	0.4441	1.1345	526,000	69.2	9.53	-	1420

TABLE D-6 continued

W_A watts	E_{SR} Volts	E_{PT} Volts	q/A BTU/HR FT^2	Δt °F	Nu	Y_1	Y_2
RUN 64			L = 49/64 in.	R_{100} = 0.05054 Ω			
0.0	0.0767	0.1812	14,200	21.6	1.41	-	-
30.2	0.0750	0.1762	13,500	18.2	1.60	17.2	-
53.3	0.0743	0.1738	13,200	15.2	1.88	26.3	-
96.0	0.0738	0.1724	13,000	13.7	2.03	37.5	-
0.0	0.0889	0.2124	19,300	27.4	1.52	-	-
30.2	0.0878	0.2082	18,700	22.3	1.81	20.3	-
53.3	0.0868	0.2040	18,100	18.3	2.13	28.2	-
96.0	0.0865	0.2024	17,900	15.4	2.51	40.2	-
0.0	0.0987	0.2388	24,100	35.5	1.46	-	-
30.2	0.0987	0.2340	23,600	24.4	2.08	22.1	-
53.3	0.0992	0.2328	23,600	18.2	2.80	37.8	-
96.0	0.0989	0.2314	23,400	16.3	3.10	41.8	-
0.0	0.1210	0.3000	37,100	52.6	1.51	-	-
30.2	0.1206	0.2879	35,500	29.0	2.63	26.2	-
53.3	0.1200	0.2840	34,800	24.8	3.02	39.4	-
96.0	0.1190	0.2804	34,100	21.5	3.40	55.9	-
0.0	0.1378	0.3471	48,900	60.8	1.72	-	-
30.2	0.1400	0.3412	48,800	40.5	2.58	37.1	-
53.3	0.1370	0.3292	46,100	31.6	3.14	50.5	-
96.0	0.1362	0.3246	45,200	26.4	3.69	63.8	-
0.0	0.1704	0.4471	77,900	87.2	1.89	-	-
30.2	0.1723	0.4321	76,100	57.2	2.84	63.2	-
53.3	0.1719	0.4205	73,900	41.5	3.82	70.3	-
96.0	0.1683	0.4074	70,100	34.9	4.31	85.9	-
0.0	0.2100	0.5729	123,000	112.5	-	-	-
30.2	0.2126	0.5384	117,000	62.4	4.00	74.1	-
53.3	0.2104	0.5255	113,000	53.6	4.50	101	-
96.0	0.2114	0.5183	112,000	42.1	5.70	107	-
0.0	0.2246	0.6010	138,000	98.5	-	-	-
30.2	0.2267	0.5739	133,000	63.0	5.00	76.3	-
53.3	0.2275	0.5634	131,000	49.2	5.70	88.3	-
96.0	0.2270	0.5558	129,000	41.9	6.60	107.2	-
0.0	0.2636	0.7124	192,000	106.2	-	-	-
30.2	0.2703	0.6841	189,000	63.8	2.65	-	252
53.3	0.2686	0.6665	183,000	51.3	4.50	-	445
0.0	0.3122	0.8586	274,000	119.2	-	-	-
30.2	0.3153	0.8160	263,000	78.2	5.47	-	449
53.3	0.3166	0.7441	257,000	58.9	5.50	-	569
96.0	0.3175	0.7827	254,000	48.1	6.64	-	756
0.0	0.3324	0.9123	310,000	119.6	-	-	-

TABLE D-6   continued

W_A watts	E_{SR} Volts	E_{PT} Volts	q/A BTU/HR FT^2	Δt ^{o}F	Nu	Y_1	Y_2
RUN 64 continued							
30.2	0.3407	0.8843	308,000	81.9	4.70	-	490
53.3	0.3397	0.8580	298,000	64.2	5.82	-	668
96.0	0.3414	0.8482	296,000	53.0	7.02	-	895
0.0	0.3695	1.0192	385,000	122.0	-	-	-
30.2	0.3742	0.9802	375,000	85.2	5.50	-	574
53.3	0.3772	0.9595	370,000	66.0	7.03	-	768
96.0	0.3778	0.9451	365,000	55.5	8.26	-	1030
0.0	0.4024	1.1132	458,000	123.2	-	-	-
30.2	0.4065	1.0709	445,000	90.0	6.16	-	601
53.3	0.4081	1.0498	438,000	74.2	7.40	-	944
96.0	0.4088	1.0362	433,000	63.8	8.51	-	1220
0.0	0.4422	1.2321	557,000	127.3	-	-	-

TABLE D-7

LIQUID: Methanol   TEMPERATURE: 113°F   FREQUENCY: 44.1 kcps

WIRE DIAMETER: 0.007"

W_A watts	E_{SR} Volts	E_{PT} Volts	q/A BTU/HR FT^2	Δt °F	Nu	Y_1	Y_2
RUN 58			L = 46/64 in.	R_{100} = 0.09421 Ω			
0.0	0.0257	0.1057	4,230	17.2	1.26	-	-
15.6	0.0258	0.1048	4,200	12.2	1.75	17.3	-
0.0	0.0354	0.1474	8,110	25.5	1.64	-	-
9.5	0.0353	0.1459	8,020	21.2	-	-	-
15.6	0.0352	0.1444	7,900	17.4	2.32	22.9	-
53.3	0.0345	0.1399	7,510	11.5	3.31	26.3	-
96.0	0.0344	0.1391	7,440	10.3	3.66	34.7	-
0.0	0.0462	0.1977	14,200	42.3	1.75	-	-
3.2	0.0461	0.1953	14,000	36.8	-	-	-
15.6	0.0460	0.1916	13,700	26.2	2.74	33.5	-
53.3	0.0450	0.1870	13,000	20.5	3.24	43.4	-
0.0	0.0516	0.2230	17,900	46.2	2.02	-	-
0.5	0.0516	0.2231	17,900	46.8	-	-	-
1.3	0.0516	0.2205	17,700	39.7	-	-	-
15.6	0.0516	0.2179	17,500	32.5	2.78	44.5	-
53.3	0.0515	0.2121	17,000	18.5	4.70	39.3	-
96.0	0.0512	0.2108	16,800	17.3	4.97	51.7	-
0.0	0.0581	0.2580	23,300	61.7	-	-	-
0.5	0.0580	0.2538	22,900	52.6	-	-	-
15.6	0.0584	0.2476	22,500	33.0	3.52	44.9	-
53.3	0.0586	0.2457	22,400	26.8	4.33	56.5	-
96.0	0.0580	0.2415	21,800	22.5	4.96	65.0	-
0.0	0.0665	0.3007	31,100	72.6	-	-	-
0.5	0.0667	0.3016	31,300	73.1	-	-	-
1.3	0.0669	0.2970	30,900	62.2	-	-	-
15.6	0.0671	0.2913	30,400	49.0	3.26	79.2	-
53.3	0.0671	0.2872	30,000	40.1	3.91	94.7	-
96.0	0.0672	0.2823	29,500	29.0	5.25	87.0	-
0.0	0.0666	0.3069	31,800	83.9	-	-	-
0.0	0.0713	0.3300	36,600	86.8	-	-	-
0.0	0.0722	0.3328	37,400	82.8	-	-	-
15.6	0.0734	0.3187	36,400	47.0	4.07	74.3	-
53.3	0.0727	0.3112	35,200	38.6	4.75	89.9	-

TABLE D-7   continued

W_A watts	E_{SR} Volts	E_{PT} Volts	q/A BTU/HR FT^2	Δt $^\circ F$	Nu	Y_1	Y_2
RUN 58 continued							
96.0	0.0726	0.3082	34,800	34.0	5.28	106.4	-
0.0	0.0769	0.3504	41,900	78.1	-	-	-
15.6	0.0778	0.3397	41,100	52.2	3.98	-	235
53.3	0.0776	0.3312	40,000	38.5	5.19	-	324
96.0	0.0778	0.3296	39,900	34.5	5.97	107	-
0.0	0.0857	0.3907	52,100	78.0	-	-	-
15.6	0.0863	0.3819	51,300	59.8	4.36	-	323
53.3	0.0858	0.3685	49,200	44.0	5.6	-	400
96.0	0.0862	0.3683	49,400	41.0	6.02	-	573
0.0	0.0966	0.4407	66,200	80.6	-	-	-
15.6	0.0970	0.4379	66,100	72.8	4.66	-	266
53.3	0.0972	0.4283	64,800	58.0	5.67	-	599
96.0	0.0970	0.4227	63,800	51.6	6.23	-	718
15.6	0.1090	0.4960	84,100	77.0	5.63	-	210
53.3	0.1090	0.4849	82,200	63.5	6.60	-	648
96.0	0.1081	0.4762	80,100	57.2	7.08	-	943
0.0	0.0397	0.1832	11,300	86.5	-	-	-
15.6	0.0396	0.1833	11,300	86.6	-	-	-
53.3	0.1258	0.5723	11,200	76.0	-	-	-
96.0	0.1258	0.5674	11,100	71.0	-	-	-
53.3	0.0444	0.2056	14,200	87.8	-	-	-
15.6	0.0445	0.2067	14,300	90.1	-	-	-
0.0	0.0443	0.2059	14,200	89.9	-	-	-
0.0	0.0472	0.2193	16,100	90.1	-	-	-
15.6	0.0472	0.2193	16,100	90.2	-	-	-
53.3	0.0472	0.2192	16,100	89.5	-	-	-
0.0	0.0520	0.2450	19,800	99.3	-	-	-
0.0	0.0541	0.2533	21,300	95.2	-	-	-
RUN 65		L = 48/64 in.		R_{100} = 0.1006 Ω			
0.0	0.0296	0.1298	5,720	16.5	1.77	-	-
15.6	0.0282	0.1231	5,180	13.2	2.00	19.12	-
53.3	0.0282	0.1226	5,160	10.5	2.50	26.4	-
0.0	0.0309	0.1366	6,290	21.6	1.49	-	-
15.6	0.0309	0.1349	6,210	15.2	2.08	21.5	-
53.3	0.0308	0.1335	6,120	11.4	2.73	28.7	-
96.0	0.0307	0.1329	6,080	10.1	3.06	36.0	-
0.0	0.0376	0.1686	9,460	29.2	1.67	-	-
15.6	0.0378	0.1656	9,320	17.7	2.70	24.2	-

TABLE D-7 continued

W_A watts	E_{SR} Volts	E_{PT} Volts	q/A BTU/HR FT^2	Δt $^\circ F$	Nu	Y_1	Y_2
RUN 65 continued							
53.3	0.0368	0.1607	8,830	14.9	3.02	34.4	-
96.0	0.0368	0.1599	8,780	12.4	3.60	40.2	-
0.0	0.0416	0.1884	11,700	35.5	1.71	-	-
15.6	0.0415	0.1827	11,300	20.8	2.78	27.7	-
53.3	0.0415	0.1812	11,200	16.8	3.40	38.0	-
96.0	0.0414	0.1799	11,100	13.9	4.07	44.6	-
0.0	0.0465	0.2105	14,600	36.2	2.09	-	-
15.6	0.0466	0.2071	14,400	24.7	3.00	33.5	-
53.3	0.0460	0.2014	13,800	17.6	4.00	39.0	-
96.0	0.0456	0.1988	13,500	15.0	4.58	48.1	-
0.0	0.0548	0.2559	20,900	53.2	2.07	-	-
15.6	0.0554	0.2483	20,500	29.4	3.60	38.8	-
53.3	0.0543	0.2408	19,500	22.8	4.40	49.2	-
96.0	0.0540	0.2383	19,200	20.2	4.86	61.4	-
0.0	0.0621	0.2938	27,200	60.1	2.40	-	-
15.6	0.0630	0.2863	26,900	36.1	3.87	51.8	-
53.3	0.0628	0.2818	26,400	28.5	4.77	61.4	-
96.0	0.0629	0.2794	26,200	24.1	5.60	74.3	-
0.0	0.0703	0.3366	35,300	67.7	-	-	-
15.6	0.0702	0.3247	34,000	47.2	3.78	74.7	-
53.3	0.0700	0.3180	33,200	36.6	4.70	84.2	-
96.0	0.0698	0.3133	32,600	31.0	5.43	90.0	-
0.0	0.0726	0.3547	38,400	81.1	-	-	-
15.6	0.0739	0.3439	37,900	51.8	3.85	85.3	-
53.3	0.0742	0.3361	37,200	35.8	5.40	83.4	-
96.0	0.0743	0.3339	37,000	31.5	6.07	91.0	-
0.0	0.0809	0.3895	47,000	71.2	-	-	-
15.6	0.0820	0.3839	46,900	54.8	4.32	-	301
53.3	0.0814	0.3719	45,100	40.5	5.57	-	370
96.0	0.0814	0.3682	44,700	34.2	6.50	-	461
0.0	0.0911	0.4396	59,700	72.8	-	-	-
15.6	0.0909	0.4345	58,900	66.0	4.56	-	337
53.3	0.0917	0.4258	58,200	49.0	5.98	-	494
96.0	0.0914	0.4199	57,200	42.8	6.70	-	602
0.0	0.1023	0.4969	75,800	75.8	-	-	-
15.6	0.1014	0.4906	74,200	73.3	-	-	-
53.3	0.1005	0.4754	71,200	60.0	6.03	-	620
96.0	0.1006	0.4729	70,900	56.2	6.39	-	685
0.0	0.1149	0.5591	95,800	77.8	-	-	-
15.6	0.1151	0.5604	96,200	78.1	-	-	-
53.3	0.1145	0.5511	94,100	70.2	-	-	-

TABLE D-7   continued

W_A watts	E_{SR} Volts	E_{PT} Volts	q/A BTU/HR FT^2	Δt $^\circ F$	Nu	Y_1	Y_2
RUN 65 continued							
96.0	0.1142	0.5422	92,300	62.2	-	-	-
0.0	0.0414	0.2026	12,500	80.7	-	-	-
15.6	0.0415	0.2034	12,600	80.9	-	-	-
53.3	0.0414	0.2024	12,500	79.3	-	-	-
96.0	0.0412	0.2003	12,300	75.6	-	-	-
0.0	0.0457	0.2246	15,300	82.6	-	-	-
53.3	0.0466	0.2262	15,500	83.1	-	-	-
96.0	0.0457	0.2245	15,300	81.8	-	-	-
0.0	0.0498	0.2477	18,400	88.5	-	-	-
0.0	0.0530	0.2630	20,800	87.1	-	-	-
0.0	0.0569	0.2841	24,100	91.2	-	-	-

TABLE D-8

LIQUID: Distilled Water   TEMPERATURE: 149°F   FREQUENCY: 108 kcps

WIRE DIAMETER: 0.010"

W_A watts	E_{SR} Volts	E_{PT} Volts	q/A BTU/HR FT^2	Δt °F	Nu	Y_1	Y_2
RUN 68			L = 49/64 in.	R_{100} = 0.05054 Ω			
0.0	0.0820	0.1958	16,400	27.8	1.27	-	-
34.2	0.0824	0.1970	16,600	28.3	-	-	-
47.0	0.0821	0.1954	16,400	25.7	-	-	-
62.0	0.0820	0.1935	16,200	21.1	1.65	12.1	-
105.0	0.0816	0.1918	16,000	18.4	1.87	31.9	-
0.0	0.0998	0.2430	14,800	39.5	1.35	-	-
62.0	0.0998	0.2392	24,400	29.8	1.76	15.7	-
105.0	0.1001	0.2364	24,200	21.9	2.38	23.3	-
0.0	0.1163	0.2851	33,900	44.5	1.64	-	-
62.0	0.1166	0.2795	33,300	31.0	2.30	16.3	-
105.0	0.1145	0.2708	31,700	23.4	2.91	24.7	-
0.0	0.1314	0.3267	43,900	54.2	1.73	-	-
34.2	0.1317	0.3230	43,500	45.7	-	-	-
62.0	0.1323	0.3180	43,000	33.4	2.76	17	-
105.0	0.1309	0.3108	41,600	26.8	3.34	26.9	-
0.0	0.1668	0.4340	74,000	83.5	1.88	-	-
62.0	0.1703	0.4200	73,100	48.4	3.23	24.1	-
105.0	0.1700	0.4097	71,200	34.2	4.46	32.2	-
0.0	0.2122	0.5624	122,000	94.7	-	-	-
16.0	0.2120	0.5629	122,000	95.1	-	-	-
24.0	0.0654	0.1676	11,200	72.2	-	-	-
62.0	0.2157	0.5396	119,000	56.3	4.27	30.1	-
105.0	0.2153	0.5316	117,000	48.2	5.19	44.9	-
0.0	0.1932	0.5165	102,000	99.8	-	-	-
62.0	0.1950	0.4877	97,200	56.3	3.68	27.6	-
105.0	0.1949	0.4744	94,500	39.3	5.15	36.6	-
0.0	0.2195	0.6062	136,000	122.2	-	-	-
62.0	0.2255	0.5726	132,000	66.8	4.20	33.2	-
0.0	0.2362	0.6337	153,000	103.2	-	-	-
62.0	0.2408	0.6136	151,000	69.1	1.11	-	68.7
105.0	0.2427	0.6006	149,000	50.5	1.50	-	130
0.0	0.2583	0.6936	183,000	102.1	-	-	-
62.0	0.2631	0.6691	180,000	66.8	1.37	-	75.4
105.0	0.2633	0.6577	177,000	55.5	1.62	-	139

TABLE D-8   continued

W_A watts	E_{SR} Volts	E_{PT} Volts	q/A BTU/HR FT^2	Δt $^\circ$F	Nu	Y_1	Y_2
RUN 68 continued							
0.0	0.2807	0.7666	220,000	113.3	-	-	-
24.0	0.2812	0.7687	221,000	114.0	-	-	-
34.2	0.2820	0.7596	219,000	103.8	-	-	-
62.0	0.2839	0.7408	215,000	81.7	1.34	-	80.6
105.0	0.2838	0.7171	208,000	61.0	1.71	-	152
0.0	0.3070	0.8413	264,000	115.0	-	-	-
62.0	0.3098	0.8147	258,000	87.0	1.51	-	88.0
105.0	0.3118	0.7905	252,000	63.0	2.04	-	165
0.0	0.3379	0.9321	322,000	121.2	-	-	-
34.2	0.3393	0.9371	325,000	122.1	-	-	-
47.0	0.3390	0.9291	322,000	116.7	-	-	-
62.0	0.3415	0.9165	320,000	102.3	1.60	-	84.9
105.0	0.3462	0.8901	315,000	73.9	2.17	-	184
0.0	0.3833	1.0694	419,000	129.2	-	-	-
62.0	0.3876	1.0372	411,000	100.3	-	-	-
105.0	0.3925	1.0169	408,000	78.0	2.66	-	207
0.0	0.4049	1.1356	470,000	132.0	-	-	-
62.0	0.4085	1.0991	459,000	103.1	-	-	-
105.0	0.4137	1.0688	452,000	76.1	3.03	-	227
0.0	0.4430	1.2697	575,000	148.4	-	-	-
62.0	0.4512	1.2249	565,000	110.2	-	-	-
105.0	0.4532	1.87$\gamma\gamma$	550,000	86.2	3.25	-	242
RUN 69		L = 47/64 in.		R_{100} = 0.04928 Ω			
0.0	0.0712	0.1635	12,400	18.70	1.43	-	-
62.0	0.0709	0.1626	12,300	17.3	1.53	10.5	-
105.0	0.0708	0.1616	12,200	15.7	1.67	18.7	-
0.0	0.0869	0.2030	18,800	29.7	1.36	-	-
62.0	0.0865	0.1994	18,400	21.3	1.85	12.2	-
105.0	0.0862	0.1980	18,200	19.2	2.04	21	-
0.0	0.0968	0.2268	23,400	31.8	1.58	-	-
62.0	0.0963	0.2231	22,900	25.5	1.93	13.7	-
105.0	0.0957	0.2196	22,400	19.9	2.42	21.7	-
0.0	0.1162	0.2792	34,600	47.7	1.55	-	-
62.0	0.1176	0.2752	34,500	32.4	2.28	16.7	-
105.0	0.1170	0.2709	33,800	25.8	2.81	26.1	-
0.0	0.1445	0.3584	55,200	69.0	1.70	-	-
62.0	0.1454	0.3477	53,900	44.8	2.57	22	-
105.0	0.1455	0.3423	53,100	34.8	3.27	33.6	-
0.0	0.1564	0.3911	65,200	73.2	1.89	-	-

TABLE D-8 continued

W_A watts	E_{SR} Volts	E_{PT} Volts	q/A BTU/HR FT^2	Δt $^\circ$F	Nu	Y_1	Y_2
RUN 69 continued							
62.0	0.1591	0.3821	64,800	46.6	2.97	23.3	-
105.0	0.1582	0.3724	62,800	34.5	3.90	32.4	-
0.0	0.1774	0.4558	86,200	90.2	-	-	-
62.0	0.1815	0.4434	85,800	57.4	3.19	28.3	-
105.0	0.1828	0.4346	84,700	39.4	4.60	36.6	-
0.0	0.2041	0.5377	117,000	106.2	-	-	-
62.0	0.2090	0.5205	116,000	68.7	3.60	34.1	-
105.0	0.2092	0.5067	113,000	51.2	4.71	47.3	-
0.0	0.2190	0.5697	133,000	98.5	-	-	-
62.0	0.2232	0.5462	130,000	58.4	4.75	28.7	-
105.0	0.2231	0.5382	128,000	49.5	5.53	45.9	-
0.0	0.2414	0.6372	164,000	108.2	-	-	-
62.0	0.2480	0.6165	163,000	68.5	1.21	-	71.4
105.0	0.2478	0.6056	160,000	57.6	1.42	-	131
0.0	0.2659	0.6914	196,000	97.2	-	-	-
62.0	0.2682	0.6715	192,000	72.1	1.36	-	77.8
105.0	0.2687	0.6527	187,000	52.8	1.81	-	144
0.0	0.2872	0.7642	234,000	112.8	-	-	-
62.0	0.2914	0.7338	228,000	75.8	1.53	-	86.3
105.0	0.2924	0.7154	223,000	57.4	1.99	-	154
0.0	0.3112	0.8288	275,000	114.4	-	-	-
62.0	0.3154	0.8030	270,000	84.0	1.65	-	88.2
105.0	0.3163	0.7918	267,000	73.0	1.86	-	170
0.0	0.3347	0.9079	324,000	127.1	-	-	-
62.0	0.3371	0.8571	308,000	83.2	1.88	-	94.1
105.0	0.3357	0.8326	298,000	66.9	2.27	-	181
0.0	0.3730	1.0084	401,000	125.8	-	-	-
62.0	0.3794	0.9840	398,000	97.3	-	-	-
105.0	0.3847	0.9533	391,000	67.3	2.97	-	207
0.0	0.4051	1.0974	474,000	127.1	-	-	-
62.0	0.4107	1.0712	469,000	100.2	-	-	-
105.0	0.4159	1.0555	468,000	82.0	2.88	-	220
0.0	0.4271	1.1683	532,000	133.1	-	-	-
62.0	0.4351	1.1382	528,000	102.1	-	-	-
105.0	0.4349	1.1108	515,000	86.2	3.04	-	234

TABLE D-9

LIUID: Methanol   TEMPERATURE: $113^{\circ}F$ FREQUENCY: 108 kcps

WIRE DIAMETER: 0.007"

W_A watts	E_{SR} Volts	E_{PT} Volts	q/A BTU/HR FT^2	Δt $^{\circ}F$	Nu	Y_1	Y_2
RUN 66			L = 48/64 in.	R_{100} = 0.1006 Ω			
0.0	0.0197	0.0855	2,510	11.2	1.14	-	-
0.0	0.0223	0.0998	3,420	11.8	1.48	-	-
0.0	0.0262	0.1150	4,490	17.2	1.33	-	-
16.0	0.0262	0.1150	4,490	17.4	-	-	-
24.0	0.0262	0.1144	4,460	15.1	-	-	-
62.0	0.0261	0.1135	4,420	12.2	1.84	11.9	-
105.0	0.0260	0.1129	4,380	10.2	2.18	16.0	-
0.0	0.0306	0.1358	6,200	22.1	1.44	-	-
62.0	0.0303	0.1328	5,990	15.7	1.95	14.2	-
105.0	0.0301	0.1310	5,880	11.2	2.67	16.9	-
0.0	0.0361	0.1621	8,720	28.7	1.57	-	-
4.3	0.0362	0.1629	8,800	29.3	-	-	-
16.0	0.0362	0.1611	8,700	23.2	-	-	-
62.0	0.0361	0.1597	8,600	19.8	2.22	16.8	-
105.0	0.0359	0.1568	8,400	12.3	3.48	18.3	-
0.0	0.0417	0.1912	11,900	42.0	1.47	-	-
62.0	0.0422	0.1878	11,800	25.8	2.35	21.0	-
105.0	0.0416	0.1823	11,300	16.6	3.48	22.2	-
0.0	0.0524	0.2445	19,100	52.8	1.90	-	-
62.0	0.0518	0.2368	18,300	40.10	2.38	31.0	-
105.0	0.0519	0.2312	17,900	25.5	3.60	31.8	-
0.0	0.0602	0.2874	25,800	66.1	-	-	-
10.0	0.0603	0.2825	25,400	53.8	-	-	-
62.0	0.0606	0.2790	25,200	44.0	3.00	35.5	-
105.0	0.0604	0.2732	24,600	33.4	3.81	40.3	-
0.0	0.0699	0.3385	35,300	73.8	-	-	-
16.0	0.0701	0.3341	34,900	64.7	-	-	-
62.0	0.0700	0.3307	34,500	59.1	3.07	48.7	-
105.0	0.0703	0.3223	33,800	40.1	4.39	49.9	-
0.0	0.0775	0.3904	45,100	97.9	-	-	-
62.0	0.0781	0.3744	43,600	67.0	-	-	-
105.0	0.0776	0.3596	41,600	46.8	1.84	-	121
0.0	0.0794	0.3901	46,200	83.7	-	-	-
62.0	0.0789	0.3834	45,100	77.0	-	-	-

TABLE D-9   continued

W_A watts	E_{SR} Volts	E_{PT} Volts	q/A BTU/HR FT^2	Δt $^\circ$F	Nu	Y_1	Y_2
RUN 66 continued							
105.0	0.0790	0.3712	43,700	56.8	1.60	-	126
0.0	0.0941	0.4618	64,800	83.0	-	-	-
62.0	0.0937	0.4576	63,900	81.3	-	-	-
105.0	0.0933	0.4455	62,000	67.0	-	-	-
0.0	0.1050	0.5170	80,900	86.5	-	-	-
62.0	0.1050	0.5170	80,900	86.3	-	-	-
105.0	0.1048	0.5108	79,800	80.0	-	-	-
0.0	0.0374	0.1849	10,300	90.2	-	-	-
62.0	0.0372	0.1840	10,200	90.3	-	-	-
105.0	0.0371	0.1825	10,100	86.4	-	-	-
0.0	0.0424	0.2103	13,300	91.3	-	-	-
62.0	0.0426	0.2111	13,400	91.5	-	-	-
105.0	0.0425	0.2102	13,300	90.5	-	-	-
0.0	0.0475	0.2375	16,800	96.4	-	-	-
105.0	0.0475	0.2374	16,800	96.1	-	-	-
0.0	0.01678	0.8474	212,000	102.2	-	-	-
0.0	0.1772	0.8973	237,000	103.1	-	-	-
0.0	0.1918	0.9723	278,000	103.8	-	-	-
RUN 67		L = 46/64 in.		R_{100} = 0.09421 Ω			
0.0	0.0211	0.0856	2,810	10.2	1.40	-	-
0.0	0.0252	0.1034	4,060	15.8	1.31	-	-
62.0	0.0252	0.1025	4,020	11.1	1.84	11.1	-
0.0	0.0341	0.1421	7,530	25.4	1.52	-	-
62.0	0.0341	0.1396	7,400	16.8	2.25	14.6	-
105.0	0.0338	0.1374	7,220	12.7	2.90	20.3	-
0.0	0.0395	0.1661	10,200	32.5	1.65	-	-
62.0	0.0396	0.1639	10,100	22.9	2.26	21.7	-
105.0	0.0394	0.1604	9,820	14.2	3.53	22.0	-
0.0	0.0468	0.2021	14,700	47.7	1.61	-	-
62.0	0.0469	0.1960	14,300	27.5	2.68	26.8	-
105.0	0.0465	0.1923	13,900	22.2	3.21	32.3	-
0.0	0.0573	0.2522	22,500	56.4	2.10	-	-
62.0	0.0573	0.2444	21,800	38.2	2.97	38.2	-
105.0	0.0571	0.2388	21,200	27.6	3.96	40.8	-
0.0	0.0667	0.3008	31,200	71.8	-	-	-
62.0	0.0660	0.2885	29,600	53.2	2.92	59.4	-
105.0	0.0663	0.2811	29,000	34.7	4.33	51.5	-
0.0	0.0756	0.3495	41,100	85.2	-	-	-

TABLE D-9   continued

W_A watts	E_{SR} Volts	E_{PT} Volts	q/A BTU/HR FT^2	Δt $^{\circ}F$	Nu	Y_1	Y_2
RUN 67 continued							
62.0	0.0762	0.3367	39,900	57.7	1.44	-	82
105.0	0.0759	0.3328	39,300	51.8	1.57	-	121
0.0	0.0825	0.3773	48,400	77.7	-	-	-
62.0	0.0829	0.3706	47,800	64.2	-	-	-
105.0	0.0826	0.3603	46,300	49.7	1.93	-	131
0.0	0.0998	0.4578	71,100	81.8	-	-	-
0.0	0.0989	0.4491	69,100	75.8	-	-	-
105.0	0.0985	0.4423	67,800	68.8	-	-	-
105.0	0.0866	0.3873	52,500	65.2	-	-	-
0.0	0.1108	0.5135	88,500	87.5	-	-	-
62.0	0.1109	0.5137	88,600	88.2	-	-	-
105.0	0.1109	0.5099	88,000	83.2	-	-	-
0.0	0.1263	0.5852	115,000	88.2	-	-	-
105.0	0.1258	0.5826	114,000	88.0	-	-	-
0.0	0.1431	0.6650	148,000	90.3	-	-	-
105.0	0.1431	0.6649	148,000	90.1	-	-	-
0.0	0.1577	0.7417	182,000	97.6	-	-	-
105.0	0.1578	0.7415	182,000	97.2	-	-	-
0.0	0.1745	0.8215	223,000	98.3	-	-	-
105.0	0.1745	0.8215	223,000	98.4	-	-	-
0.0	0.1851	0.8716	251,000	98.5	-	-	-

TABLE D-10

LIQUID: Methanol   TEMPERATURE: 113°F   FREQUENCY: 306 kcps

WIRE DIAMETER: 0.007"

W_A watts	E_{SR} Volts	E_{PT} Volts	q/A BTU/HR FT^2	Δt °F	Nu	Y_1	Y_2
RUN 70			L = 47/64 in.		R_{100} = 0.09723 Ω		
0.0	0.0233	0.0977	3,460	11.7	1.51	-	-
92.0	0.0232	0.0975	3,450	11.8	-	-	-
125.0	0.0231	0.0968	3,410	10.2	1.70	4.67	-
0.0	0.0278	0.1176	4,980	15.4	1.65	-	-
125.0	0.0278	0.1171	4,960	12.7	1.96	5.28	-
160.0	0.0278	0.1164	4,920	11.2	2.24	7.96	-
0.0	0.0339	0.1449	7,470	21.3	1.80	-	-
125.0	0.0335	0.1422	7,260	16.0	2.31	6.11	-
160.0	0.0334	0.1410	7,170	13.3	2.75	8.78	-
0.0	0.0394	0.1718	10,300	31.3	1.70	-	-
74.0	0.0394	0.1718	10,300	31.5	-	-	-
92.0	0.0394	0.1702	10,200	27.3	-	-	-
125.0	0.0396	0.1691	10,200	19.7	2.65	7.0	-
160.0	0.0393	0.1668	9,980	16.8	3.04	10.3	-
0.0	0.0468	0.2051	14,600	36.5	2.07	-	-
92.0	0.0466	0.2017	14,300	29.2	-	-	-
125.0	0.0464	0.1997	14,100	25.8	2.81	8.4	-
160.0	0.0457	0.1955	13,600	22.1	3.15	12.2	-
0.0	0.0617	0.2818	26,400	59.1	2.36	-	-
125.0	0.0624	0.2748	26,100	37.8	3.59	11.2	-
160.0	0.0620	0.2700	25,500	31.1	4.24	15.7	-
0.0	0.0525	0.2350	18,800	47.0	2.09	-	-
125.0	0.0528	0.2290	18,400	29.4	3.24	9.29	-
160.0	0.0518	0.2231	17,600	24.2	3.73	13.0	-
0.0	0.0678	0.3157	32,600	70.0	-	-	-
74.0	0.0681	0.3098	32,100	56.4	-	-	-
125.0	0.0680	0.3061	31,700	48.7	3.41	13.7	-
160.0	0.0674	0.2971	30,500	36.2	4.37	17.5	-
0.0	0.0755	0.3637	41,800	93.1	-	-	-
125.0	0.0767	0.3493	40,800	58.4	3.57	15.9	-
160.0	0.0770	0.3422	40,100	44.3	4.72	20.4	-
0.0	0.0794	0.3712	44,900	74.0	-	-	-
92.0	0.0795	0.3659	44,300	66.3	-	-	-

TABLE D-10   continued

W_A watts	E_{SR} Volts	E_{PT} Volts	q/A BTU/HR FT^2	Δt $°F$	Nu	Y_1	Y_2

RUN 70   continued

125.0	0.0794	0.3622	43,800	61.1	3.80	16.4	-
160.0	0.2508	1.1261	430,000	51.8	4.36	23.4	-
0.0	0.0924	0.4351	61,200	80.5	-	-	-
125.0	0.0921	0.4273	59,900	71.7	-	-	-
160.0	0.0865	0.3939	51,900	59.8	-	-	-
0.0	0.1112	0.5273	89,300	83.8	-	-	-
125.0	0.1107	0.5221	88,000	80.5	-	-	-
160.0	0.1103	0.5125	86,100	71.2	-	-	-
0.0	0.1251	0.5988	114,000	90.0	-	-	-
125.0	0.1251	0.5987	114,000	89.8	-	-	-
160.0	0.1250	0.5936	113,000	84.8	-	-	-
0.0	0.1466	0.7033	157,000	90.2	-	-	-
160.0	0.1471	0.7055	158,000	90.1	-	-	-
0.0	0.1652	0.7989	201,000	95.2	-	-	-
0.0	0.1760	0.8507	228,000	95.0	-	-	-
0.0	0.1879	0.9121	261,000	96.8	-	-	-

RUN 71   L = 47/64 in. R_{100} = 0.09723 Ω

0.0	0.0219	0.0919	3,060	12.3	1.27	-	-
0.0	0.0258	0.1090	4,290	14.2	1.54	-	-
125.0	0.0256	0.1073	4,180	11.2	1.90	4.94	-
160.0	0.0255	0.1068	4,150	10.1	2.09	7.55	-
0.0	0.0311	0.1328	6,280	21.5	1.49	-	-
125.0	0.0310	0.1308	6,170	14.9	2.11	5.80	-
160.0	0.0309	0.1298	6,110	11.3	2.75	8.05	-
0.0	0.0355	0.1523	8,230	24.2	1.75	-	-
125.0	0.0352	0.1496	8,010	19.3	2.12	6.73	-
160.0	0.0351	0.1478	7,900	13.3	3.02	8.78	-
0.0	0.0410	0.1777	11,100	29.1	1.96	-	-
125.0	0.0408	0.1739	10,800	20.4	2.71	7.14	-
160.0	0.0407	0.1727	10,700	17.5	3.13	10.52	-
0.0	0.0497	0.2220	16,800	47.0	1.87	-	-
125.0	0.0496	0.2144	16,200	27.8	3.00	8.94	-
160.0	0.0499	0.2134	16,200	22.3	3.72	12.3	-
0.0	0.0585	0.2640	23,500	53.4	2.30	-	-
125.0	0.0582	0.2541	22,500	34.0	3.43	10.2	-
160.0	0.0578	0.2514	22,200	29.6	3.87	15.2	-
0.0	0.0714	0.3311	36,000	69.2	-	-	-
125.0	0.0713	0.3231	35,100	55.2	3.36	15.0	-

TABLE D-10   continued

W_A watts	E_{SR} Volts	E_{PT} Volts	q/A BTU/HR FT^2	Δt ^oF	Nu	Y_1	Y_2
RUN 71 continued							
160.0	0.0716	0.3173	34,600	42.1	4.28	19.6	-
0.0	0.0720	0.3401	37,300	80.3	-	-	-
125.0	0.0733	0.3307	36,900	53.1	3.66	14.6	-
160.0	0.0736	0.3246	36,400	39.2	4.83	18.6	-
0.0	0.0861	0.4035	52,900	75.8	-	-	-
125.0	0.0860	0.3948	51,700	63.0	-	-	-
160.0	0.0863	0.3882	51,000	51.0	5.25	23.2	-
0.0	0.0988	0.4635	69,700	76.6	-	-	-
125.0	0.0986	0.4595	69,000	72.2	-	-	-
160.0	0.0974	0.4463	66,200	61.8	-	-	-
0.0	0.1143	0.5391	93,800	79.9	-	-	-
125.0	0.1143	0.5388	93,700	79.8	-	-	-
160.0	0.1147	0.5355	93,500	73.6	-	-	-
0.0	0.1244	0.5912	112,000	84.2	-	-	-
125.0	0.1250	0.5939	113,000	84.4	-	-	-
160.0	0.0389	0.1842	10,900	82.7	-	-	-
0.0	0.0430	0.2045	13,400	84.3	-	-	-
160.0	0.0430	0.2045	13,400	84.2	-	-	-
0.0	0.0489	0.2339	17,400	89.0	-	-	-
0.0	0.1693	0.8185	211,000	95.2	-	-	-
0.0	0.1849	0.8953	252,000	96.3	-	-	-
0.0	0.1975	0.9642	290,000	101.3	-	-	-

APPENDIX E

CRITICAL SOUND PRESSURE DATA

TABLE E-1

LIQUID: Distilled Water   FREQUENCY: 20.6 kcps

V* volts	W_A watts	P_{CR} atm.	P_{peak} atm.	T_w $^\circ$F	Δt $^\circ$F	q/A BTU/hr ft^2
Liquid Temperature = 149°F						
10.0	7.0	.27	.50	282	133.1	500,000
10.0	7.0	.27	.50	277	128.1	430,000
7.5	4.8	.20	.34	262	113.1	310,000
6.0	3.0	.17	.28	259	110.2	250,000
3.0	1.0	.092	.14	241	92.1	170,000
2.5	0.8	.080	.13	237	88.3	120,000
5.0	2.0	.16	.24	211	62.8	66,000
7.5	4.8	.20	.34	196	47.0	38,000
10.0	7.0	.27	.50	182	33.3	28,000
15.0	15.6	.34	.60	164	14.8	10,000
Liquid Temperature = 113°F						
7.5	4.8	.19	.34	265	152.1	590,000
6.0	3.0	.17	.28	262	149.0	500,000
3.0	1.5	.12	.14	241	128.2	360,000
5.0	1.5	.12	.21	223	110.0	163,000
6.0	3.0	.17	.28	210	97.4	92,300
10.0	7.0	.25	.44	194	81.1	76,000
15.0	15.6	.34	.58	180	67.3	57,000

* V = voltage drop across the transducers.

TABLE E-2

LIQUID: Methanol   FREQUENCY: 20.6 kcps

V* volts	W_A watts	P_{CR} atm.	P_{peak} atm.	T_w °F	Δt °F	q/A BTU/hr ft^2
Liquid Temperature = 113°F						
10	7.0	0.16	0.30	129	16.3	4,100
10	7.0	0.16	0.30	136	23.8	7,800
7.5	4.8	0.14	0.25	142	28.8	11,200
5	2.0	0.11	0.17	156	43.4	19,400
3	1.0	0.076	0.12	167	54.4	25,000
2	0.8	0.055	0.087	178	65.5	39,000
3	1.0	0.076	0.123	185	72.2	60,000
5	2.0	0.11	0.17	187	74.2	90,000
10	7.0	0.16	0.30	189	76.7	105,000
Liquid Temperature = 95°F						
12.5	12.0	0.20	0.36	130	35.1	8,600
7.5	7.0	0.14	0.27	142	47.4	11,500
5	4.8	0.12	0.23	152	57.3	16,000
3	1.0	0.072	0.11	170	75.4	33,000
3	1.0	0.072	0.11	179	84.4	41,500
5	2.0	0.10	0.16	186	91.0	55,000
10	7.0	0.14	0.27	192	97.0	77,000

TABLE E-3

LIQUID: Distilled Water   LIQUID TEMPERATURE: 149°F

V^* volts	W_A watts	P_{CR} atm.	P_{peak} atm.	T_w °F	Δt °F	q/A BTU/hr ft^2
Frequency = 44.1 kcps						
25	23.2	.36	.62	179	30.0	24,000
20	15.6	.31	.55	188	38.5	30,800
15	9.5	.26	.51	198	49.0	45,100
10	4.6	.19	.33	216	67.0	61,200
3	0.5	.13	.20	239	90.0	95,100
7.5	3.2	.16	.25	251	102.0	158,000
10	4.6	.19	.33	261	112.0	217,000
20	15.6	.31	.55	277	128.3	352,000
25	23.2	.36	.62	282	133.0	505,000
Frequency = 108 kcps						
175	47.0	.63	1.1	177	27.8	16,400
175	47.0	.63	1.1	189	39.5	24,800
150	34.2	.53	.89	203	54.2	43,900
125	34.2	.45	.66	249	99.8	102,000
125	24.0	.45	.66	244	94.7	122,000
125	24.0	.45	.66	251	102.0	183,000
150	34.2	.53	.89	262	113.3	220,000
150	34.2	.53	.89	264	115.0	264,000
175	47.0	.63	1.1	270	121.2	322,000

TABLE E-4

LIQUID: Methanol   LIQUID TEMPERATURE: 113°F

V volts	W_A watts	P_{CR} atm.	P_{peak} atm.	T_w °F	Δt °F	q/A BTU/hr ft^2
Frequency = 44.1 kcps						
15	9.5	.23	.47	138.5	25.5	8,110
7.5	3.2	.15	.24	155.0	42.3	14,200
5	1.3	.13	.20	159.0	46.2	17,900
3	0.5	.09	.13	173.0	61.7	23,300
5	1.3	.13	.20	185.0	72.0	31,000
10	4.6	.17	.31	191.0	78.1	41,900
15	9.5	.23	.47	193.0	80.6	66,000
Frequency = 108 kcps						
125	24	.42	.76	130	17.2	4,510
125	24	.42	,76	135	22.1	6,200
100	16	.34	.58	142	28.7	8,720
75	10	.25	.38	166	52.8	19,100
75	10	.25	.38	179	66.2	25,800
100	16	.34	.58	186	73.3	35,200
175	47	.42	.76	196	83.0	64,800
Frequency = 306 kcps						
175	125	,92	-	124.7	11.7	3,460
175	125	.92	-	128.4	15.4	4,980
150	92	.83	-	144.3	31.3	10,300
150	92	.83	-	149.5	36.5	14,600
125	74	.71	-	183.0	70.0	32,600
150	92	.83	-	187.0	74.0	44,900
175	125	.92	-	196.8	83.8	89,300

APPENDIX F

SAMPLE CALCULATIONS

I. SAMPLE CALCULATION FOR THE PERCENTAGE OF SOIL REMOVED

Using data from Run A1 in Table C-1 where W_A = 86.0 watts, CPM_i = 36200, CPM_f = 32500, Background = 486 CPM

$$S_R(\text{Percentage Soil Removed}) = \frac{CPM_i - CPM_f}{\frac{2}{3}(CPM_i)} \times 100\%$$

$$= \frac{(36200 - 486) - (32500 - 486)}{\frac{2}{3}(36200 - 486)} \times 100\%$$

$$= 15.5\%.$$

II. SAMPLE CALCULATION FOR THE HEAT TRANSFER RESULTS

The formulae used are as follows:

$$I = E_{SR}/0.02$$

$$q = 3.415\ E_{PT}I$$

$$q/A = 3.415\ E_{PT}\ I\ /\pi D_w \ell$$

$$R_{PT} = E_{PT} / I \ ; \qquad\qquad T_{PT} = \left(\frac{R_{PT} - R_o}{R_{100} - R_o}\right)\ 100.$$

Taking R_{100}/R_o = 1.3925

$$T_{PT} = \frac{354.777\ E_{PT}}{R_{100}\ I} - 254.777$$

$$\Delta T = T_{PT} - T_L$$

where D_w - wire diameter, ft

E_{SR} - voltage drop across the standard resistor, volts

E_{PT} - voltage drop across the test section of the platinum wire, volts

I - current, amp

ℓ - length of the test section, ft

q/A - heat flux, BTU/hr ft^2

R_o - resistance of the test section at $0^\circ C$, Ω

R_{100} - resistance of the test section at $100^\circ C$, Ω

R_{PT} - resistance of the test section at T_{PT}, Ω

T_{PT} - temperature of the wire, $^\circ C$

T_L - temperature of the liquid, $^\circ C$.

Using data from Run 30 in Table D-1, where

$T_L = 95^\circ F$ $(35^\circ C)$, $W_A = 15.6$ watts,

$E_{SR} = 0.0705$ volts, $E_{PT} = 0.1535$ volts

$D_w = 0.010$ in. $= 0.000833$ ft, $\ell = 48/64$ in. $= 0.0625$ ft

$R_{100} = 0.05021$ Ω

1. Calculation of Δt and q/A

I $= 0.0705/0.02 = 3.525$ amp

$$q/A = \frac{3.415 \times 0.1535 \times 3.525}{3.1415 \times 0.000833 \times 0.0625}$$

$= 11,300$ BTU/hr ft^2

$$T_{PT} = \frac{354.777 \times 0.1535}{0.05021 \times 3.525} - 254.777$$

$= 52.6^\circ C = 127^\circ F$

$\Delta T = 52.6 - 35 = 17.6^\circ C = 31.6^\circ F$

2. <u>Calculation of Nu_w and $(Gr\ Pr)^{1/2}S_R^{1/2}/P_{CR}$</u>

When $W_A = 15.6$ watts, $S_R = 2.7\%$

when $T_{PT} = 127^oF$, $P_{CR} = 0.21$ atm

$$T_f = \frac{T_L + T_{PT}}{2} = \frac{95 + 127}{2} = 111^oF$$

$k_L = 0.117$ BTU/ft hr ^oF, $\qquad \beta = 6.72 \times 10^{-4}\ ^oF^{-1}$

$\rho_L = 48$ lb/ft^3 $\qquad\qquad \mu = 1.05$ lb/ft-hr

$Cp = 0.625$ BTU/lb ^oF

$$h = \frac{q/A}{\Delta t} = \frac{11300}{31.6} = 358\ \text{BTU/hr ft}^2\ ^oF$$

$$Nu = \frac{hD_w}{k_L} = \frac{358 \times 0.000833}{0.117} = 2.55$$

$$Gr = \frac{g\ \beta\ \rho_L^2\ \Delta t\ D_w^3}{2} = \frac{32.2 \times 3600^2 \times 6.72 \times 10^{-4} \times 48^2 \times 31.6 \times .000833^3}{1.05^2}$$

$$= 10.5$$

$$Pr = \frac{C_p \mu}{k_L} = \frac{0.625 \times 1.05}{0.117} = 5.6$$

$$(Gr\ Pr)^{1/2}(S_R)^{1/2}/P_{CR} = (10.5 \times 5.6)^{1/2}(2.7)^{1/2}/0.21$$

$$= 59.5$$

3. <u>Calculation of Nu_B and $Re^{1/2}Pr^{2/3}S_R^{1/2}/PC_R$</u>

Using data from Run 30 in Table D-1 where

$W_A = 15.6$ watts, $\qquad\qquad S_R = 2.7\%$

$$E_{SR} = 0.1496 \text{ volts}, \quad E_{PT} = 0.3529 \text{ volts}$$

$$I = 0.1496/0.02 = 7.48 \text{ amp}$$

$$q/A = \frac{3.415 \times 0.3529 \times 7.48}{3.14 \times 0.000833 \times 0.0625} = 55{,}100 \text{ BTU/hr ft}^2$$

$$T_{PT} = \frac{354.777 \times 0.3529}{0.05021 \times 7.48} - 254.777$$

$$= 78.2^\circ C = 173^\circ F \; ; \quad \Delta T = 173 - 93.8 = 79.2^\circ F$$

$$T_f = \frac{93.8 + 173}{2} = 136^\circ F$$

$$k_L = 0.116 \text{ BTU/ft hr } ^\circ F, \qquad \lambda = 480 \text{ BTU/lb}$$

$$\rho_L = 47.1 \text{ lb/ft}^3, \qquad \mu_L = 0.90 \text{ lb/ft-hr}$$

$$\rho_v = 1/\mathcal{N}_v = 1/18.6 \text{ lb/ft}^3$$

$$D_B = 12 \times 10^4 \text{ ft (see calculation for } D_B \text{ below)}$$

$$Re = \frac{q}{A} \frac{\rho_L D_B}{\lambda \mu_L \rho_v} = \frac{55100 \times 47.1 \times 12 \times 10^{-4} \times 18.6}{480 \times 0.90} = 134$$

$$Pr = 4.80 \qquad\qquad P_{CR} = 0.073 \text{ atm}$$

$$Nu_B = \frac{hD_B}{k_L} = \frac{55100 \times 12 \times 10^{-4}}{79.2 \times 0.116} = 6.94$$

$$Re^{1/2} Pr^{2/3} S_R^{1/2}/P_{CR} = (134)^{1/2} (4.8)^{2/3} (2.7)^{1/2}/.073 = 746$$

4. Calculation of Radial Gradient in Temperature Within the Wire

Assuming that the thermal conductivity is constant and the electric heat is uniformly generated, McAdams et al.[*] derived the following equation:

* McAdams, W.H., J.N. Addoms, R.M. Rinaldo and R.S. Day, ChemEng.Prog. 44, 639 (1948)

$$T_s = T_w - \frac{(q/A) \, D_w}{8K}$$

where T_s = surface temperature of the wire, $^{\circ}F$

T_w = measured mean temperature of the wire, $^{\circ}F$

q/A = heat flux, BTU/hr ft^2

D_w = wire diameter, ft

k = thermal conductivity of the wire, BTU/hr ft $^{\circ}F$.

Using data from Run 53 in Table D-3 where D_w = 0.000833 ft,

$$q/A = 590,000 \text{ BTU/hr ft}^2$$

$$\Delta T = 152\,^{\circ}F$$

$$T_L = 113\,^{\circ}F$$

$$T_w = 152 + 113 = 265\,^{\circ}F$$

$$\frac{(q/A)D_w}{8k} = \frac{590,000 \times 0.000833}{8 \times 42} = 1.5\,^{\circ}F$$

$$T_s = T_w - 1.5 = 263.5\,^{\circ}F.$$

It can be seen that the error involved in neglecting the radial temperature gradient of the wire is less than 0.6%. At lower hea t flux values, the error is even smaller.

III. CALCULATION OF RESONANCE SIZE

From Equation (1) in Part II

$$R_o = \frac{0.326 \, P_o^{1/2}}{f \, \rho_L^{1/2}}$$

where R_o - resonance radius, cm

ρ_L - density of the liquid, g/cm^3

f - frequency, kcps

P_o - ambient pressure, atm.

Since P_o = 1 atm, values of R_o at different frequencies are calculated and given in the following table:

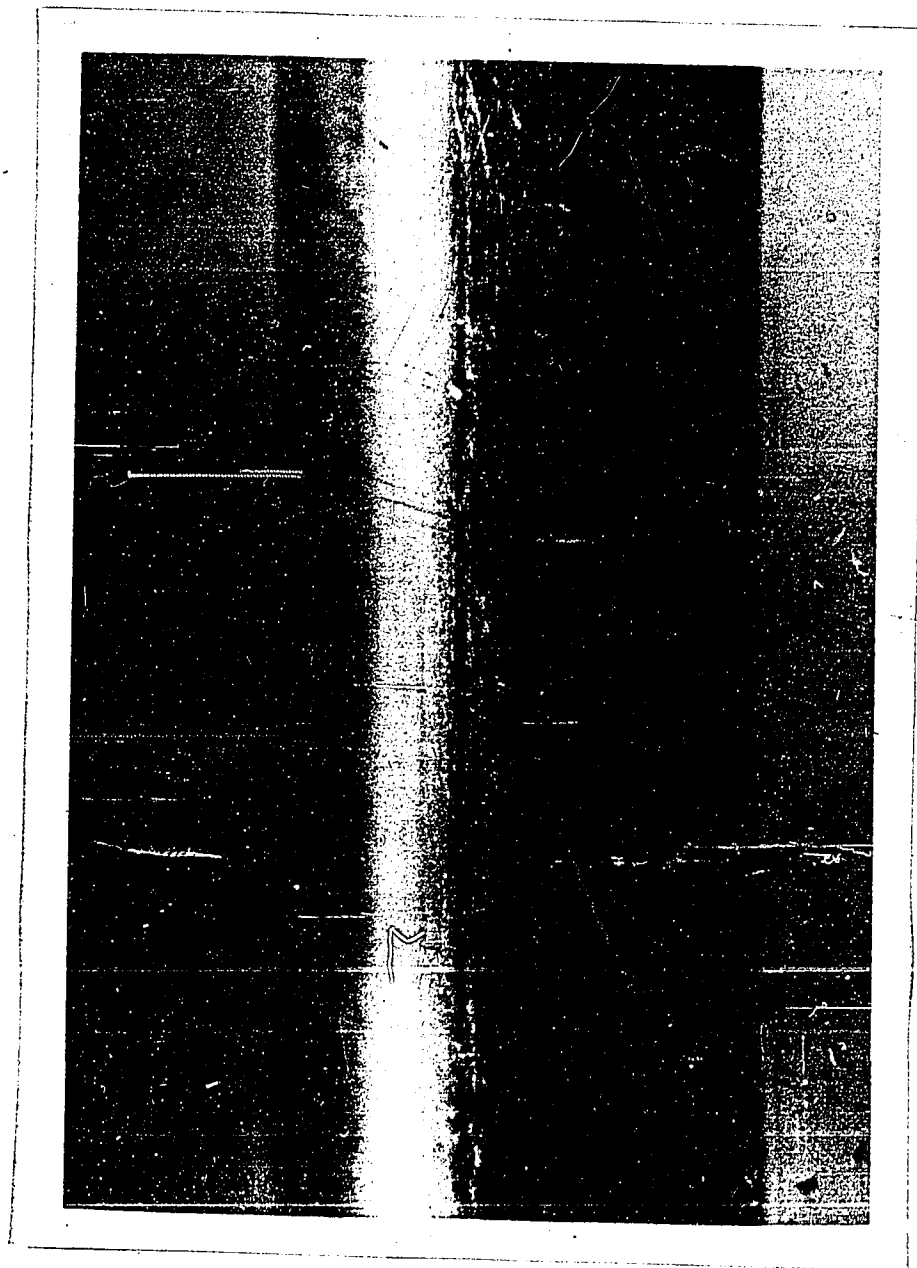| Liquid	Density g/cm^3	f kcps	R_o cm	$D_B = 2R_o$ ft $x10^4$
Water	0.980	20.6	0.0160	10.5
Methanol	0.755	20.6	0.0182	12.0
Water	0.980	44.1	0.00748	4.9
Methanol	0.755	44.1	0.00850	5.6
Water	0.980	108	0.00305	2.0
Methanol	0.755	108	0.00347	2.3
Methanol	0.755	306	0.00122	0.72

APPENDIX G

PHOTOGRAPHIC STUDY OF THE SURFACE CONDITIONS

OF PLATINUM WIRE

The photographs shown in the following pages were taken through a microscope with a 160 x magnification.

FIGURE 1   Photograph of a new platinum wire D_w = 0.010 in. Magnification = 160 x   (G-2).
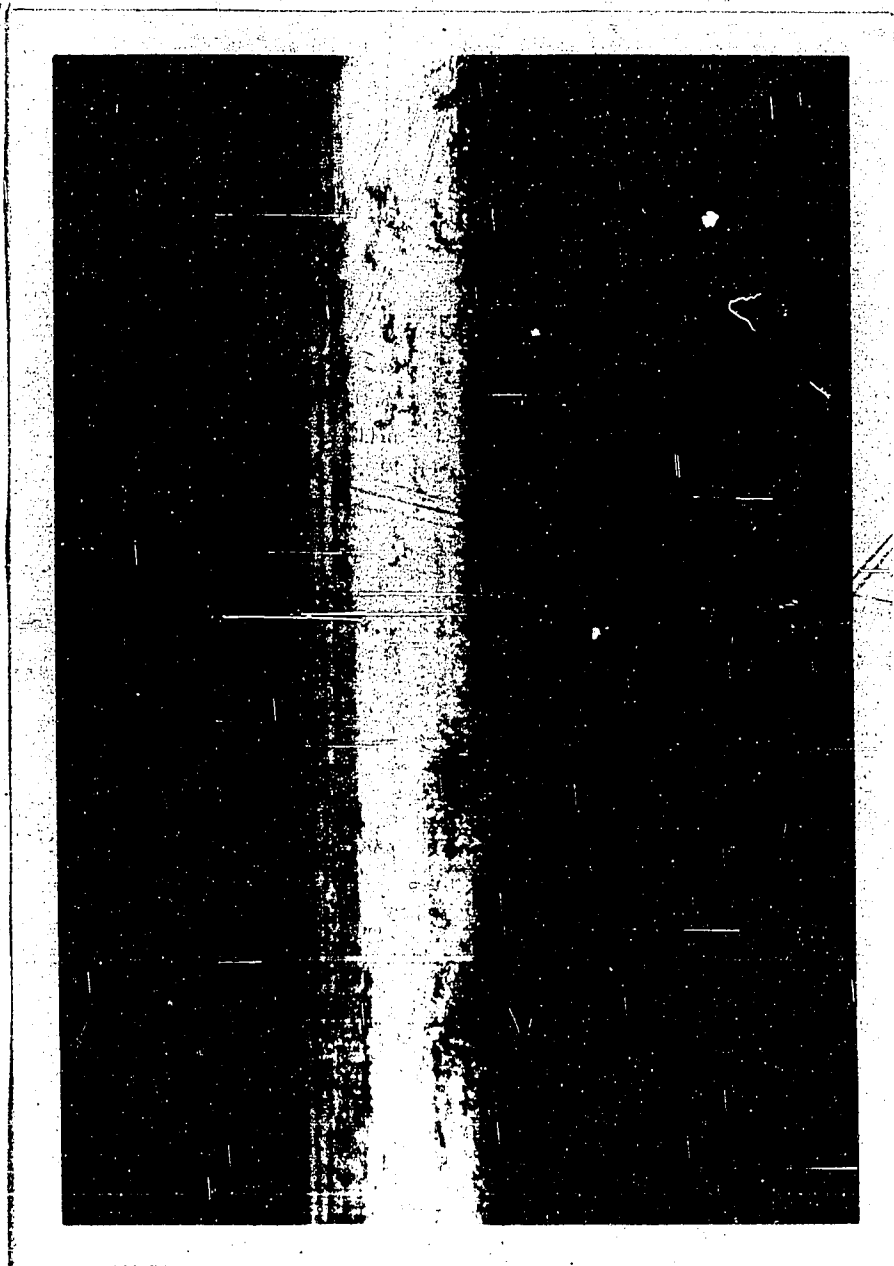
FIGURE 2   Photograph of a platinum wire after 3 tests. D_w = 0.007 in. Magnification 160 x.   (G-3)

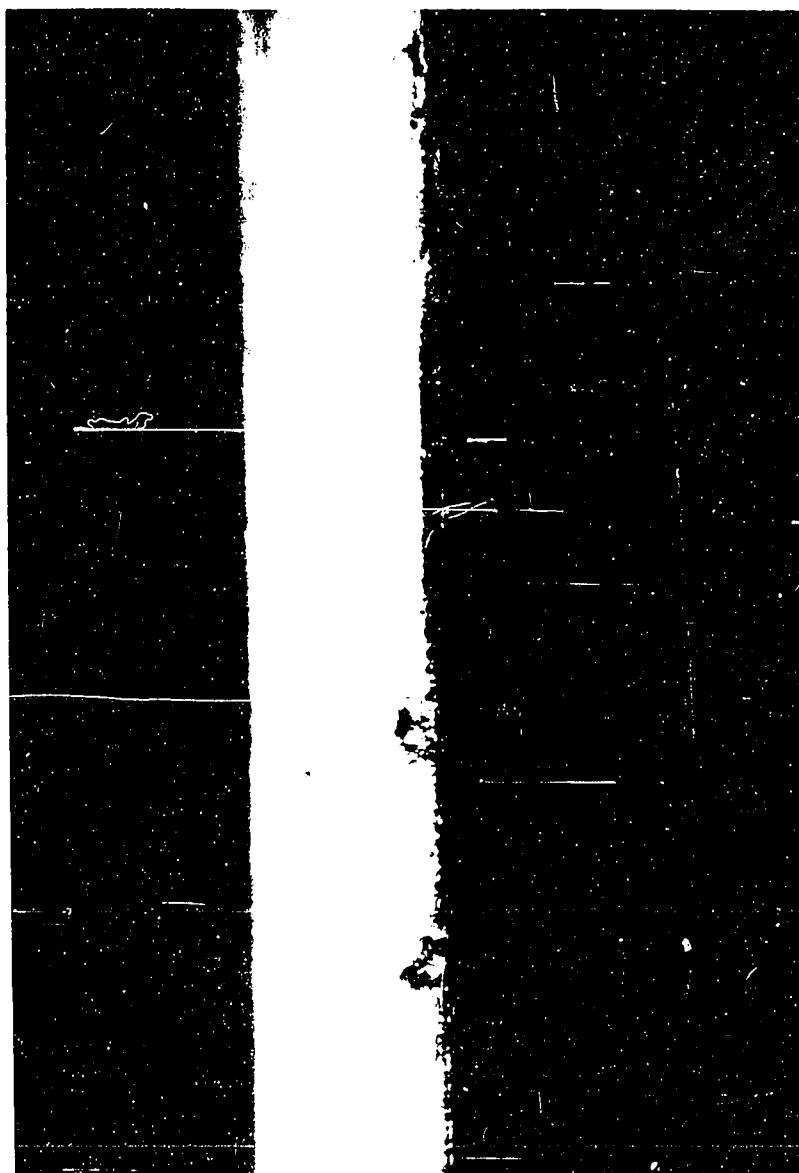FIGURE 3   Photograph of a platinum wire after 5 tests. D_w = 0.007 in. Magnification = 160 x.   (G-4).